Thesis submitted for the degree of

Doctor of Philosophy

At the University of Leicester

By

Areej Mashhour Tawfiq Assaf, MSc.

Department of Infection, Immunity and Inflammation

University of Leicester

April 2008

ProQuest LLC
789 East Eisenhower Parkway
P.O. Box 1346
Ann Arbor, MI 48106-1346

To Mom and Dad
With love

Statement of Originality

This accompanying thesis submitted for the degree of PhD entitled "Human Toll-Like Receptor (TLR) 9 Expression and Function in Haematological and Non-haematological Malignancies" is based on work conducted by the author in the department of Infection, Immunity and Inflammation at the University of Leicester mainly during the period between March 2005 and April 2008.

All the work recorded in this thesis is original unless otherwise acknowledged in the text or by references.

None of the work has been submitted for another degree in this or any other university.

Signed:———— Date: ————

Acknowledgement

First, sincere gratitude to Dr. Michael Browning for his supervision, excellent academic guidance, help, support and encouragement during the last two and half years. His wide knowledge and logical way of thinking has been of a great help to me. He was always available when I needed his advice.

The work presented here was done in the Department of Infection, Immunity and Inflammation, University of Leicester so I would like to thank Dr. Bernard Burke for his help in the luciferase assay, Dr. Jeni Luckett for her help in confocal microscopy and all the staff and colleagues of the department who helped me out over the years.

I would like to give my sincere thanks to Dr. Cynthia A. Leifer, USA, for her great scientific help and valuable advice in the expression of hTLR9 and for providing the TLR9 construct genes and their empty plasmids. A special thanks to Dr. Raj Patel, department of Biochemistry, for his friendly and wise support in western blotting and inhibitors, and Prof. M. Manson, department of Biochemistry, for providing the inhibitors and their antibodies. Further thanks goes to Prof. Loems Ziegler-Heitbrock, department of Infection, Immunity and Inflammation, for providing the luciferase construct, Prof. Andreas Gescher, department of Cancer Studies and Molecular Medicine, for providing the Curcumin and Dr. John Curnow, University of Birmingham for using Luminex® 100 instrument.

It is a pleasure to also extend my thanks to my colleagues who worked in the Lab during my study, for their help and support. I am very grateful to my friends Ghada, Hind and Noura; I owe them a lot for their care, support and encouragement during the hard times in Leicester. Never ending thanks to all my friends in UK and Jordan for their support and encouragement through out the years in Leicester.

Finally, I am deeply indebted to my family especially to Mom and Dad whose prayers, encouragement, support, patience and love have always been lightening my way. Simply, words cannot convey my appreciation, gratitude and love for them.

Abstract

Human Toll-like receptor (TLR) 9 expression and function in haematological and non-haematological malignancies.

Areej Mashhour Tawfiq Assaf

The toll like receptors (TLRs) are mammalian type I transmembrane proteins that play an essential role in the activation and regulation of innate and adaptive immunity through the recognition of specific molecular patterns of pathogens. In humans, ten TLRs (TLR 1–10) have been identified. Toll-like receptor 9 is expressed in B cells and plasmacytoid dendritic cells and recognises bacterial and viral DNA and oligodeoxynucleotides (ODNs) with unmethylated deoxycytosine-deoxyguanosine (CpG) motifs. Activation via TLR9 is thought to depend on activation of MAPK, PI3K/AKT and IκB/NF-κB pathways and leads to cytokine release, upregulation of immunologically relevant surface markers and increased cellular proliferation. The immune stimulatory effects of CpG ODNs are being exploited as a novel therapeutic approach to the treatment of human diseases and tumours.

This thesis addresses the expression and function of human TLR9 in haematological and non-haematological tumour cells. I have shown that most B linage tumour cell lines expressed TLR9, with the exception of myeloma cell lines U266, Karpas 707H and the EBV-lymphoblastoid HMy2 cell line, whereas all non-haematological cell lines tested were negative or very weakly positive. TLR9 positive B-cells/B-cell lines, responded to CpG-ODN activation by activating intracellular signalling pathways, cytokine release, surface marker upregulation and cellular proliferation, whereas TLR9 negative cells did not.

Data on the ability of pretreatment with low doses of CpG-ODN to induce a refractory state (tolerance) on Burkitt's lymphoma BJAB cells indicates that low doses of CpG-ODN tolerised NF-κB activation and, to some extent, cellular proliferation and surface marker upregulation. Moreover, reactivating NF-κB on BJAB cells after being tolerised with low dose of CpG-ODN is time dependent with the tolerising effect lasting up to two weeks after a single dose of CpG-ODN.

Finally, inhibiting the signalling pathways (ERK, $p38^{MAPK}$, PI3K/AKT and NF-κB) with selective inhibitors U0126, SB203580, LY294002 and Curcumin respectively, has shown different effects on basal and CpG-ODN activated surface marker expression, cellular proliferation and cytokine release. Furthermore, different signalling pathways mediate different functional effects of CpG-ODN/TLR9 activation, and suggest that ERK and p38 MAPK pathways are involved in CpG-ODN mediated NF-κB activation. This work should shed a new light on the mechanisms of action of CpG activation on TLR9 signalling in immune and non-immune cells and on its immunotherapeutic use in the treatment of cancer.

Table of Content

Abbreviations

β-ME:	β-Mercaptoethanol.
AP-1:	Activator protein-1
APC:	Antigen presenting cell.
ATF2:	Activating transcription factor 2
B-CLL:	B-cell chronic lymphocytic leukemia
BL:	Burkitt's lymphomas
BMDM:	Bone marrow–derived macrophages
BSA:	Bovine serum albumin
CCR:	Chemokine receptor.
CCR7:	CC chemokine receptor 7
CD:	Cluster of differentiation.
CpG:	2′-deoxyribo (Cytidine-phosphate-Guanidine) dinucleotides.
CPM:	Count per minute.
CTLs:	Cytotoxic T-lymphocytes
DC:	Dendritic cell.
DEPC:	Diethylpyrocarbonate
DLBCL:	Diffuse large B-cell lymphoma
DNA-PK:	DNA-dependent protein kinase
dNTP:	Deoxynucleotide triphosphate
dsRNA:	Double-stranded RNA.
ERK:	Extracellular signal-regulated kinase
ER:	Endoplasmic reticulum
FACS:	Fluorescence-activated cell sorting
FCS:	Fetal calf serum.
FITC:	Fluorescein isothiocyanate.
FL:	Follicular lymphoma
FSC:	Forward scatter
FW:	Forward
GM-CSF:	Granulocyte-macrophage colony- stimulating factor.
HA:	Haemagglutinin
HRP:	Horse raddish peroxidase
ICAM-1:	Intercellular adhesion molecule 1

IFN:	Interferon
Ig:	Immunoglobulin.
IκB:	Inhibitor of nuclear factor-κB
IKK:	Inhibitor of nuclear factor-κB kinase.
IL:	Interleukin.
IL-IR:	Interleukin-1 receptor
IP:	Immunoprecipitation
IRAK:	IL-IR -associated kinase.
IRF:	Interferon-regulatory factor.
JNK:	c-Jun N-terminal Kinase
KO:	Knock-out
LCL:	Lymphoplastoid cell line
LPS:	Lipopolysaccharide.
LRR:	Leucine-rich repeat.
LTA:	Lipotechoic acid.
ODN:	Oligodinucleotides
mAbs:	Monoclonal antibodies.
MAPK:	Mitogen-Activated Protein Kinase
M-CSF:	Macrophage colony-stimulating factor.
MCL:	Mantle cell lymphoma
mDC:	Myeloid dendritic cells.
MFI:	Mean channel fluorescence intensity
MHC:	Major Histocompatibility Complex
MZL:	Marginal zone B-cell lymphoma
mRNA:	messenger RNA
MyD88:	Myeloid differentiation primary-response protein 88.
NF-κB:	Transcription factor nuclear factor-kappa B
NK:	Natural killer.
NOD:	Nucleotide–binding oligomerization domain
PAMPs:	Pathogen-associated molecular patterns.
PBMC:	Peripheral blood mononuclear cells.
pDC:	Plasmacytoid dendritic cells.
PBS:	Phosphate buffer saline
PE:	Phycoerythrin.

PI3K:	phosphatidylinositol 3 kinase [PI3]-kinases
RIG1:	Retinoic acid–inducible protein 1
PMSF:	Phenylmethanusulphonylfluoride
PRRs:	Pattern recognition receptors.
PS:	Phosphorothioate
RLU:	Relative light unit
RT:	Room temperature
RW:	Reverse
ssRNA:	Single-stranded RNA.
SAPK:	Stress-activated protein kinases
SLL:	B-cell small lymphocytic lymphoma
SSC:	Side-scatter
STAT1:	Signal Transducer and Activator of Transcription 1
TAK1:	Transforming-growth-factor-β-activated kinase.
TGF:	Transforming growth factor.
$T_{H:}$	Helper T cells
TIR:	Toll-interleukin 1 receptor-resistance domain (Toll/IL-I) receptor.
TIRAP:	TIR domain-containing adaptor protein.
TLRs:	Toll-like receptors.
TM:	Transmembrane (proteins)
TNF:	Tumour necrosis factor.
TRAF:	Tumour-necrosis-factor-receptor-associated factor.
TRAIL:	TNF-related apoptosis-induced ligand
TRAM:	TRIF-related adaptor molecule.
TRIF:	TIR-domain-containing adaptor protein inducing IFN-β.
Ubc:	Ubiquitin-conjugating
VPS34:	Class III vacuolar protein sorting 34
WB:	Western blotting

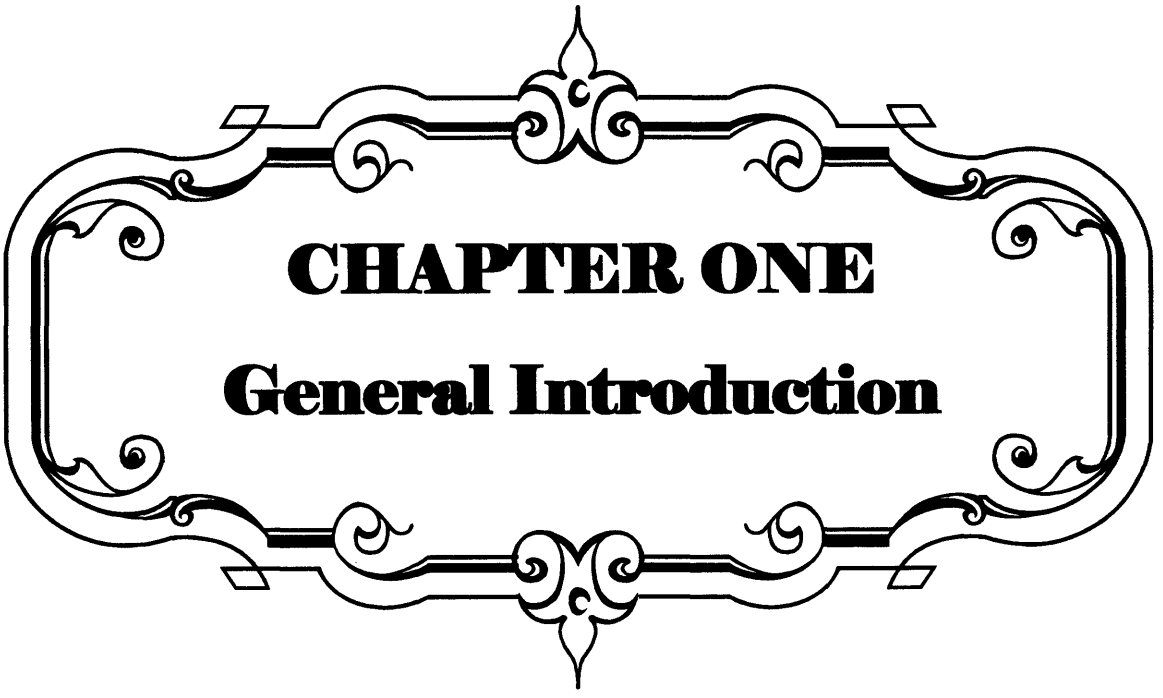

CHAPTER ONE

General Introduction

CHAPTER ONE
General introduction

1.1 The Immune System:

The immune system, the body's line of defence, is a collection of cells and tissues distributed throughout the body, collectively referred to as lymphoid tissues, protecting the body from any invading pathogen. Lymphoid tissues are either primary lymphoid organs, such as the bone marrow and thymus, where lymphocytes develop from lymphoid stem cells and then enter the circulation, or secondary lymphoid organs and tissues, such as lymph nodes, where lymphocytes are most active in defending the body against diseases.

Self/non-self discrimination is an important aspect within the immune system. This ability to distinguish self from non-self is very important for protecting the body from the invading pathogens and in eliminating modified or altered cells (e.g. malignant cells), whilst not attacking the bodies own normal cells and tissues. Pathogens can replicate intracellularly (parasites, viruses and some bacteria) or extracellularly (parasites, fungi and most bacteria), requiring different strategies for immunological targeting.

Upon the exposure to a pathogen, two complementary systems are activated, the innate and the adaptive immune systems. The adaptive immune system is a highly sophisticated response that is organised by two classes of specialised cells, namely B and T lymphocytes. It expresses remarkable diversity of receptors, which specifically target the invading organism, and by providing an immunological memory that prevents the infection from repetition. The secondary lymphoid organs, such as the spleen and lymph nodes, are the home for the circulating B and T lymphocytes, which re-circulate between the lymphoid tissues and the blood and lymph. In these locations, "naive" lymphocytes scan for the presence of antigens. B cells develop in the bone marrow, which is considered a primary lymphoid organ, but it also acts as a secondary organ because of the presence of antibody-secreting plasma cells. T lymphocytes develop in the thymus from precursor cells produced by the bone marrow. Dendritic cells present in the peripheral tissues pick up pathogens in the form of antigenic determinants during infection, and migrate to the lymphoid tissues carrying the antigens with them. Then,

these antigens will be processed and presented to T lymphocytes within the lymphoid tissues. The appropriate T lymphocytes respond to the antigen by either killing the infected cells directly, or secreting cytokine mediators. The latter may facilitate an antigen-specific B lymphocyte response, leading to humoral immunity by the secretion of antibody specific for the pathogen, and production of memory B-cells. However, it takes three to five days for sufficient numbers of T and B cell clones of antigen-specific lymphocytes to be produced and to differentiate into effector cells, allowing enough time for most of the pathogens to damage the host. Hence, the need for innate immune mechanisms, which act against the invading organisms from the time of infection without a lag phase.

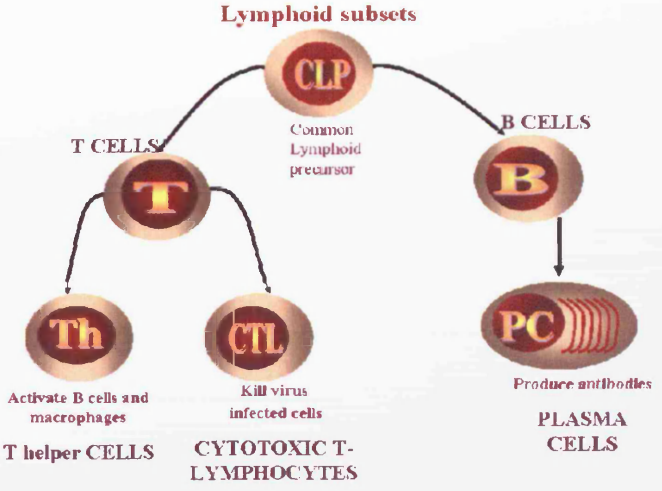

Figure 1.1 Lymphocyte subsets in the human leukocytes and their functions.

T cells recognise the non-self target, such as pathogens, as antigen-derived peptides coupled to the major histocompatibility complex (MHC) molecules, leading to the production of killer or helper T cells. Killer T cells recognise the antigens coupled to class I MHC molecules, while helper T cells recognise antigen associated with class II MHC molecules. Helper T cells control the immune response by directing others to kill the infected cells or organisms. The activation of helper T cells triggers the release of cytokines such as interleukin-2 (IL-2), IL-4, IL-5, IL-6, or interferon gamma (IFN–γ) that influence the activity of many cell types, in addition to the upregulation of molecules expressed on the T cell's surface and stimulation of B cell proliferation and differentiation into antibody secreting B cells (Figure 1.1).

In contrast to adaptive immunity, the innate immune recognition is mediated by a set of germline encoded, non-clonal receptors that recognise conserved pathogen associated

molecular patterns (PAMPs), referred to as pattern recognition receptors (PRR). Innate immunity involves both cells such as phagocytes, and soluble factors such as antimicrobial peptides and the complement pathway. Innate immune mechanisms will be activated immediately after the infection to control the infecting pathogen's replication until the lymphocytes can begin to deal with that infection. Unlike the adaptive immunity, the innate immunity is not antigen–specific, and does not exhibit memory or lasting protective immunity, and there is a limited selection of recognition molecules.

The innate immune system protects the body by rapidly detecting the infectious agent, regardless of its type, based on the profile of PAMPS exposed. It categorises the type of those invading agents as to whether they are located extracellularly or intracellularly and by the nature of the PAMPs expressed. Depending on the type of infection, distinct subsets of innate immune cells produce the appropriate cytokines and chemokines to limit the spread of the infection and activate the appropriate adaptive immune response to eliminate the infection and prevent its recurrence. Adaptive immunity is influenced by the production of helper T (T_H) cell subsets and their resulting production of "effector" cytokines. Stimulated naïve T_H cells differentiate into effector cells that promote either cell-mediated immune response (T_H1-type response), or humoral (antibody-mediated) immune response (T_H2-type response), working together to mount an appropriate defence. The balance between them is modulated by chemical messengers, the cytokines. T_H1 cytokines such as IL–2, IFN–γ, and IL–12 stimulate the cell-mediated response and suppress the humoral response. T_H2 cytokines, such as IL–10, IL-6 and IL-4, stimulate the humoral response and suppress the cell-mediated response. For extracellular pathogens, pro-inflammatory cytokines such as tumour-necrosis factors–α (TNF-α) will be produced, whereas, mainly type-I interferons are produced in case of the intracellular pathogens.

The innate immune system detects the invading pathogen by using one or more members of several general families of PRRs on innate cells that detect PAMPS on pathogens. PRRs include the toll like receptors (TLRs), Nucleotide–binding oligomerization domain (NOD), Retinoic acid–inducible protein 1 (RIG1), mannose receptor and C-type lectins such as dendritic cell–specific intracellular adhesion molecule 3 – grabbing non–integrin (DC–SIGN).

The best understood family of PRRs is the Toll like receptors, that recognise distinct PAMPs and result in the upregulation of cell surface molecules and cytokine/chemokine mediators, directing innate as well as acquired immune response (Schnare M *et al.*, 2001; Underhill DM *et al.*; 2002; Vasselon T *et al.*, 2002).

1.2 Toll like Receptors:

In 1997, Medzhitov and colleagues characterized a human homologue of the Drosophila Toll protein that is able to induce an immune response. This human protein was similar to the Drosophila Toll protein and the human interleukin-1 receptor, and so it was known as Toll Like receptor (TLR). Since then, a family of mammalian toll-like receptors has been identified that constitutes one of the first lines of defence in the body against invading pathogens. Upon their activation by the specific components of the microbes, they play a crucial role in the function of the innate immune system. TLRs are germline–encoded immunoreceptors that are essential sensors in detecting and responding to a broad diversity of invading microbial and viral pathogens (Takeda K *et al.*, 2003). They respond by detecting bacterial cell wall components and pathogen–derived nucleic acids, triggering immune responses at both the innate and adaptive levels.

Toll-like receptors are type I transmembrane (TM) proteins. They are composed of an N-terminal signal peptide extracellular domain, which contains leucine-rich repeats involved in recognising the ligands (PAMPs). Also, TLRs contain a transmembrane domain and a cytoplasmic domain, which is largely made up of the (TIR) Toll-interleukin 1 receptor-resistance domain (Toll/IL-1) that is required for the downstream signalling (Figure 1.2) (Akira S 2001; Medzhitov R *et al.*, 2001).

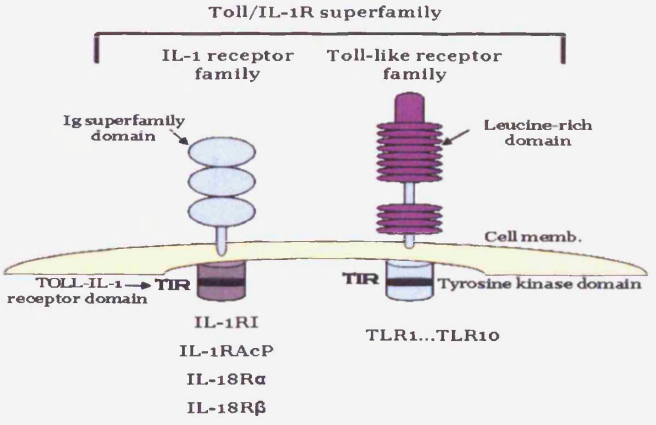

Figure 1.2: Toll like receptor's structure compared with the interleukin I (IL-1) receptor family.

In mammals, the well conserved TLR family is presently known to consist of 11 members, at least 10 members of which are expressed in humans (Rock FL *et al.*, 1998; Du X *et al.*, 2000; Hemmi H *et al.*, 2000; Akira S *et al.*, 2003) (Figure 1.3). The Toll-like receptors (TLR1, TLR2, TLR4, TLR5 and TLR6) that distinguish fungal and bacterial membrane constituents, are confined on the plasma membrane and can be recruited to phagosomes, whereas those that recognise viral and bacterial nucleic acid (TLR3, TLR7, TLR9 and to some extent TLR8) are allocated intracellularly to the membranes of the endosomal compartment (Latz E *et al.*, 2004a; Latz E *et al.*, 2004b; O'Neill LA 2004) (Figure 1.3). These receptors are expressed on a large number of immune cells as well as some epithelial cells, playing a crucial role in the activation of the innate immune response to the invading microbial pathogens (Muzio M *et al.*, 2000). The surface expression of TLRs measured by monoclonal antibodies showed a very low level of expression. This would correspond to a few thousand molecules per cell in monocytes, whilst only a few hundred or less in immature dendritic cells (Visintin A *et al.*, 2001). On the other hand, the expression of those receptors is modulated in response to different stimuli, such as dsRNA for TLR3 and lipopolysaccharides for TLR4 (Cario E *et al.*, 2000; Akira S *et al.*, 2003), and it is observed in other cells such as intestinal epithelial cells, vascular endothelial cells, and cardiac myocytes.

The family of human toll like receptors (hTLRs) recognise distinct PAMPs (Figure 1.3), such as lipoproteins (TLR 1, 2 & 6), dsRNA (TLR3), lipopolysaccharides (LPS) (TLR4), flagellin (TLR5), single stranded RNA, synthetic imidazoquinolines and loxoribine (TLR 7&8) and unmethylated CpG oligodinucleotides (TLR9) (Cario E *et al.*, 2000; Akira S *et al.*, 2003). The interaction of the TLR and its PAMP ligand initiates an intracellular signal, which leads to the production of different chemical mediators and the upregulation of immunologically relevant surface markers. This would direct the innate as well as the acquired immune responses in the activated cells (Iwasaki A *et al.*, 2004; Ishii KJ *et al.*, 2005). The main characteristics that differentiate individual TLRs are expression profiles, subcellular localisation, ligand recognition, and signalling pathways activated.

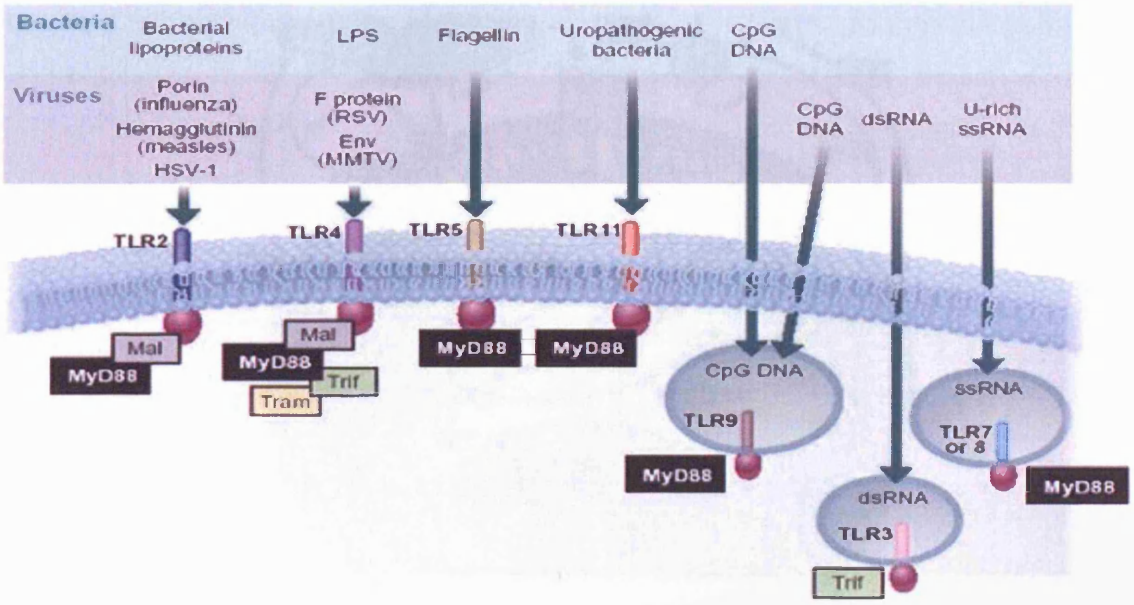

Figure 1.3. TLRs 1-9 and their PAMPs. (**www.fz-borstel.de/en/research/icb/ni/index.htm**).

Although TLRs are known to be transmembrane proteins, only those (TLR1, TLR2, TLR4, TLR5 and TLR6) which recognise the unique molecular structures of fungal and bacterial cells are localised on the plasma membrane, from where they could be taken to the phagosomes. However, those TLRs (TLR3, TLR7 & TLR9) which recognise viral and bacterial nucleic acids are intracellularly localised (Funami K *et al.*, 2004; Latz E *et al.*, 2004b; Leifer CA *et al.*, 2004; Kajita E *et al.*, 2006). The location of these receptors is thought to be an important factor in determining their ability to mount the innate immune responses to such known diversity of pathogenic microorganisms. The activation of TLRs, in general, results in the stimulation of the innate immune response, including upregulation of immunologically relevant surface markers, increase cell proliferation and cytokine/chemokine release (Akira S *et al.*, 2001). Figure 1.4 illustrates the TLRs ligands and the different innate immune responses induced by the activation of each TLR with its specific ligand.

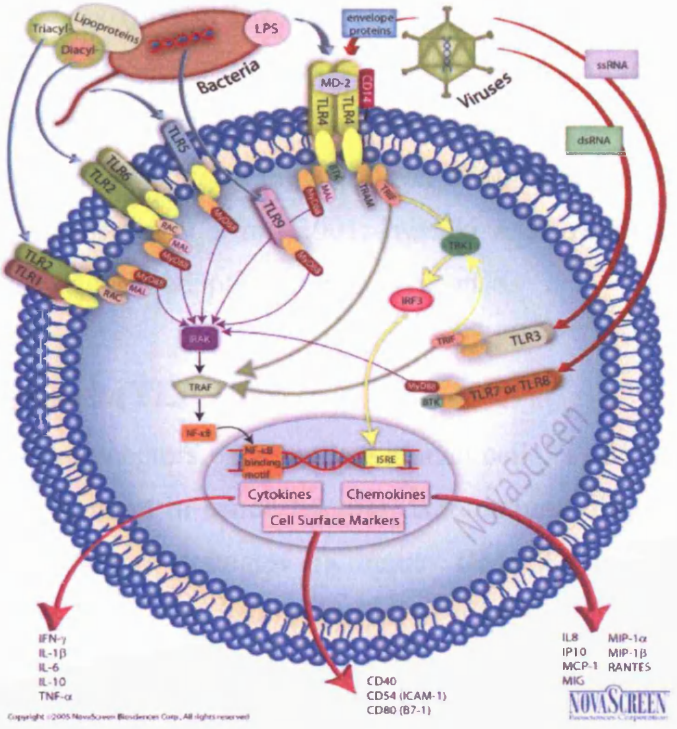

Figure 1.4. The immunostimulatory effects of the Toll-Like Receptors. (Nova screen Biosciences Corporation).

TLR members are differentially expressed on immunological and non-immunological cells. The cells of the innate immune system express different types of the TLRs. Most of the TLRs (except TLR3) are known to be expressed in monocytes-macrophages, whereas B-cells express all TLRs except TLR3 and TLR8 (Hornung V *et al.*, 2002; Brouke E *et al.*, 2003; Dasari P *et al.*, 2005). TLR3 has been found to be expressed in neutrophils, T cells, natural killer cells, and immature dendritic cells (Dasari P et al., 2005). Furthermore, TLRs were found to be expressed by some non-immune cells such as airway smooth muscle cells which significantly express all TLRs, human corneal cells which express TLR4, and the epithelial cells of the lower female genital tract which showed a high expression level of TLR 2, 3, 5 and 6 (Song PI *et al.*, 2001; Zarember KA *et al.*, 2002; Funami K *et al.*, 2004; Droemann D *et al.*, 2005; Sukkar MB *et al.*, 2006; Herbst-Kralovetz MM *et al.*, 2008). Importantly in humans, mature dendritic cell (DC) and its precursors (pre-DC), including monocytes (pre-DC1), plasmacytoid DC precursors (pre-DC2), and $CD11c^{+}$ immature DCs (imDCs), were found to express most TLRs (Kadowaki N *et al.*, 2001; Visintin A *et al.*, 2001; Dasari *et al.*, 2005). Visintin A *et al.*, (2001) reported that human monocytes express all TLRs except TLR3, and TLRs 1-4 & 6 are expressed in immature DCs whereas mature DC express only TLR1 and 6. In 2003, Bourke E and colleagues reported the expression of TLRs 1, 6, 7, 9 and 10 on

plasmacytoid dendritic cells (pDC). The activation of DC and its precursors would produce chemokines and cytokines upon TLR activation. For example, the activation of TLR2 and 4 in monocytes produce TNF-α and IL-6 while the activation of TLR9 in pDC is responsible for the production of the high level of type I IFN (IFN-α and IFN-β), (Akira S *et al.*, 2001; Kadowaki N *et al.*, 2001; Iwasaki A *et al.*, 2004; Dasari *et al.*, 2005) influencing the subsequent adaptive immune response.

1.3 Toll like receptor 9 (TLR9):

Amongst the ten Toll-like receptors expressed in human cells, TLR9 receives growing attention due to its involvement in cancer studies, autoimmune diseases as well as in immunomodulatory therapeutic strategies (Klinman DM. 2004). The TLR9 gene contains an open reading frame that was identified in a search of the human genomic DNA database with a Human Genome Blast program (http://www.ncbi.nlm.nih.gov/BLAST/), and its gene has been found to be localised on chromosome 3p21.3 with accession number NT-001625 (Figure 1.5). Human TLR9 contains 1032 amino acid residues with a calculated molecular weight of 115.9 kDa.

```
   1 MGFCRSALHP LSLLVQAIML AMTLALGTLP AFLPCELQPH GLVNCNWLFL
  51 KSVPHFSMAA PRGNVTSLSL SSNRIHHLHD SDFAHLPSLR HLNLKWNCPP
 101 VGLSPMHFPC HMTIEPSTFL AVPTLEELNL SYNNIMTVPA LPKSLISLSL
 151 SHTNILMLDS ASLAGLHALR FLFMDGNCYY KNPCRQALEV APGALLGLGN
 201 LTHLSLKYNN LTVVPRNLPS SLEYLLLSYN RIVKLAPEDL ANLTALRVLD
 251 VGGNCRRCDH APNPCMECPR HFPQLHPDTF SHLSRLEGLV LKDSSLSWLN
 301 ASWFRGLGNL RVLDLSENFL YKCITKTKAF QGLTQLRKLN LSFNYQKRVS
 351 FAHLSLAPSF GSLVALKELD MHGIFFRSLD ETTLRPLARL PMLQTLRLQM
 401 NFINQAQLGI FRAFPGLRYV DLSDNRISGA SELTATMGEA DGGEKVWLQP
 451 GDLAPAPVDT PSSEDFRPNC STLNFTLDLS RNNLVTVQPE MFAQLSHLQC
 501 LRLSHNCISQ AVNGSQFLPL TGLQVLDLSH NKLDLYHEHS FTELPRLEAL
 551 DLSYNSQPFG MQGVGHNFSF VAHLRTLRHL SLAHNNIHSQ VSQQLCSTSL
 601 RALDFSGNAL GHMWAEGDLY LHFFQGLSGL IWLDLSQNRL HTLLPQTLRN
 651 LPKSLQVLRL RDNYLAFFKW WSLHFLPKLE VLDLAGNQLK ALTNGSLPAG
 701 TRLRRLDVSC NSISFVAPGF FSKAKELREL NLSANALKTV DHSWFGPLAS
 751 ALQILDVSAN PLHCACGAAF MDFLLEVQAA VPGLPSRVKC GSPGQLQGLS
 801 IFAQDLRLCL DEALSWDCFA LSLLAVALGL GVPMLHHLCG WDLWYCFHLC
 851 LAWLPWRGRQ SGRDEDALPY DAFVVFDKTQ SAVADWVYNE LRGQLEECRG
 901 RWALRLCLEE RDWLPGKTLF ENLWASVYGS RKTLFVLAHT DRVSGLLRAS
 951 FLLAQQRLLE DRKDVVVLVI LSPDGRRSRY VRLRQRLCRQ SVLLWPHQPS
1001 GQRSFWAQLG MALTRDNHHF YNRNFCQGPT AE
```

Figure 1.5. The amino acid sequence of human TLR9. The predicted signal peptide residues 818-835 is shown in blue and underlined. (http://www.ncbi.nlm.nih.gov/entrez/viewer.fcgi?db=nuccore&id=20302169).

TLR9 shares significant homology with the other TLR members, including putative intracellular/extracellular and transmembrane domain sequences (Du X *et al.*, 2000; Hemmi H *et al.*, 2000).

1.3.1 TLR9 expressing cells:

It is expected that each TLR is capable of detecting its specific ligand depending on its unique pattern of cellular and tissue expression. TLRs, in general, are expressed in many tissues, except for TLR9 which is expressed in limited number of human cells. Furthermore, TLR9 expression varies between species; in mice, it is expressed in pDC and B cells as in humans, but also in monocytes/macrophages and myeloid dendritic cells (mDC) (Iwasaki A *et al.*, 2004). Resting human immune cells, B cells and plasmacytoid dendritic (pDC) cells are the main expressing cells for TLR9 whereas resting macrophages do not express TLR9 in humans (Kadowaki N *et al.*, 2001; Krug A *et al.*, 2001; Hornung V *et al.*, 2002; Dasari P *et al.*, 2005; Vollmer J 2005; Hoene *et al.*, 2006). Some studies have reported human TLR9 expression in other immune cells such as activated neutrophils (Hayashi F *et al.*, 2003) and in some natural killer (NK) cells (Roda J *et al.*, 2005), and also in eosinophils and T lymphocytes (Nagase H *et al.*, 2003; Hornung V *et al.*, 2002). On the other hand, Hornung V *et al.*, 2002 reported that monocytes, NK cells, and T cells express low hTLR9 level, but they do not respond to CpG activation. Other studies have reported TLR9 expression in other human cell types, such as pulmonary epithelial cells and lung cancer, airway smooth muscles, keratinocytes and intestinal epithelial cells (Pedersen G *et al.*, 2005, Platz J *et al.*, 2004, Chuang TH *et al.*, 2000, Zarember KA *et al.*, 2002, Lebre M *et al.*, 2007 and Droemann D *et al.*, 2005). TLR9 expression and localisation is very important for the induction of the immune response upon their recognition and activation with CpG DNA motif.

1.3.2 TLR9 localisation:

Several members of the TLR family are expressed on the plasma membrane of cells (Leifer CA *et al.*, 2004). The nature and cellular localisation of TLR9 in primary human cells remain controversial; it is mainly accepted to be intracellularly expressed. However, it may also be on cell membrane in certain circumstances (Eaton-Bassiri A *et al.*, 2004; Leifer CA *et al.*, 2004). TLR9 is primarily an endosomal protein detecting CpG-DNA ligands only as these compounds become internalised (Cunningham-Rundles C *et al.*, 2006). Most of the literature (Latz E *et al.*, 2004b; Leifer CA *et al.*,

2004) found that the majority of human TLR9 was expressed intracellularly. Several independent studies had shown that TLR9 is localised in late endosome or lysosomes, where it recognises double stranded unmethylated CpG motifs (CpG DNA) (Hemmi H *et al.*, 2000; Latz E *et al.*, 2004a; Latz E *et al.*, 2000b; Leifer CA *et al.*, 2004). However, a recent study showed that TLR9 can also appear on the cell surface of some tonsillar lymphocytes, especially after LPS activation (Eaton-Bassiri A *et al.*, 2004).

The immune response induced by the stimulation of TLR9 depends on the type of the cells TLR9 is expressed in, and the nature of TLR9 ligand required for this stimulation. Although the localisation of TLR9 in the immune cell seems to be important for the immune response induction, no clear data shows its importance for the function of the receptor. However, knowing that all TLRs that share specificity for nucleic acids are located predominantly intracellularly strongly indicates that the localisation might be related to the recognition of the ligand's type. This is revealed in TLR9 as it recognises viral or bacterial DNA, but not (normally) mammalian DNA (Funami K *et al.*, 2004, Kajita E *et al.*, 2006, Latz E *et al.*, 2004a and Leifer CA *et al.*, 2004). On the other hand, Barton GM. and colleagues (2006) found that surface expression of TLR9 did not alter or change the ability of the receptors to recognize CpG DNA, but it gained the ability to recognise mammalian DNA, indicating that TLR9 intracellular localisation mostly controls the access of the receptor to CpG DNA. In previous studies done by Latz group (Latz E *et al.*, 2004a; Latz E *et al.*, 2004b), TLR9 was found to be initially localised in the endoplasmic reticulum (ER). The activation of TLR9 requires its specific agonist (CpG motif) to be internalised via a clathrin-dependent endocytic pathway before rapidly moving to a tubular lysosomal compartment. Also, endosomal maturation is thought to be essential for the immunostimulatory activity (Latz E *et al.*, 2004b). In lymphocytes, this uptake is energy and temperature dependent and is greatly increased by cell activation (Krieg AM 2006). In the absence of CpG DNA, TLR9 is kept in the ER, but upon CpG DNA uptake it gains access to the incoming endosomes that contain CpG DNA by directly fusing ER with the endosome (Latz E *et al.*, 2004b; Leifer C *et al.*, 2004). Ishii and colleagues reported the involvement of phosphatidylinositol 3 kinase [PI3]-kinases (PI3K) in the vesicular uptake of CpG DNA and its contribution with the endosomal maturation (Ishii K *et al.*, 2002). After CpG DNA internalisation, it will bind to TLR9 and upon their binding it will rapidly recruit and activate the adaptor molecule,

myeloid differentiation factor, MyD88 through their binding with Toll/IL-1 receptor (TIR) domains to trigger downstream signalling pathways (Wesche *et al.*, 1997; Hacker H *et al.*, 2000; Nejad A *et al.*, 2002; Latz E *et al.*, 2004b).

Subcellular mislocalisation of TLRs may cause dysregulation of the immune response. As a result, their ability to bind to the specific ligands would be affected by either lack of accessibility or over exposure to others.

1.4 TLR9 ligands:

TLR9 recognizes 2′-deoxyribo (cytidine-phosphate-guanosine) (CpG) dinucleotides that are not found in vertebrate DNA, but are present at relatively high frequency in bacterial DNA and many viruses, as they are not methylated at C5 of the cytosine base in bacteria and viruses (Krieg A *et al.*, 1995). In 1995, CpG DNA motif was described. Five years later, TLR9 was recognised as the targets of the CpG motif containing DNA. Genomic DNA of vertebrates contains highly methylated cytosine (~70-80%) of the CpG DNA, does not normally induce an immune response, possibly because they have reduced numbers of stimulatory CpG motifs (about five-fold from the expected frequency), are methylated, their uptake into immune cells is inefficient, and they contain a higher frequency of inhibitory DNA motifs (Krieg AM 2002b; Stacey K *et al.*, 2003). Native DNA has a phosphodiester backbone that can easily be degraded by nucleases. However, mammalian self-CpG DNA was found to activate TLR9 in some autoimmune diseases such as systemic lupus erythematosus (SLE) (Yung RL *et al.*, 1995; Richardson B, 2003; Viglianti GA *et al.*, 2003). In 2000, Akira's group reported the signal transducing receptor for CpG DNA to be the TLR9 glycoprotein (Hemmi H *et al.*, 2000). Bacterial/Viral CpG DNA has been described and characterized for the presence of unmethylated deoxycytidyl-deoxyguanosine dinucleotide CpG DNA and its activation via TLR9, but it was expensive and difficult to produce.

1.5 CpG-Oligodeoxydinucleotide (ODN):

In order to make stable TLR9 agonists, scientists made synthetic, single stranded hypomethylated oligodeoxynucleotides (CpG-ODN) that have a nuclease-resistant phosphorothioate (PS) backbone (Humans: GTCGTT; Mice: GACGTT) (Figure 1.6). The synthetic CpG-ODNs are mostly of 18 to 25 nucleotides and frequently contain more than one CpG motif. Studies done on CpG DNA showed its stimulatory effect on

B-cells, natural killer cells, dendritic cells and monocytes/macrophages in mice. This effect was the same with the synthetic ODN form, but it was found to depend to a great degree on the precise bases flanking the CpG dinucleotide, ODN backbone and the number of CpG motifs (Krieg AM 1999).

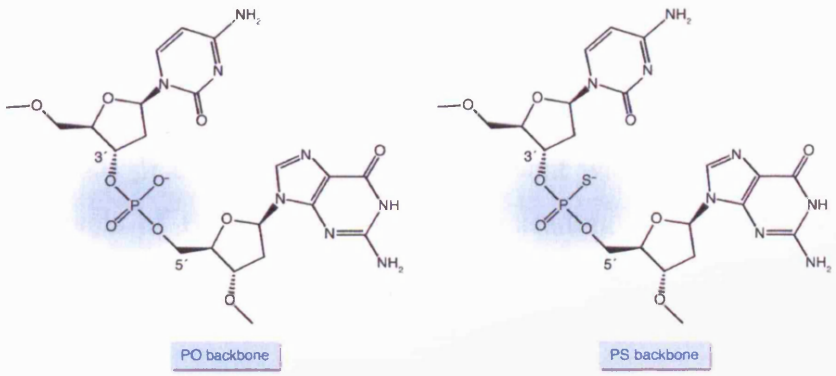

Figure 1.6. Backbones of native phosphodiester (PO) (CpG DNA) and modified PS DNA (CpG-ODN) (Krieg, AM 2007).

The immunostimulatory effects of synthetic CpG-ODN products encouraged scientists to develop TLR9 agonist motifs that can be used for the treatment of cancer, infectious diseases, asthma and allergies. In this context, several studies have been done using the CpG-ODN as an immunotherapeutic agent that promotes T_H1- T-cell immune responses and prominent release of IFN-γ, IL-12, and IL-18 (Klinman D *et al.*, 1996; Vollmer J 2005).

1.5.1 Types of CpG-ODN:

Several reports have categorized CpG-containing immunostimulatory ODNs into two major groups that are distinguishable based on their ability to provoke the unique cellular response and their distinct activity on plasmacytoid dendritic cells (Krieg AM 2002b). The two major groups differ in the nucleotide backbone composition and have specific sequence variations which are the main reasons for their functional variances. The first one is known as CpG-A ODN and was identified by A. Krieg (Wellesley, MA, USA), G. Hartmann (Munich, Germany) and colleagues; they are also termed as CpG-D ODNs by D. Klinman (Bethesda, MD, USA) and colleagues. This class contains mixed phosphodiester–phosphorothioate backbones and a single hexameric purine–pyrimidine–CG–purine–pyrimidine motif, capped at each end by a phosphorothioate poly G tail (Verthelyi D *et al.*, 2001). It was found to induce weak

activation of B-cells, but strongly induced IFN-α by pDC in addition to high level induction of natural killer cell activation (Krug *et al.*, 2001; Krieg AM 2001; Verthelyi *et al.*, 2001).

The second class was termed by Krieg, Hartmann and colleagues as CpG-B ODNs (Hartmann G and Krieg AM 2000) and by Klinman and colleagues as CpG-K ODNs (Klinman D *et al.*, 1996). Active CpG-ODNs type B are composed of multiple TCGTT and/or TCGTA motifs on a phosphorothioate backbone (Hartmann G *et al.*, 2000; Liang H *et al.*, 2000). It is a very potent T_H2 adjuvant with anti-tumour activity. It stimulates high levels of B-lymphocyte activation leading to cellular proliferation, secretion of cytokines and IgM, and induces monocytes/dendritic cells to produce the proinflammatory cytokine IL-6, but they showed low levels of expression of IFN-α (Krieg AM 2001; Verthelyi *et al.*, 2001; Gursel M *et al.*, 2002).

Additional differences were described in the *in vitro* effects of CpG-A and CpG-B ODNs on human immune cells. CpG-B ODNs act on pDCs to promote TNF-α and IL-8 secretion, increased survival and maturation (defined by upregulation of CD80, CD86 and MHC II), but low and transient secretion of type I interferon (IFN-γ) (Kerkmann M *et al.*, 2003). Whereas, CpG-ODN type A was found to trigger limited pDC maturation, but sustained high level of IFN-α/β which in turn mediates DCs maturation (Krug *et al.*, 2001; Kerkmann M *et al.*, 2003). This type of CpG-ODN, also, was not able to stimulate B cells directly (Krug *et al.*, 2001). Furthermore, the response of monocytes to these two types of ODNs was particularly informative. CpG-ODN type-B triggers monocytes to proliferate and secrete IL-6, whereas CpG-ODN type-A stimulated them to differentiate into dendritic antigen-presenting cells (APCs). When both types are mixed, a cross inhibition occurred by inhibiting another's effects on monocytes (Gürsel M *et al.*, 2002). Cells from TLR9-deficient mice and Hek293 human embryonic kidney tumour cells expressed a nonresponsive phenotype to CpG-DNA type-B (Bauer S *et al.*, 2001).

In 2003, Marshall JD and colleagues identified a third class of CpG-ODN, named as CpG-ODN type-C, that contains a complete phosphorothioate backbone and a CpG containing palindromic motif. This ODN effectively stimulated B cells to proliferate, secrete cytokines, express costimulatory antigens and induced strong IFN-α production. In addition, it specifically activated pDCs to undergo maturation and

secrete cytokines, including very high levels of IFN-α (Marshall JD *et al.*, 2003). CpG-ODN type-C has a combined feature of both types A and B. Table 1.1 summarise the three different CpG-ODN classes identified (Class A, Class B and Class C). It shows an example and its sequence for each class, structural features and immune effects as described by Krieg AM (2007).

Classes of CpG ODN

ODN class	Example ODN	Structural features	Immune effects
A-class (for IFN-α inducing; also called D-type)	GGgggacgatcgtcgGGGGG (also known as ODN 2216)	Poly G region at the 3′ and/or 5′ ends; usually with a few PS-modified internucleotide linkages at the 5′ and 3′ ends for nuclease resistance, but the center portion of the ODN with the CpG motif(s) must be PO	Induces exceptionally strong pDC IFN-α secretion and moderate expression of costimulatory molecules Induces very little B cell activation
B-class (for B cell–activating; also called K-type)	TCGTCGTTTTGTCGTTTTGTCGTT (also known as CPG 7909 and PF-3512676)	Fully PS-modified backbone, no major secondary structure; most important CpG motif for activating human TLR9 is at the 5′ end	Induces very strong B cell proliferation and differentiation Induces pDC expression of costimulatory molecules and modest IFN-α secretion
C-class (for combined activities)	TCGTCGTTTTCGGCGCGCGCCG (also known as ODN 2395)	Fully PS-modified backbone, 1 or more 5′ CpG motifs; self-complementary palindrome in middle or 3′ end enables formation of duplex or hairpin secondary structure	Induces strong B cell proliferation and differentiation Induces pDC IFN-α secretion and expression of costimulatory molecule

Capital letters in ODN sequences indicate 3′ PS internucleotide linkage; lower-case letters in ODN sequences indicate 3′ PO internucleotide linkage; underlining indicates self-complementary palindromes; bold letters indicate CpG motifs thought to contribute the most to immune stimulation. PO, phosphodiester.

Table 1.1.Different classes of CpG ODN. (Krieg AM. 2007).

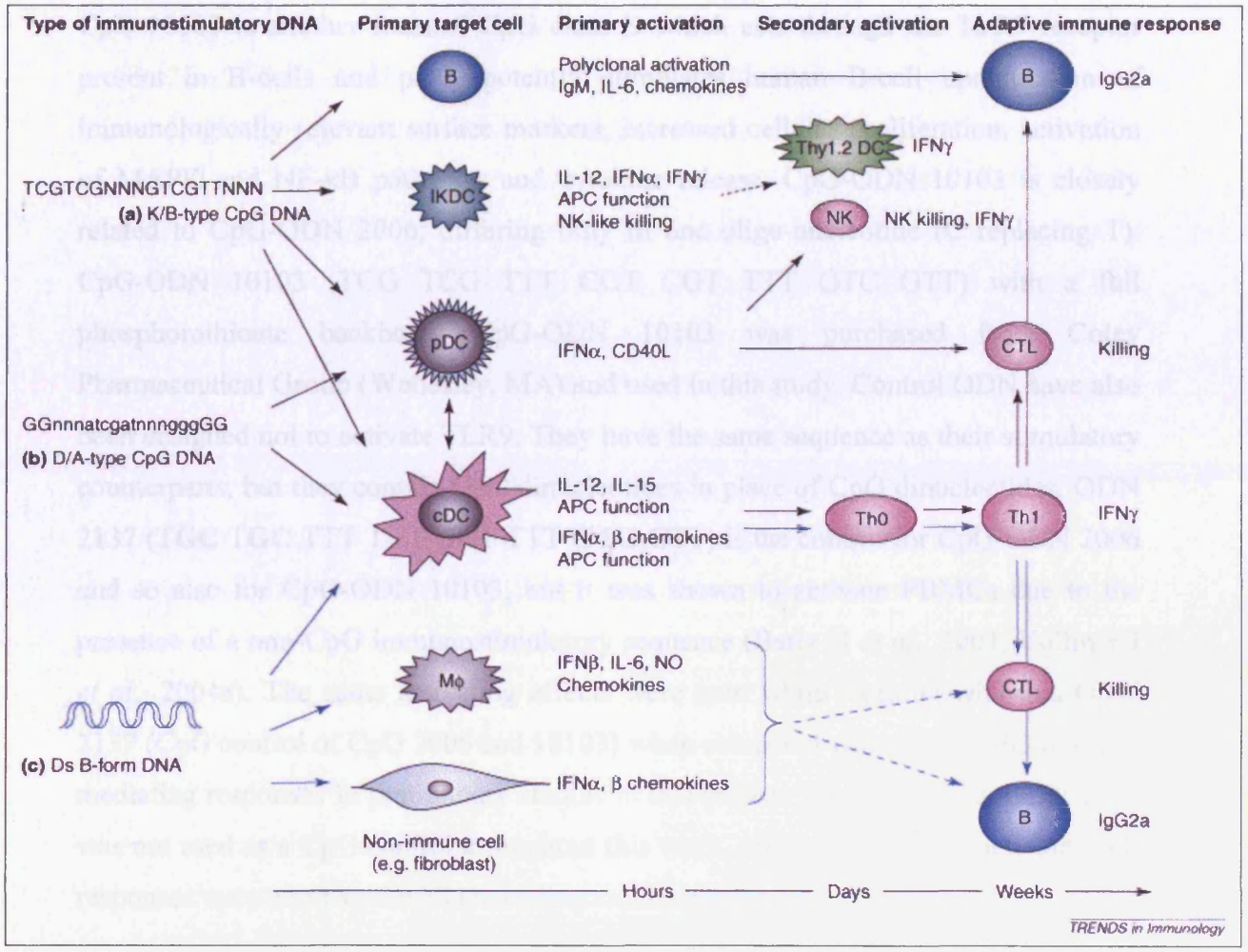

Figure 1.7. Innate and adaptive immune regulation by the different types of CpG oligodeoxynucleotides (ODNs). (Ishii K *et al.*, 2006).

Figure 1.7 illustrates the differential activity induced by the three types of CpG-ODNs. It shows both types A and B stimulating pDC to produce type I IFNs, while CpG-ODN type-B, but not type-A activating B cells to proliferate and produce cytokines and immunoglobulins. Type-C activates both cell types (pDC and B-cells), but to a lesser extent than type A or type B alone (Ishii K *et al.*, 2006).

As a conclusion, working with B-lymphocytes requires CpG-ODN type-B for the best activation. The type-B, CpG motif 2006 (5'- TCG TCG TTT **T**GT CGT TTT GTC GTT -3' (24 mer)) oligo-nucleotide was identified and developed (Hartmann G. and Krieg AM. 2000). 2006 CpG-ODN is the most popular type-B product to have the significant stimulatory response, and hence has been used in the majority of studies to activate human B–cells (Jahrsdorfer B *et al.*, 2005, Vollmer J *et al.*, 2004a, Krieg AM 2002a; Krieg AM 2002b; Latz E *et al.*, 2004a).

CpG 10103 is another form of CpG class B which acts through the TLR9 receptor present in B-cells and pDC, potently stimulates human B-cell upregulation of immunologically relevant surface markers, increased cellular proliferation, activation of MAPK and NF-κB pathways and cytokine release. CpG-ODN 10103 is closely related to CpG-ODN 2006, differing only in one oligo-nucleotide (C replacing T). CpG-ODN 10103 (TCG TCG TTT **C**GT CGT TTT GTC GTT) with a full phosphorothioate backbone, CpG-ODN 10103 was purchased from Coley Pharmaceutical Group (Wellesley, MA) and used in this study. Control ODN have also been designed not to activate TLR9. They have the same sequence as their stimulatory counterparts, but they contain GpC dinucleotides in place of CpG dinucleotides. ODN 2137 (T**GC** T**GC** TTT TGT **GC**T TTT **GTG C**TT) is the control for CpG-ODN 2006 and so also for CpG-ODN 10103, but it was shown to activate PBMCs due to the presence of a non-CpG immunostimulatory sequence (Bartz H *et al.*, 2004; Vollmer J *et al.*, 2004a). The same activating effects were seen while working with this ODN 2137 (CpG control of CpG 2006 and 10103) when compared with CpG 10103 immune mediating responses in preliminary studies in this project. For this reason, ODN 2137 was not used as a CpG control throughout this work, and the CpG-ODN activated cell responses were compared with the resting cell responses.

1.5.2 Specific cellular responses to CpG-ODN:

1.5.2.1 TLR9 dependent responses:

Most types of immune cells do not express TLR9 and they have been found not to be activated by TLR9 agonist, CpG-ODN. Cellular responses to bacterial DNA and synthetic oligodeoxynucleotide containing unmethylated CpG-dinucleotides (CpG-ODN) were found to be directly related to activation of TLR9 expressed in those immune cells. In humans, TLR9 expression is thought to be functional in resting B lymphocytes and pDCs. TLR9 expression was found in other non-resting cells such as activated neutrophils (Hayashi F *et al.*, 2003), some natural killer cells (Roda J *et al.*, 2005) and in a low level in pulmonary epithelial cells (Platz J *et al.*, 2004) in addition to other non-immune cells. As the level of the expressed TLR9 was variable on those cells, CpG-ODN mediated responses were variable too. In some cells, CpG-ODN required the presence of other factors to stimulate its activation. In neutrophils, the response to CpG-ODN required Granulocyte-Macrophage Colony-Stimulating Factor (GM-CSF) pretreatment (Hayashi F *et al.*, 2003). Moreover, IFN-γ treatment

significantly increased both TLR9 mRNA expression and CpG DNA responsiveness of human PBMC (Takeshita F *et al.*, 2001). In contrast, the low expression level of TLR9 mRNA in pulmonary epithelial cells seems not to be significantly regulated by IFN-γ (Platz J *et al.*, 2004). Moreover, NK cells express low levels of TLR9 mRNA (Hournung V *et al.*, 2002) and respond to CpG-ODN activation, but their response to produce IFN-γ after CpG-ODN activation was negligible. However, CpG-ODN mediated IFN-γ production in NK cells was enhanced in the presence of Ab-coated tumour cells (Roda J *et al.*, 2005). In conclusion, CpG-ODN mediated response is dependent on the presence and level of TLR9 expression. Indeed, this supports the CpG-ODN non-responsiveness in TLR9 negative cells whereas, in TLR9 negative cells transfected with human TLR9 gene, CpG-ODN responsiveness was reconstituted (Bauer S *et al.*, 2001; Takeshita F *et al.*, 2001; Chuang T *et al.*, 2002).

TLR9-mediated B-cell activation:

CpG-ODN mediates responses that vary depending on cell type. In general, the activation of TLR9 expressing cells with CpG-ODN enhanced the secretion of some cytokines such as interleukin-1β (IL-1β), IL-6, IL-12, IL- 18, TNF-α, IFN-α, and IFN-γ that promote acquired immunity (Klinman D *et al.*, 1996; Yi A *et al.*, 1996; Kamstrup S *et al.*, 2001). CpG-ODN/TLR9 activation of B cells enhances immunoglobulin production (IgM), and the expression of costimulatory molecules (CD80 and CD86) and molecules involved in B-cell/T-cell interaction expressed on B-lymphocytes (MHC class II and CD54). Furthermore, CpG-ODN activated B-cells become resistant to apoptosis by increasing their cellular proliferation (Krieg A *et al.*, 1995; Klinman D *et al.*, 1996; Decker T *et al.*, 2000a; Decker T *et al.*, 2000b; Hartmann, G *et al.*, 2000; Jahrsdorfer B *et al.*, 2001; Verthelyi *et al.*, 2001; Henault M *et al.*, 2005).

CpG-ODN/TLR9 activation in B cells triggers the induction of T_H2-like pattern of cytokines such as IL-6, IL-10 and TNF-α which are known to have direct or indirect anti-tumor effects (Klinman D *et al.*, 1996; Henault M *et al.*, 2005). Figure 1.8 illustrates some of the CpG DNA induced immune responses in the different cells expressing TLR9. In B-cells it shows the enhancing effect of CpG DNA to induce cellular proliferation, surface marker upregulation, immunoglobulin production and T_H2-like cytokines release. Whereas, NK cells,

monocytes/macrophages and DCs activation enhances T_H1 and T_H2-like cytokine secretion, in addition to surface marker upregulation (Krieg AM 2001).

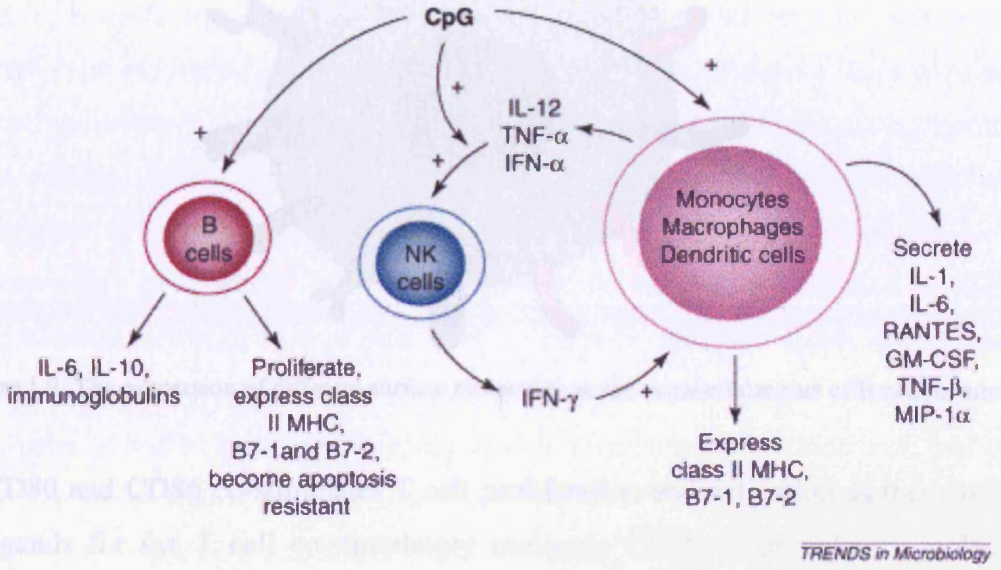

Figure 1.8. CpG DNA-induced immune responses on B cells, natural killer (NK) cells and monocytes, macrophages and dendritic cells. CpG DNA activation induces cellular proliferation, surface marker upregulation, immunoglobulin and cytokine/chemokine release in the different immune cells. (Krieg.AM 2001).

A variety of cellular receptors and antigens are involved in the regulation of the immune response. On the extracellular part of the B cell membrane, there are surface marker proteins that play a vital role in the growth and differentiation of B cells. Figure 1.9 shows some of the surface molecules expressed on the surface of B cells, including the adhesion molecules CD54, costimulatory molecules CD80 and CD86 and other surface molecules such as MHC II and CD40. CpG-ODN/TLR9 in B-cells render the cells more immunogenic and undergoing normal cell maturation and differentiation (Decker T *et al.*, 2000a; Decker T *et al.*, 2000b; Hartmann G *et al.*, 2000; Jahrsdörfer B *et al.*, 2001).

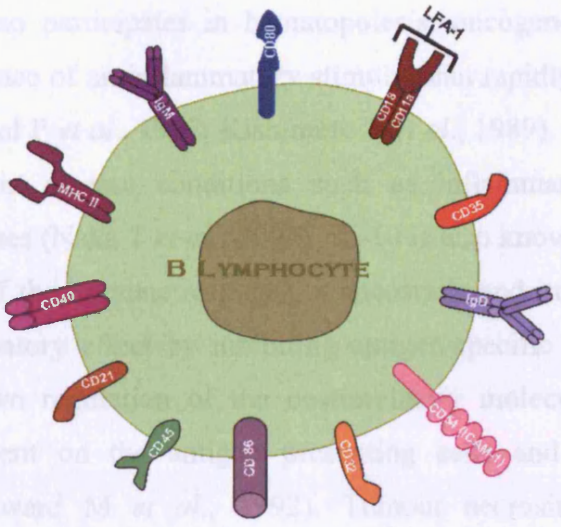

Figure 1.9. The expression of different surface molecules on the extracellular part of B cell membrane.

CD80 and CD86 co-stimulates T cell proliferation and activation as they work as ligands for the T cell co-stimulatory molecule CD28. Costimulatory molecules CD80 and CD86 interact with CD28 on T lymphocytes inducing the synthesis of IL-2 that is necessary for the optimal activation of T lymphocytes and preventing T-cell death.

Cell surface intercellular adhesion molecule 1 (ICAM-1; CD54) is expressed at low levels on resting lymphocytes, and upon cell stimulation, CD54 expression increases, and participates as an adhesion molecule as well as costimulatory molecule to enhance T-cell activation. In normal B cells, it mediates homotypic adhesion while in tumour cells, it is expressed in high levels and it is closely related to the degree of cell maturation (Boyd AW *et al.*, 1989 and Terol MJ *et al.*, 2003). MHC class II is required for antigen presentation to $CD4^+$ helper T cells. Cytokines released from CpG-ODN activated cells can modulate the adaptive immune response to diminish pathogens and tumour cells.

When B cell receptor is simultaneously engaged, CpG-induced B cell proliferation is greatly induced (Tasker L *et al.*, 2003). Optimal CpG-ODN type-B is a strong mitogen for B cells, enhancing them to enter the G1 phase of cell cycle and within few hours to secrete of IL-6 and IL-10. CpG-ODN induced IL-6 expression is needed to enhance IgM secretion by B cells, whereas CpG-ODN induced IL-10 release enhances IgA secretion, but it is a negative-regulator for the amount and duration of IL-12 secretion. IL-6 is a multifunctional regulator of immune

responses. It also participates in hematopoiesis, oncogenesis and inflammation where the presence of an inflammatory stimulus can rapidly induce its production in B-cells (Sehgal P *et al.*, 1987; Kishimoto T *et al.*, 1989). Its pathologic role was seen in different disease conditions such as inflammatory autoimmune and malignant diseases (Naka T *et al.*, 2002). IL-10 is also known for its importance in the regulation of the immune response, homeostasis and inflammation. It exhibits an anti-inflammatory effect by inhibiting antigen-specific T cell proliferation in addition to down regulation of the costimulatory molecules (involved in T_H1 responses) present on the antigen presenting cells and inhibition of TNF-α production (Howard M *et al.*, 1992). Tumour necrosis factor α is another proinflammatory cytokine, production of which is enhanced with CpG-ODN uptake. It has an important role in regulating inflammatory responses, cell cycle proliferation and apoptosis, in addition to which it has the ability to activate adhesion molecule expression, enhance leukocyte trafficking, and thus enhance inflammatory cell recruitment. TNF-α indirectly activates the Nuclear Factor-κB (NF-κB) by inducing IκB proteolysis through the phosphorylation of IκB by IκB kinase (IKK) (Han Y *et al.*, 1999).

Overall, CpG-ODN/TLR9 stimulates the innate immunity, and CpG-ODN induced cytokines have a role in modulating the adaptive immune response to remove some pathogens by polarizing $CD4^+$ T cells to either T_H1 or T_H2 phenotype (Krieg AM 2002a; Krieg AM 2002b) (Figure 1.10).

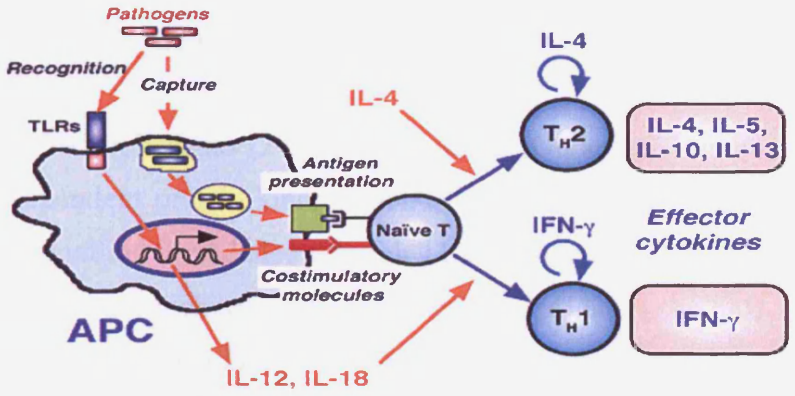

Figure 1.10. Regulatory effect of TLRs on T helper cell development and balance. The activation of TLRs leads to the production of cytokines and upregulation of surface markers that regulate the development and balance in the T_H cells inducing the release of effector cytokines. (Akira S. *et al.*, 2001).

1.5.2.2 TLR9 independent response:

In addition to its ability to stimulate B cells, dendritic cells and macrophages to induce an immune response via TLR9-dependent pathway, CpG DNA and synthetic CpG-ODN are capable of providing survival signals to the immune system in a TLR9-independent pathway (Park Y *et al.*, 2002). Park and colleagues (2002) stated that CpG-ODN is able to protect B cells and DCs from spontaneous apoptosis by activating NF-κB and AKT (a serine/threonine protein kinase that mediates various downstream effects of PI3K) without activating TLR9.

In 2000, Raz and colleagues (Chu W *et al.*, 2000) show that immunostimulatory CpG-DNA not only activates bone marrow–derived macrophages (BMDM) via TLR9, but it also directly triggers DNA-dependent protein kinase (DNA-PK) activation, a member of phosphatidlinositol 3 (PI3) kinase-like family, which can phosphorylate IκB-kinaseβ, leading to the activation of the transcription factor NFκB needed for the production of many inflammatory cytokine genes in BMDM. A few models were done to explain the connections between DNA-PK and TLR9, but no single one was favoured. Figure 1.11 illustrates Raz and colleagues' TLR9 dependent and TLR9 independent model, as described by Aderem A and Hume DA (2000), showing how both pathways would lead to the NFκB activation. This model showed a few weaknesses, showing the TLR9 pathway to be analogous to the TLR4 pathway. For that reason, Aderem and Hume suggested a second model (Figure 1.12). They have stated that DNA-PK can mediate the activation of CpG-ODN/TLR9 downstream signalling pathway in which each TLR9 and DNA-PK might activate NFκB signalling pathway separately.

However, Ishii and colleagues (2002) found that CpG-mediated immune activation was a DNA-dependent protein kinase (DNA-PK)–independent process in BMDM, and that CpG signalling is mediated through TLR9, but not DNA-PK, in three strains of DNA-PK KO mice which responded normally to CpG DNA. In 2005, Dragoi AM and colleagues reported that DNA-PKcs is an important intermediate in the CpG-DNA-triggered AKT signaling pathway, and it is not a downstream molecule of TLR9 in response to CpG-ODN activation. They detected the involvement of a DNA-PK which possibly activates AKT leading to the activation of IKK and NF-κB indicating that DNA-PK acts upstream of AKT upon CpG-ODN stimulation (Dragoi AM *et al.*, 2005). In contrast, Sester and colleagues (2006) stated that AKT

activation by CpG-ODN was completely dependent on TLR9 in BMDM, and was required for survival. They also indicated that, there is no evidence for TLR9-independent responses to CpG DNA in Akt activation. As a result, CpG-ODN activation is mostly TLR9-dependent, while studies are still trying to determine an independent pathway.

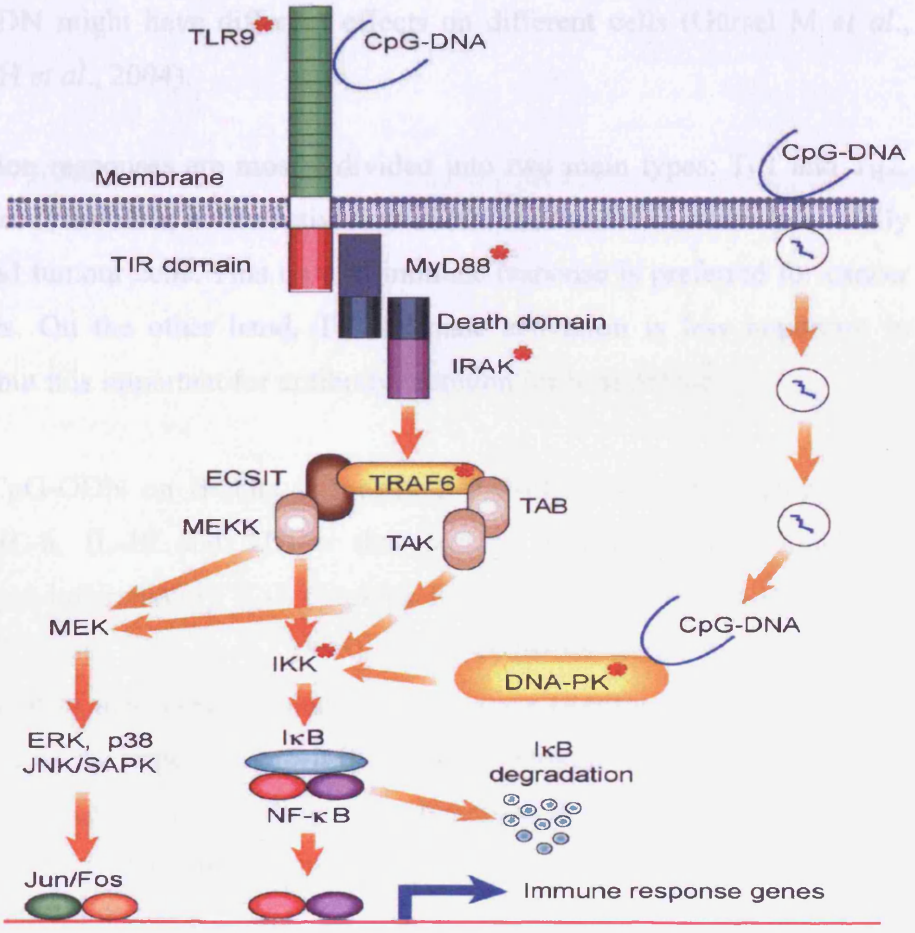

Figure 1.11. Involvement of CpG DNA in TLR9 and DNA-PK Signaling Pathways. (Aderem A and Hume DA, 2000).

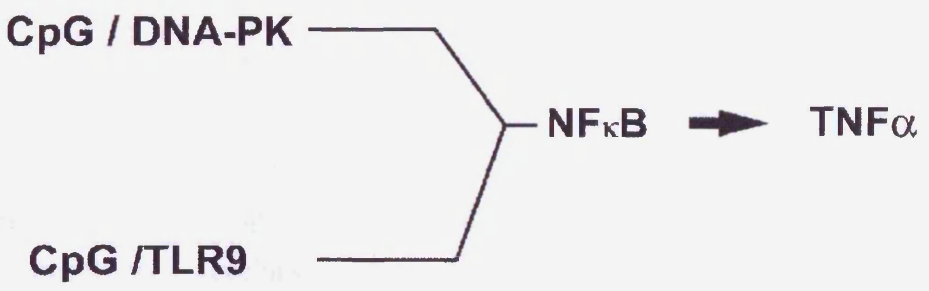

Figure 1.12. TLR9 and DNA-PK interaction proposed model by Aderem A and Hume D.A (2000).

1.5.3 Therapeutic uses of CpG-ODN:

CpG DNA and ODNs have the ability to trigger the immune response leading to host protection. Studies done on animals found that CpG-ODN might be of therapeutic use for allergic diseases, as vaccine adjuvants, and in cancer immunotherapy. Also, different types of CpG-ODN have distinct effects on the same cells, and even same type of CpG-ODN might have different effects on different cells (Gürsel M *et al.*, 2002; Dalpke AH *et al.*, 2004).

Immune activation responses are mostly divided into two main types: T_H1 and T_H2. The T_H1 response is involved in the activation of NK cells and CTLs that lyse virally infected cells and tumour cells. This type of immune response is preferred for cancer immunotherapies. On the other hand, T_H2 immune activation is less important in cancer therapy, but it is important for antibody secretion for host defence.

The effect of CpG-ODN on B-cells is mostly a T_H2-like response, leading to the production of IL-6, IL-10 and TNF-α that perform critical immunomodulatory functions. The pro-inflammatory IL-6 cytokine facilitates B and T cells growth and differentiation (Klinman DM *et al.*, 1996). IL-10 cytokines function as a counter-regulatory mechanism that down regulates T_H1 response (Redford TW *et al.*, 1998). Moreover, TNF-α is an important pro-inflammatory cytokine that has a role in the immediate host defence against invading microorganisms in addition to its role in the necrosis in some types of tumours, while it promotes cell growth in other types of tumour cells (Locksley RM *et al.*, 2001).

Different potential therapeutic uses for the immunomodulatory CpG-ODN have been reported in Klinman DM (2004). Four major immunotherapeutic applications for CpG-ODN were characterized. The first one is the ability of CpG-ODN to induce protective host immunity against infectious pathogens by stimulating the innate immune response. The second applicable use of CpG-ODNs is acting as a vaccine adjuvant, promoting the immunogenicity of the co-administreted antigens. This improves the function of antigen presenting cells (APC) that induces an adaptive immune response to the co-administered vaccines by the production of cytokine/chemokine milieu. CpG-ODNs have also been evaluated for their use in reducing allergic responses, by stimulating an antigen-specific T helper 1 (T_H1)-cell response, which would inhibit

T_H2 mediated asthma. Finally, CpG-ODN activation of the TLR9 signalling cascade results in the activation of natural killer (NK) cells and cytotoxic T lymphocytes (CTLs) that exhibits an anti-tumour effect, showing its immunotherapeutic uses for the treatment of different types of cancers. The four different applications of CpG-ODN are summarised in Figure 1.13.

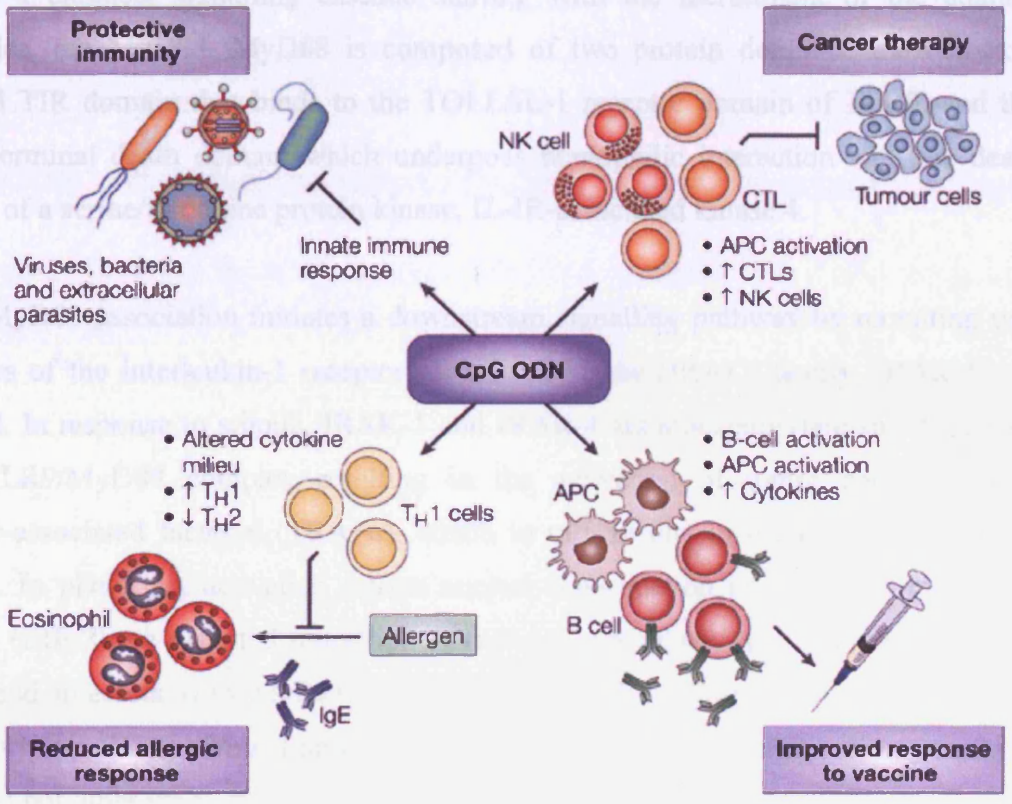

Figure 1.13. Potential therapeutic uses of CpG oligodeoxynucleotides (ODNs). CpG-ODN is potentially used in four main applications, to protect against pathogens, reduce allergic responses, improve response to vaccine and for the tumour therapy. (Klinman D 2004).

1.6 Signal transduction of CpG-ODN / TLR9 activation:

TLR9 signal transduction is similar to that for TLR7 and TLR8, but it is more specific and complex. Ahmad-Nejad P *et al.*, (2002) and Latz *et al.*, (2004a) reported that CpG-ODN signalling requires internalization of CpG-ODN to an endosomal compartment, which enhances the endosomal maturation (acidification) and CpG motif recognition via TLR9, which is delivered to the late endosome from the endoplasmic reticulum (ER). A recent study on mice reported that, a multi-transmembrane-domain-containing protein (UNC93B1) has an essential role in TLR9 trafficking from ER to the endosome, by

binding to the nucleotide-sensing TLR9 in the ER to deliver TLR9 to endosomes (Brinkmann MM *et al.*, 2007; Kim YM *et al.*, 2008). A phosphoinositide 3-kinase (PI 3-kinase), possibly class III vacuolar protein sorting 34 (VPS34), is needed for the endosomal fusion and plays an important role in the uptake of CpG-ODN and the activation process (Ishii KJ *et al.*, 2002; Kuo CC *et al.*, 2006). CpG-ODN/TLR9 binding induces a classical signalling cascade starting with the recruitment of the adaptor molecules, the MyD88. MyD88 is composed of two protein domains; the carboxy-terminal TIR domain that binds to the TOLL/IL-1 receptor domain of TLR9, and the amino-terminal death domain which undergoes homophilic interaction with the death domain of a serine/threonine protein kinase, IL-IR-associated kinase 4.

TLR9/MyD88 association initiates a downstream signalling pathway by recruiting two members of the interleukin-1 receptor associated kinase (IRAK) family, IRAK-1 and IRAK-4. In response to stimuli, IRAK-1 and IRAK-4 autophosphorylate and dissociate from TLR9/MyD88 complex resulting in the activation of tumor necrosis factor receptor-associated factor 6 (TRAF6), which in turn results in the oligomerization of TRAF6. In pDC, this activation causes nuclear translocation of interferon regulatory factor 7 (IRF-7), an essential transcription factor that regulates type I IFN induction in pDCs, and interacts with MyD88, IRAK-1 and TRAF-6. This binding activates and phosphorylates IRF-7 stimulating IFN-α promoters. IRF-7 is constitutively expressed in pDC, but not other types of cells (Kawai T *et al.*, 2004; Kawai T *et al.*, 2006).

TRAF6 oligomerization leads to the activation of two distinct signalling pathways; the mitogen-activated protein (MAP) kinase, and the activation of nuclear factor NF- κB pathways, resulting in the production of pro-inflammatory cytokines and chemokines (Akira S *et al.*, 2006). An ubiquitin-conjugating (Ubc) enzyme, Ubc13, forms a complex with TRAF6, which lead to the activation of Transforming Growth Factor-β (TGFβ)-activated kinase 1 (TAK1). Ubc13 and TAK1 are needed for CpG-ODN/TLR9 induced activation of NF-κB by IκB kinase (IKK) complex. They are also necessary for the induction of the activator protein-1 (AP-1) by the MAP kinase (Ishii KJ and Akira S 2006).

The nuclear factor-$_{K}$B (NF-$_{K}$B) pathway starts with the activation of TAK1 in the cytoplasm, leading to the activation of the inhibitor of NF-$_{K}$B kinase complex (IKKs).

IKK phosphorylates I_KB, leading to its proteolytic degradation that activates NF-κB transcription factor to translocate to the nucleus to induce the expression of its target genes, leading to the production of proinflammatory cytokines. NF-$_K$B transcription factor exhibits an anti-apoptotic activity through induction of death suppressing genes and it enhances cellular proliferation, where both functions play a critical role in oncogenesis and cancer therapy (Lin A *et al.*, 2003). In addition to the NF-κB-dependent signalling pathways controlled by these IKK complexes, CpG-ODN induced TAK1 activates the mitogen-activated protein (MAP) kinase pathways (Wesche *et al.*, 1997; Häcker H *et al.*, 2000; Ahmad- Nejad P *et al.*, 2002).

Three major MAPK pathways have been identified in response to TAK1 activation, leading to the activation of AP-1 complexes. The first one is the classical MAP kinases; extracellular signal-regulated kinase (MEK/ERK) regulates the cellular proliferation and differentiation. The second one is c-Jun N-terminal Kinase (JNK), known as stress-activated protein kinases (SAPK/JNK). Finally, $p38^{MAPK}$ pathway is involved in the regulation of several transcription factors such as ATF-2 (activating transcription factor 2) and Stat1 (signal transducer and activator of transcription 1). JNK and $p38^{MAPK}$ signalling pathways are responsive to stress stimuli and involved in cell differentiation and apoptosis (Häcker H *et al.*, 2000; Hemmi H *et al.*, 2000).

Figure 1.14 shows the proposed model for TLR9 signalling in B cells. Upon the uptake of CpG-ODN, TLR9 would directly bind to CpG-ODN and recruit MyD88 to form a large complex with multiple molecules, including IRAK4 and TRAF6. This can activate NF-κB (through IKK) and the MEK/ERK, JNK, and p38 MAPK pathways, leading to the activation of AP-1 complexes. When NF-κB and AP-1 proteins enter the nucleus, they would activate the target genes involved in B cell activation, proliferation, and immunoglobulin (Ig) production (Hacker H *et al.*, 2000; Hemmi H *et al.*, 2000; Kawai T *et al.*, 2007).

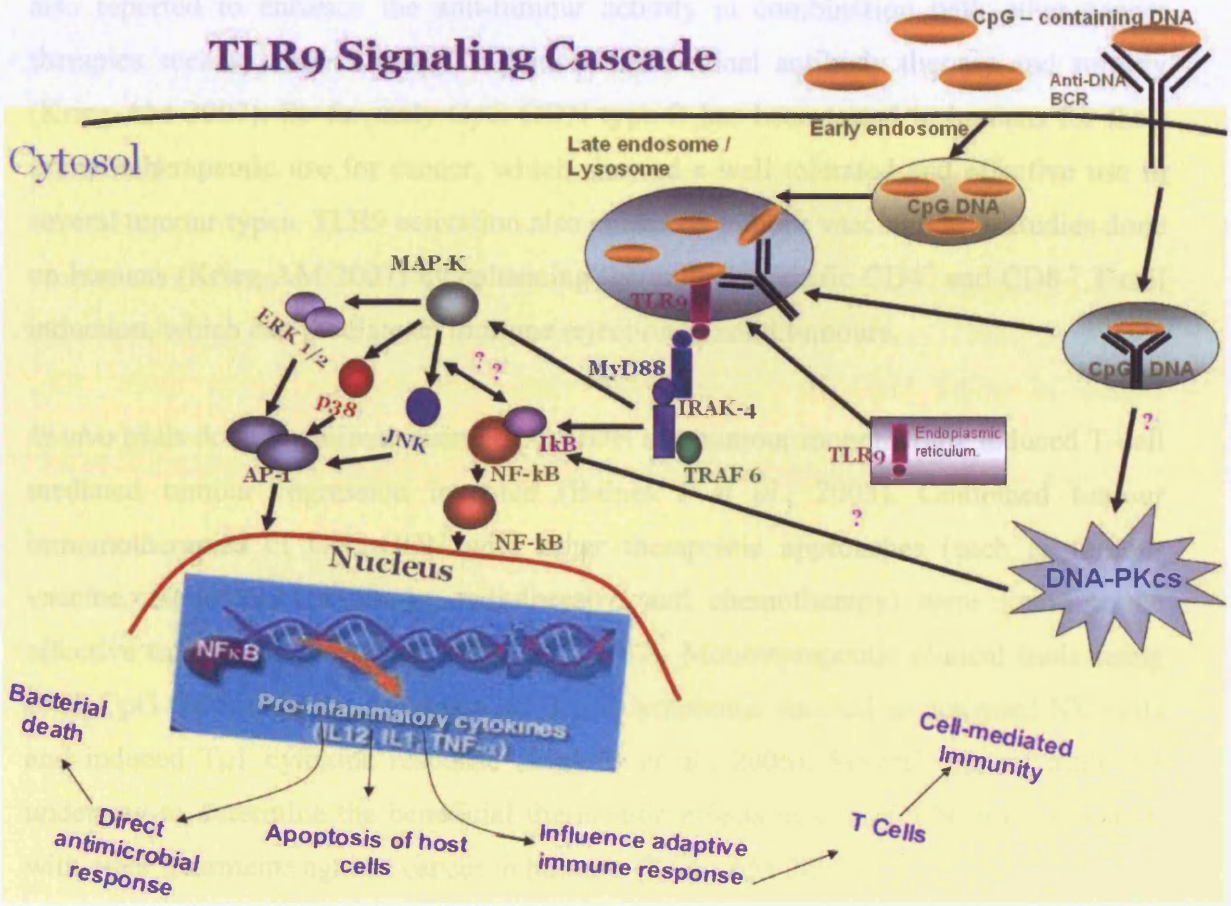

Figure 1.14. Proposed TLR9/CpG-ODN signalling pathway in B-cells. Once CpG-ODN internalization into the cell occurs, they will be exposed to TLR9 in endosomes translocated from the endoplasmic reticulum by a process controlled by type III PI 3-kinase. Direct binding of TLR9 to CpG-ODN recruits MyD88 to form a large complex with multiple molecules, including IRAK4 and TRAF6, to activate NF-κB (through IKK) which results from the phosphorylation of the IκB proteins that normally sequester NF-κB proteins in the cytoplasm. The TAK1 also activates the JNK and p38 MAPK pathways, leading to the activation of AP-1 complexes. Both the NF-κB and AP-1 proteins enter the nucleus where they activate target genes involved in B-cell activation, proliferation, and immunoglobulin (Ig) production. Abbreviations: AP-1, activating protein; BCR, B cell receptor; IκB, inhibitor of NF-κB; IKK, IκB kinase; IRAK, IL-1R-associated kinase; TAK1, TGF-β-activated kinase; and TRAF, TNF-receptor-associated factor 1.

1.7 Tumour immunotherapy and CpG-ODN:

Tumour immunotherapy depends on the stimulation of the immune response to induce a strong tumour specific response that can stop and/or kill existing tumour cells. CpG-ODN is known as efficient adjuvant to stimulate the induction of the tumour specific immune response (Krieg AM 2006; Weeranata RD *et al.*, 2006). The anti-tumour activity of CpG-ODN type-B has been applied in different ways. It can be used as a tumour monotherapy that might mediate NK cell or T cell activation. CpG-ODN was

also reported to enhance the anti-tumour activity in combination with other cancer therapies such as chemotherapy, radiation, monoclonal antibody therapy and surgery (Krieg AM 2007). So far, only CpG-ODN type-B has been tested in humans for their immunotherapeutic use for cancer, which showed a well tolerated and effective use in several tumour types. TLR9 activation also enhanced tumour vaccination in studies done on humans (Krieg AM 2007) by enhancing the antigen-specific $CD4^+$ and $CD8^+$ T cell induction, which can mediate an immune rejection of solid tumours.

In vivo trials done on animals using CpG-ODN as a tumour monotherapy induced T-cell mediated tumour regression in mice (Baines J *et al.*, 2003). Combined tumour immunotherapies of CpG-ODN with other therapeutic approaches (such as tumour vaccine, monoclonal antibody, radiotherapy, and chemotherapy) were found to be effective tumour-suppressants (Kreig AM 2007). Monotherapeutic clinical trials using 7909 CpG-ODN done on humans with B-cell lymphoma showed an activated NK cells and induced T_H1 cytokine response (Link B *et al.*, 2006). Several clinical trials are underway to determine the beneficial therapeutic effects of CpG-ODN in combination with other treatments against cancer in humans (Kreig AM 2007).

CpG-ODN induced response results from TLR9 activation and can promote tumour regression by directly activating the anti-tumour factors as IFN-α and TRAIL or indirect activation of NK cell-mediated tumour cell killing (Kreig AM 2006). Nevertheless, the full therapeutic benefits of the use of CpG-ODN type-B alone or in a combination with other therapeutic agents for the treatment of cancer remain to be determined. On the other hand, the effectiveness of the other CpG-ODN classes in cancer therapy needs more investigations.

1.8 Cancer cells and CpG-ODN / TLR9 activation:

Whilst the expression of TLR9 and its responsiveness towards CpG ODN activation in the immune system has been studied extensively, their effect on tumour cells has received relatively little attention. The expression of TLR9 was confirmed in a range of human cell malignancies showing the variable expression levels and pattern of effector functions (cellular proliferation, induction of cytokine synthesis and upregulation of costimulatory ligand molecules) which varied between different tumour cell types (Decker T *et al.*, 2000a; Decker T *et al.*, 2000b; Takeshita F *et al.*, 2001; Jahrsdorfer B

et al., 2001; Bourke E *et al.*, 2003; Henult M *et al.*, 2005; Jahrsdorfer B *et al.*, 2005; Wang H *et al.*, 2006).

Such findings raised a fundamental question about the relationship between TLR9 expression and function in response to CpG-ODN activation in different tumour cell types. Moreover, as CpG-ODN has been widely used as a therapeutic agent for tumour immunotherapy, it is therefore important to ascertain the effects of CpG ODN on tumour cells. This would also evaluate fully the potential of CpG ODN in cancer immunotherapy.

Cancer cells result from a single cell transformation resulting in unregulated cell proliferation. Neoplastic B cells are generated from normal B cells, blocking and altering any stage of B cell differentiation. The abnormalities that occur in the normal cells leading to malignancy are not restricted to immune cells, but also occur in non-immune cells such as epithelial tumours in the kidney, cervix, prostate, breast, lung and rectum epithelial cells, or other tissues of the body such as melanocytes.

1.8.1 CpG-ODN/TLR9 in B cell malignancies:

Depending on the various stages of B lymphocyte differentiation, several lymphoid neoplasms arise (Figure 1.15). Most B cell neoplasms are derived from mature naïve B cells, such as B-cell chronic lymphocytic leukemia (B-CLL), B-cell small lymphocytic lymphoma (SLL), and mantle cell lymphoma (MCL). Follicular lymphoma (FL) and diffuse large B-cell lymphoma (DLBCL) are derived from germinal centre B cells, whereas B cell acute lymphoblastic leukaemias (B-ALL) originate predominantly from precursor B-cells. Memory B cells can develop into marginal zone B-cell lymphoma (MZL) and B-CLL. Plasmacytoma is related to plasma cells, and when a clone of abnormal plasma cells multiplies in bone marrow a plasma cell cancer emerges producing multiple myeloma.

Knowing the stages of normal B cell differentiation is helpful in understanding for the biology of B-cell neoplasia. In Figure 1.15, altering one of the different stages of normal B cell differentiation and maturation develops certain type of lymphoma/leukaemia depending on its stage. Although malignant cells originate from their normal counterparts, they differ from their normal counterparts in a number of

respects. Malignant cells exhibit a low tendency to undergo apoptosis in response to normal signals (Lagneaux L *et al.*, 1998). They also have altered expressions of a variety of adhesion and costimulatory surface molecules, and lose the ability to function as an effective antigen-presenting cell (Chaperot L *et al.*, 1999).

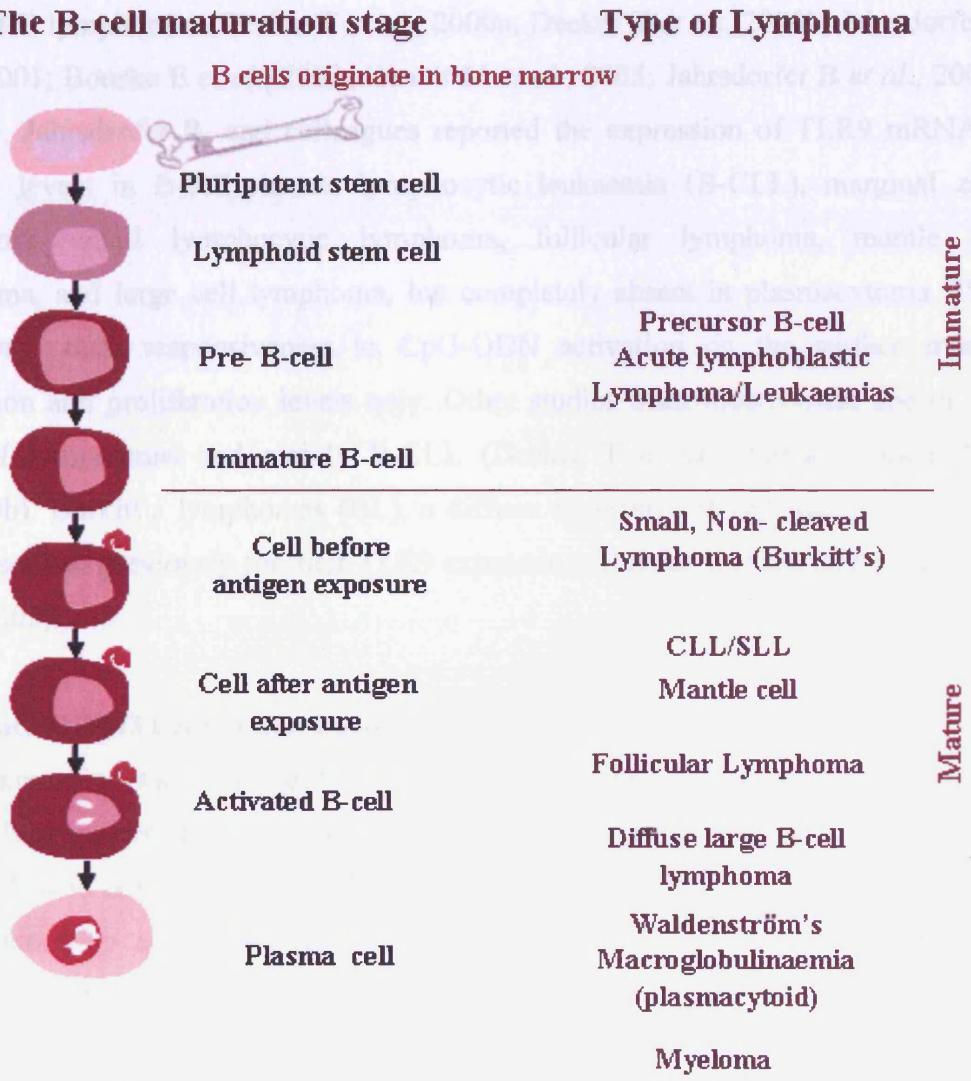

Figure 1.15. The maturation stage of the cell of origin determines the type of lymphoma.

As TLR9 expression is detected in normal B cells, in this work I will be focusing on malignancies of B cell origin. Normal B cells originate from stem cells in the bone marrow and they undergo a differentiation and maturation process. The mature B cells migrate to different parts of the body to perform their unique functions at each stage. Any changes in the development stages of B cell's differentiation and maturation, results in a specific kind of malignancy (Figure 1.15). Furthermore, most of B cell malignancies occur in the mature stage, such as Burkitt's lymphoma and mantle cell

lymphoma, but that does not mean it can not occur before maturation as in precursor B-lymphoblastic leukaemia/lymphoma (precursor B-cell ALL) (WHO classifications from Prakash S *et al.*, 2007).

Several studies reported the expression of TLR9 and responsiveness to CpG-ODN in different B lymphomas (Decker T *et al.*, 2000a; Decker T *et al.*, 2000b; Jahrsdorfer B *et al.*, 2001; Bourke E *et al.*, 2003; Henult M *et al.*, 2005; Jahrsdorfer B *et al.*, 2005). In 2005, Jahrsdrofer B. and colleagues reported the expression of TLR9 mRNA at variable levels in B-cell chronic lymphocytic leukaemia (B-CLL), marginal zone lymphoma, small lymphocytic lymphoma, follicular lymphoma, mantle cell lymphoma, and large cell lymphoma, but completely absent in plasmacytoma. They also tested their responsiveness to CpG-ODN activation on the surface marker expression and proliferation levels only. Other studies dealt mostly with one or two types of lymphomas and mainly B-CLL (Decker T *et al.*, 2000a; Decker T *et al.*,2000b). Burkitt's lymphomas (BL), a diffuse aggressive B cell malignancy, have been described previously for their TLR9 expression (Bourke E *et al.*, 2003; Henult M *et al.*, 2005).

1.8.2 CpG-ODN/TLR9 in non-haematological malignancies:

TLR9 expression was also found to be present in a variety of malignant solid tumours such as lung cancer, intestinal cancer, and tumours in spleen, while its expression was weak to low in non-malignant tissues (Takeshita F *et al.*, 2001; Wang H *et al.*, 2006). Also, Platz J *et al.*, (2004) reported a weak expression of the TLR9 in primary respiratory epithelial cells (Platz J *et al.*, 2004; Wang H *et al.*, 2006).

In preliminary experiments done in our laboratory by Hélia Esteves, University of Leicester, BSc. dissertation, a panel of cell lines derived from different ranges of non-haematological tumour cell lines, including epithelial cancers and melanomas, appeared to express TLR9 by intracellular monoclonal antibody staining and flow cytometry, but showed no response to culture in the presence of CpG-ODN. Such findings raised a fundamental question about the expression of TLR9 in non-haematological tumour cells and hence needed more investigations to determine their expression to TLR9.

1.9 Aims of the project:

The aims of this project were to address the relationship between TLR9 expression and response to CpG ODN in both haematological and non-haematological cancer cells. In this study, the expression of TLR9 was investigated in different types and/or stages of B cell malignancies and in solid tumour cells using flow cytometry, immunoprecipitation and western blotting, and confocal microscopy, while RT-PCR was used for the detection of TLR9 mRNA expression.

The expression of TLR9 was also studied in relation to its pattern of effector functions upon the activation with CpG-ODN. To investigate the cellular responses to CpG-ODN stimulation, I studied upregulation of immunologically relevant cell surface markers (CD54, CD80, CD86 and MHC class II), cellular proliferation, intracellular signalling (MEK/ERK, p38, AKT and NF-κB pathways) and induction of cytokine synthesis (TNF-α, IL-6 and IL-10).

Another aim was to investigate whether CpG-ODN has the ability to induce a refractory state in tumour B-lymphocytes that might develop when the cells are pre-exposed to a low dose of CpG-ODN, and to determine the duration and nature of such state. To achieve this purpose, cells were treated with a low dose of 10103 CpG-ODN for different time intervals and studied for their CpG-ODN induced immune responses upon their treatment with a subsequent activating dose of CpG-ODN.

Finally, to determine the molecular mechanisms that lead to the CpG-ODN mediated responses, I studied the involvement of the different signalling pathways in the activation of TLR9 by CpG-ODN, and used a panel of inhibitors specific for the different intracellular signalling pathways to evaluate the effects of these pathways on different functional responses to CpG-ODN. The downstream signalling activities of NF-κB, ERK 1/2, p38 and AKT pathways were investigated in Burkitt's lymphoma, BJAB, cells.

The studies outlined would provide valuable information on the response of TLR9 positive tumour cells, as opposed to cells of the immune system, to CpG-ODN as a potential immunotherapeutic agent. In addition, they should shed new light on the

mechanisms of action of CpG activation of TLR9 signalling in immune and non-immune cells.

Summary of aims:

- **TLR9 expression in haematological and non-haematological tumour cells.**
- **The relationship between TLR9 expression and CpG-ODN mediated responses in haematological and non-haematological tumour cells.**
- **The effect of low doses of CpG-ODN on subsequent TLR9/CpG-ODN mediated responses.**
- **The molecular mediated mechanisms of intracellular signalling induced by CpG-ODN activation in BJAB Burkitt's lymphoma B-Cells.**

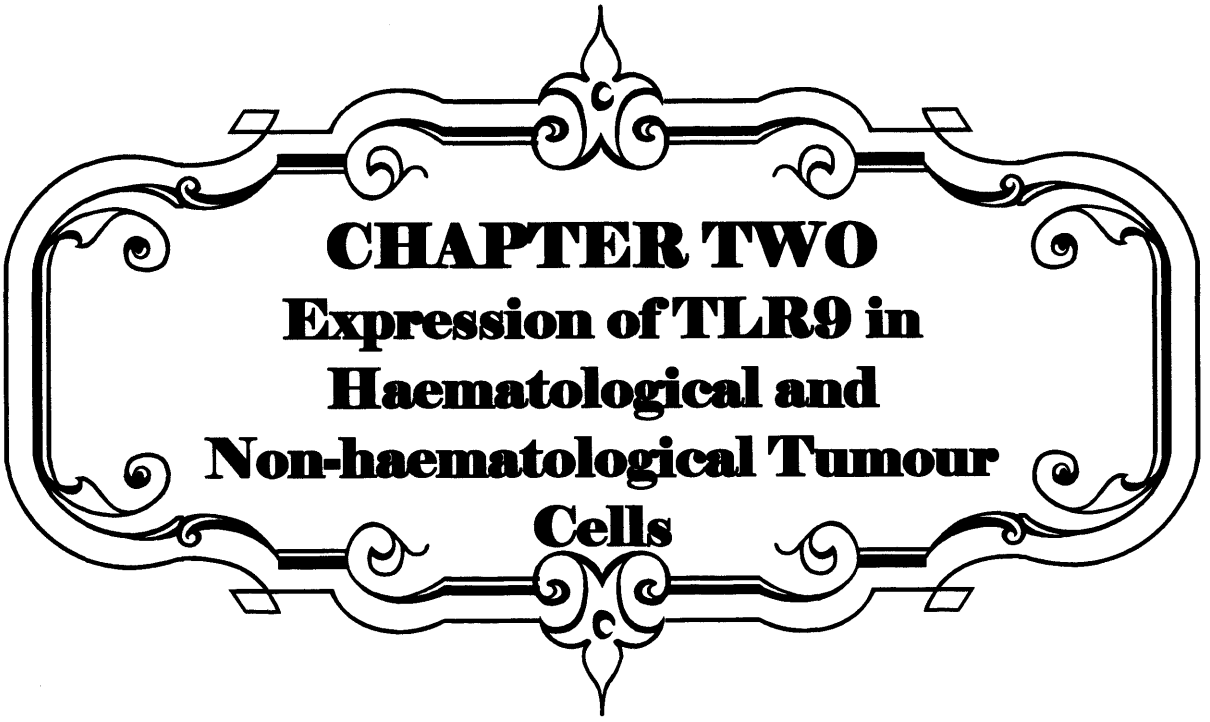

CHAPTER TWO

Expression of TLR9 in Haematological and Non-haematological Tumour Cells

CHAPTER TWO
Expression of TLR9 in haematological and non-haematological tumour cells

2.1 Introduction:

Among TLRs, TLR9 has been proposed as playing a significant role in the treatment of cancer, asthma, infectious diseases, and allergies (Vollmer J 2005). TLR9 specifically recognizes unmethylated deoxycytidyl deoxyguanosine dinucleotide (CpG) motifs, present at 20-fold higher frequency in bacterial or viral DNA than in mammalian DNA as they are suppressed and methylated in the mammalian DNA (Krieg AM *et al.*, 1995). This recognition leads to the stimulation of innate immune cells, by triggering the signalling pathways leading to the production of T_H1-like proinflammatory cytokines, interferons and chemokines (Krieg AM *et al.*, 1995).

Many studies have been done to determine the expression and localisation of TLR9 and its functional relation with CpG DNA activation to enhance the treatment of infectious diseases and cancer. In humans, TLR9 was found to be highly expressed in B-cells, plasmacytoid dendritic cells (pDC), natural killer (NK) cells and activated macrophages/monocytes (Hornung V *et al.*, 2002; Dasari P *et al.*, 2005; Vollmer J 2005; Hoene *et al.*, 2006), and these cell types were shown to be activated by CpG DNA, leading to upregulation of immunologically relevant surface markers, increased cellular proliferation, activating signalling pathways and cytokine release. Resting human B-cells express significant levels of TLR9, whereas its cellular localization remains controversial, but intracellular localisation is generally agreed. However, conflicting data were reported as to whether TLR9 was expressed at the cell surface in addition to the intracellular localisation. Some papers reported that the majority of human TLR9 is intracellularly expressed, and it could be surface accessible following CpG DNA activation (Latz E *et al.*, 2004a; Latz E *et al.*,2004b). In recent studies, TLR9 expression was detected by flow cytometry on the surface of B lymphocytes from whole blood and peripheral mononuclear cells (PBMCs), in B cells of severely injured patients prone to sepsis and in distinct populations of tonsillar B-cells (Eaton-Bassiri A *et al.*, 2004; Dasari P *et al.*, 2005; Baiyee EE *et al.*, 2006). Eaton-Bassiri *et al.*, (2004) reported that human PBMCs show approximately 10% of cells with TLR9 surface expression, while Latz E *et al.*, (2004b) failed to detect cell surface TLR9 expression in TLR9-transfected

Hek293 cells. In other cell transfection studies, non-permeablised Hek293 cells transfected with HA-TLR9 specifically bound FITC-anti-HA Ab, showing that at least a fraction of the TLR9 was on the cell surface of the transfected cell lines, but its location was not specified (Takeshita F *et al.*, 2001). Overall, these data indicate that TLR9 mainly expressed intracellularly, but can be detected on cell surface too.

Malignant B cells represent to a large extent, B cells blocked at various stages of differentiation. Human B-cell malignancies originate from different stages of B-cell differentiation. Jahrsdrofer B *et al.*, (2005) tested different types of non-Hodgkin's B-cell lymphoma and found significant differences in the expression of TLR9 and activation upon CpG stimulation. TLR9 expression was also found to be present in a variety of malignant solid tumours such as lung cancer, intestinal cancer, and tumours in spleen, while its expression was weak to low in non-malignant tissues (Takeshita F *et al.*, 2001). Also, Platz *et al.*, reported a weak expression of the TLR9 in primary respiratory epithelial cells (Platz J *et al.*, 2004).

Preliminary experiments done in our laboratory (Hélia Esteves, University of Leicester, BSc. Dissertation) tested a panel of cell lines derived from different haematological and non-haematological tumours for the expression of TLR9, using monoclonal antibody staining and flow cytometry. All the cell lines tested, including epithelial cancers and melanomas, showed positive (intracellular) staining with the TLR9 antibody, as compared with an isotype control Ab, following permeabilisation, suggesting intracellular TLR9 expression. No human cell lines were identified that did not apparently express TLR9, as detected by this method. Based on these results, I wanted to verify the extent of TLR9 expression in human haematological and non-haematological tumour cell lines, and identify its cellular localisation, if present. The aims of this chapter were, first to establish techniques to detect TLR9 expression by cells, using mAb staining and flow cytometry, immunoprecipitation and western blotting, confocal microscopy, and semi-quantitative reverse transcriptase qRT-PCR. Next, to determine the levels of TLR9 expression in a panel of B-cell lines and solid (non-haematological) tumour cell lines. Finally, to determine the localisation of TLR9 in tumour cells and in human cells transfected with TLR9.

2.2 Materials and Methods:

2.2.1 Antibodies:

The following antibodies were used:

2.2.1.1 Unconjugated antibodies

2.2.1.1.1 Toll like receptor (TLR) 9 antibodies

- Anti-TLR9 mAb (IMG-305A, IMGENEX, USA) monoclonal antibody raised against a KLH-conjugated synthetic peptide corresponding to amino acids 268-284 of human TLR9 isoform A.
- Anti-TLR9 (N-15) Sc-13215 goat polyclonal IgG with its epitope mapping near the N-terminus of the hTLR9 (Santa Cruz Biotechnologies, Santa Cruz, USA).
- Affinity purified anti-human TLR9 rat mAb (eB72-1665, eBioscience, USA) generated against amino acids 273-288 of human TLR9.

2.2.1.1.2 Isotype controls, other Antibodies and blocking peptides

- Anti-Haemagglutinin (HA) high affinity rat mAb-clone 3F10 (Roche Applied Sciences, UK).
- Affinity purified rat IgG2a isotype control (eB 12-4321, eBioscience, USA).
- Blocking peptides for polyclonal anti-human TLR9 (eB66-P929, eBioscience, USA).

2.2.1.2 Conjugated Antibodies

2.2.1.2.1 Toll like receptor (TLR) 9 Antibodies;

- Phycoerythrin (PE)-conjugated rat mAb anti-human TLR9 (eB72-1665, eBioscience, USA), generated against a portion of human toll-like receptor 9 (aa 273-288).
- Anti-TLR9-PE (IMG-305D, IMGENEX, USA) mAb raised against a KLH-conjugated synthetic peptide corresponding to amino acids 268-284 of human TLR9.

2.2.1.2.2 Isotype control, other antibodies and reagents.

- Anti-IgG1 (mouse)-PE isotype control (Beckman Coulter, UK).
- Anti-IgG1 (mouse)-FITC isotype control (Beckman Coulter, UK).
- Anti-Rat IgG2a-PE isotype control (eBioscience, USA).
- Anti-IgG1-PE isotype control (Immunotech, Marseille, France).
- Anti-CD20 -FITC (Beckman Coulter, UK).
- Peroxidase-labelled anti-mouse IgG (Amersham Biosciences, Little Chalfont, UK).
- Polyclonal rabbit anti-rat IgG-HRP (DAKO, A/S, Denmark).
- Rabbit IgG TrueBlot™: HRP anti-rabbit IgG (eBioscience, USA).
- Swine anti-rabbit immunoglobulins/ horseradish peroxidase (HRP) (DAKO, A/S, Denmark).
- HRP-conjugated anti-mouse Ig (Amersham Biosciences, Little Chalfont, UK).
- HRP-conjugated anti β-actin antibodies (Santa Cruz Biotechnologies, Santa Cruz, USA)
- Anti-HA peroxidase high affinity rat mAb-clone 3F10 (Roche Applied Sciences, UK).
- Goat polyclonal to rat IgG H&L FITC Abs (Abcam , UK)
- NBD C_6–ceramide complexed to BSA (Invitrogen, UK).

2.2.2 Cell culture, cells and cell lines

2.2.2.1 Human peripheral blood mononuclear cells.

Human peripheral blood mononuclear cells (PBMCs) were isolated from heparinized (Heparin sodium - 10 I.U/ml final concentration; Sigma-Aldrich, UK) blood of healthy adult donors. 25ml of 1:1 diluted blood in growth medium RPMI-1640 supplemented with 10% Foetal Bovine Serum (FBS), streptomycin (100μg/ml), pencillin (100U/ml), and 2mM L-glutamine (all from Sigma-Aldrich, UK) were added slowly over 15ml of Lymphoprep ™ (Nycomed Diagnostics, Oslo, Norway). Centrifugation with a speed of 1480rpm/20minutes at room temperature (RT) was done, with the brake off. Cells were isolated from the buffy layers and washed with RPMI-1640 medium. Cell pellets collected after centrifugation at 1480rpm for 5 minutes at RT were counted and suspended with growth medium.

2.2.2.2 $CD19^+$ B-cell separation.

$CD19^+$ B cells were positively selected and separated from PBMCs isolated from 50 ml heparinized blood of healthy adult donors (see 2.2.2.1) using 20µl of $CD19^+$ Microbeads magnetic cell sorter (MACS) per $1x10^7$total cells (MACS; Miltenyi Biotech, Bisley, UK). CD19 Microbeads are used for direct magnetic labelling of $CD19^+$ B cells. The LS^+/VS^+ separation MACS Columns (MACS, Miltenyi Biotech, Bisley, UK) were placed in a MiniMACS separator– a strong permanent magnet – then the MACS Column matrix would provide a magnetic field strong enough to retain cells labelled with minimal amounts of CD19 Microbeads. MiniMax washing buffer (filtered 0.5% bovine serum albumin in phosphate buffer saline – PBS, pH 7.2) was used to wash the columns, allowing cells not labelled with $CD19^+$ beads to be washed from the columns. The columns were released from the magnetic field and $CD19^+$ B-cells were eluted and kept in growth medium. $CD19^+$ B-cells were tested for purity by flow cytometry using anti-CD20 FITC (Beckman Coulter, UK) and it was routinely greater than 95% positive.

2.2.2.3 Tumour cells and cell lines used in this study.

Cells and cell lines illustrated in Table 1.1 were cultured in growth medium (RPMI-1640) supplemented with 10% Foetal Bovine Serum (FBS), streptomycin (100µg/ml), penicillin (100U/ml), and 2mM L-glutamine (all from Sigma-Aldrich, UK), at 5% CO_2, in a humid environment at 37°C. Human embryonal kidney cell lines, Hek293, were cultured in Iscove's Modified Dulbecco's Medium (Sigma-Aldrich) supplemented as above. Cells were split twice weekly into fresh growth medium.

Cell Types	Cell lines	Description		Stage of differentiation
B-cells	*CD19+*	*Ex vivo* cells	Normal B-cells	Mature B-cell
Haematological tumour cells	*KR076*		Tumour CLL	Mature B-cell
	FC029		Mantle cell lymphoma	Mantle cell
	TH044			
	JVM-2	Cell lines		
	HMy-2		EBV transformed B lymphoblastoid cell	Activated B-cell
	RAMOS		Burkitt's Lymphoma	Mature B cell
	RAJI			
	BJAB			
	ELIJAH			
	U266		Multiple Myeloma	Plasma cell
	Karpas 707H			
	RPMI 8226			Lymphoblast like-Plasma cell
	TANOUE		Precursor B-ALL	Acute lymphoblastic leukaemia
	380			Lymphoblast (immature B-cell)
	LiLa			
	KG-1		Acute myeloid leukaemia	Myelogenous blast
	HL-60		Promyelocytic Leukemia	Promyelocyte
Non-Haematological tumour cells	*Hek293*	Cell lines	Human embryonal kidney	Kidney epithelium
	HeLa		Human cervical carcinoma	Cervical epithelial cell
	Du-145		prostate carcinoma	Prostatic epithelial cell
	HRT-18		Rectum-anus, adenocarcinoma	Rectum epithelial cell
	WM1361A		Melanoma	Melanocyte
	CORL-47		Small cell lung cancer	Small cell of the airway epithelium
	MCF-7		Breast cancer adenocarcinoma	Breast epithelial cell

Table 2.1. Characteristics of the *ex vivo* cells and cell lines used in the different protocols in this study.

2.2.2.4 Transfection of Hek293 and HeLa tumour cells with TLR9.

Human embryonal kidney cell line Hek293 (kindly provided by Dr. Sek Chow, University of Leicester, UK) and the cervical carcinoma cell line HeLa were transfected with two hTLR9-containing plasmid constructs and with their empty plasmids as a control. Cells were plated in six-well plates (Nunclon™ Surface, Nunc products, UK) at 5 x 10^5 cells/well and stable transfection (with indicated cDNAs) was done on the following day using Effectene Transfection Reagent (Qiagen, UK) according to the manufacturer's instructions. The cells were transfected separately for 24 hours at 37°C and 5% CO_2 with 0.4 µg/well of the full-length linear human TLR9 vector plasmids either conjugated to haemagglutinin (pDisplay-HA/hTLR9) or unconjugated (pCIneo-hTLR9). Another 0.4µg/well of empty vector pDisplay and pCIneo were used as a mock transfection control. Figures 2.1 and 2.2 illustrate the empty plasmids used for the transfection. The four expression plasmids were a kind gift from Cynthia A. Leifer, USA. The plasmid constructs were prepared from human TLR9 cDNA which was inserted into pCIneo (Promega, Madison, WI). TLR9 cDNA (26–1032), lacking its leader sequence, but keeping its stop codon, was cloned into pDisplay (Invitrogen Life Technologies, UK), to generate a HA-tagged TLR9 (Takeshita *et al.*, 2001). All TLR9 gene constructs had been shown to activate NF-κB when stimulated with CpG (Leifer CA *et al.*, 2004).

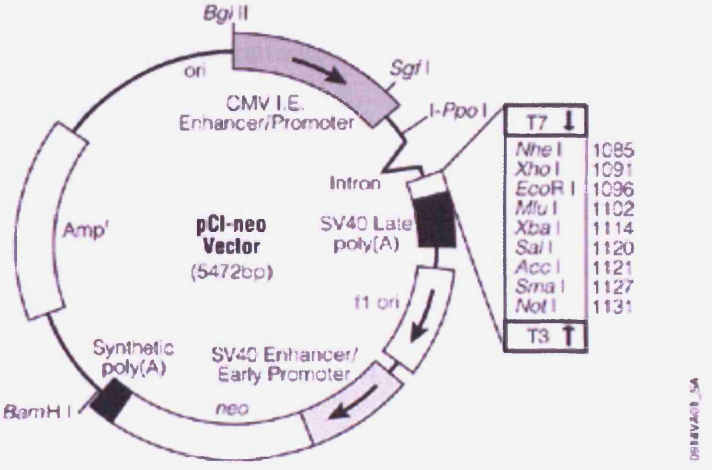

Figure 2.1: pCI-neo vector (Promega, Madison, WI)

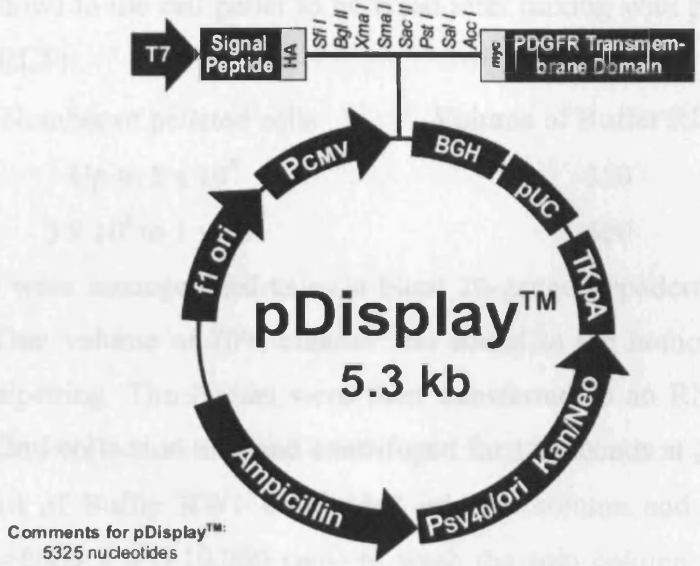

Comments for pDisplay™:
5325 nucleotides

CMV promoter: bases 1-596
T7 promoter: bases 638-657
Murine Ig kappa-chain V-J2-C signal peptide: bases 737-799
Hemagglutinin A epitope: bases 800-826
Multiple Cloning Site: bases 827-873
myc epitope: bases 874-903
PDGFR transmembrane domain: bases 907-1056
Bovine growth hormone polyadenylation signal: bases 1069-1288
pUC origin: bases 1378-2051
Thymidine kinase polyadenylation site: bases 2458-2187
Neomycin/Kanamycin resistance gene: bases 3421-2366
SV40 origin and promoter: bases 3797-3456

Figure 2.2: pDisplay vector (Invitrogen Life Technologies,UK).

Post transfection, Hek293 and HeLa cells were washed with phosphate buffer saline (PBS) and cultured in fresh growth medium with 0.5 mg/ml G418 (Geneticin, Sigma-Aldrich, UK). Stably transfected cells were selected with G418 for one to two weeks, splitting the cells twice weekly. After two weeks, the transfectants were tested for expression of TLR9 using PCR (section 2.2.3). Stable transfectants were transferred to flasks and maintained with 0.3mg/ml G418-Geneticin concentration under their normal growth conditions, and were frozen in aliquots in liquid nitrogen. Transfected cell lines were grown in culture for up to 5 weeks before being replaced with freshly thawed cells. Expression of TLR9 was determined by RT-PCR for each batch used.

2.2.3 mRNA expression of hTLR9

2.2.3.1 Total RNA extraction

Total RNA was extracted according to the manufacturer's instructions using RNeasy blood Mini Kits (QIAGEN, UK). Up to $1x10^7$ cells were washed with PBS and the cell pellet was loosened by flicking the tube. Buffer RLT was added (according to

the table below) to the cell pellet to be lysed after mixing with β-ME (10μl to each 1ml buffer RLT).

Number of pelleted cells	Volume of Buffer RLT (μl)
Up to 5 x 10^6	350
5 x 10^6 to 1 x 10^7	600

The lysates were homogenized using a blunt 20-gauge hypodermic needle (0.9mm diameter). One volume of 70% ethanol was added to the homogenized lysate and mixed by pipetting. The lysates were then transferred to an RNeasy spin column placed in a 2ml collection tube and centrifuged for 15 seconds at ≥8000 x *g* (≥10,000 rpm). 700 μl of Buffer RW1 was added into the column and centrifuged for 15 seconds at ≥8000 x *g* (≥10,000 rpm) to wash the spin column membrane and the flow-through was discarded. The column was transferred into a new 2-ml collection tube and 500 μl of Buffer RPE was added into the spin column and centrifuged for 15 seconds at ≥8000 x*g* (≥10,000 rpm). Another wash to the column was done using 500 μl of Buffer RPE for 2 minutes at ≥8000 x *g* (≥10,000 rpm). The spin column was transferred into a 1.5 ml collection tube and 30-40μl of RNase-free water was applied directly onto the spin column membrane, and centrifuged for 1 minute at ≥8000 x *g* (≥10,000 rpm). The concentration of RNA extracted was determined by measuring the absorbance at 260 nm (A_{260}) and at 280 nm (A_{280}). The RNA concentration (μg/μl) was calculated from this equation:

(A_{260}) x 40 x Dilution factor/1000μl.

The total RNA extracted was either reverse transcribed into single-stranded cDNA or kept at –70 °C until use.

2.2.3.2 First-Strand cDNA Synthesis

Five micrograms of cDNA was prepared from the total RNA extract according to the manufacturer's instructions by the Superscript™ First strand synthesis system for RT-PCR (Invitrogen, UK). One microliter of 10mM deoxynucleotide (dNTP) mix, 1μl of 0.5μg/μl oligo (dT) and DEPC-treated water were added to 5μg of total RNA in a total volume of 10μl were incubated at 65°C/5minutes, then placed on ice for 1-2 minutes. Two microliters of 10X RT buffer, 4μl of 25mM $MgCl_2$, 2μl of 0.1M DTT and 1μl of RNaseOUT™ (RNase inhibitor) were added to each RNA/primer mix and incubated at 42°C/2minutes. One microliter of Superscript II RT (50 units)

was added to each mix and incubated at 42°C/50minutes. The reactions were terminated at 70°C/15minutes and then chilled on ice. Tubes were spun to collect the content and 1µl RNase H was added to each tube and incubated at 37°C/20minutes. The cDNA prepared was either used immediately in PCR or kept at –20 °C until use.

2.2.3.3 Reverse-transcriptase-polymerase chain reaction (RT-PCR):

cDNA (from 5µg total RNA) was amplified using platinum® Taq DNA polymerase (Invitrogen, UK) in 10 mM dNTP mix, 5µl of 10x PCR buffer minus Mg,1.5µl of 50mM $MgCl_2$, 0.4µl from 5units/µl of Taq DNA polymerase, 1µl of 10µM forward primer (FW), 1µl of 10µM reverse primer (RW) and autoclaved water to a final volume of 50µl. The primers used for TLR9 PCR were either:

TLR9-FW1	5'-CAACAACCTCACTGTGGTGC-3',	
TLR9-RW1	5' GAGTGAGCGGAAGAAGATGC-3'	Or
TLR9-FW2	5'-ACAACAACATCCACAGCCAAGTGTC-3'	
TLR9-RW2	5'-AAGGCCAGGTAATTGTCACGGAG-3'	

For the house keeping gene, β-actin, primers used were:

β-actin FW	5'-GCTCGTCGTCGACAACGGCTC-3'
β-actin RW	5'-CAAACATGATCTGGGTCATCTTCTC-3'

TLR9 Primers of FW1 and RW1 would result in a 511bp product length while FW2 and RW2 yield a PCR product of 250bp length. β-actin primers gave a 353bp product. All primers were obtained from MWG (MWG, Ebensburg, Germany).

The cDNA mix was incubated in a thermal cycler at 95°C for 2minutes to completely denature the template and activate the enzyme. Thirty cycles of PCR amplification were done as follow:

Denature	95°C for 30 seconds.
Anneal	58°C for 30 seconds.
Extend	72°C for 2.5 minutes.

After thirty cycles, they were then incubated at 72°C for 7minutes, and the reaction was maintained at 4°C after completion of PCR. The products were either stored at -20°C until use or they were separated by running 12µl of the product with 3µl of blue loading gel (Sigma, UK) on 1.8% agarose gel electrophoresis (120V/30minutes)

along with a molecular weight marker (100bp DNA Ladder, BioLabs, U.K) and stained with ethidium bromide. Electrophoresis documentation was done with Kodak DC 120 zoom digital camera (Eastman Kodak Company, USA).

2.2.3.4 Semi-quantitative Real-Time Polymerase Chain Reaction (qRT-PCR):

A semi-quantitative RT-PCR was performed using the LightCycler system (Roche Diagnostics, Mannheim) according to the manufacturer's instructions. Amplification of cDNA was carried out using the SYBR green (Quanti Tect SYPR® Green PCR Kit, QIAGEN, UK), which is a fluorescent dye that binds to the minor groove of the DNA double helix. In solution, the unbound dye exhibits very little fluorescence, however, fluorescence is greatly enhanced upon DNA-binding. After annealing of the primers, a few dye molecules can bind to the double strand. DNA binding results in a dramatic increase of the SYBR Green I molecules which emit light upon excitation. Fluorescence intensity is measured after each amplification cycle to monitor the increasing amount of amplified DNA. PCR for TLR9 was performed using the TLR9 primers described previously (section 2.2.3.3). To quantify the product, a standard cDNA was prepared from pCl-neo/TLR9 plasmid starting with $1x10^{-2}$ng/µl for standard one, and making five fold dilutions for the other three standards ($2x10^{-3}$, $4x10^{-4}$ and $8x10^{-5}$ng/µl). The standard curve gave a linear regression line after the real-time PCR reaction (Figure 2.3). 1.5µl of 5µM of each primer, 7.5µl of master mix SYBR Green I and 3.5µl of RNase free water were added to 1µl of the 5µg cDNA of a final volume of 15 µl placed in Light cycler capillaries (20µl) (Roche Diagnostics, Mannheim). Thermal cycling was initiated with an incubation step at 50°C for 2 minutes, followed by a first denaturation step at 95°C for 15 minutes, and continued with 45 cycles of 95°C for 15 seconds, 58°C for 30 seconds, and 72°C for 15 seconds.

The β-actin house keeping gene PCR was run under the same conditions and was used to normalise the TLR9 results. Melting curve analysis was used to control the specificity of the amplification products. No amplification of non-specific products was noticed for any of the primer sets used. Concentration of TLR9 mRNA normalised against β-actin house keeping gene is expressed as arbitrary unit (AU).

Amplification and melting curve analysis:

For the analysis of expression of TLR9 mRNA in the different cell lines, the specificity of amplification was controlled by analysing the standard curve (Figure 2.3), melting curve (Figure 2.4) and the number of cycles in the sigmoidal curves in addition to the analysis of crossing points (Figure 2.5). Figure 2.4 was used as an example of analysis of Light Cycler curves. Curves were analyzed by determining the cycle number at which the amplification curves intersected with a horizontal line drawn across at a signal level when SYBR green fluorescence increases exponentially. This signal increases in direct proportion to the amount of PCR product in a reaction. A significant increase in fluorescence above the baseline value measured during the 15-25 cycles indicates the detection of accumulated PCR product.

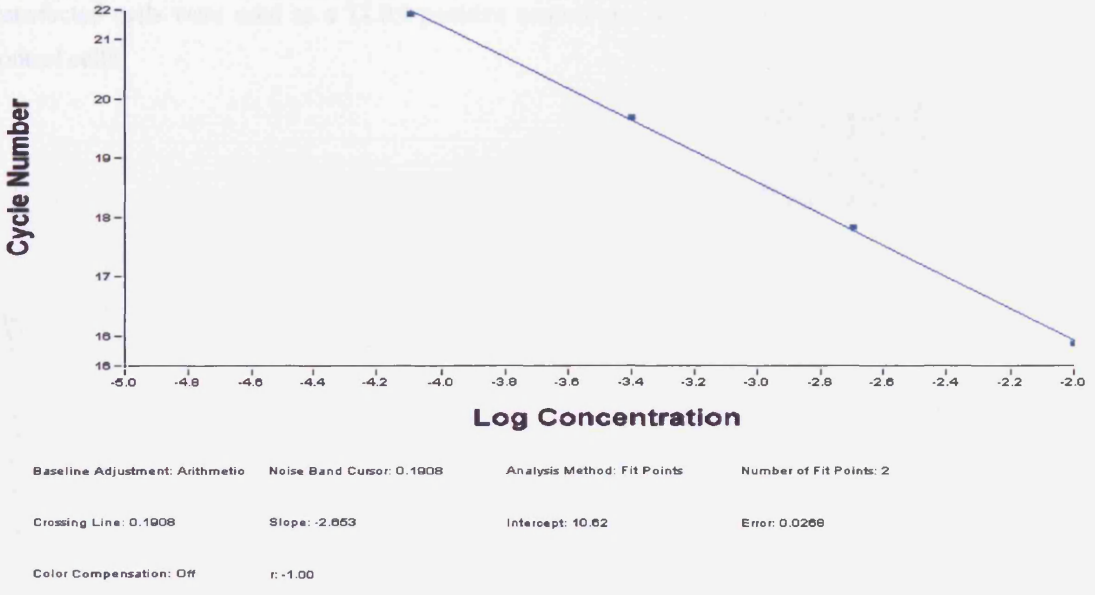

Figure 2.3: linear regression line graph, from serial dilutions of standard TLR9 DNA (pCI-neo/TLR9 plasmid). From the standard curve, the amount of cDNA region of interest in the different cell lines was estimated and normalized using the house keeping gene results to give a semi-quantitative value.

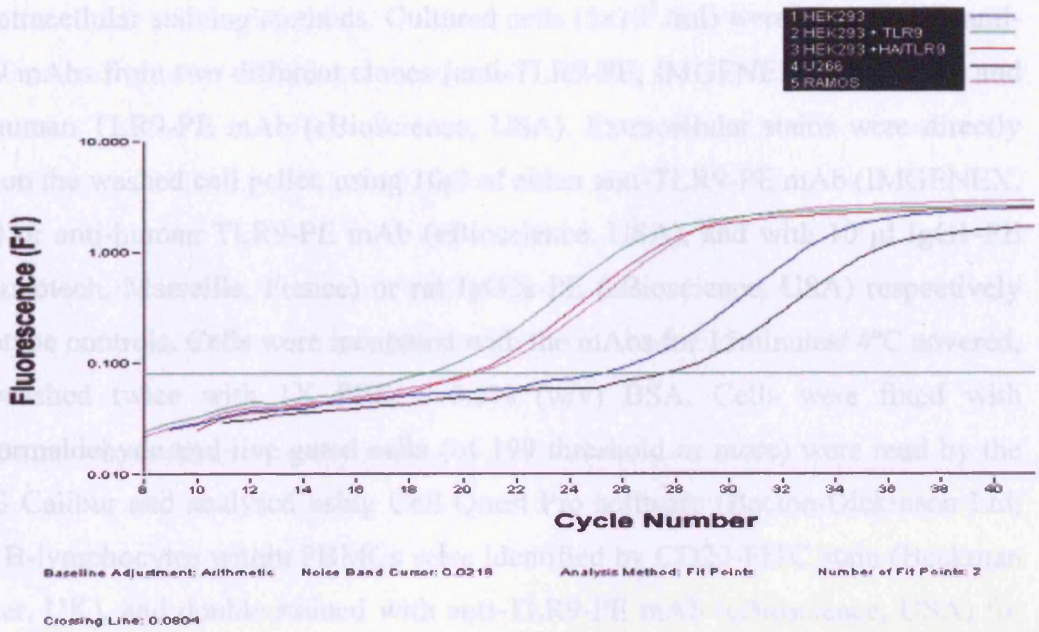

Figure 2.4: Hek293 with its TLR9 transfectants and tumour B-cells amplification sigmoidal curves of their different cDNA templates. Curves were analyzed by determining the cycle number at which the amplification curves intersected with a horizontal line. Hek293 TLR9 transfected cells were used as a TLR9 positive control and the null Hek293 as TLR9 negative control cells.

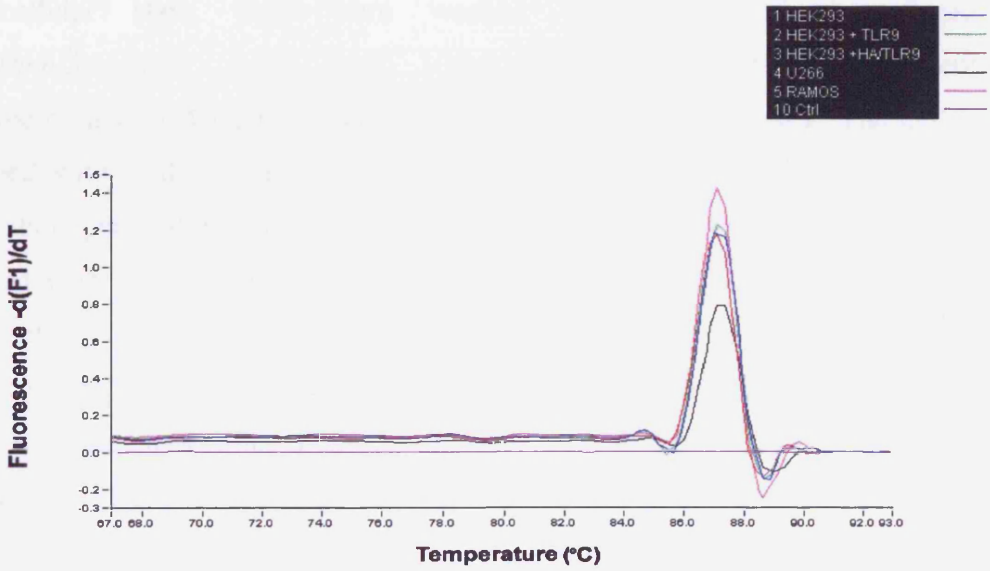

Figure 2.5: Melting curve analysis of TLR9 mRNA for Hek293 with its transfectants and tumour B-cells, with the linear negative control line showing no non-specific amplifications.

2.2.4 Protein expression of hTLR9:

2.2.4.1 Immunofluorescent staining and flow cytometry:

To determine the expression and cellular localization of TLR9 in normal and malignant human cells, flow cytometric analysis was performed using a FACS Calibur flow cytometer (Becton-Dickinson Ltd, Cowley, UK) and both cell surface

and intracellular staining methods. Cultured cells ($5x10^5$ /ml) were stained with anti-TLR9 mAbs from two different clones (anti-TLR9-PE, IMGENEX, USA) mAb and anti-human TLR9-PE mAb (eBioscience, USA). Extracellular stains were directly done on the washed cell pellet, using 10µl of either anti-TLR9-PE mAb (IMGENEX, USA) or anti-human TLR9-PE mAb (eBioscience, USA), and with 10 µl IgG1-PE (Immunotech, Marseille, France) or rat IgG2a-PE (eBioscience, USA) respectively as isotype controls. Cells were incubated with the mAbs for 15minutes/ 4°C covered, and washed twice with 1X PBS – 0.5% (w/v) BSA. Cells were fixed with paraformaldehyde and live gated cells (of 199 threshold or more) were read by the FACS Calibur and analysed using Cell Quest Pro software (Becton-Dickinson Ltd, UK). B-lymphocytes within PBMCs were identified by CD20-FITC stain (Beckman Coulter, UK), and double stained with anti-TLR9-PE mAb (eBioscience, USA) for the surface expression of TLR9. A parallel group were blocked using an equal concentration of the blocking peptide for polyclonal anti-human TLR9 (eBioscience, USA) and anti-TLR9-PE mAb (eBioscience, USA) in intracellular and extracellular staining to detect the efficiency of the method and the sensitivity of antibody. For intracellular stain, cells were washed with 1X PBS, centrifuged at 1500rpm/5minutes, fixed with 100µl of intraStain fixative reagent A (Dakocytomation, Glostrup, Denmark) and left for 15minutes/RT. The cells were washed with 2ml 1X PBS – 0.5% (w/v) BSA before the addition of the 100µl intraStain permeabilisation reagent B (Dakocytomation, Glostrup, Denmark) and stained with 10µl of anti-TLR9 conjugated to PE (IMG-305D and eB72-1665) or 10µl of the premixed anti-TLR9-PE and its blocking peptide (same done for extracellular staining). The cells were also stained separately with 10µl IgG1-PE (Immunotech, Marseille, France) or with Rat IgG2a-PE (eBioscience, USA) respectively for isotype controls. Cells were incubated for 15minutes/RT, washed twice with 1X PBS – 0.5% (w/v) BSA, centrifuged and fixed with 0.5ml of paraformaldehyde. Results were read in the FACS Calibur, and analysed using Cell Quest Pro software (Becton-Dickinson Ltd, UK).

Normal PBMCs and Burkitt's lymphoma BJAB cell lines were also examined for their TLR9 expression before and after CpG-ODN activation (three days with 3µg/ml 10103 CpG-ODN) to determine if TLR9 expression will change after CpG-ODN activation.

Fluorescence values were brought together after gating on a combination of forward scatter (FSC) and side-scatter (SSC) features. Data from 10,000 events were acquired using CellQuest software (BD Biosciences, UK). The signals were acquired in a linear mode for FSC and SSC characteristics, and in a logarithmic mode for fluorescence intensities. Measurements included percentage of total population, and median in addition to mean channel fluorescence intensity (MFI) in energy channels.

2.2.4.2 Immunoprecipitation and Western blot.

Immunoprecipitation and western blotting were done to detect the expression of TLR9 protein on the tested cell lines.

2.2.4.2.1 Cell lysis:

A) Tri Reagent

PBMCs and tumour cell pellets ($5x10^6$ – $1x10^7$cells) were washed with PBS and lysed in 200 µl Tri Reagent™ (Sigma, Pool, UK). The lysate was centrifuged at 12,000xg for 10minutes at 4°C, and 40µl of chloroform was added. Cells were centrifuged (12,000xg/15minutes/4°C) and the RNA phase removed. Protein supernatant was isolated by centrifugation (2,000xg/5minutes/4°C) after the addition of 60µl of 100% ethanol. To precipitate the protein, 300µl isopropanol were added. The samples were incubated at RT for 10minutes, centrifuged at 12,000 g for 10 minutes/4°C forming a pellet on the side and bottom of the tube. The supernatant was removed and the protein pellet washed twice with 0.3 M guanidine MC1/95% ethanol. Samples were kept in wash solution for 20 minutes/RT, and then centrifuged at 7,500 xg for 5minutes/4°C. The protein pellet was dried and dissolved in 1% sodium dodecylsulfate (SDS) and the insoluble material was removed by centrifugation. A microplate assay was done, and protein concentrations were determined using The Bio-Rad *DC* (detergent compatible) protein assay (BioRad, Hercules, USA) according to the manufacturer's instructions. This is a colorimetric assay for protein concentration following detergent solubilisation, based on a modification of the traditional Lowry method. 10µl of β-Mercaptoethanol (β-ME) in Laemmli loading dye 1:20 (reduced) (62.5 mM Tris-HCl, pH 6.8, 2% SDS, 25% glycerol, 0.01% Bromophenol Blue) (BioRad, Hercules, USA) were added to 10 µl of the lysed protein and then all heated to 95°C for 5minutes before loading them on to the

gel to detect the protein presence in the sample by western blotting after polyacrylamide gel electrophoresis (see section 2.2.4.2.3).

B) Latz *et al.*, (2004a) Lysis buffer:

The washed pellets of $5x10^6$ cells were incubated on ice for 30minutes with 1ml of cold lysis buffer containing 137mM NaCl, 20mM Tris-HCl, pH 7.4, 1mM EDTA, 0.5% Triton X-100 containing 60mM *n*-octylglucoside, 25mM iodoacetamide, and a mixture of protease inhibitors (10µl/ml leupeptin,10µl/ml aprotinin and 1mM phenylmethylsulfonyl fluoride (all from Sigma, UK) (Latz *et al.*, 2004a). Ultracentrifugation (15,000 xg) was done for 15minutes/4°C and the supernatants collected for immunoprecipitation.

C) RIPA Lysis buffer:

One ml of cold RIPA buffer containing 1% NP-40, 0.5% Nadeoxycholate, 50mM Tris HCl, 150mM NaCl, 1mM Na-fluoride, 30mM Na Pyrophosphate, 2mM EDTA, 0.1% SDS, 100µM Na orthovanadate 1mM phenylmethanusulphonylfluoride (PMSF) (Sigma,UK) and protease inhibitors (Sigma,UK) of 10µg/ml Leupeptin,10µg/ml Aprotinin and 10µg/ml Pepstatin were added to the washed pellet of $5x10^6$ cells for 30 minutes on ice. After lysis, the samples were centrifuged at 15,000 xg for 15minutes/4°C and the supernatants collected for immunoprecipitation.

2.2.4.2.2 Immunoprecipitation

Five $x10^6$ cells were lysed with 1ml of either the Latz *et al.*, lysis buffer or RIPA lysis buffer for 30minutes on ice (section 2.2.4.2.1, B or C). Cell lysates were centrifuged, and nuclei were removed. The lysates were divided into two aliquots and incubated with 5µg of TLR9 Abs or isotype control mAb. The anti-TLR9 Abs used were anti-TLR9 mAb (IMG-305D, IMGENEX, USA), purified anti-TLR9 (eB72-1665, eBioscience, USA) or anti-HA high affinity rat mAb-clone 3F10 (Roche Applied Sciences, UK) for the HA-tagged TLR9 transfectants. The isotype control was incubated with 5µg of mouse IgG1 or rat IgG2a respectively. All were placed on a rotator for 1hour/4°C. Immune complexes were precipitated by the addition of 50µl of 20% protein G sepharose slurry (Amersham Biosciences, USA) equilibrated in lysis buffer. The immunoprecipitate (IP) was left overnight rotating

in the cold. After extensive washing with lysis buffer, the immunoprecipitate was solubilised by boiling in 30µl Laemmli loading dye with β-ME (reduced) (BioRad, Hercules, USA). The immune complex was loaded on precast 7.5% SDS-PAGE gels (Ready gel Tris-HCL gels, BioRad, Hercules, USA) for western blotting as described in the following section.

2.2.4.2.3 Western blotting system:

Western blotting of whole cell lysates (Tri-reagent lysis buffer) or immunoprecipitates (Latz *et al.*, lysis buffer or RIPA lysis buffer) was done according to the instructions of the mini-protean®II electrophoresis and blotting system (BioRad, Hercules, USA). Immunoprecipitates (20µl) were loaded on precast 7.5% SDS-PAGE gels (Ready gel Tris-HCL gels, BioRad, Hercules, USA) and submitted to electrophoresis at 20mA for the stacking gel (10minutes) and 30mA for the resolving gel (40minutes) to fractionate the protein according to size using premixed 1X Tris/Glycine running buffer (BioRad, Hercules, USA), followed by transfer of proteins into a Hybond-C Super nitrocellulose membranes (Amersham Biosciences, Little Chalfont, UK) at 300mA for 90 minutes in ice using 1X Tris/Glycine/SDS blotting buffer (BioRad, Hercules, USA). The membrane blots were washed in 1X PBS – 0.1% Tween 20 three times for 5 minutes each time on the orbital shaker. To prevent non-specific binding, the membranes were incubated and blocked in 5% non-fat powdered milk in 1X PBS – 0.1% Tween 20 for 1 hour. The membranes were washed with 1X PBS – 0.1% Tween 20 three times for 10 minutes each time and then they were blotted with 1:500 of anti-TLR9 (anti-TLR9 mAb (IMGENEX, USA) or anti-TLR9 (N-15) Sc-13215 goat polyclonal IgG (Santa Cruz Biotechnologies, Santa Cruz, USA) in 1% non-fat powdered milk in 1X PBS – 0.1% Tween 20 for 24-48hours. The membranes were then washed in 1X PBS – 0.1% Tween 20 three times for 10 minutes each time. A secondary antibody of 1:5000 horseradish peroxidase (HRP) conjugated anti-mouse IgG $F(ab')_2$ fragments (Amersham Biosciences, Little Chalfont, UK) or 1:10,000 rabbit anti-goat IgG HRP respectively in 1% non-fat powdered milk in 1X PBS–0.1% Tween 20 were incubated for 1 hour. The membranes were then washed in 1X PBS – 0.1% Tween 20 three times for 10 minutes each time. The protein bands were visualized using Chemiluminescence

ECL Blotting detection kit and exposed to Hyperfilm™ ECL Western (both from Amersham Biosciences, Little Chalfont, UK) for 45minutes.

The Tri-reagent lysed blots (without immunoprecipitation) were stripped with 0.15M Glycine (pH 2.2) and 1% SDS in 1X PBS – 0.1% Tween 20 for 10 minutes three times, then blocked with 5% non-fat powdered milk in 1X PBS – 0.1% Tween 20 for 1 hour. Then, they were reblotted for β-actin as a control of protein load for the samples using β-actin/HRP antibody (Santa Cruz Biotechnologies, Santa Cruz, USA) at 1:5,000 dilution for 2hours. The membranes were then washed in 1X PBS – 0.1% Tween 20 three times for 10 minutes each time. The β-actin membranes were developed within 15 seconds using ECL Blotting detection kit and images were observed.

2.2.4.3 Immunofluorescence staining and confocal microscopy method:

To determine the expression and cellular localisation of TLR9, immunofluorescence staining and confocal microscopy were used.

2.2.4.3.1 Cell preparation:

A) Adherent cells:

$1x10^5$ cells/ml of the TLR9 transfected Hek293 and HeLa cell lines and their mock transfectants were left to grow overnight on 13mm sterile cover slips in 12 well plates, after treating the coverslips with 100µl poly-d-lysin (PDL) (1:100 in PBS) for 60minutes/RT. Cell culture medium was removed and cells were fixed with 1ml 10% formal saline for 30minutes/RT and then washed three times with water. Cells then were stained with Gogli stain NBD C_6–ceramide complexed to BSA (Invitrogen, UK) (section 2.2.4.3.1, B).

B) Suspension cells:

Pellets of $1x10^5$ cells/ml tumour B-cells were fixed for 30minutes/RT with 10% formal saline before cytospinning on cytoslide microscope slides (Shandon, USA) (150xg/3minutes) using a Shandon cytospin 2 centrifuge. Each cell line was spun onto four slides, placed in humid chamber, and stained with Golgi stain NBD C_6–ceramide complexed to BSA (Invitrogen, UK).

2.2.4.3.2 Golgi stain:

Cytoslides with cells were washed in HBSS/HEPES to be fixed for 10minutes in 10% formal saline. Ice-cold HBSS/HEPES was used to wash each sample several times before incubating them for 30minutes/4°C with 100 µl of 5µM Ceramide-BSA complex (NBD C_6–ceramide complexed to BSA; Invitrogen,UK). Cells were rinsed with HBSS/HEPES three times and incubated for 30-90 minutes/RT with 2mg/ml BSA to enhance Golgi stain. Cells were rinsed with HBSS/HEPES then fixed with 10% formal saline before staining for expression of TLR9.

2.2.4.3.3 Confocal microscopy immunofluorescence stain:

One ml 1X TBS was added to all cells for 5 minutes/RT. For intracellular stain cells were permeablised using 1ml of 1X TBS 0.1% Triton-x for 10minutes/RT whereas for extracellular stain they were left with 1X TBS. 500µl of 5% goat serum were used to block the cells. After 60 minutes / RT goat serum was removed and cells were stained with the primary antibodies. For each cell line, two slides were stained intracellularly and the other two extracellularly for 1hour/RT with the target antibody diluted 1:20 in goat serum. In each set, one slide was stained with the isotype control, affinity purified rat IgG2a (eBioscience, USA), and the other with affinity purified anti-human TLR9 rat mAb (eBioscience, USA). For the haemagglutinin tagged TLR9 transfected cells, anti-haemagglutinin (HA) high affinity rat mAb-clone 3F10 (Roche Applied Sciences, UK) was used. A secondary stain was used after washing three times with 1% TBS, using goat FITC-labelled polyclonal Ab to rat IgG (Abcam, UK), 1:400 dilution in 5% goat serum for 1hour/RT. Cells were washed three times with 1%TBS. Cover slips from the adherent cells were removed from the 12 well plate and mounted on a slide using VECTASHIELD HardSet mounting medium with DAPI (Vector laboratories, USA) which contains a counterstain for DNA. Suspension cells were mounted directly on the cytoslides to be examined by fluorescence confocal microscopy. Cytoslides were mounted with immersion oil and read at different filters using TE300 semi-automatic Nikon microscope; Blue (Dapi excitation filter wavelength; 365nm) for the nucleus (DNA) stain, Green (FITC excitation filter wavelength; 475nm) for TLR9 stain and Red (CY5 excitation filter wavelength; 630nm) for the background to compare.

2.2.5 Statistical analysis

Each experiment was repeated at least two times. Data points stand for the mean of triplicate results for RT-PCR and replicates for the other techniques. Data were analysed using Student's paired t-test using GraphPad prism 4 software version 4.03. Results were considered significant when p value was less than 0.05, and very significant when p value was less than 0.001.

2.3 Results:

Investigating the expression and function of TLR9 in haematological and non-haematological tumour cells is critical to understand the potential of CpG ODN as an immunotherapeutic agent in the treatment of cancer. To this end, the cellular expression of TLR9 in human tumour cells was investigated using a panel of anti-human TLR9 antibodies. In this work, flow cytometry, immunoprecipitation/western blotting, and confocal microscopy investigations were done to identify the expression of TLR9 protein in the different human tumour cell lines, and RT-PCR was used to identify expression of TLR9 mRNA.

In preliminary experiments done in our laboratory (Helia Esteves, University of Leicester, BSc. dissertation) using *ex vivo* tumour B cells and panels of haematological and non-haematological human tumour cell lines, the intracellular expression of TLR9 was seen by anti-TLR9-PE mAb (IMGENEX, USA) staining and flow cytometry in all B-cell tumours tested (data not shown). The expression of TLR9 was also seen, however, in a range of non-haematological tumour cell lines, including epithelial cancers and melanomas, and no TLR9-negative cells/cell lines were identified. Initially, it was my aim to further investigate TLR9 (mRNA and protein) expression in haematological and non-haematological tumour cells, based on these preliminary results.

2.3.1 Toll-like receptor 9 mRNA expression in the human cells:

Based on most publications, the expression of TLR9 by immune cells has mostly been through the detection of mRNA using PCR-based methods (Hougrnung V *et al.*, 2002). I therefore established a reverse transcriptase (RT) PCR for the detection of TLR9 mRNA, based on the published method, and a semi-quantitative RT-PCR assay for determining levels of expression. For the study of the expression of TLR9 in haematological and non-haematological tumour cell lines, cDNA was prepared from 5μg total RNA of each cell line. RT-PCR was carried out for the different cell lines. Figures 2.6 and 2.7 represent RT-PCR of haematological and non-haematological tumour cells respectively. $CD19^+$ B cells isolated from PBMCs from three normal individuals were all positive for TLR9 mRNA expression (Figure 2.6a). Haematological tumour cells showed TLR9 bands of the predicted size, indicating expression of TLR9 mRNA in most of the cell lines, with the exception of the myeloma cells (U266 and Karpas 707H cell lines) and the EBV transformed B

lymphoblastoid cell (HMy-2 cell) (Figure 2.6b). Karpas and U266 cells were therefore used as negative controls for TLR9 in subsequent PCR. The TLR9 transfected Hek293 cells showed a clear TLR9 specific band while it was weak for HeLa HA/TLR9, with no visible band for HeLa TLR9 (Figure 2.7). In contrast, the untransfected HeLa and Hek293 cells showed only a very faint band or no band, indicating a very low to undetectable TLR9 expression level. TLR9 expression in TLR9 transfected Hek293 cells appeared higher compared with HeLa HA/TLR9 transfected cells. All the non-haematological tumour cells tested (Corl-47, MCF-7, HRT-18, MW1361A and Du-145) showed negative or very weak TLR9 mRNA expression (Figure 2.7).

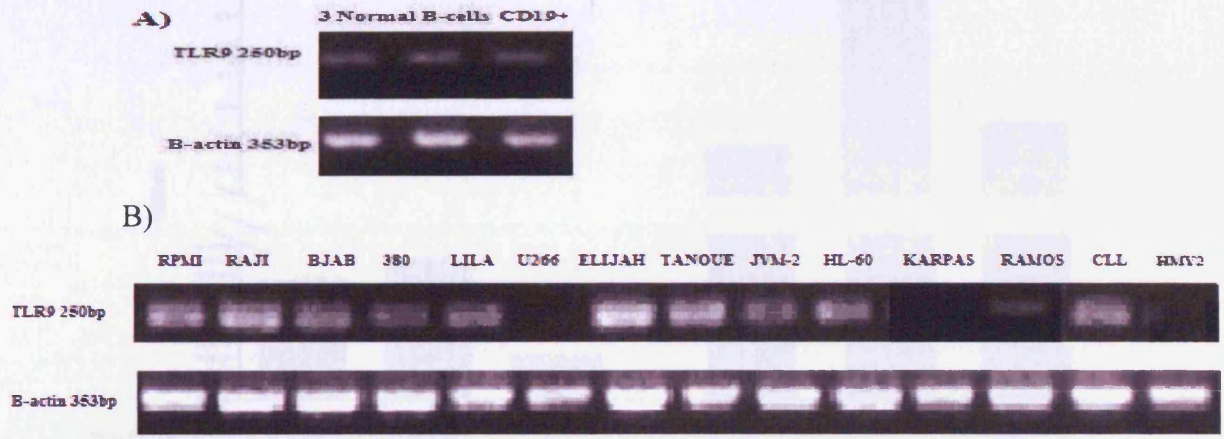

Figure 2.6. TLR9 mRNA expression by RT-PCR in normal B-cells (A), and in tumour B-cells (B). Upper bands show TLR9 specific PCR, and lower bands β-actin house keeping gene. This experiment was repeated in two independent times and primers with the same results.

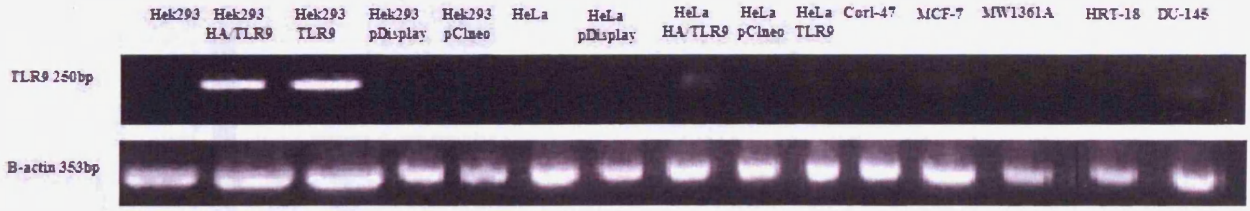

Figure 2.7. Variable levels of TLR9 mRNA expression by RT-PCR in different non-haematological tumour cells and TLR9 transfected cells, compared with β-actin house keeping gene. This experiment was repeated in two independent times and primers with same results.

To determine the level of TLR9 mRNA in each cell line tested, a semi-quantitative method was established, using a standard curve derived from five-fold dilutions from the pCl-neo/TLR9 plasmid, and by relating the PCR signals to the standard curve (Figure 2.3), and normalised with the house keeping gene β-actin.

2.3.1.1 TLR9 mRNA expression in haematological cells by qRT-PCR.

Results obtained from qRT-PCR were broadly consistent with the RT-PCR results (Figures 2.8 & 2.9). Six different healthy adult volunteer's PBMCs or $CD19^+$ B-cells (three from each) expressed TLR9, but at different levels (Figure 2.8). TLR9 mRNA level in $CD19^+$ B-cells was at least ten times higher than in PBMCs (Figure 2.8), which was expected as TLR9 is mostly expressed by B-cells in PBMCs. TLR9 mRNA expression levels in haematological tumour cells normalised with the house keeping gene β-actin showed a marked degree of variability in relation to the TLR9 mRNA level (Figure 2.9).

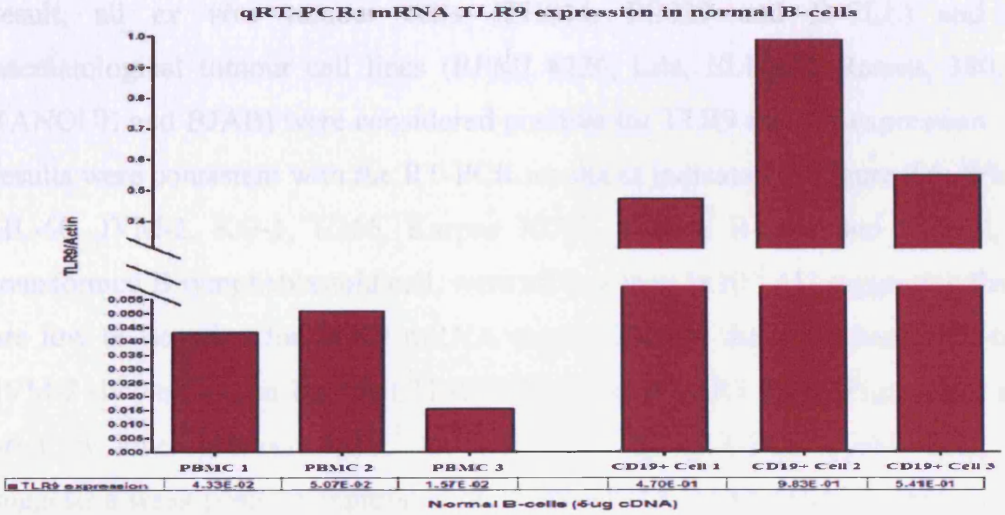

Figure 2.8: Semi-quantitative RT- PCR for TLR9, after normalisation with the house keeping gene β-actin from three PBMCs and three $CD19^+$ B-cell samples from six healthy donors.

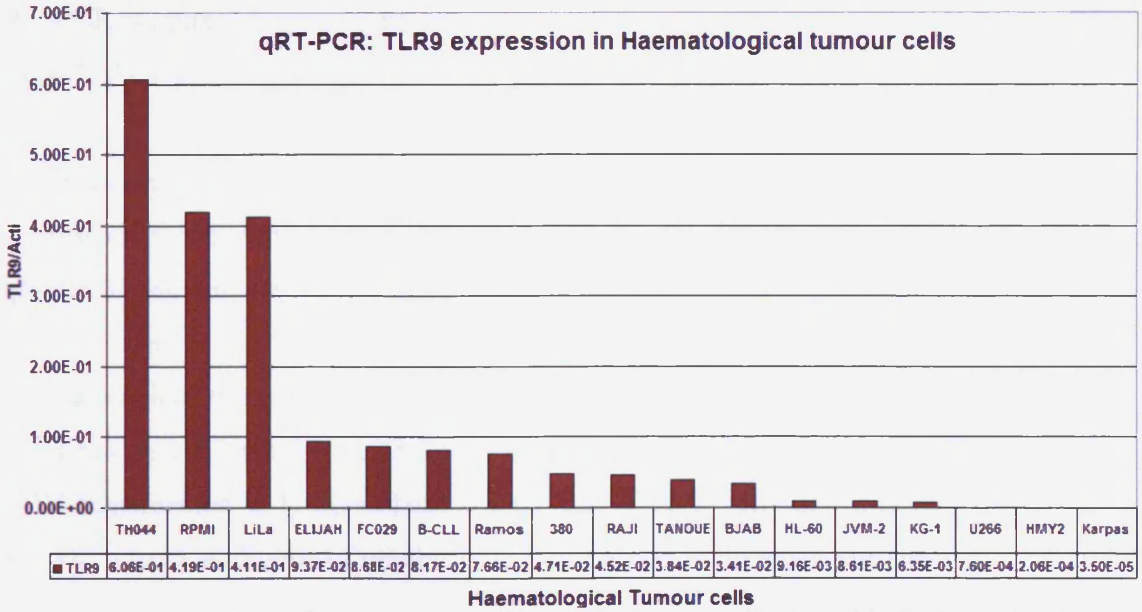

Figure 2.9: Semi-quantitative RT- PCR for TLR9 after normalisation with the house keeping gene β-actin, in a panel of human haematological tumour-cell lines.

Table 2.2 summarises the TLR9 mRNA arbitrary expression levels detected by qRT-PCR after normalising the results with β-actin house keeping gene. $CD19^+$ B-lymphocytes showed the highest TLR9 expression when determined from three different healthy donors showing mRNA level more than $4x10^{-1}$AU. Normal PBMCs showed a high TLR9 expression of more than $1.0x10^{-2}$AU, but less than $CD19^+$ B-cells. Cells in Table 2.2 are organised according to their TLR9 mRNA arbitrary expression levels showing the highest in the *ex vivo* cells. As $CD19^+$/PBMCs cells are known to express TLR9 (Baiyee EE *et al.*, 2006), I will consider data of TLR9 mRNA level greater than $1.0x10^{-2}$AU to be positive for TLR9 expression. As a result, all *ex vivo* tumour cells (TH044, FC029 and B-CLL) and some haematological tumour cell lines (RPMI 8226, Lila, ELIJAH, Ramos, 380, Raji, TANOUE and BJAB) were considered positive for TLR9 mRNA expression. These results were consistent with the RT-PCR results as indicated in Figure 2.6. Whereas, HL-60, JVM-2, KG-1, U266, Karpas 707H tumour B-cells and HMy-2, EBV transformed B lymphoblastoid cell, were all less than $1x10^{-2}$ AU suggesting that they are low or negative for TLR9 mRNA expression. On the other hand, HL-60 and JVM-2 showed a clear but faint TLR9 mRNA band by RT-PCR (Figure 2.6) and an arbitrary level between $1x10^{-3}$ to $1x10^{-2}$ AU by qRT-PCR (Table 2.2), which suggests a weak positive expression of TLR9 mRNA. TLR9 mRNA expression level in KG-1 cell lines was also between $1x10^{-3}$ and $1x10^{-2}$ AU suggesting also a weak positive expression whereas U266, Karpas and HMy-2 showed no TLR9 band by RT-PCR (Figure 2.6) and TLR9 mRNA expression level by qRT-PCR was less than $1x10^{-3}$ AU suggesting a negative TLR9 mRNA expression.

As discussed above and indicated in Table 2.2, I have defined TLR9 mRNA expression to be considered strong positive when the arbitrary levels detected by qRT-PCR are greater than $1.0x10^{-2}$ AU, weak positive for less than $1.0x10^{-2}$ but greater than $1x10^{-3}$ AU and negative for $1x10^{-3}$ AU or less. Therefore, haematological tumour cells showed an expression of TLR9 mRNA in most of the cell lines tested, with the exception of the myeloma cell lines U266 and Karpas and EBV transformed B lymphoblastoid cell line HMy-2, although different cell lines showed a marked degree of reliability in basal levels of TLR9 expression.

Cells	Cell type	Description	TLR9 mRNA level AU
Donor -1	*Ex vivo* $CD19^+$ cells	Normal B-Lymphocytes	9.83E-01
Donor -2			5.41E-01
Donor -3			4.70E-01
Donor -4	*Ex vivo* PBMCs cells	Peripheral blood mononuclear cells	5.07E-02
Donor -5			4.33E-02
Donor -6			1.57E-02
TH044	*Ex vivo* cells	Mantle cell lymphoma	6.06E-01
RPMI 8226	Cell lines	Multiple Myeloma	4.19E-01
LiLa		Precursor B-ALL	4.11E-01
ELIJAH		Burkitt Lymphoma	9.37E-02
FC029	*Ex vivo* cells	Mantle cell lymphoma	8.68E-02
B-CLL		Tumour CLL	8.17E-02
Ramos	Cell lines	Burkitt Lymphoma	7.66E-02
380		Precursor B-ALL	4.71E-02
RAJI		Burkitt Lymphoma	4.52E-02
TANOUE		Precursor B-ALL	3.84E-02
BJAB		Burkitt Lymphoma	3.41E-02
HL-60		Promyelocytic Leukemia	9.16E-03
JVM-2		Mantle cell lymphoma	8.61E-03
KG-1		Acute myeloid leukaemia	6.35E-03
U266		Multiple Myeloma	7.60E-04
HMy-2		EBV transformed B lymphoblastoid cell	2.06E-04
Karpas 707H		Multiple Myeloma	3.50E-05

Table 2.2 Summarises the TLR9 mRNA expression levels detected by qRT-PCR for the haematological cells after normalising their results with β-actin house keeping gene. Results are the mean of three independent experiments.

2.3.1.2 TLR9 mRNA expression in non-haematological cells by qRT-PCR.

To quantitate the level of TLR9 mRNA expression in non-haematological tumour cells and transfected and untransfected Hek293 and HeLa cells, I did qRT-PCR (Figure 2.10). Table 2.3 indicates the mRNA arbitrary levels of TLR9 normalised with the house keeping gene β-actin. Analysing the arbitrary TLR9 mRNA expression level detected by qRT-PCR in the same way indicated in section (2.3.1.1), HRT-18 and HeLa cell lines showed weak expression (between $1x10^{-3}$ and $1x10^{-2}$ AU) whereas Hek293, Corl-47, WM1361A, DU-145 and MCF-7 were all less than $1x10^{-3}$ AU suggesting negative TLR9 mRNA expression.

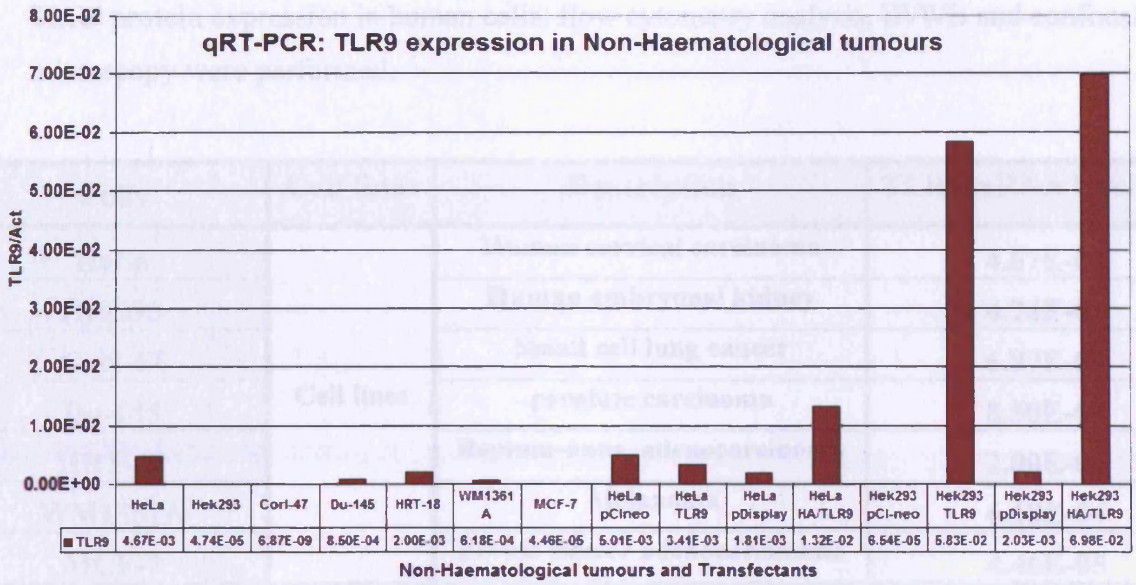

Figure 2.10: Semi-quantitative RT- PCR for TLR9 after normalisation with the house keeping gene β-actin, from different non-haematological tumour cells and TLR9 transfected Hek293 and HeLa cells.

TLR9 transfected and mock transfected Hek293 and HeLa cells were investigated for TLR9 mRNA expression levels. TLR9 and HA/TLR9 transfected Hek293 cell line showed a positive TLR9 expression with more than $1x10^{-2}$AU TLR9 mRNA, whereas transfected HeLa cells showed a strong positive TLR9 mRNA expression in HA/TLR9 transfected HeLa cells, but not in HeLa/TLR9 cells. In HeLa HA/TLR9, TLR9 mRNA level was $1.3x10^{-2}$AU (in the range of the positive expression) while in HeLa TLR9 it was $3.5x10^{-3}$ AU indicating a weak positive expression. On the other hand, TLR9 mRNA expression levels in mock-transfected Hek293 and HeLa cells showed weak to negative expression by qRT-PCR (Table 2.3). Although HeLa and its mock transfected cells should be TLR9 negative cells, they showed TLR9 mRNA levels between $1x10^{-3}$ to $6x10^{-3}$ AU. This might indicate that they are not completely negative for TLR9 mRNA expression. On the other hand, HeLa TLR9 cells showed a TLR9 mRNA level of $3.5x10^{-3}$ AU indicating that the cells were not efficiently transfected.

2.3.2 TLR9 protein expression in malignant human cells:

Several B cell malignancies have been shown to express TLR9 (Decker T *et al.*, 2000a; Decker T *et al.*, 2000b; Jahrsdorfer B *et al.*, 2001; Brouke E *et al.*, 2003). RT-PCR methods were sufficient to determine TLR9 mRNA expression, but to determine

TLR9 protein expression in human cells, flow cytometry analysis, IP/WB and confocal microscopy were performed.

Cells	Cell lines	Description	TLR9 mRNA level AU
HeLa	Cell lines	Human cervical carcinoma	4.67E-03
Hek293		Human embryonal kidney	4.74E-05
Corl-47		Small cell lung cancer	6.87E-09
Du-145		prostate carcinoma	8.50E-04
HRT-18		Rectum-anus, adenocarcinoma	2.00E-03
WM1361A		Melanoma	6.18E-04
MCF-7		Breast cancer adenocarcinoma	4.46E-05
HeLa pClneo	Mock transfect	Human cervical carcinoma	5.01E-03
HeLa pDisplay			1.81E-03
HeLa TLR9	TLR9 transfect		3.41E-03
HeLa HA/TLR9			1.32E-02
Hek293 pCl-neo	Mock transfect	Human embryonal kidney	6.54E-05
Hek293 pDisplay			2.03E-03
Hek293 TLR9	TLR9 transfect		5.83E-02
Hek293 HA/TLR9			6.98E-02

Table 2.3 summarises the TLR9 mRNA expression levels detected by qRT-PCR in the non-haematological cells and transfected Hek293 and HeLa cells after normalising their results with β-actin house keeping gene. Results are the mean of three independent experiments.

2.3.2.1 Flow cytometry:

Flow cytometric analysis was performed for surface and intracellular expression. The cells of interest were gated in a live gate (region R1) according to their forward and side scatter profiles as shown in Figure 2.11.

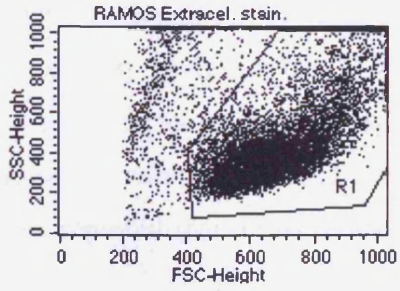

Figure 2.11. Forward and side scatter profile for the extracellular stain of RAMOS cell lines. A live gate was applied to the viable cell population (R1) and used for subsequent analysis of TLR9 expression by the cells.

Figures 2.12 and 2.13 represents TLR9 protein extracellular and intracellular expression by flow cytometry in several B-cells and cell lines ($CD19^+$ normal *ex vivo* B-cell, KR076 *ex vivo* B-CLL, Burkitt's Lymphoma cell line RAMOS, Lymphoblast-like myeloma cell line RPMI-8226, myeloma cell line Karpas 707H and myeloma cell line U266), using a directly conjugate anti-human TLR9-PE mAb (eBioscience, USA).

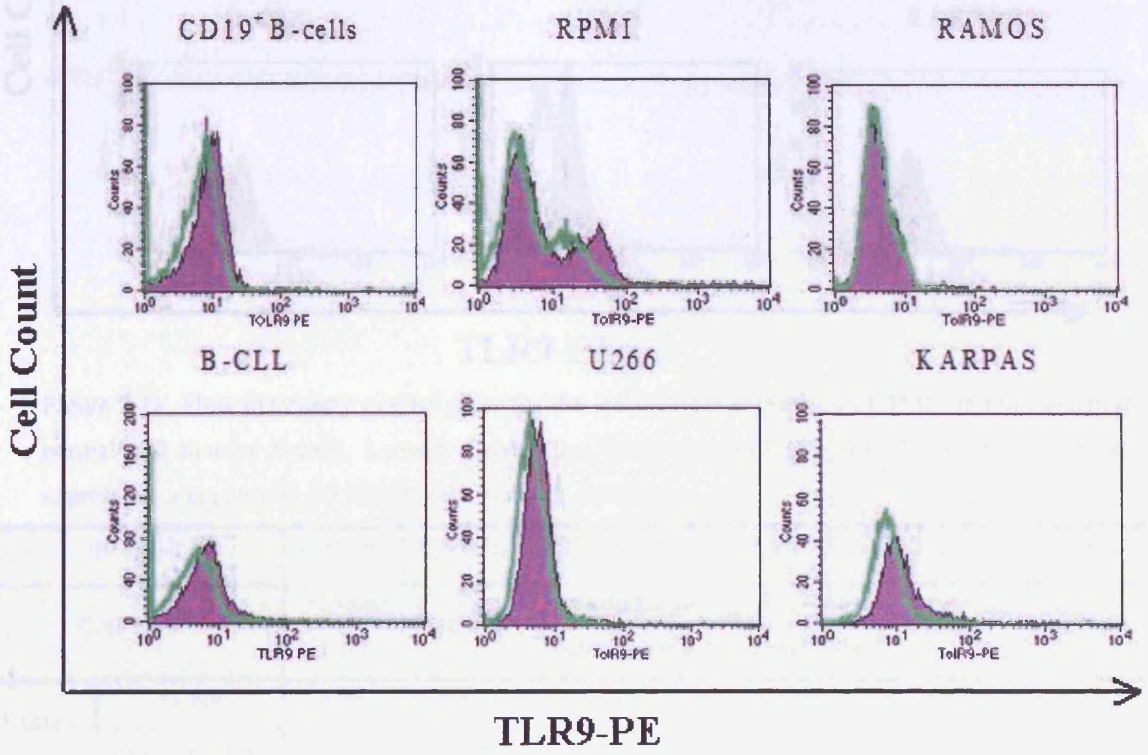

Figure 2.12. Flow cytometry overlay plots for the extracellular expression of TLR9 in representative normal and tumour B-cells. Legend: Green line: isotype control IgG1-PE. Purple blocks: TLR9 expression using anti-TLR9 PE Ab (eBioscience, USA).

Ex vivo $CD19^+$ and KR076 B-cells, RAMOS, and RPMI 8226 showed a positive TLR9 mRNA level whereas Karpas 707H and U266 were negative as indicated in section (2.3.1.1). The overlay plots for the TLR9 extracellular expression (Figure 2.12) showed little or no evidence of surface expression in most of the cells except for RPMI which showed a subpopulation of cells positive for extracellular TLR9 expression. It has been reported that TLR9 is extracellularly expressed at least in a subset of normal $CD19^+$ B-cells (Eaton-Bassiri A *et al.*, 2004; Dasari P *et al.*, 2005; Baiyee EE *et al.*, 2006; Grandjenette C *et al.*, 2007). TLR9 surface stain was consistently slightly higher than isotype control in $CD19^+$ cells, B-CLL and RPMI cells, but they also showed that in U266 and Karpas (TLR9 mRNA negative cells).

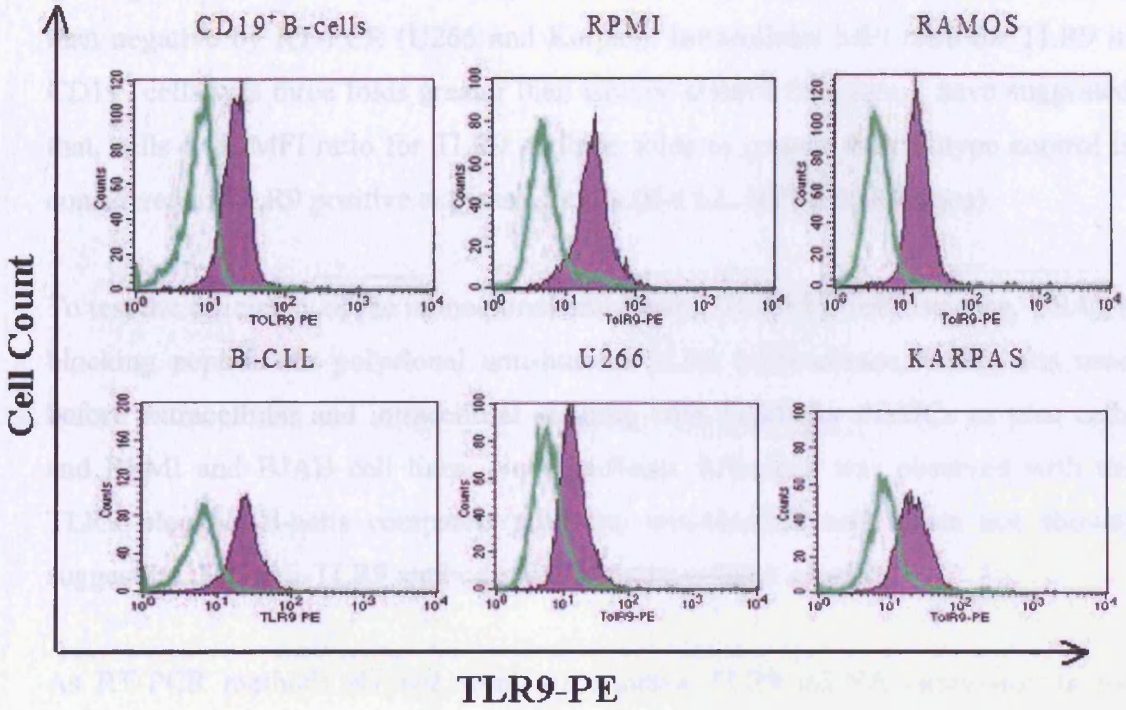

Figure 2.13. Flow cytometry overlay plots for the intracellular expression of TLR9 in representative normal and tumour B-cells. Legend: Green line: isotype control IgG1-PE. Purple blocks: TLR9 expression using anti-TLR9 PE Ab. (eBioscience, USA).

B-cells		CD19$^+$	KR076	RPMI 8226	RAMOS	U266	Karpas
Cell Type		Normal B-cell	B-CLL	Lymphoblast-like myeloma	Burkitt Lymphoma	Myeloma	Myeloma
Extra-cellular	TLR9	8.98	6.55	3.72	3.92	5.62	9.73
	Isotype Ctrl.	6.67	4.37	3.11	3.79	4.37	6.79
	TLR9/Isotype	**1.35**	**1.5**	**1.2**	**1.03**	**1.29**	**1.43**
Intra-cellular	TLR9	21.67	23.29	24.36	15.54	13.58	19.99
	Isotype Ctrl.	7.17	5.94	4.78	3.85	8.22	7.77
	TLR9/Isotype	**3.02**	**3.92**	**5.09**	**4.04**	**1.6**	**2.5**

Table 2.4 The median fluorescence intensity for the intracellular and extracellular TLR9 staining using anti-TLR9 PE Ab (eBioscience, USA) of B-lymphocytes from normal and tumour of different B-cell lines compared with the control isotype IgG1 IgG1-PE (Immunotech, Marseille, France). This experiment was done in two independent times.

Despite differences in the B-cell differentiation stages, CD19$^+$ B-cells were found to express TLR9 protein (Dasari P *et al.*, 2005; Baiyee EE *et al.*, 2006; Grandjenette C *et al.,* 2007). Table 2.4 shows that extracellular MFI consistently slightly higher for TLR9 than isotype control in B-cells, but no correlation with expression by qRT-PCR. On the other hand, intracellular MFI was higher for TLR9 than isotype control,

and higher ratio for cells positive by RT-PCR ($CD19^+$, B-CLL, RPMI and Ramos) than negative by RT-PCR (U266 and Karpas). Intracellular MFI ratio for TLR9 in $CD19^+$ cells was three folds greater than isotype control therefore, I have suggested that, cells with MFI ratio for TLR9 of three folds or greater than isotype control is considered as TLR9 positive expressing cells (B-CLL, RPMI and Ramos).

To test the efficiency of the monoclonal anti-human TLR9-PE (eBioscience, USA), a blocking peptide for polyclonal anti-human TLR9 (eBioscience, USA) was used before extracellular and intracellular staining with TLR9 for PBMCs *ex vivo* cells and RPMI and BJAB cell lines. No significant difference was observed with the TLR9 blocked B-cells compared with the non-blocked cells (data not shown) suggesting that, anti-TLR9 antibody might not be antigen specific.

As RT-PCR methods showed weak to negative TLR9 mRNA expression in the epithelial cancers and melanomas (Figure 2.7 and Table 2.3), while the preliminary experiments done in our laboratory by Hélia Esteves (University of Leicester, BSc. Dissertation) showed a weak intracellular TLR9 protein expression (in HRT-18, CORL-47, DU-145, MCF-7 and WM1361A cell lines), using monoclonal antibody staining in flow cytometry (data not shown), I did not re-investigate their TLR9 protein expression using flow cytometry and rely on her results suggesting that, TLR9 Ab was not antigen specific.

To confirm the specificity of the flow cytometric staining observed by the anti-TLR9 mAbs, TLR9 positive control cell lines were made by stably transfecting human TLR9 into the $TLR9^{low}$ Hek293 and HeLa cell lines (http://www.invivogen.com/family.php?ID=165 and Eaton-Bassiri A *et al.*, 2004). The TLR9 mRNA expression in untransfected, mock transfected and TLR9 transfected Hek293 and HeLa cell lines were tested by qRT-PCR (Figure 2.10 and Table 2.3). Hek293 TLR9, Hek293 HA/TLR9 and HeLa HA/TLR9, but not HeLa TLR9, showed a positive TLR9 mRNA expression levels by qRT-PCR (section 2.3.1.2). The TLR9 transfected and mock transfected Hek293 and HeLa cells were stained intra- and extracellularly for TLR9 expression. Overlay plots obtained by flow cytometric analysis of live gated cells are shown in Figures 2.14 and 2.15 for extracellular and intracellular expression respectively. The median fluorescence

intensities for TLR9 and IgG1 isotype and their ratio are shown in Tables 2.5 and 2.6 for Hek293 and HeLa cells respectively.

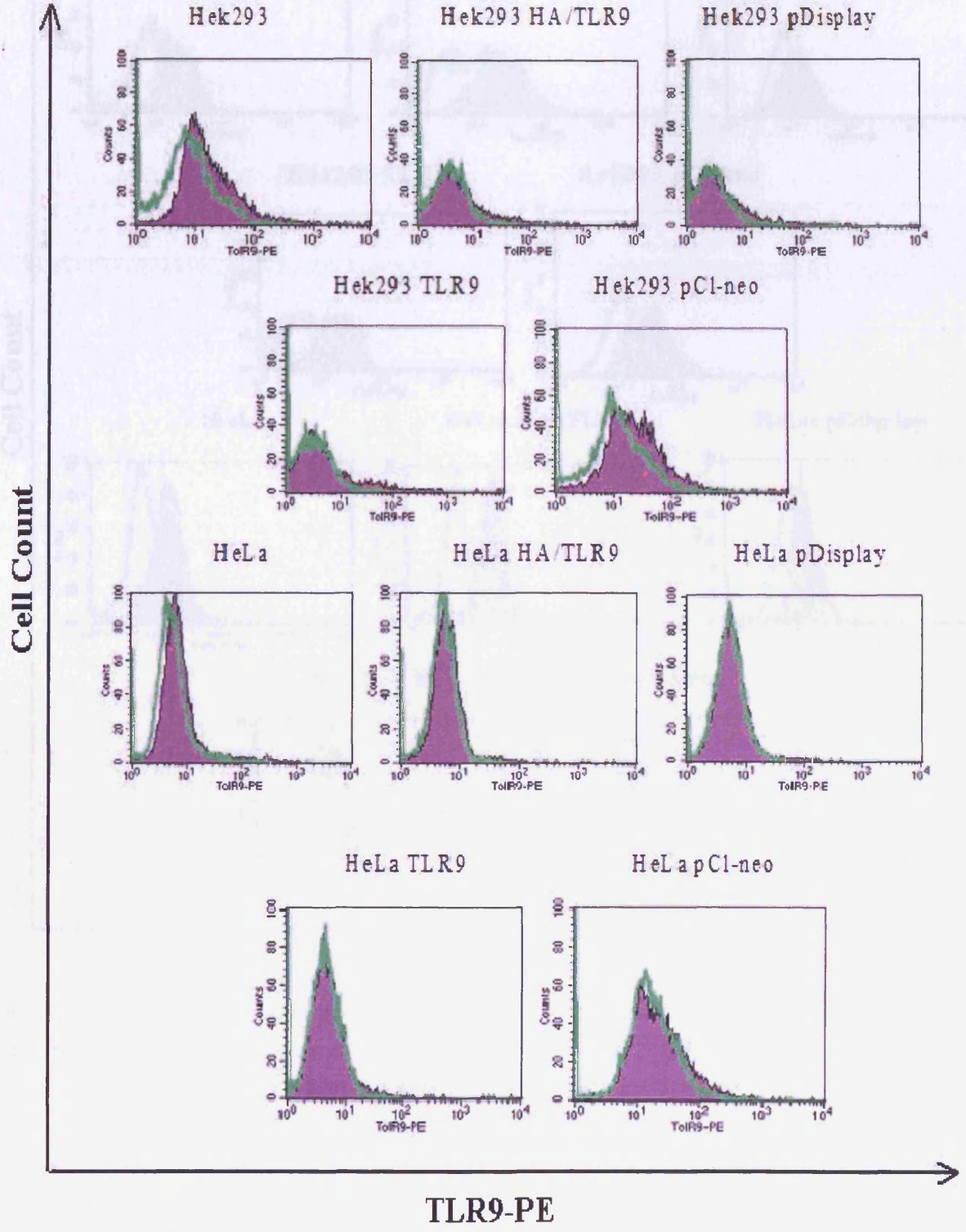

Figure 2.14. Flow cytometry overlay plots for the extracellular expression of TLR9 in Hek293 and HeLa cells and their transfectants. Legend: Green line: isotype control IgG1-PE. Purple blocks: TLR9 expression using anti-TLR9 PE Ab (eBioscience). This experiment was repeated in two independent times.

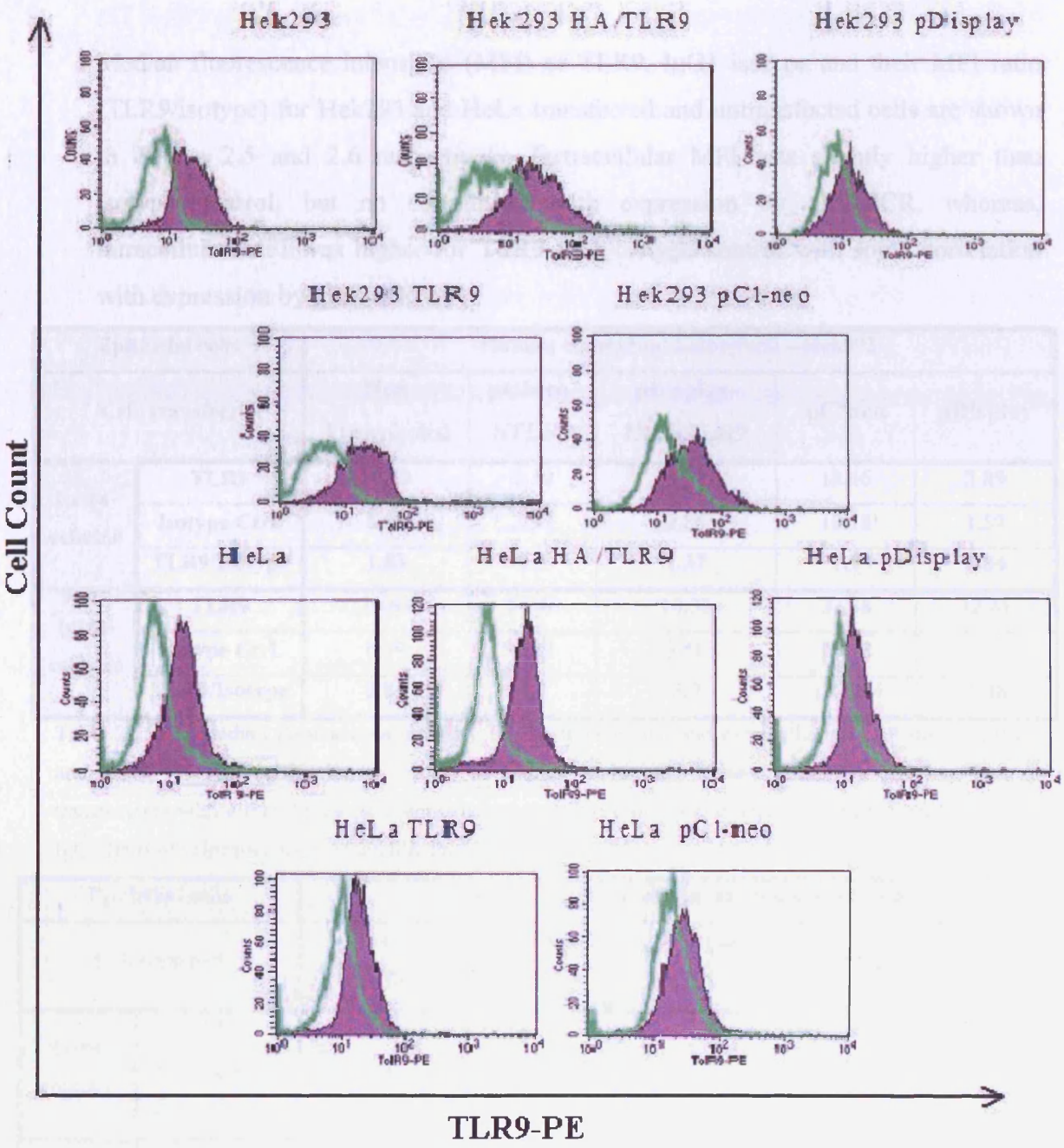

Figure 2.15. Flow cytometry overlay plots for the intracellular expression of TLR9 in Hek293 and HeLa cells and their transfectants. Legend: Green line: isotype control IgG1-PE. Purple blocks: TLR9 expression using anti-TLR9 PE Ab (eBioscience, USA). This experiment was repeated in two independent times.

TLR9 transfected Hek293 and HeLa cells overlay plots showed no clear shift in TLR9 extracellular expression compared with untransfected or mock transfected Hek293 and HeLa cells (Figure 2.14). In contrast, untransfected, TLR9 transfected and mock transfected Hek293 and HeLa cells showed a shift to the right from the isotype control in TLR9 intracellular stain (Figure 2.15), but the MFI ratio between TLR9 and isotype control showed some relative variations (Tables 2.5 and 2.6).

Median fluorescence intensities (MFI) of TLR9, IgG1 isotype and their MFI ratio (TLR9/isotype) for Hek293 and HeLa transfected and untransfected cells are shown in Tables 2.5 and 2.6 respectively. Extracellular MFI was slightly higher than isotype control, but no correlation with expression by qRT-PCR, whereas, intracellular MFI was higher for TLR9 than isotype control with some correlation with expression by qRT-PCR.

Epithelial cells		**Human embryonal kidney cell – Hek293**				
Cell transfect		**Non Transfected**	**pCIneo-hTLR9**	**pDisplay-HA/hTLR9**	**pCIneo**	**pDisplay**
Extra-cellular	**TLR9**	12.63	3.59	3.92	19.46	2.89
	Isotype Ctrl.	6.92	2.33	2.86	10.18	1.57
	TLR9/Isotype	**1.83**	**1.5**	**1.37**	**1.9**	**1.84**
Intra-cellular	**TLR9**	19.63	14.46	14.33	27.38	12.41
	Isotype Ctrl.	6.79	3.89	3.68	10.18	8.35
	TLR9/Isotype	**2.89**	**3.7**	**3.9**	**2.68**	**1.48**

Table 2.5. The median fluorescence intensity for the intracellular and extracellular TLR9 staining, using anti-TLR9 PE Ab. (eBioscience, USA), of human embryonal kidney (Hek293) cell line and its transfectants with either TLR9 gene construct or the empty plasmid, compared with the control isotype IgG1 IgG1-PE (Immunotech, Marseille, France).

Epithelial cells		**Human cervical carcinoma cell line – HeLa**				
Cell transfect		**Non Transfected**	**pCIneo-hTLR9**	**pDisplay-HA/hTLR9**	**pCIneo**	**pDisplay**
Extra-cellular	**TLR9**	6.32	4.61	5.94	18.11	5.23
	Isotype Ctrl.	4.87	4.26	5.14	15.26	4.91
	TLR9/Isotype	**1.30**	**1.08**	**1.15**	**1.19**	**1.07**
Intra-cellular	**TLR9**	15.68	18.94	18.11	26.18	14.86
	Isotype Ctrl.	6.21	9.73	5.09	16.70	8.35
	TLR9/Isotype	**2.5**	**1.95**	**3.56**	**1.57**	**1.78**

Table 2.6. The median fluorescence intensity for the intracellular and extracellular TLR9 staining, using anti-TLR9 PE Ab (eBioscience, USA), of human cervical carcinoma cell line (HeLa) cell line and its transfectants with either TLR9 gene construct or the empty plasmid, compared with the control isotype IgG1 IgG1-PE (Immunotech, Marseille, France).

Analysing the intracellular MFI TLR9/isotype control ratio in the same way as suggested previously for B-cells, ratios greater than three was suggested positive for intracellular TLR9 protein expression by flow cytometry, which was consistent with

RT-PCR results. Intracellular MFI ratio of TLR9/isotype control showed more than three for cells positive by RT-PCR (Hek293 TLR9, Hek293 HA/TLR9 and HeLa HA/TLR9) while it was less than three in cells negative by RT-PCR (Hek293, Hek293 pCl-neo, HeLa, HeLa TLR9, HeLa pDisplay and HeLa pCl-neo).

As PBMCs and BJAB cells were found to express TLR9 mRNA by RT-PCR, they were investigated for their TLR9 protein expression, before and after three days with 3µg/ml 10103 CpG-ODN. PBMCs and BJAB extracellular stain did not show a significant expression for TLR9 protein in resting or in CpG-ODN activated cells (data not shown). In contrast, intracellular stain showed some TLR9 protein expression in resting PBMCs and BJAB cells, which was enhanced two folds upon their activation with CpG-ODN, as indicated in Figure 2.16.

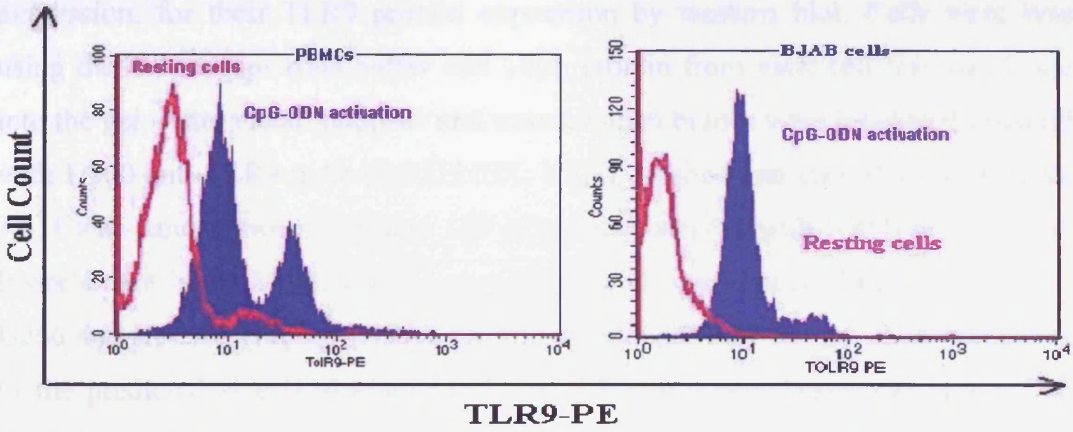

Figure 2.16. Flow cytometry overlay plots for the intracellular expression of TLR9 in resting and CpG-ODN activated normal PBMCs (left) and tumour BJAB (right) B-cells. Legend: Red line: TLR9 expression in Resting cells. Purple blocks: TLR9 expression in CpG-ODN activated cells. This experiment was done only once.

Extracellular expression of TLR9 by $CD19^{+}$ B-cells, some B-cell malignancies and TLR9 transfected Hek293 and HeLa cells has been reported by some groups, using indirect colour labelling techniques (Eaton-Bassiri A *et al.*, 2004; Baiyee EE *et al.*, 2006), also their TLR9 intracellular expression was expected from publications (Cynthia A *et al.*, 2004; Latz E *et al.*, 2004b; Fransson M *et al.*, 2007; Nakano S *et al.*, 2008) and from TLR9 mRNA levels detected in section (2.3.1). In this study, no clear evidence of extracellular staining, however, possible weak intracellular staining in TLR9 positive cells but data not conclusive. CpG-ODN activation increased levels of intracellular expression of TLR9 in PBMCs and BJAB cells, but not extracellular

expression. These observations made it imperative to confirm TLR9 protein expression by alternative methods, in order to validate the flow cytometric data.

2.3.2.2 Immunoprecipitation and Western blot.

As the data from the flow cytometry experiments did not completely agree with previously published literature for the expression of TLR9 in B-cells and other cells, and did not fully support the RT-PCR data, western blotting was performed to try to detect TLR9 protein expression by the different cell lines.

In the initial experiments, I used U266, Karpas and untransfected Hek293 cell lines, negative for TLR9 mRNA expression by PCR, as negative controls in western blotting and studied RPMI and Ramos cell lines, positive for TLR9 mRNA expression, for their TLR9 protein expression by western blot. Cells were lysed using the Tri-reagent lysis buffer and 10μg protein from each cell line was loaded into the gel. After electrophoresis and transfer, membranes were incubated overnight with 1:300 anti-TLR9 mAb (IMGENEX, USA), washed and stained with secondary Ab. Clear band between 100 and 150 kDa was observed with RPMI cells and to a lesser extent in RAMOS, while a very faint band was seen in Karpas, and none in U266 and Hek293 (Figure 2.17A). On the other hand, they did not show clear bands of the predicted size (116 kDa) for TLR9. The same membrane was stripped and blotted with 1:300 of the polyclonal Ab of anti-TLR9 (N-15) goat polyclonal IgG (Santa Cruz, USA). This did not show an observable band of the appropriate size (Figure 17B) in any of the cell lysates, while β-actin was detected at similar levels in all lysates (Figure 2.17C).

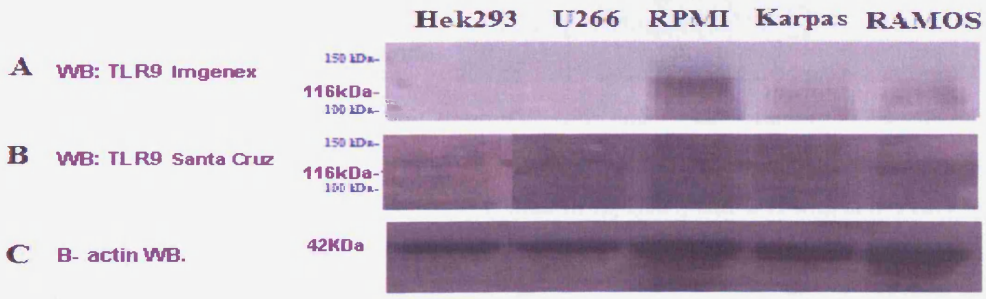

Figure 2.17. Tumour B-cells lysed by Tri Reagent™ (Sigma, UK) and blotted using two different TLR9 antibodies. Hek293 cells were used as a negative control. A) Membrane blotted with Anti-TLR9 mAb (IMGENEX, USA). B) The same membrane after stripping and blotting using polyclonal Anti-TLR9 antibody (Santa Cruz,USA). C) Protein levels of loaded samples using β-actin antibodies. U266, Karpas and Hek293 cell lines were used as a negative control (based on PCR results).

Given that the level of endogenously expressed TLR9 is very low in B-cells (Chen W *et al.*, 2005), western blotting using Tri-reagent lysis buffer may not be sufficiently sensitive to detect TLR9 protein, even when present. Dr. Leifer (Cornell University. NY, USA; personal communication) recommended the use of the lysis buffer used in Latz *et al.*, 2002 and to do immunoprecipitation before western blotting (Latz *et al.*, 2002). Lysing the tumour B-cells, immunoprecipitating the clear lysate with 1:300 anti-TLR9 (N-15) goat polyclonal IgG (Santa Cruz, USA), and western blotting with the same antibody, did not show any band at appropriate size (Figure 2.18A), but a 105 kDa band was seen in each lane. Similar results were seen after stripping the membrane and re-probing it with 1:500 anti-TLR9 mAb (IMGENEX, USA), (Figure 2.18b). Again a band at 105 kDa size was detected in all of the cells tested with IMGENEX mAb (Figure 2.18B). An additional band was seen in U266, Ramos and Hek293 cells at the size of 150 kDa, but none of the cell lines showed any band at the 116 kDa size after western blotting them by IMGENEX mAb (Figure 18B). Dr. Cynthia Leifer (USA, personal communication) observed that a band at about 160 kDa for TLR9 in the anti-TLR9 IP from the Ramos cells should be seen. Also, HA-TLR9 tagged Hek293 transfected cell should show an expression at about 160 KDa by western blotting.

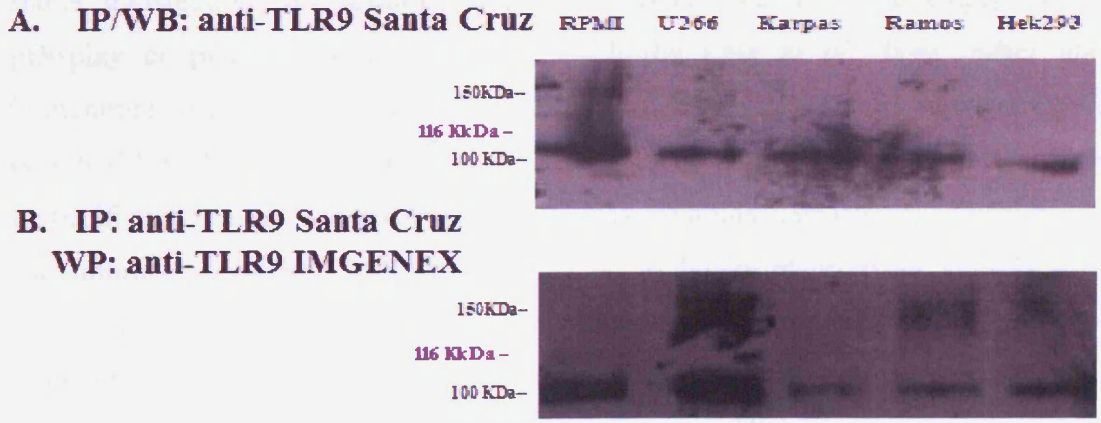

Figure 2.18. Immunoprecipitation of different tumour B-cells and Hek293 tumour cells using anti-TLR9 antibody (Santa Cruz, USA). A) IP and WB with the same antibody (anti-TLR9 antibody (Santa Cruz, USA). B) IP with anti-TLR9 antibody (Santa Cruz, USA) and WB with anti-TLR9 mAb (IMGENEX, USA). U266, Karpas and Hek293 cell lines were used as a negative control (based on PCR results).

Using a third TLR9 specific antibody, IP/WB with rat anti-TLR9 (eBioscience, USA) also could not detect the presence of hTLR9 of the predicted size (116 kDa), but in most of the cells an 80kDa band was observed (data not shown).

In view of the fact that flow cytometry could not reveal which cell lines are clearly positive or negative for TLR9 protein expression, and that immunoprecipitation and western blotting indicated bands between 80-150 kDa seen in both TLR9 positive and TLR9 negative cells by RT-PCR, a control group of experiments was carried out. Ramos, RPMI, U266 and Hek293 cell lines were immunoprecipitated with affinity purified rat IgG2a isotype control (eBioscience, USA) in parallel with anti-TLR9 antibodies (eBioscience, USA), and were then western blotted with the 1:500 anti-TLR9 (eBioscience, USA). Bands of 120 kDa and 90 kDa were seen only with all the isotype control IPs. On the other hand, a 200 kDa band was seen in cells immunoprecipitated with anti-TLR9 Ab (eBioscience, USA), but not with isotype control IPs (data not shown) although U266 and Hek293 are TLR9 negative by PCR.

Several reports studying TLR9 function had used Hek293 cell lines as a TLR9 negative model for transfection studies (Eaton-Bassiri A *et al.*, 2004; Latz E *et al.*, 2004; Latz E *et al.*, 200b; Hoene *et al.*, 2006). To have a definite positive control for the IP/WB, Hek293 and HeLa cells were transfected with expression plasmids containing full length TLR9, with and without HA-tag, using pDisplay-HA/hTLR9 or pCIneo-hTLR9 expression plasmids, and chemically selected in G418 to generate stable transfection. As controls, cells were transfected with the empty vector pDisplay or pClneo. Cells were lysed with the Latz *et al.*, lysis buffer and immunoprecipitated and blotted with either purified anti-TLR9 (eBioscience, USA) or anti-HA high affinity rat mAb-clone 3F10 (Roche Applied Sciences, UK) which is specific for HA-tag that is present in pDisplay plasmids. The isotype control lysate was immunoprecipitated with mouse IgG1 or rat IgG2a respectively. IP/WB with anti-TLR9 (eBioscience, USA) did not show the band of interest (data not shown). Immunoprecipitation and western blotting with 1:50 anti-HA peroxidase high affinity rat mAb-clone 3F10 (Roche Applied Sciences, UK) showed two bands over 100kDa (110 and 140 kDa), only in Hek293 HA/TLR9 cells, but not in HeLa HA/TLR9 cells, whereas their isotype controls and the non transfected Hek293 and HeLa cells showed a weak band at 150 kDa (Figure 2.19A). Re-blotting the same membrane with 1:500 affinity purified anti-hTLR9 (eBioscience, USA) overnight, no bands were seen between 100-150 kDa in the Hek293 HA/TLR9 nor the other cells (Figure 2.19B).

A. IP/WB: anti-HA Ab

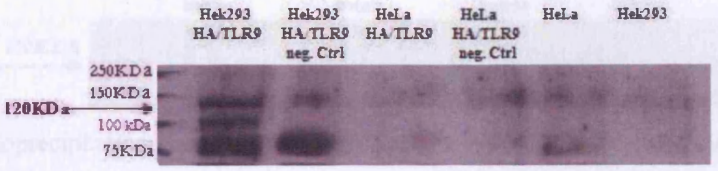

B. IP: anti-HA Ab
WB: anti-TLR9 Ab

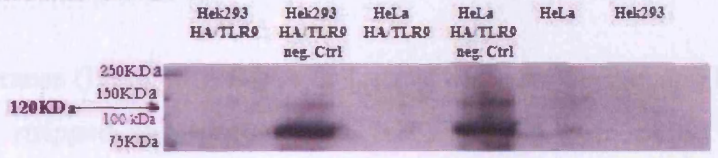

Figure 2.19. Immunoprecipitation / western blot for the presence of TLR9 protein in different HA-tagged transfectants of Hek293 and HeLa tumour cells using anti-HA antibody (Roche Applied Sciences, UK) and anti-TLR9 antibody (eBioscience, USA) after lysis with Latz *et al*, lysis buffer. Isotype controls for each cell line were used as a negative control. A) IP/WB with anti-HA Ab (Roche Applied Sciences, UK). B) IP with anti-HA Ab (Roche Applied Sciences, UK) and WB with anti-TLR9 antibody (eBioscience, USA).

Knowing that researchers used large amounts of protein for the IP (Hoene *et al.*, 2006), as the endogenous level of TLR9 was low (Chen W *et al.*, 2005), and some used RIPA lysis buffer to lyse the cells, experiments were repeated using $1x10^7$ of cells lysed by the two different lysing buffers (Latz *et al.*, or RIPA lysis buffer), and immunoprecipitated in 1:50 anti-HA high affinity rat mAb-clone 3F10 (Roche Applied Sciences, UK) overnight. Meanwhile, the isotype control cells were IP with affinity purified Rat IgG2a Ab (eBioscience, USA). Western blotting was followed with anti-HA rat mAb-HRP clone 3F10 (Roche Applied Sciences, UK). Blots lysed with RIPA lysis buffer, showed a 120 kDa faint band only in Hek293 and HeLa cells transfected with pDisplay-HA/hTLR9 (Figure 2.20), but not in the lanes precipitated with isotype control antibodies. Anti-HA rat mAb is specific for HA-tag which is present in pDisplay plasmids. pDisplay transfected Hek293 and HeLa cells showed a band slightly lower than 120kDa. Using Latz *et al.*, lysis buffer and IP/WB same cells, a band at 120kDa was only detected in Hek293 HA/TLR9 (data not shown).

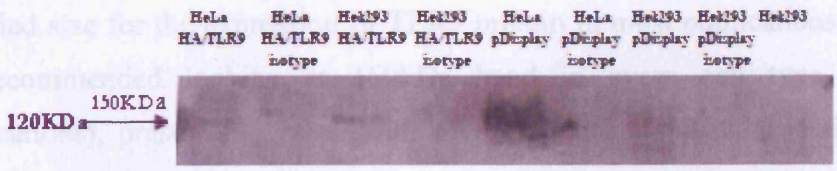

Figure 2.20. Immunoprecipitation / western blot with anti-HA Ab (Roche Applied Sciences, UK) for the presence of TLR9 protein using RIPA lysis buffer in HA-tagged TLR9 transfected epithelial tumour cells Hek293 and HeLa and their empty plasmid controls. IgG isotype for each cell line and untransfected Hek293 cells were used in immunoprecipitation as negative control.

The same membranes (lysed with RIPA or Latz *et al.*, lysis buffers and IP with anti-HA mAb) were stripped and blotted with 1:200 affinity purified rat anti-hTLR9 (eBioscience, USA). RIPA lysed blots showed a 120 kDa band for HeLa HA/TLR9 and a faint one for Hek293 HA/TLR9 (Figure 2.21A), but non-specific bands of other sizes were seen on the other cells. For Latz *et al.*, lysed blots, a band at 120 kDa was clearly detected in Hek293 HA/TLR9, but non-specific bands were seen in the other cells (Figure 2.21B).

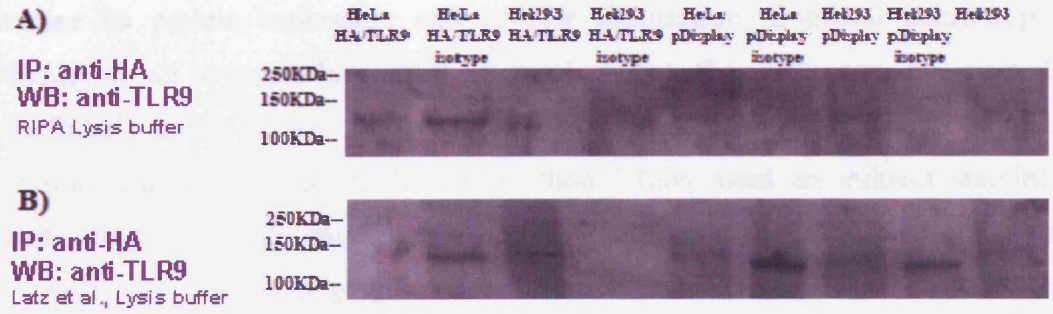

Figure 2.21. Immunoprecipitation with anti-HA Ab (Roche Applied Sciences, UK) and Western blotting with anti-TLR9 antibody (eBioscience, USA) for the presence of TLR9 protein using two different lysis buffers in HA-tagged TLR9 transfected epithelial tumours and their empty plasmid controls. IgG isotype for each cell line and untransfected Hek293 cells were used in immunoprecipitation as negative control. A) Cells lysed with RIPA lysis buffer. B) Cells lysed with Latz *et al.*, lysis buffer.

Overall, the use of three different antibody products specific for TLR9 in immunoprecipitation and western blotting could not consistently detect the expression of TLR9 in the haematological and non haematological tumours or stable TLR9 transfectants in a significant way, with some doubts about their quality for this purpose. Using large amount of anti-HA Abs in IP/WB and lysing the protein in RIPA lysis buffer showed a faint band of approximately the right size, although even the right size of the TLR9 band is of doubt. Although 115-120 kDa is predicted to be

the specified size for the expression of TLR9 protein in most publications, Leifer C (USA) recommended looking at 160kDa band in every cell type (personal communications), presumably as a result of post translational modification of the protein. The non-transfected cells did not show TLR9 expression with any of the different ways of immunoprecipitation and western blotting.

The data suggest that levels of TLR9 protein expression, even following forced, transgenic expression, may be too low to reliably detect by western blotting, with or without prior immunoprecipitation. Such results made it essential to verify TLR9 protein expression in tumour cells through a third method.

2.3.2.3 Confocal immunofluorescent microscopy:

To this point, I had shown the expression of TLR9 at the mRNA level by RT-PCR. In addition, I had investigated TLR9 protein detection by flow cytometry or IP/WB, however, they did not yield reliable results. A third method was therefore used to determine its protein expression and cellular localisation. Confocal microscopy technique is an immunofluorescent method where the cells can be stained extracellularly and/or intracellularly with anti-TLR9 mAb to detect the TLR9 protein expression and its localisation. In this method I have used an indirect staining method, using an affinity purified anti-human TLR9 rat mAb (eBioscience, USA) and a secondary Ab, goat polyclonal anti- rat IgG FITC Abs (Abcam, UK) to determine the expression of TLR9 protein in normal and tumour cells. To detect the efficiency and specificity of the technique, I have tested them on TLR9-transfected Hek293 cells which showed previously a high level of TLR9 mRNA expression. Hek293 TLR9 cells were stained with anti-TLR9 mAb cell-surface, and permealised for intracellular TLR9 expression.

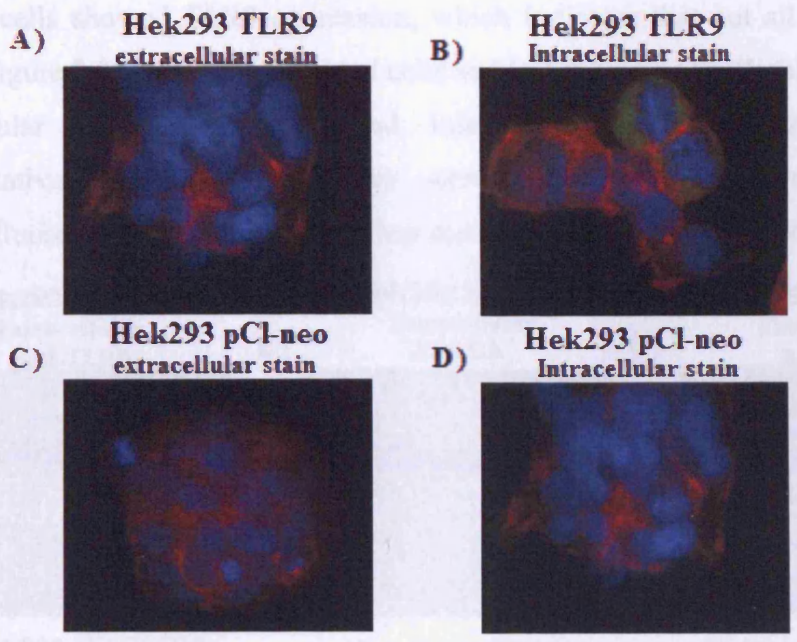

Figure 2.22. Confocal microscopy images of transfected Hek293 cells stained for extracellular (a & c) and intracellular (b & d) expression of TLR9 (green). (a & b) Hek293 TLR9 transfected cells, or mock plasmid pCl-neo transfected cells (c & d). Hek293 transfected cells were incubated with 1:20 dilution of affinity purified anti-human TLR9 rat mAb (eBioscience, USA). This experiment was done once in duplicate.

Figure 2.22 shows intracellular, but not extracellular expression of TLR9 in (some) TLR9 transfected, but not mock transfected Hek293 cells, also TLR9 construct gene was not expressed by all TLR9 transfected Hek293 cells indicating low transfection efficiency. To investigate the specificity of TLR9 antibody used in the last part, HA/TLR9 transfected Hek293 cells were tested using either anti-human TLR9 rat mAb (eBioscience, USA) or anti-HA high affinity rat mAb-clone 3F10 (Roche Applied Sciences, UK) to detect TLR9, or haemagglutinin attached to TLR9 gene, construct respectively. Hek293 cells transfected with HA/TLR9 or its mock construct (pDisplay) were stained extracellularly and intracellularly to determine the presence and localisation of HA, and hence the expression of TLR9 gene. As indicated in Figure 2.23, extracellular staining of HA/TLR9 transfected or mock transfected Hek293 cells did not show any expression. Meanwhile, intracellular staining with anti-TLR9 or anti-HA mAbs showed a significant stain of Hek293 HA/TLR9 transfected cells due to the presence of TLR9 and/or HA genes, indicating intracellular expression of TLR9 in Hek293 HA/TLR9 cells, but no expression was seen in the mock transfected controls. No clear difference was noticed in staining between the two different antibodies. However, only 30-40% of TLR9 transfected

Hek293 cells showed TLR9 expression, which indicates that not all cells express TLR9 (Figure 2.23). Mock transfected cells and isotype stained cells (shown only for extracellular Hek293 pDisplay and intracellular Hek293 HA/TLR9 as a representative example respectively) were used as a negative control in immunofluorescence staining, where they did not show TLR9 expression.

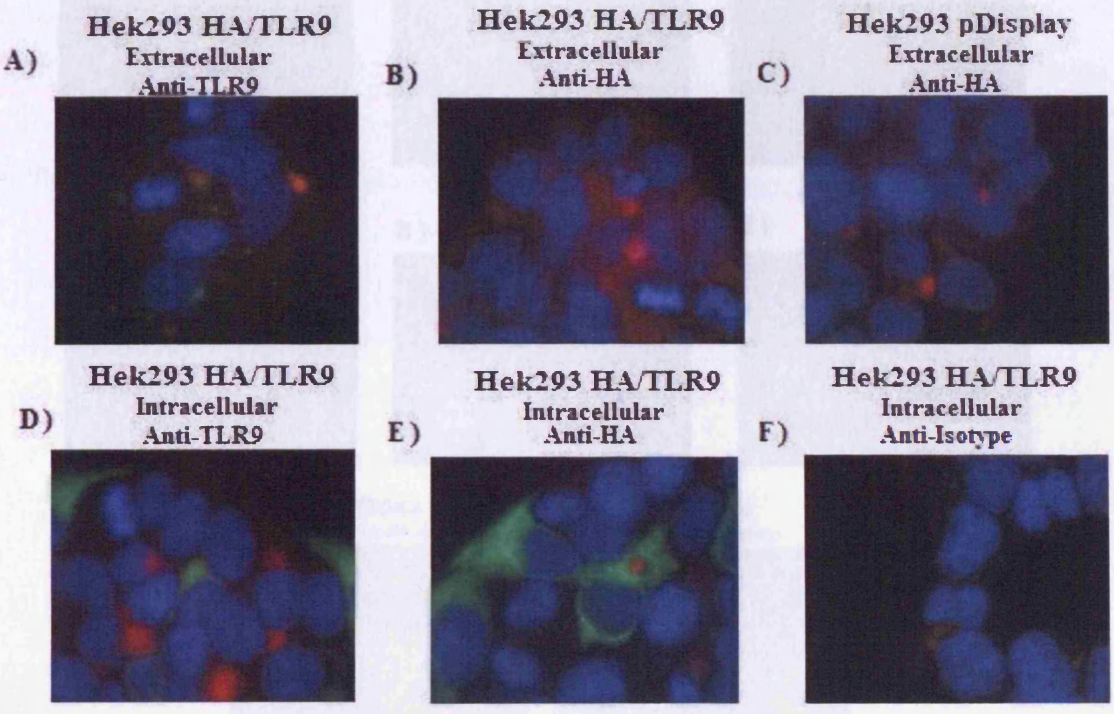

Figure 2.23. Confocal microscopy images of transfected Hek293 cells with pDisplay HA/TLR9 and pDisplay alone. Extracellular (a-c) and intracellular (d-f) staining for expression of TLR9 (green) (d & e) or mock plasmid pDisplay transfected Hek293 cells (c). Hek293 HA/TLR9 transfected cells and mock transfected cells were stained with Golgi stain (red) (NBD C_6 –ceramide complexed to BSA (Invitrogen, UK) and incubated with 1:20 dilution of affinity purified anti-human TLR9 rat mAb (eBioscience, USA) (a&d) or with anti-haemagglutinin (HA) high affinity rat mAb-clone 3F10 (Roche Applied Sciences, UK) (b, c & e). Mock Hek293 pDisplay cells and Hek293 HA/TLR9 cells stained with the isotype antibody (f) were used as negative control. This experiment was done once in duplicate.

To further address the expression and localisation of TLR9, tumour cells (TH044, LILA, U266, Karpas 707H, BJAB and Hek293 HA-TLR9 transfected cells) were stained with ceramide-BSA complex, which is a red fluorescent structural marker for Golgi Complex (NBD C_6–ceramide complexed to BSA; Invitrogen, UK), and counterstained for TLR9 expression using anti-human TLR9 rat mAb (eBioscience, USA) (Figures 2.24). As B-lymphocytes contain a large nucleus and very little cytoplasm, the Golgi complex was relatively not resolved with high precision in these cells, but still TLR9 gave distinguishable green staining that colocalised with

the red Golgi stain. On the other hand, TLR9 stain in Hek293 HA-TLR9 transfected cells was seen in the cytoplasm and not in Golgi complex (Figure 2.23), indicating that TLR9 transfected cells might reside in a different cellular compartment.

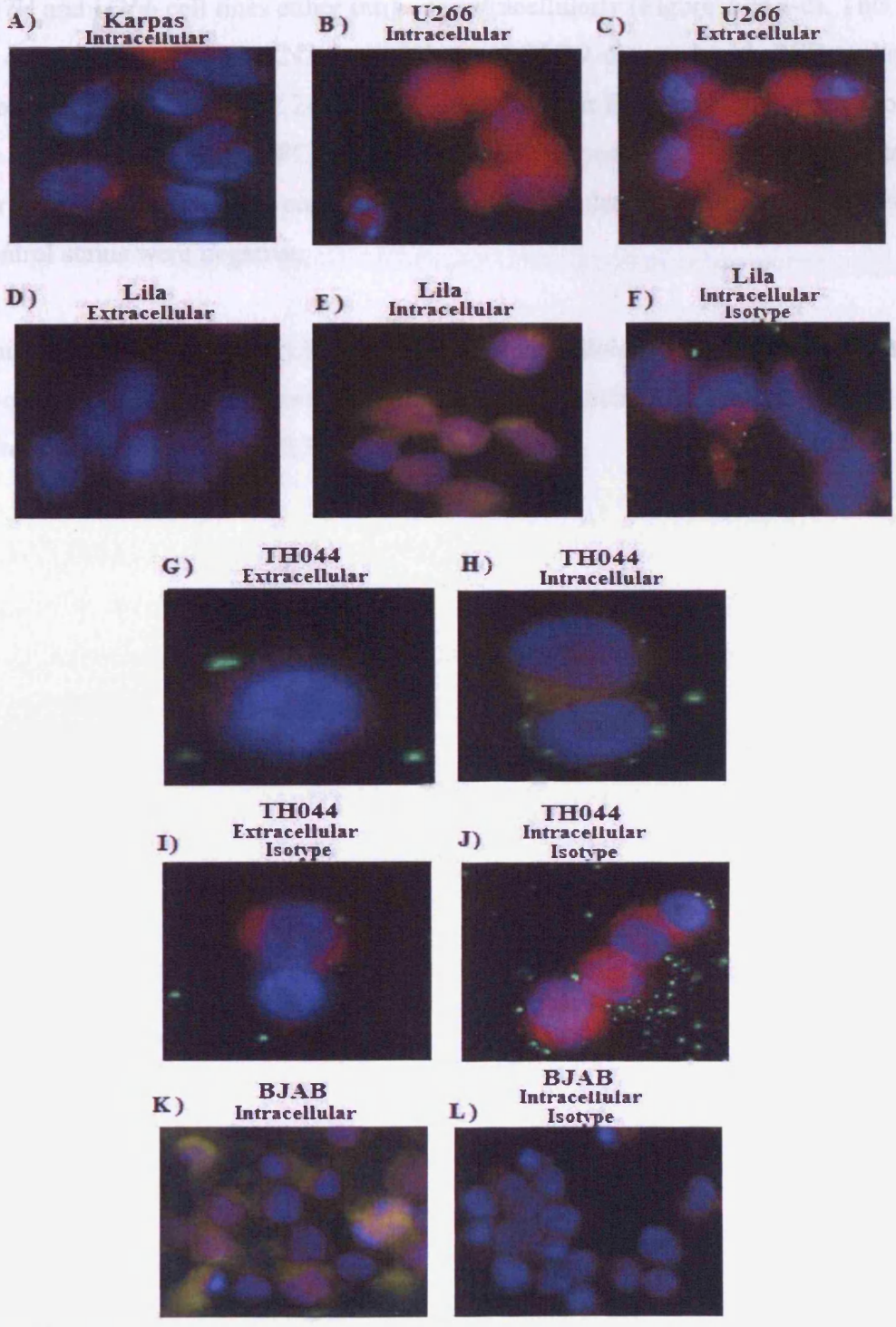

Figure 2.24. Confocal microscopy images of tumour B-cells extracelluarly and intracellularly stained for TLR9 (green) and Golgi stain (red) (NBD C_6–ceramide complexed to BSA (Invitrogen, UK). Cells were incubated with 1:20 dilution of affinity purified anti-human TLR9 rat mAb (eBioscience, USA) or with the isotype antibody a negative control. This experiment was done once in duplicate.

Figure 2.24 shows some representative images for TLR9 expression in *ex vivo* TH044 cells, and tumour B-cells (Karpas, U266, Lila and BJAB) from different differentiation stages. TLR9 protein was not detected in multiple myeloma Karpas 707H and U266 cell lines either intra- or extracellularly (Figure 2.24 a-c). This result is consistent with the mRNA expressions of TLR9 detected with PCR techniques (section 2.3.1.1). Figure (2.24 d-k) represents tumour B-cells that had been shown to be TLR9 positive by RT-PCR. None of them was positive by extracellular staining for TLR9, whereas all were positive by intracellular staining for TLR9. Isotype control stains were negative.

This would indicate that TLR9 is expressed intracellularly in TLR9 positive tumour B-cells and is not expressed extracellularly, which was consistent with flow cytometry results (section 2.3.2.1).

2.3 Discussion

Understanding the expression of functionally active TLR9 in human normal and tumour cells is an important consideration for the use of CpG in tumour immunotherapy. Whilst most studies have investigated the expression and role of TLR9 in normal cells of the immune system, considerably less is known about its expression and function in tumour cells. Detecting the TLR9 level of expression and the limits of activation in tumour cells would reveal its importance for influencing the immune system in relation to the potential role of TLR9 agonists in cancer immunotherapy. The goal of this part of the study was to investigate the extent and levels of TLR9 expression across a range of tumour types, and to identify tumour cell lines that are characterised by a high level of TLR9 expression for further studies on the role of TLR9 in these cells following stimulation with CpG ODN.

Although it was expected that the localisation of TLR9 and its translocation upon activation would add another important link with the innate immunity, there are no clear data available to show the importance between the localisation and function of the receptor. Barton and colleagues (2006) reported that the intracellular localisation of the TLR9 ensures that activation happens only upon the recognition of foreign CpG DNA, but not self-DNA. On the other hand, they showed that the surface expression of TLR9 did not prevent this recognition, but conferred the ability to recognise mammalian DNA. They suggested that the intracellular localisation is not required for the recognition, but it is significant in controlling the accessibility of TLR9 to the different DNA sources, and its localisation is crucial in differentiating self from non-self nucleic acids (Barton GM *et al.*, 2006). The method by which TLR9 gains access to internalised CpG ligands in human is still incompletely understood, although some recent studies on mice indicated the involvement of a multi-transmembrane-domain-containing protein (UNC93B1) in TLR9 trafficking from ER to the endosome (Brinkmann MM *et al.*, 2007; Kim YM *et al.*, 2008).

Previous studies have reported that TLR9 mRNA was found at high levels in normal tissues extracted from skeletal muscles and spleen (Du, X *et al.*, 2000; Nishimura M *et al.*, 2005). In humans, high signal intensities were also detected for TLR9 transcripts in the cytoplasm of lung cancer tissue specimens and they were functionally active while normal lung tissues showed weak expression of TLR9 (Droemann D *et al.*, 2005). Platz

J and colleagues reported a weak expression of TLR9 in respiratory epithelial cell lines and primary epithelial cells (Platz J *et al.*, 2004). These data suggested that TLR9 may be more widely expressed than solely in cells of the immune system.

To determine the expression of TLR9 in the haematological and non-haematological tumour cells I used methods to detect it on both levels of mRNA and protein expression. Determining the expression of TLR9 at the mRNA level was done by RT-PCR, and qRT-PCR, whereas the protein level by flow cytometry, western blotting, and confocal microscopy. In this work, I have established a positive control model by transfecting a TLR9 construct gene (alone or with haemagglutinin tag) into cell lines known not to express (or only to express at very low levels) TLR9, Hek293 and HeLa cell lines. A stable transfection was achieved, and TLR9 expression was detected at the mRNA level. Hek293 transfection showed a higher level of TLR9 mRNA expression than in HeLa cells, which was very low to almost negative for HeLa TLR9 cell line. Hek293 and HeLa cells were also transfected with the empty plasmid for each construct gene, where those mock transfectants showed no expression for TLR9. This would indicate that TLR9 mRNA expression detected by PCR was from the presence of TLR9 construct gene. Having validated the PCR method in this way, I used it to detect the expression of TLR9 mRNA in normal B-cells and a variety of tumour cells representing different stages of B-cell differentiation.

TLR9 mRNA expression was detected in many haematological normal and tumour cells. Normal peripheral blood mononuclear cells (PBMCs) and separated B-cells ($CD19^+$ B-cells) were tested from six healthy adults (three for each), detecting TLR9 mRNA in each case. $CD19^+$ *ex vivo* B-cells showed a clear TLR9 band expression by RT-PCR, and a highly significant expression level by qRT-PCR (more than $4x10^{-1}$ AU), that was the highest compared with the PBMCs and tumour cells. Normal PBMCs cells showed a significant expression of TLR9 mRNA (more than $1x10^{-2}$ AU). This was expected, as TLR9 is mostly expressed by B-cells which represent approximately 5% of cells in PBMCs. Most of the haematological tumour cells tested showed TLR9 mRNA expression, with a variation in its levels in each cell. Cells (PBMCs, $CD19^+$, TH044, FC029 and B-CLL *ex vivo* B-cells and RPMI, Ramos, Raji, ELIJAH, BJAB, 380, Lila and Tanoue tumour B-cells) expressed more than $1x10^{-2}$AU TLR9 mRNA level, and were considered positive for TLR9, whereas in HL-60, JVM-2 and KG-1 tumour cells

were considered low/equivocal, as TLR9 mRNA level was between $1x10^{-3}$ and $1x10^{-2}$ AU. Tumour cells (U266, Karpas 707H and HMy-2) with less than $1x10^{-3}$AU TLR9 mRNA level were considered negative for TLR9 expression. These results are consistent with publications where Ramos, RPMI 8226, PBMCs, BJAB cells were used as a positive control for TLR9 expression (Leifer CA *et al.*, 2004; Takeshita F *et al.*, 2004; Baiyee EE *et al.*, 2006; Longo PG *et al.*, 2007 respectively). Brouke E and colleagues (2003) reported that, Epstein-Barr virus (EBV)–transformed cell lines and other cell lines representative of mature B-cell neoplasias (Burkitt's lymphoma and follicular lymphoma) expressed TLR9 mRNA, whereas pre-B cell lines were negative. Also, Jahrsdorfer B and colleagues (2005) reported that TLR9 mRNA was present in B-CLL but absent in plasmacytoma isolated from bone marrow of patients with multiple myeloma, this was consistent with my results were B-CLL cells expressed TLR9 mRNA while Karpas and U266 multiple myeloma cell lines did not.

To determine TLR9 mRNA expression in non-haematological tumour cells, epithelial and melanoma cell lines MCF-7, CORL-47, HeLa, Hek293, DU-145, HRT-18 and WM1361A were tested. According to their TLR9 mRNA expression levels most of them were less than $1x10^{-3}$AU indicating negative TLR9 mRNA expression. HeLa and HRT-18 tumour cell lines showed a weak/low positive TLR9 mRNA expression (more than $1x10^{-3}$AU, but less than $1x10^{-2}$AU). TLR9 transfected Hek293 cells were more than $1x10^{-2}$AU indicating that they are TLR9 mRNA positive cells. Untransfected and mock transfected Hek293 cells did not express TLR9 mRNA as they showed mRNA level less than $1x10^{-3}$ AU. In TLR9 transfected HeLa cells, HeLa HA/TLR9 were the only cells that showed TLR9 mRNA level, above $1x10^{-2}$ AU, whereas it did not show a significant TLR9 mRNA expression in HeLa TLR9 cells (less than $1x10^{-3}$AU). Untransfected and mock transfected HeLa cells showed low/equivocal TLR9 mRNA level (between $1x10^{-3}$ and $1x10^{-2}$ AU). Such results were also found in others work (Hoene V *et al.*, 2006).

The expression levels in human epithelial tumour cell lines and mock transfected Hek293 cells were almost similar to the 'negative' cell lines U266, Karpas and HMy-2. HeLa TLR9 cells showed some TLR9 mRNA expression, to levels similar to weak positive B-cell lines, HL-60, JVM-2 and KG-1, suggesting that they were not highly transfected. In contrast, TLR9 transfected Hek293 cells showed TLR9 mRNA levels similar to Ramos and 380 tumour B-cells, suggesting that Hek293 was successfully

transfected with TLR9 and HA/TLR9. The very low basal levels of TLR9 mRNA expression in the epithelial tumours might render them to be non-functional as toll like receptors.

Several reports indicated the expression of TLR9 protein by flow cytometry. Extracellular expression of TLR9 by B-cells and TLR9 transfected Hek293 and HeLa cells has been investigated by some groups, using indirect colour labelling techniques (Eaton-Bassiri A *et al.*, 2004; Baiyee EE *et al.*, 2006). Their TLR9 intracellular expression was also reported in several publications (Cynthia A *et al.*, 2004; Latz E *et al.*, 2004b; Fransson M *et al.*, 2007; Nakano S *et al.*, 2008). In this study, looking for the TLR9 protein expression by flow cytometry using a direct stain revealed that the surface protein expression of TLR9 in resting human B cells ($CD19^+$) and a broad range of different cell types were low to undetectable. TLR9 transfected Hek293 and HeLa cells also showed no clear surface expression of TLR9. Similarly, indirect immunofluorescent staining and confocal microscopy could not show a clear surface expression in TLR9 transfected Hek293 cells and the other TLR9 positive (by RT-PCR) tumour cells tested. On the other hand, conflicting data have been reported concerning the cell surface TLR9 expression. Eaton-Bassiri and colleagues (2004) reported that the average frequency of cell surface TLR9 expressing PBMCs was 10.1% ± 5.7% of live gated cells, relative to 0.9% ± 0.4% for isotype control. Dasari P *et al.*, (2005) had detected the surface expression of TLR9 on 15-90% of resting B cells using a three colour flow cytometry method. Meanwhile, initial TLR9 transfection studies (Takeshita F *et al.*, 2001; Chaung TH *et al.*, 2002) staining with the anti-tagged Abs (HA- and Flag- tags respectively) found that TLR9 was expressed on their cell surface after TLR9 transfection. Later on, Latz E *et al.*, (2004b), using the eBioscience rat anti-human TLR9 mAb, could not detect cell surface TLR9 expression by confocal microscopy on TLR9 transfected Hek293 cells. In my study, cell lines tested were not identical in their MFI for surface staining with anti-TLR9 mAb, which was consistently higher than the isotype control, but with no correlation with TLR9 mRNA expression by RT-PCR.

As a conclusion, detecting TLR9 surface expression in tumour cells may depend on a number of factors including cell type and method used. Researchers who have been able to detect TLR9 surface expression worked mostly on normal B-cells or macrophages/monocytes and used an indirect method of either three colour stain for

TLR9 (Dasari P *et al.*, 2005) or indirectly looking for a conjugated tag (Takeshita F *et al.*, 2001; Chaung TH *et al.*, 2002). Working with a direct staining technique to detect TLR9 protein might not be sufficiently sensitive to give clear results.

Moreover, an apparent intracellular expression of TLR9 was noticed in cells showing MFI ratios more than three between TLR9 and the isotype control, which was broadly consistent with the results by RT-PCR. Comparing the MFI ratio for the intracellular expression of TLR9 in haematological tumour cells with the positive control of resting $CD19^+$ B-cells, U266 and Karpas tumour B-cells (TLR9 negative by RT-PCR) showed less than three folds. The data suggest that, MFI TLR9/isotype control ratio of greater than three might correlate with intracellular TLR9 protein expression. However, using a blocking peptide did not make any noticeable difference in comparison with the non-blocked stained PBMCs for the intracellular expression of TLR9, suggesting that staining with the anti-TLR9 antibody compared with the isotype control was not antigen specific. CpG-ODN activated PBMCs and BJAB cells showed a significant upregulation in the intracellular expression of TLR9 compared with the resting non-activated cells. Furthermore, TLR9 transfected Hek293 cells and HeLa HA/TLR9 tumour cell did show a clear increase in MFI ratio compared with the untransfected or mock transfected Hek293 and HeLa cells which was consistent with qRT-PCR results. These results are consistent with other researchers where they found that TLR9 is retained intracellularly and not detected on the cell surface in cells endogenously expressing TLR9 as Ramos cell line or in TLR9 transfected Hek293 cells (Leifer CA *et al.,* 2004).

In summary for the flow cytometry results, no clear evidence of extracellular expression of TLR9 by $CD19^+$ B-cells, some B-cell malignancies and TLR9 transfected Hek293 and HeLa cells, but possible weak intracellular expression in cells positive for TLR9 by PCR, but data not conclusive. CpG-ODN activation increased levels of intracellular expression of TLR9 protein in PBMCs and BJAB cells, but not extracellular expression.

Several reports studying TLR9 function had used Hek293 cell lines as a TLR9 negative model for transfection studies (Eaton-Bassiri A *et al.*, 2004; Latz E *et al.*, 2004b; Leifer CA *et al.,* 2004; Hoene *et al.*, 2006). Hoene and colleagues (2006), have used Hek293 cells as a model and transfected them with hTLR9 gene construct, to have a positive model for their study. Their RT-PCR and FACS data indicated that untransfected

Hek293 cells also express TLR9, but at very low levels (Hoene *et al.*, 2006). This was consistent with my results for Hek293 and HeLa cells.

TLR9 protein expression was detectable using immunofluorescent confocal microscopy and showed an intracellular TLR9 expression in TLR9 transfected Hek293 cells, and TLR9 positive (by PCR) TH044, LILA and BJAB cell lines, while it was negative for the mock transfected Hek293 cells, TLR9 negative (by PCR) U266 and Karpas 707H multiple myeloma cell lines and the negative controls stained with the isotype antibodies. Less than 50% of TLR9 transfected Hek293 cells showed an expression for TLR9 by confocal microscopy. This might be due to several factors affecting stable transfection. Stable transfection with linear DNA yields optimal integration of DNA into the host genome, but it also results in lower DNA uptake by the cells. The plasmid promoter is critical for efficient expression of the transfected gene, as strong CMV promoter in the transfected plasmid might not be functional all the time. Also, transfected DNA in stable transfection cells is integrated into the host chromosome, and so depending on the site of integration, the flanking sequences might strongly influence the expression of the DNA by either increasing or decreasing the expression of the gene of interest. Finally, the cells with the inserted plasmid might lose their growth advantage if the gene product has a negative effect, and the constitutive expression might decrease with time (Qiagen transfection resource book, http://www1.qiagen.com/literature/brochures/tfbr/1020182_BRO_TF_0302WW.pdf).

In summary, cells that showed mRNA expression of TLR9 (by PCR), also showed intracellular TLR9 protein by confocal microscopy, and (to a degree) by flow cytometry, but did not show clear evidence of cell surface expression. As the same monoclonal antibody was used in these two methods, the data suggests that an indirect staining method and confocal microscopy was a more sensitive method for detecting TLR9 expression than a directly conjugated monoclonal antibody and flow cytometry.

As publications stated (An H *et al.*, 2002; Chen W *et al.*, 2005; Baiyee EE *et al.*, 2006), TLR9 expression can be upregulated upon the activation of the cells. I have checked the protein expression of TLR9 using immunofluorescent flow cytometry on resting and CpG-ODN activated PBMCs and BJAB cells. Intracellular TLR9 protein expression was significantly enhanced in the activated cells whereas it did not show any upregulation in

the surface expression of TLR9 protein. I did not check TLR9 upregulation using the other techniques, as it was not of the main aims in this work, as I mainly wanted to check TLR9 expression in tumour cells. This could be done in future work, to detect the effect of different factors on the upregulation of TLR9 in tumour cells.

Western blotting was also used to look for the expression of TLR9 protein in normal and tumour cells. I did not find any consistent bands of an appropriate size, and there was poor correlation between western blotting and either PCR or immunofluorescence techniques. Cells were lysed with three different lysis buffers for the detection of TLR9 protein before western blotting, and no consistent bands of the appropriate size were seen in cells from each lysis buffer. Furthermore, since the endogenous TLR9 protein is low (Chen W *et al.*, 2005), immunoprecipitation was a necessity before western blotting. In addition, different clones of TLR9 antibodies were used in IP and WB to determine the expression of TLR9 protein, and primary antibodies directed against either TLR9 or HA-tagged proteins to determine TLR9 expression in HA/TLR9 transfected cells were also used. While the size of hTLR9 is predicted to be 115.9 kDa (Chuang, TH *et al.*, 2000), in most of the published reports the size of the hTLR9 protein band was variable, ranging from 100 to 200 kDa (Leifer CA *et al.*, 2004; Hoene V *et al.*, 2006) and others did not even mention the size (Chen W *et al.*, 2005). In my experiments, western blots used did not show a detectable TLR9 protein band when lysed by either of the lysis buffers (Tri reagent and Latz *et al.*, buffers). IP/WB using anti-TLR9 antibodies revealed variable and weak bands ranging from 80-150 kDa. However, bands of a similar size were also observed with the negative controls for the TLR9, indicating that these were not TLR9 specific. Tumour B-cells did not show a clear significant band for TLR9 protein expression. Researchers working on tumour B-cells showed TLR9 protein expression by western blotting after stimulating the cells (Chen W *et al.*, 2005), while in my experiments I only attempted to detect their expression in a resting, non-active state.

Using immunoprecipitation of HA-tagged transfectants with large amounts of anti-HA antibodies, after lysing with RIPA lysis buffer, and blotting with the same anti-HA antibody, I was able to detect a faint band of the predicted size (120 kDa) in Hek293 and HeLa HA/TLR9 transfectants, whilst using Latz *et al.*, lysis buffer showed it only in Hek293 HA/TLR9 transfectants. Immunoprecipitation with anti-HA did not show a significant difference in the HA/TLR9 transfected Hek293 and HeLa cells from the

mock transfectants, when anti-TLR9 mAb was used for western blotting, using the two different lysis buffers. Hek293 TLR9, Hek293 HA/TLR9 and HeLa HA/TLR9 were shown to express TLR9 mRNA by qRT-PCR, but almost ten times less than RPMI cell lines which are known for their low endogenous TLR9 protein expression (Chen W *et al.*, 2005). As a conclusion, anti-TLR9 mAb might be of low affinity/avidity, or the technique is not sensitive enough to detect the low TLR9 protein expression.

Although TLR9 antibodies used were produced to be applicable in FACS and IP/WB, doubts were raised concerning their sensitivity, as other researchers could not get reliable results for the detection of TLR9 protein expression (Hoene V *et al.*, 2006). Whether this was due to the sensitivity of the antibodies or to the sensitivity of the techniques, is not clear as their results were not conclusive. My results were consistent with a recent study (Hoene V *et al.*, 2006), which found that the use of TLR9 antibodies was not conclusive, and the necessity for working with high amounts of total cellular protein was required. From that, the necessity to use a sensitive detection method is consistent with the low expression levels of TLR9 in the cells.

Recent studies (Latz E *et al.*, 2004b) found that the majority of human TLR9 was expressed intracellularly, but that TLR9 could also be surface accessible following exposure to CpG-DNA. Failure to detect the cell surface TLR9 expression on human cells does not mean that they are not expressed on the surface, but there might be low surface expression level that was not detected in my assay. Theoretically, expression of TLR9 at the cell surface might be of crucial relevance for primary human antigen-presenting cells, and required for those receptors to play an active role in cellular activity or immune function (Eaton-Bassiri A *et al.*, 2004). Not being able to detect the surface expression of TLR9 in PBMCs, a known positive control for TLR9 expression, compared with published data (Eaton-Bassiri A *et al.*, 2004; Dasari P *et al.*, 2005) indicates that the sensitivity of the antibody or the method was not sufficient to detect the surface expression. Furthermore, most of the researchers looked at the expression of TLR9 by immune cells using RT-PCR–based methods (Hornung V *et al.*, 2002; Brouke E *et al.*, 2003; Baiyee EE *et al.*, 2006). There is less information available about the cellular localisation of TLR9 due to the limited availability of monoclonal antibodies directed against TLR9. For that, those who studied the expression by using monoclonal antibodies, used indirect staining for immunofluorescence techniques and indicated that, in PBMCs TLR9 was expressed on the cell surface and intracellularly (Eaton-Bassiri A

et al., 2004; Dasari P *et al.*, 2005; Baiyee EE *et al.*, 2006). However, Latz E and colleagues (2004b) and Leifer CA and her colleagues (2004) stated that TLR9 expression was absent from the plasma membrane of resting TLR9 transfected Hek293 cells, but present intracellularly which was consistent with my results.

Eaton-Bassiri and colleagues (2004) have reported the specificity and sensitivity of flow cytometric human TLR9 staining, by making their own anti-human TLR9 mAb, and validated their results using immunofluorescence confocal microscopy technique. Hence, they were able to detect TLR9 expression at the cell surface of primary human cells, indicating that the failure to detect cell surface expression on primary human cells may be due to low level of cell surface TLR9 expression, technique sensitivity and antibody affinity (Eaton-Bassiri A *et al.*, 2004). The need to generate a number of monoclonal antibodies with high specificity and sensitivity for TLR9 is highlighted by these data. The 8th International Workshop on human Leukocytes Differentiation Antigen (HLDA8) Dec. 2004 (www.hlda8.org), had generated a number of monoclonal antibodies for the different TLRs, but still need a highly sensitive one for the detection of the low TLR9 expression.

In summary, this study reveals that the analysis of TLR9 expression in human tumour cells is favoured by using immunofluorescence confocal microscopy and PCR, which are sensitive methods. Immunofluorescence confocal microscopy method was the most convenient method to localise the TLR9 protein expression, which was clearly expressed intracellularly. qRT-PCR, a semi-quantitative method to assess the number of transcripts of the target mRNA, was the most convenient method for TLR9 mRNA expression. In agreement with the immunofluorescent flow cytometry results, I was not able to detect TLR9 expression on the surface of TLR9 transfected Hek293 and HeLa cells or B-cell lines, although they showed (weak) intracellular TLR9 expression by immunofluorescent flow cytometry and confocal microscopy. WB/IP was not a specific and sensitive method for the detection of the low TLR9 protein expression levels. Therefore, immunofluorescence confocal microscopy was specific and sensitive enough to show the expression of TLR9 protein and correlated with RT-PCR, indicating that the antibodies used were indeed TLR9 specific. However, levels of expression of mRNA may not correlate with expression of the protein. Longo PG and Colleagues (2007) reported considerable variations in the levels of TLR9 mRNA and protein in normal

PBMCs and B-CLL cells, but with no correlation with their CpG-ODN mediated cellular proliferation response. This was also seen in my results, however, more immunofluorescence staining and functional studies of TLR9-mediated cell activation would be required to determine whether mRNA detection correlated with expression of a functional protein.

2.4 Conclusion

TLR9 expression was not convincingly demonstrated by flow cytometry and IP/WB using monoclonal antibody stains of isolated human PBMC and/or haematological and non-haematological tumour cells or TLR9 transfectants stained for cell surface or intracellular TLR9 expression. This may be due to limitations of antigen recognition, antibody affinity/avidity by directly conjugated monoclonal antibodies in flow cytometry, and unconjugated antibodies in IP/WB, or due to low levels of protein expression, or a combination of the two. Another important factor that might contribute is the sensitivity of the techniques. Immunofluorescent results obtained by confocal microscopy using the same antibodies and an indirect staining method were consistent with RT-PCR results, suggesting that antibody specificity was not the problem. The differences between the flow cytometry, IP/WB, immunofluorescent stain and the RT-PCR for the expression of TLR9 in this work suggest that immunofluorescence confocal microscopy and PCR-based methods were the most sensitive techniques for the detection of TLR9.

In conclusion, all of the tested haematological tumour cells were TLR9 positive with the exception of multiple myeloma U266 and Karpas cell lines and EBV transformed B lymphoblastoid HMy-2 cell line, whereas all of the non-haematological tumour cells were negative for TLR9 expression, using PCR based methods. These results support the assumption that different types of malignancies express TLR9 to markedly different levels and are therefore likely to respond differently to treatment with CpG-ODN. This would give the TLR9 positive tumour expressing cells a higher chance of immunological treatment, depending on their response. Finally, CpG-ODN can activate B-cells leading to upregulation of the intracellular TLR9 protein expression compared to the resting cells. The expression of functionally active TLR9 in human tumour cells would trigger the immune responses at both the innate and adaptive levels, promoting a valuable method for the treatment of cancer. Accordingly, tumour cells that express a functionally active level of TLR9 would have a better chance to be treated effectively. Unfortunately, for tumour-immunologists, the cellular patterns of TLR9 expression vary between different types of tumours and thus their response to CpG-ODN. For that reason, further experiments, including RT-PCR and staining with specific and sensitive TLR9 antibodies, seem necessary to clarify TLR9 expression patterns in various tissues and to correlate that with the functional studies of TLR9-mediated cell activation.

CHAPTER THREE

CpG-ODN Mediated Responses and TLR9

CHAPTER THREE
CpG-ODN mediated responses and TLR9

3.1 Introduction:

The immune system has developed defence mechanisms against viral and bacterial infections by detecting subtle differences in the chemical structure between microbial and host DNA. It uses TLR9 (in the cells that express TLR9) for this detection by looking for unmethylated CpG dinucleotides which are relatively common in viral and bacterial genomes, but uncommon in mammalian DNA (Hemmi H *et al.*, 2000). A critical advance in understanding the mechanism of action for TLR9 was to identify its synthetic agonist, CpG-ODN. Different classes of CpG-ODN are characterised, each with distinct effects on the immune response, and CpG-B ('K'-type) is particularly effective for activating B-cells. The human type-B CpG motif2006 CpG-ODN (5'- TCG TCG TTT **T**GT CGT TTT GTC GTT -3' (24 mer) oligo-nucleotide was identified and developed (Hartmann G. and Krieg AM. 2000). 2006 CpG-ODN was used in the majority of studies to activate human B–cells (Krieg AM 2002a; Krieg AM 2002b; Latz E *et al.*, 2004a; Vollmer J *et al.*, 2004a; Jahrsdorfer B *et al.*, 2005). In the first few months of this study, I worked with 2006 CpG-ODN, which was then replaced with 10103 CpG-ODN by Coley pharmaceutical group-USA. 10103 CpG-ODN (5'- TCG TCG TTT **C**GT CGT TTT GTC GTT -3' (24 mer) is the new CpG-ODN type-B that activates B-cells and modulates the immune response in the same way as 2006 CpG-ODN. 10103 CpG-ODN differs from 2006 CpG-ODN by a single base, indicated in bold type in the sequence above. ODN 2137 (5'-TGC TGC TTT TGT **GC**T TTT GT**G** CTT-3') in which the CpG motifs of ODN 2006 are inverted to GpC (indicated in bold type in the sequence above), and which as a result possesses six TG dinucleotides (thymidine-rich), was used as a non-CpG control in some of the studies.

The discovery of the receptor-ligand interaction between TLR9 and CpG-ODN shed new light on the TLR9 identity and helped in identifying the functional effect of CpG-ODN on cell lines and primary cells. Optimal CpG-B ODN is a strong mitogen for B-cells. Limited information is known about tumour cells and their responses to CpG-ODN activation, but such activation via TLR9 would be expected to make the tumour cells more visible for innate and acquired immunity. Not all immune cells are known to express TLR9 and not all the tumour cells examined in this work expressed TLR9

(Chapter Two), therefore the response of the immune cells to the tumours might vary, depending on whether the tumour cells are activated directly by CpG-ODN. CpG-ODN mediates several immune responses in normal human B-cell (Jahrsdorfer B *et al.*, 2001; Verthelyi *et al.*, 2001; Henault M *et al.*, 2005; Grandjenette C *et al.*, 2007). CpG-ODN activated B-cells strongly proliferate and upregulate the expression of costimulatory surface antigens, in addition to other immune mediated responses.

Jahrsdrofer B *et al.*, 2005, tested different B-cell malignancies, and found that most of them expressed TLR9 and responded to CpG DNA activation, with the exception of plasmacytoma cells. As B-cell malignancies are derived from a potential antigen-presenting cell, they might express TLR9 at constitutively high levels. Following CpG-ODN stimulation, intracellular TLR9 would internalize into an endoplasmic compartment where CpG-ODN motif would recognize and bind TLR9, leading to the rapid activation of adaptor molecules, MyD88, IRAK-1, IRF-7, and TRAF-6 (Akira S *et al.*, 2003; Akira S *et al.*, 2004). This would go into a signalling cascade leading to the rapid activation of several mitogen-activated protein kinases, including ERK1/2, p38 ^{MAPK} protein kinase, c-Jun NH_2-terminal kinase (JNK), and PI3-kinase/AKT, in addition to NF-κB complex, the down stream target of p38 ^{MAPK}. Finally, CpG-ODN activation of tumour cells might result in the induction of cytokines such as TNF-α, IL-6, IL-10, IL-12 and IFN-γ (Wooldridge JE *et al.*, 1997; Smith JB *et al.*, 1998).

In normal B-cells, activation of TLR9 would activate those downstream signalling kinase pathways resulting in the upregulation of the relevant surface markers (MHC class II, CD54, CD80 and CD86) and cellular proliferation. Although haematological tumour cells tested here are mostly B-cells, not all showed TLR9 expression, as discussed in Chapter Two. However, there is only limited information on the CpG-ODN sensitivity of tumour B-cells. Therefore, the aims of the present study were firstly to identify CpG-ODN responsive tumour cells, the relationship between the expression of hTLR9 and the CpG-mediated response in human tumour cells, and to determine the role of hTLR9 in CpG-mediated response in the human tumour cells. In addition to that, to detect the CpG-mediated response in the TLR9 transfected Hek293 and HeLa cells. This should define and characterize the CpG-ODN mediated response in CpG responsive tumour cells.

3.2 Materials and Methods:

3.2.1 Materials:

- 10103 CpG ODN (Coley Pharmaceutical, Canada)
- Anti-CD54-PE (ICAM-1) mAb, Beckman Coulter, UK)
- Anti-CD80-FITC mAb (clone MAB104, Beckman Coulter, UK)
- CD86-PE mAb (clone HA5.2B7, Beckman Coulter, UK)
- Anti-MHC II-FITC mAb (mouse anti-human HLA-DP DQ, Dako , UK)
- IgG1-PE isotype control monoclonal antibody (Beckman Coulter, UK)
- IgG1-FITC isotype control mAb (Beckman Coulter, UK).
- Rabbit polyclonal anti-p-IκB-α Ab (Ser 32)-R Santa Cruz Biotechnologies, Santa Cruz, USA)
- Rabbit polyclonal IgG anti-IκB-α Ab (C-21), sc-371 Santa Cruz Biotechnologies, Santa Cruz, USA)
- Peroxidase-labelled anti-mouse IgG (NIF824, Amersham Biosciences, Little Chalfont, UK).
- Peroxidase labelled anti-rabbit Ab (NIF824, Amersham Biosciences, Little Chalfont, UK)
- β-actin/HRP antibody (Santa Cruz Biotechnologies, Santa Cruz, USA)
- α-tubulin/HRP antibody (Santa Cruz Biotechnologies, Santa Cruz, USA)
- Mouse polyclonal anti- p-ERK (E-4) Ab (Santa Cruz Biotechnologies, Santa Cruz, USA)
- Rabbit polyclonal affinity purified anti-ERK1 of rat origin (sc-94 Santa Cruz Biotechnologies, Santa Cruz, USA)
- Rabbit AKT/PKB [pS473] mAb (BioSource™ , Invitrogen, UK)
- Goat polyclonal affinity purified antibody to Akt1 of human origin (C-20), (sc-1618 Santa Cruz Biotechnologies, Santa Cruz, USA)
- A non radioactive p38 MAP Kinase assay kit (New England BioLab, UK)
- Beadlyte® Human Multi-cytokine Beadmaster™ Kit (Milipore, UK)
- [methyl-^{3}H] thymidine (GE Healthcare, UK, Ltd)
- *Salmonella abortus equii* lipopolysaccharide (LPS) (Alexis Biochemicals, Lausen, Switzerland).

3.2.2 Methods:

3.2.2.1 CpG ODN activation dose and time course:

To study the stimulatory effects of CpG-ODN, I had to determine the optimal activating dose and time of CpG-ODN to mediate a response in tumour cells. Although publications recommended 5μg/ml of 2006 CpG-ODN type-B as an optimal dose to activate human B–cells (Jahrsdorfer B *et al.*, 2005), I needed to determine the proper concentration required to activate the different stages of malignant B-cells. At the beginning of the project, I have used 2006 CpG-ODN (Coley's Pharmaceutical) to activate the tumour cells, but Coley's Pharmaceutical company changed it to 10103 CpG-ODN, so I had to move on and use 10103 CpG-ODN afterward till the end of the project. Although 10103 CpG-ODN has the same effect as 2006 CpG-ODN (personal contact with Coley's Pharmaceutical), I had to ensure that it is showing the same activation response. Furthermore I had to determine the activating dose and time required for CpG-ODN stimulation. This was evaluated by studying the surface expression and upregulation of relevant immunological markers.

TLR9 positive cells ($5x10^5$ cells/ml) were either left untreated or stimulated with 0.1μg/ml, 1μg/ml, 3μg/ml and 12μg/ml 10103 CpG ODN (Coley Pharmaceutical, Canada) for three days in supplemented growth medium and incubated in 5% CO_2 at 37°C. Surface marker expression was measured by flow cytometry as described in section (3.2.2.7) to determine the optimal activating dose for the relevant surface markers' upregulation.

After determining the optimal activating dose, the cells were tested to determine the best time for the activation. $5x10^5$cells/ml were treated with the appropriate activating does of 10103 CpG ODN for one and three days to detect the best time for the activation. The activity was determined by looking at the upregulation of the relevant surface markers using flow cytometry.

3.2.2.2 Effect of 2137 non-CpG control vs. 10103 CpG-ODN:

Considering that ODN 2137 is produced as a non-CpG control ODN, I have used it for a control group of TLR9 expressing tumour cells, and compared their results with

the 10103 CpG-ODN. Both groups were tested for the upregulation of the surface markers CD54, CD80, CD86 and MHC II.

3.2.2.3 Cell viability:

Cells were tested for their viability before and after the activation by counting the number of viable cells, after mixing 20µl of cells with 20µl of trypan blue (Fischer Scientific, UK). Percentage of the viable cells (excluding trypan blue) was calculated from the total number of cells.

3.2.2.4 Western blot analysis of intracellular signalling pathway activation:

CpG-ODN mediates MAPK, AKT and NF-κB/IκB-α downstream signalling. To determine the intracellular downstream signalling effect of CpG-ODN mediated activation, Burkitt's Lymphomas (RAMOS and BJAB) cells were tested for their activation of intracellular signalling pathways. In addition, TLR9 transfected Hek293 cells and mock transfected Hek293 cells were tested for some activation products.

BJAB, Burkitt's lymphoma B-cell ($5x10^6$cells/ml) was activated with 3µg/ml 10103 CpG-ODN for up to 120 minutes to investigate the involvement of the different signalling pathways mediated by CpG-ODN activation. Antibodies against ERK1/2, AKT-1 and p38 activation product ATF-2, were used in western blots to determine their activation by detecting the relevant phosphorylated product.

Five $x10^6$cells/ml Burkitt's lymphomas (RAMOS and BJAB) and TLR9 and pDisplay transfected Hek293 human cells were either left unactivated or activated for various times (up to 120 minutes) using the appropriate activating dose of 10103 CpG-ODN (10µg/µl for Ramos and 3µg/ml for the other cell lines). For a known control, PBMCs were treated with 1µg/ml of *Salmonella abortus equii* lipopolysaccharide (LPS) (Alexis Biochemicals, Lausen, Switzerland), as indicated to induce pIκB activation in macrophages (Kim CS *et al.*, 2001).

A) Preparation of cell lysate:

To determine the activation of ERK and PI3K/AKT pathways, BJAB cells were either left in medium alone (indicated as time 0) or activated with CpG-ODN for up to 120 minutes for the ERK pathway, and 90 minutes for AKT pathway. Cells

were centrifuged and washed with PBS for each time interval and then lysed for 30 minutes on ice with 0.5ml lysis buffer (20mM Tris HCl (pH 7.5), 15mM NaCl, 2.5mM Sodium Pyrophosphate, 1mM EDTA, 1mM EGTA, 1% Triton X-100S, 1mM Na orthovanadate, 1mM β-glycerolphosphate, and protease inhibitors (Sigma,UK) of 10μg/ml Leupeptin, 10μg/ml Aprotinin and 10μg/ml Pepstatin). For the $p38^{MAPK}$ pathway, cells were IP/WB and determined using a non radioactive p38 MAP Kinase assay (New England BioLab, UK) as described in section (3.2.2.5).

Similarly, $5x10^6$cells/ml of cells activated with CpG-ODN (RAMOS, BJAB, Hek293 TLR9 and Hek293 pDisplay) or LPS (PBMCs) for up to 90 minutes were centrifuged and washed with PBS for IκB-α determination. The pellet of the washed cells was lysed for 30 minutes on ice using 0.5ml RIPA lysis buffer (1% NP-40, 0.5% Nadeoxycholate, 50mM Tris HCl, 150mM NaCl, 1mM Na-fluoride, 30mM Na-pyrophosphate, 2mM EDTA, 0.1% SDS, 100μM Na-orthovanadate 1mM phenylmethanusulphonylfluoride (PMSF) and protease inhibitors (Sigma) of 10μg/ml Leupeptin, 10μg/ml Aprotinin and 10μg/ml Pepstatin). After lysis, the samples were centrifuged at high speed (14,000 rpm) for 10 minutes at 4°C. The supernatants were collected and dried using Bench-Top Freeze Dryer (ModulyoD Freeze Dryer, Thermo Fisher Scientific, UK).

B) Gel Electrophoresis procedure.

After the BJAB cell lysis for the determination of ERK1/2 and AKT-1, the samples were centrifuged at 14,000rpm for 10 minutes at 4°C and supernatant collected in a new tube. The lyophilized supernatant for the IκB-α determination was dissolved in 50μl of the lysis buffer. Protein concentration was estimated using a microplate assay done according to the instructions of the mini-protean®II and blotting system (BioRad, Hercules, USA). 20 μl of ERK and AKT lysed cells were suspended in 20μl 2X loading dye with β-ME (reduced) (BioRad, Hercules, USA) and boiled for 5 minutes/95°C. 20μl of IκB-α lysate was resuspended in 20μl Laemmli loading dye with β-ME (reduced) (BioRad, Hercules, USA) and boiled for 5 minutes at 95°C. 25μl of ERK, AKT or IκB-α lysate from each interval time was loaded on precast 12% SDS-PAGE gels (Ready gel Tris-HCL gels, BioRad, Hercules, USA) and submitted to electrophoresis at 20mA for the stacking gel (10

minutes) and 30mA for the resolving gel (40 minutes) to fractionate the protein according to size, using premixed 1X Tris/Glycine buffer (BioRad, Hercules, USA). Afterwards the proteins were transferred into a Hybond-C Super nitrocellulose membrane (Amersham Biosciences, Little Chalfont, UK) at 300mA for 90 minutes on ice using 1X Tris/Glycine/SDS buffer (BioRad, Hercules, USA).

C) Immunoblotting procedure.

The membrane blots were washed in 1X PBS – 0.1% Tween 20 three times for 5 minutes each time on the orbital shaker. To prevent the non-specific binding, the membranes were incubated in 5% non-fat dry milk in 1X PBS – 0.1% Tween-20 for 1 hour. The membranes were washed in 1X PBS – 0.1% Tween-20 for 10 minutes and then the membranes were blotted with the specific antibody needed for each pathway in 1X PBS – 0.1% Tween 20 for at least 18hours. For ERK 1/2, blots were stained with 1:1000 mouse polyclonal anti- p-ERK (E-4) (Santa Cruz Biotechnologies, Santa Cruz, USA) in 1% non-fat dry milk in 1X PBS – 0.1% Tween-20 for 24 hours. This primary monoclonal antibody epitope corresponds to a sequence containing phosphorylated Tyr 204 of ERK of human origin. On the other hand, the membrane with AKT-2 lysates was blotted with 1:1000 rabbit monoclonal AKT/PKB [pS473] in 1% non-fat dry milk in 1X PBS – 0.1% Tween-20 for 24 hours. The membranes for the IκB-α were blotted with 1:500 rabbit polyclonal anti-p-IκB-α (Ser 32)-R (Santa Cruz Biotechnologies, Santa Cruz, USA) in 1% non-fat dry milk in 1X PBS – 0.1% Tween-20 for 24-48 hours. This primary antibody is recommended for detection of Ser 32 phosphorylated IκB-α of mouse, rat and human origin. The membranes were then washed in 1X PBS – 0.1% Tween-20 three times for 10 minutes each time. A secondary antibody was diluted in 4% non-fat dry milk in 1X PBS – 0.1% Tween 20 and incubated for 1 hour. Peroxidase-labelled anti-mouse IgG (NIF824, Amersham Biosciences, Little Chalfont, UK) at 1:1000 dilution was used for pERK 1/2 blots, while peroxidase labelled polyclonal swine anti-rabbit immunoglobulins/HRP (Dako Cytomation, UK) 1:1000 dilution was used for pAKT-1 and IκB-α blots. Membranes were washed in 1X PBS – 0.1% Tween 20 three times for 10 minutes each time. The protein bands were visualized by Chemiluminescence ECL Blotting detection kit and exposed to Hyperfilm™ ECL Western (Amersham Biosciences, Little

Chalfont, UK) for 1 minute to get bands at 42 and 44 kDa for pERK 1/2, 60 kDa for pAKT-1 and 38 kDa for pIκB-α.

D) Stripping and membrane re-blotting procedure:

After investigating the presence of the phosphorylated form of ERK1/2 and AKT following activation by CpG-ODN, the membranes were tested for the total ERK1/2, AKT-1 and IκB-α proteins. The membranes were washed 10 minutes in 1X PBS – 0.1% Tween 20 and stripped with 0.15M Glycine (pH 2.2) and 1% SDS in 1X PBS – 0.1% Tween 20 for 10 minutes three times. To stain the membranes for the total proteins of each, they were blocked with 5% non-fat powdered milk in 1X PBS – 0.1% Tween 20 for 1 hour before blotting with ERK (sc-94), AKT-1 (C-20) or IκB-α (C-21) specific antibodies. A rabbit polyclonal antibody of ERK (sc-94 Santa Cruz Biotechnologies, Santa Cruz, USA) was used for the detection of ERK 1/2, whilst goat polyclonal affinity purified antibody raised against a peptide mapping at the C-terminus of AKT-1 of human origin (C-20) (sc-1618 Santa Cruz Biotechnologies, Santa Cruz, USA) was used for AKT-1 determination, and rabbit polyclonal IgG anti- IκB-α ((C-21): sc-371 Santa Cruz Biotechnologies, Santa Cruz, USA) was used for the IκB-α. Both ERK and AKT antibodies used were diluted 1:1000, whereas it was 1:500 for IκB-α. Antibodies were diluted with 1% non-fat powdered milk in 1X PBS – 0.1% Tween 20 and blots were incubated for 24-48 hours. After washing the membranes three times (10 minutes each time) with 1X PBS – 0.1% Tween 20, the membranes were exposed for 1 hour to a secondary antibody diluted in 4% non-fat powdered milk in 1X PBS – 0.1% Tween 20. The secondary antibodies used were either 1:1000 peroxidase labelled polyclonal swine anti-rabbit immunoglobulins/HRP (Dako Cytomation, UK) for ERK and IκB-α, or 1:2000 of polyclonal rabbit anti-goat immunoglobulin/HRP (Dako Cytomation, UK) for AKT-1. Three washes in 1X PBS – 0.1% Tween 20 for 10 minutes each were done. ERK 1/2 blots showed 42/44kDa bands, while 60kDa bands for AKT-1 blots and 40kDa for IκB-α blot were visualized within 1 minute after the exposure to the ECL.

E) Loading control determination procedure:

To ensure that each well was loaded with the same concentration of protein, blots were stained for a house keeping gene. The same membranes were washed for 10

minutes in 1X PBS – 0.1% Tween 20 and blocked with 5% non-fat powdered milk in 1X PBS – 0.1% Tween 20 for 1 hour. Then, ERK1/2 and IκB-α blots were stained for expression of α-tubulin using α-tubulin/HRP antibody (Santa Cruz Biotechnologies, Santa Cruz, USA) at 1:10,000 dilution for 2 hours, and AKT-1 blots and some of IκB-α blots for the expression of β-actin using β-actin/HRP antibody (Santa Cruz Biotechnologies, Santa Cruz, USA) at 1:5,000 dilution for 2 hours. The membranes were then washed in 1X PBS – 0.1% Tween 20 three times for 10 minutes each time. The α-tubulin and β-actin blotted membranes were developed within 15 seconds using ECL Blotting detection kit, and images at 42kDa for β-actin and 60kDa for α-tubulin were observed. Band intensities were quantified using a GS-710 densitometer (Bio-Rad, UK). The relative ratio of phosphorylated and total bands to the house keeping bands was determined. The activated Hek293 TLR9 cells were compared with the TLR9 negative construct in activated Hek293 pDisplay cells.

3.2.2.5 p38 MAP Kinase activation upon TLR9 stimulation.

A non-radioactive p38 MAP Kinase assay kit (New England BioLab, UK) was used to detect $p38^{MAPK}$ activation product (ATF-2) in BJAB cells in the presence or absence of 3μg/ml of 10103 CpG-ODN.

A) Preparation of cell lysate.

BJAB, Burkitt's Lymphoma B-cell ($5x10^6$cells/ml), was activated with 3μg/ml 10103 CpG-ODN for up to 120 minutes. Cells were centrifuged and washed with PBS for each time interval and lysed for 30 minutes on ice with 500μl of ice-cold 1X cell lysis buffer (20mM Tris (pH 7.5), 150mM NaCl, 1mM EDTA, 1mM EGTA, 1mM PMSF, 1% Triton, 2.5mM Sodium pyrophosphate, 1mM b-Glycerolphosphate, 1mM Na_3VO_4, 1μg/ml Leupeptin). ATF-2 activation occurs inside the nucleus, so lysed cells were sonicated on ice four times for 15 seconds/4 cycles each using soniprep 150 sonicator (Sanyo) to ensure the lysis of the nucleus. Cells were micro-centrifuged 14,000xg for 10 minutes at 4°C and protein concentration was determined using Lowry method.

B) Immunoprecipitation/Western blotting procedure.

100µg protein from lysed and sonicated cells was immunoprecipitated using 20µl bead slurry with immobilized phospho-p38^{MAPK} (Thr180/tyr184) monoclonal antibody, and incubated with gentle rocking overnight at 4°C. Cell lysate/immobilized antibody was then micro-centrifuged at 14,000xg for 30 seconds and washed two times with 500µl of 1X ice cold cell lysis buffer. Pellets were washed twice with 500µl of 1X kinase buffer (25mM Tris (pH 7.5, 5mM β-Glycerolphosphate, 2mM DTT, 0.1mM Na3VO4, 10mM MgCl2) and kept on ice. Each pellet was resuspended in 50µl of 1X kinase buffer supplemented with 200µM ATP and 1µl of kinase substrate ATF-2 fusion protein (GST fused to ATF-2 codons 19-96 produced from E. coli expressing pGEXKG) to be incubated for 30 minutes at 30°C. Reactions were terminated with 25µl 3xSDS sample buffer, vortexed and micro-centrifuged for 30 seconds at 14,000 xg. Samples were heated to 95-100°C for 2-5 minutes and 30µl were loaded on 12.5% SDS-PAGE (Ready gel Tris-HCL gels, BioRad, Hercules, USA). 10µl of bionylated protein marker were loaded. The SDS-PAGE was submitted to electrophoresis at 20mA for the stacking gel (10 minutes) and 30mA for the resolving gel (40 minutes) to fractionate the protein according to size using premixed 1XTris/Glycine buffer (BioRad, Hercules, USA). Afterwards the proteins were transferred into a Hybond-C Super nitrocellulose membrane (Amersham Biosciences, Little Chalfont, UK) at 300mA for 90 minutes on ice using 1X Tris/Glycine/SDS buffer (BioRad, Hercules, USA).

The membrane blots were washed in 1X PBS – 0.1% Tween 20 three times for 5 minutes each time on the orbital shaker. To prevent non-specific binding, the membranes were incubated in 5% non-fat powdered milk in 1X PBS – 0.1% Tween 20 for 1 hour. The membranes were washed with 1X PBS – 0.1% Tween 20 three times for 10 minutes, and blotted with 1:1000 phospho-ATF-2 (Thr76) antibody in 1X PBS – 0.1% Tween 20 with 5% w/v BSA overnight at 4°C. The membranes were then washed three times with 1X PBS – 0.1% Tween 20 for 10 minutes each. A secondary antibody was added with 1:2000 HRP-conjugated antibody to detect the pATF-2 bands, and HRP-conjugated anti-biotin antibody (1:1000) to detect biotinylated protein markers, in 10 ml of blocking buffer (4% non-fat powdered milk in 1X PBS – 0.1% Tween 20) with gentle agitation for one

hour at room temperature. The membrane was washed in 1X PBS – 0.1% Tween 20 three times for 10 minutes each time. The protein bands were visualized by Chemiluminescence ECL Blotting detection kit and exposed to Hyperfilm™ ECL Western (Amersham Biosciences, Little Chalfont, UK) for 1 minute to get the images of a band at 38 kDa. Band intensity was quantified using a GS-710 densitometer (Bio-Rad, UK).

3.2.2.6 Nuclear factor-κB luciferase assay, transient transfection assay.

Transient transfections using Effectene Transfection Reagent (Qiagen, UK) were done according to the manufacturer's instructions, using plasmid DNA of NF-κB luciferase reporter construct (Figure 3.1) (a kind gift from Prof. L Ziegler-Heitbrock, Department of Infection, Immunity and Inflammation, University of Leicester, UK). The plasmid NF-κB luciferase reporter vector contained three copies of the prototypic NF-κB sequence from the mouse kappa light-chain enhancer cloned upstream of the TATA box of the pβTATA luci reporter plasmid.

Cells transiently transfected with the construct gene were either the adherent Hek293 and HeLa epithelial cell lines transfected with pCIneo-hTLR9 or the empty plasmid pClneo, or the suspension cells of PBMCs, RPMI 8226, BJAB and CLL B-cells. The day before transfection, $5x10^5$ cells/ml for the adherent cells and $5x10^6$ cells/ml for the suspension cells per well in six well plates were cultured in 3ml supplemented growth medium and incubated under their normal growth conditions (37°C and 5% CO2).

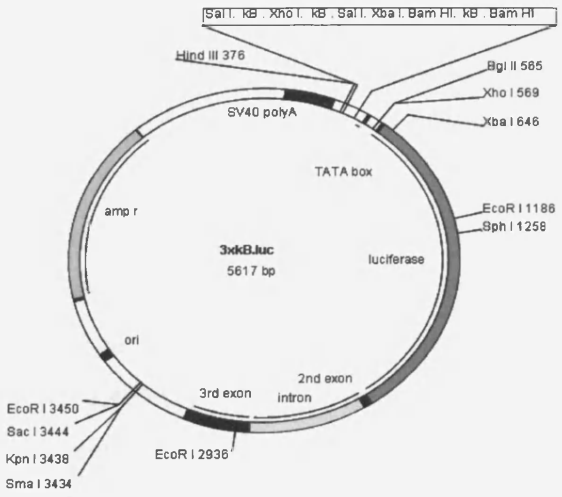

Figure 3.1. 3xNFκB luciferase reporter gene constructs.

3xNFκB.luc DNA construct (0.4 μg/well) were dissolved in TE buffer, pH 7-8 (minimum DNA concentration: 0.1 μg/μl) with the DNA-condensation buffer, Buffer EC, in a total volume of 100 μl, and 3.2 μl enhancer were added and all mixed by vortexing for one second and left for 2-5 minutes at room temperature. 10μl of Effectene Transfection Reagent were added to the DNA-Enhancer mixture and mixed by pipetting up and down 5 times or by vortexing for 10 seconds to be left for 10 minutes at room temperature. Meanwhile, the growth medium was aspirated from cells and the cells were washed once with PBS. 1.6 ml fresh supplemented growth medium were added to the cells. Another 600μl supplemented growth medium were added to the transfection complexes and mixed by pipetting up and down twice, and were immediately added to the well gently to ensure uniform distribution of the transfection complexes. Cells were incubated with the transfection complexes under their normal growth conditions. After 24 hours cells were washed from the growth medium and fresh supplemented medium was added.

Following transfection, each cell line was split into two groups each in three wells in 24 well plates (1ml/well). One group of cells was left as resting cells and the other group was activated with 3μg/ml 10103 CpG-ODN, and left to grow in the normal conditions for 18 hour. Control groups of non-transfected cells were split and treated in the same way. Afterward, cells were harvested, washed with PBS and the pellet was dissolved in 150μl of 1X reporter lysis buffer (Promega, UK). Twenty microliters of lysate was used for assay with 100μl of luciferase assay system (Promega, UK). The luciferase activity was measured using a Sirius luminometer, which measures standard glow (Berthold Detection Systems, Germany). Protein concentration using Lowry method was measured for each lysate to normalize the data and results were analyzed using GraphPad software.

3.2.2.7 Cytokine assay:

A multiplex cytokine assay was done in collaboration with Dr. John Curnow, University of Birmingham, UK, using a Beadlyte® Human Multi-cytokine Beadmaster™ Kit (Milipore, UK) for the measurement of the secretion of three cytokines (IL-6, IL-10 and TNF-α) in resting and 10103 CpG-ODN activated cells. In a flat bottom 96 well plate, $5x10^5$ cells/ml of tumour or normal B-cells, or $1x10^5$ cells/ml of non-haematological tumour cells were split into three wells (triplicates)

and left to grow without treatment (resting cells). Another group was prepared in the same way, but stimulated with 3μg/ml 10103 CpG-ODN. After 36 hours of incubation, supernatants were collected and frozen at -80°C until ready for the assay. Cytokine assay was done according to the manufacturer's instructions. IL-6 (14.0pg/ml), IL-10 (10.0pg/ml) and TNF-α (10.0pg/ml) standards were mixed and resuspended in eight different concentrations after 1:4 serial dilutions in assay buffer (PBS, 0.05% tween-20 and 1% BSA). Luminex filter plates provided with the kit were rehydrated with 200μl/well washing solution (PBS, and 0.05% Tween-20) and aspirated using vacuum manifold (Millipore, UK). Bead solution conjugated to analyte-specific antibodies to IL-6, IL-10 and TNF-α was diluted 1:9 in assay buffer, and 25μl/well was added. Beads were washed with 200μl/well washing solution and aspirated.

In the 96 well plate, 25μl of assay buffer and 50μl of the serially diluted standards (for the standard curve), blank (negative control, assay buffer alone) or cell supernatants were added to the wells. The concentration of the cytokine released by each cell was tested in triplicate for each culture condition. Luminex filter plates were covered and incubated at room temperature on an orbital shaker. Two hours later, plates were washed three times with 200μl/well washing solution and aspirated. Beadlyte® Anti-Human Multi-cytokine, Biotin (biotinylated detector antibody) was diluted 1:9 in assay buffer and 100μl of the diluted solution was added to each well. Plates were covered and incubated at room temperature on an orbital shaker for one hour. The wells were washed three times with 200μl/well of washing solution. To detect the presence of the cytokines, 25μl/well of Streptavidin-Phycoerythrin (RPE) solution was added after diluting it 1:9 in assay buffer. Plates were covered and incubated at room temperature on an orbital shaker for half an hour before washing and aspiration three times in washing solution, and 100μl/well of assay buffer was added at the end. At this stage, plates were ready to measure the concentrations of each cytokine compared with the relevent standard curve. Each well contained a four-member solid-phase sandwich, the bead- polystyrene microsphere with the analyte-specific antibodies of IL-6, IL-10 and TNF-α attached to the Luminex filter plates, cytokines (analytes) present in the samples, the analyte-specific biotinylated detector antibody which binds to one of the four available sites on the streptavidin-RPE that is conjugated to a fluorescent protein. The mean

fluorescent intensity (MFI)/60 seconds for each well was read using Luminex® 100 instrument. IL-6 was read at region 38, IL-10 at region 36 and TNF-α at region 06 using star station-2 program. IL-6, IL-10 and TNF-α concentrations were analyzed using GraphPad prism 4 software.

3.2.2.8 Flow Cytometry:

Flow cytometry was used to investigate the expression of the adhesion molecule CD54, costimulatory molecules CD80 and CD86, and Major Histocompatibility Complex (MHC) class II to detect if they would be upregulated upon activation of the cells with CpG ODN.

Cultured cells ($5x10^5$ /ml) were stimulated with the activating dose (3μg/ml for most cells) of 10103 CpG for three days (optimum time) in parallel with a control group left without activation. Cells were washed with PBS and the pellet stained with one of the following surface marker monoclonal antibodies (10μl in each), CD54-PE, CD80-FITC, CD86-PE (Beckman Coulter, UK) and MHC II-FITC (anti-human HLA-DP DQ, Dako, UK). Two other tubes were labelled with 10 μl IgG1-PE and IgG1-FITC each (Beckman coulter, UK) as an isotype control for PE and FITC conjugates. All tubes were incubated for 15min/ RT covered. Pellets washed twice with 1X PBS – 0.5% (w/v) BSA and fixed with 0.5ml 2% paraformaldehyde. Live gated cells (of 199 threshold or more) were read by the FACS Calibur flow cytometer and analysed using Cell Quest Pro software (Becton-Dickinson Ltd, UK).

Mean and median fluorescence intensity values were calculated after gating based on a combination of forward scatter (FSC) and side-scatter (SSC) features. Data of 10,000 events were acquired and analysed in a linear mode for FSC and SSC characteristics, and in a logarithmic mode for fluorescence intensities. Measurements included percentage of total population positive for each surface marker, and median in addition to mean channel fluorescence intensity (MFI) in energy channels.

3.2.2.9 Cellular Proliferation:

A direct proliferation assay for the detection of the DNA synthesis was used as an indicator of cell growth, by using incorporation of a radioactive nucleotide ([methyl-

^{3}H] thymidine). The incorporation of ^{3}H-thymidine into DNA is directly proportional to the amount of cell division occurring in the culture.

One x10^5 cells/well in flat bottom 96 well plate of tumour B-cell lines (Ramos, RPMI, RAJI, U266, Karpas 707H and BJAB), non-haematological hTLR9 transfected Hek293 and HeLa tumour cells, or *ex vivo* cells (PBMC, B-CLL, and TH044) were left to grow in triplicate wells for three days in the presence or absence of 3μg/ml 10103 CpG-ODN (except Ramos, which was cultured with 10μg/ml 10103 CpG-ODN), and pulsed with [methyl-^{3}H] thymidine (1μCi/well) (GE Healthcare, UK, Ltd) for the next 16-18 hours. A negative control of media alone was done. The cells were harvested on printed filtermat A (Glass fibre filter 1450-421, Wallac, Finland) using Harvester 96 Tomtec MACHII, (Wallac Finland) and left to dry. When dried, the filters were sealed in sample bag (1450-432, Perkin Elmer, Life science, UK) after adding the liquid scintillation cocktail Betaplate scint (Berkin Elmer life science, UK), and the incorporation of [^{3}H] thymidine in cellular DNA was measured on a 1450 Microbeta plus liquid scintillation counter (Wallac, Finland). ^{3}H-thymidine incorporation data for each cell was analysed using GraphPad prism 4 software.

3.2.2.10 Statistical analysis:

Each experiment was done in triplicates except for western blotting and some of the flow cytometric results. Data points stand for the mean of the three parallel samples measuring S.E.M. Data were analysed using Student's paired t-test using GraphPad prism 4 software version 4.03. Results were considered significant when p value was less than 0.05, and very significant when p value was less than 0.001.

3.3 Results:

CpG ODN, type-B, was recommended in publications as TLR9 agonist used to activate human B lymphocytes and other cells (Krieg AM 2002a; Krieg AM 2002b; Latz E *et al.*, 2004a; Vollmer J *et al.*, 2004a). For optimal stimulatory activity of CpG-ODN, the expression of the adhesion molecule CD54 antigen (ICAM-1), the costimulatory molecules CD80 and CD86 and the Major Histocompatibility Complex (MHC) class II were determined before and after CpG-ODN stimulation.

3.3.1 Optimal dose and time for CpG-ODN activation:

Jahrsdorfer B and colleagues (2001), recommended three days of activation with 2006 CpG-ODN for the best immune response. Table 3.1 represents some of the TLR9 positive B-cells tested for their optimal concentration of CpG-ODN after three days of activation. Cells were activated with 0.1, 1, 3, or 12μg/ml 10103 CpG-ODN. In general, the tumour B-cells tested showed the best response with 3μg/ml 10103 CpG-ODN, except for the Burkitt's Lymphoma Ramos cell line which was between 3μg/ml to 12μg/ml. The responsiveness to CpG-ODN was variable in each cell tested. B-CLL *ex vivo* cells and RPMI multiple myeloma showed similar levels of responsiveness at both 3 and 12 μg/ml 10103 CpG-ODN. In Ramos Burkitt's lymphoma cell line, 12μg/ml showed a greater upregulation for CD54 and MHC II than 3μg/ml, indicating that 12μg/ml of 10103 CpG-ODN is an optimal dose for this activation. For the determination of the optimal dose for the TLR9 transfected Hek293 and HeLa epithelial cells, 3μg/ml and 10μg/ml of 10103 CpG-ODN activation doses were used. Table 3.2 illustrates the effect of the two doses on TLR9 transfected Hek293 and HeLa epithelial cells. Neither 3μg/ml nor 10μg/ml of 10103 CpG-ODN showed an activation leading to upregulation of the relevant surface markers. The basal expression levels of the four tested surface markers were low in Hek293 transfected cells, and the same were seen with the non-transfected Hek293 cells (data not shown). CpG-ODN activation did not change their expression. TLR9 transfected HeLa cells showed the same basal CD54 expression level as in non-transfected HeLa cells (data not shown), but they did not show any changes in the four surface markers' expression, upon the CpG-ODN stimulation (Table 3.2).

Cells	Markers	Non Active	0.1 µg/µl	1µg/µl	3 µg/µl	12 µg/µl
B-CLL	CD54	106.49	146.55	260.1	853.34	1005.4
	CD80	7.68	9.76	14.49	20.11	18.35
	CD86	14.6	18.55	30.57	31.81	34.36
	MHC II	711.75	928.52	1171.5	1710.5	1815.3
Ramos	CD54	380.75	408	1008	890	1098
	CD80	8.65	8.29	10.12	9.27	10.6
	CD86	39.68	34.7	67.09	55.1	69.7
	MHC II	54.58	32.9	47.53	52.5	72.1
RPMI 8226	CD54	715.39	1031	1249	1230	1560
	CD80	2.39	2.94	5.65	8.98	6.64
	CD86	102.33	52.26	59.78	74.57	61.36
	MHC II	2.22	2.52	6.58	10.87	9.31

Table 3.1. Tumour B-cell lines activated with different concentrations of 10103 CpG-ODN for three days to determine the activating dose that would optimally upregulate the relevant surface markers. Data represents MFI readings for each surface marker. This experiment was done only once.

Although the published papers recommended three days of activation (Jahrsdorfer B *et al.*, 2001), testing the best time for the activation of TLR9 positive cells in this project was also essential. Cells were treated with the appropriate activating dose for up to three days to determine the optimal activation time. Table 3.3 summarises some of the tested cells for one and three days activation with CpG-ODN, and shows that three days is the more appropriate time for the activation. B-CLL showed a significant upregulation of the four surface markers after three days, while CD80 was not upregulated after one day of CpG-ODN activation. Ramos and BJAB Burkitt's Lymphomas showed activation after one day, but the activation and upregulation of CD54, CD86 and MHC II were higher after three days as indicated in Table 3.3. Based on these results, all TLR9 positive cell lines tested showed an optimal activation response with 3µg/ml 10103 CpG-ODN after three days except, for Ramos in which the optimal dose was 12µg/ml.

Cells	Markers	Non Active	3 µg/µl	10 µg/µl
Hek293 TLR9	CD54	13.57	5.27	4.14
	CD80	8.46	6.80	15.46
	CD86	11.19	6.17	5.54
	MHC II	6.58	4.73	4.63
Hek293 HA/TLR9	CD54	4.59	4.66	3.88
	CD80	4.26	4.01	4.49
	CD86	4.53	4.41	4.01
	MHC II	4.04	3.99	4.45
HeLa TLR9	CD54	87.72	67.79	22.58
	CD80	4.99	3.76	7.72
	CD86	5.22	2.77	6.79
	MHC II	4.12	3.30	2.95
HeLa HA/TLR9	CD54	90.21	69.53	73.72
	CD80	4.61	4.84	5.38
	CD86	4.36	4.61	4.70
	MHC II	5.03	4.34	5.87

Table 3.2. TLR9 transfected Hek293 and HeLa Cells activated for three days with 3µg/ml and 10µg/ml 10103 CpG-ODN to check the activating dose that would optimally stimulate surface markers upregulation. Data represents the MFI readings for each surface marker. This experiment was done only once.

Days / Markers		B-CLL 3 µg/ml	RAMOS 10 µg/ml	BJAB 3 µg/ml
Non active	CD54	75.54	1054	665.65
	CD80	8.07	23.9	50.25
	CD86	8.89	27.9	507.91
	MHC II	246.61	14.9	368.12
Day One	CD54	480.86**	1542**	1359.57**
	CD80	6.39	11.22	69.27
	CD86	13.11*	102.3**	816.83*
	MHC II	615.04**	195.4**	417.01
Day Three	CD54	1033.17***	1729**	1547.59***
	CD80	20.20*	18.17	133.46*
	CD86	135.98***	84.77**	1107.52**
	MHC II	914.83***	207.6**	261.59

Table 3.3. Tumour B-cells time course for one and three days, for optimal time for 3µg/ml 10103 CpG-ODN to activate cells (Ramos with 10µg/ml). Data presents the MFI for one time experiment.* $P<0.05$, ** $P<0.005$, *** $P<0.001$ (compared to non active cells).

3.3.2 Effect of 2137 non-CpG control vs. 10103 CpG-ODN:

Using 2137 ODN as non- CpG control ODN showed almost the same effect as 10103 CpG-ODN on the upregulation of the relevant immunological surface markers. Figure 3.2 illustrates the expression of one of the tested surface markers (CD54) in two cell lines, Ramos and RPMI, after their treatment with either 2137 ODN (the green line) or 10103 CpG-ODN (the blue blocks) at equivalent doses. These observations indicate that control 2137 non-CpG ODN activated Ramos and RPMI cells to the same extent as 10103 CpG-ODN. Also, reports indicated that the thymidine content in ODN 2137 would be sufficient to stimulate human B-cell activation (Vollmer J *et al.*, 2004b), therefore I did not use it as a control ODN in my subsequent experiments.

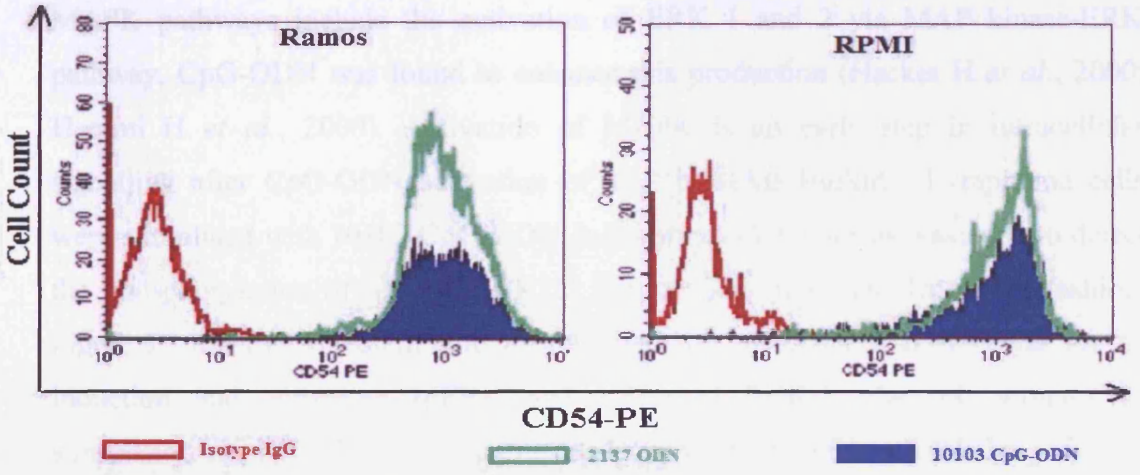

Figure 3.2. Flow cytometry overlay plots for the extracellular staining of CD54 in Ramos and RPMI cell lines. Cells were either treated with 3μg/ml 2137 ODN (green line) or with 3μg/ml 10103 CpG-ODN (blue blocks), and compared with the isotype control (red line). This experiment was repeated in three independent experiments.

3.3.3 CpG-ODN mediates responses:

Having established the optimal activating dose and time of 10103 CpG-ODN for different cell lines, I have investigated the CpG-ODN mediated responses in TLR9 positive and negative expressing cells (as determined by RT-PCR). Cells were studied for CpG-ODN mediated intracellular signalling, cytokine release, surface marker upregulation and cellular proliferation.

3.3.3.1 CpG-ODN mediated intracellular signalling:

Activation of NF-κB, ERK1/2, AKT-1 and $p38^{MAPK}$ intracellular signalling pathways was detected after CpG-ODN activation of TLR9, using western blot

analysis in a time-dependent fashion. BJAB cells were used as a model for the determination of those intracellular pathways, after CpG-ODN activation. Ramos and PBMCs were also studied for the IκB-α phosphorylation after CpG-ODN treatment. Furthermore, to determine the association of TLR9 in IκB-α degradation, TLR9 transfected Hek293 and HeLa cells were activated with CpG-ODN. Mock transfected Hek293 and HeLa cells were activated with CpG-ODN and used as control. This would also indicate whether TLR9 in transfected cells was functional.

3.3.3.2 Mitogen-activated protein kinase (MAPK) signalling pathway:

A) ERK 1/2 pathway:

MAPK pathways include the activation of ERK 1 and 2 via MAP kinase-ERK pathway. CpG-ODN was found to enhance this production (Hacker H *et al.*, 2000; Hemmi H *et al.*, 2000). Activation of MAPK is an early step in intracellular signalling after CpG-ODN activation of TLR9. BJAB Burkitt's Lymphoma cells were stimulated with 10103 CpG-ODN and western blot analysis was done to detect the phosphorylation of MAPK ERK1/2 (Figure 3.3) in a time-dependent fashion. Figure 3.3 illustrates western blots for the effect of CpG-ODN on BJAB cells, for the induction and activation (pERK/total ERK) of ERK-1 after 60 minutes of stimulation and ERK-2 after 120 minutes. The phosphorylation of ERK 1/2 indicates that activation of TLR9 via CpG-ODN in BJAB cells provoked MAP kinase-ERK pathway activation leading to the production of pERK 1/2 activated product. In recent published data, Longo PG and colleagues reported similar results in B-CLL cells (Longo PG *et al.*, 2007).

BJAB cells showed a constitutive basal activation of ERK 1/2, but initial decrease in pERK/ERK at 10 to 60 minutes of CpG-ODN stimulation was seen. CpG-ODN activated BJAB cells, gradually returned towards normal after 60 minutes, as indicated in Figure 3.3.

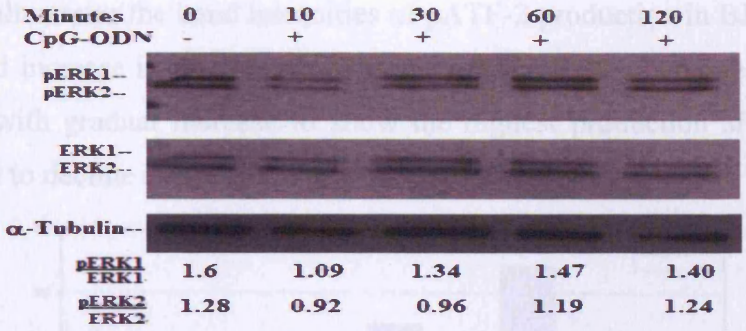

Figure 3.3. Activation of MAPK/ERK pathway by CpG-ODN in Burkitt's Lymphoma BJAB cells. BJAB cells ($5x10^6$cells/ml) were stimulated with CpG-ODN (3μg/ml) for up to 120 minutes. Equal amounts of whole cell lysates (30μl/lane) were subject to Western blotting using antibodies against the phosphorylation of ERK1/2. Total ERK1/2 was determined for the same blot. α-tubulin for each sample was used as a house keeping protein loading control. This experiment was repeated in two independent times.

B) p38 ^{MAPK} pathway:

The purpose of this part was to investigate the role of p38 ^{MAPK} and its downstream target, activating transcription factor 2 (ATF2), during TLR9 signalling in BJAB tumour cells. The activation of p38 ^{MAPK} produces phospho- p38 ^{MAPK} that activates the downstream signalling. This activation increases phosphorylation of ATF2 in a $p38^{MAPK}$-dependent manner. BJAB Burkitt's lymphoma cells were treated with 10103 CpG in a time-dependent manner, and phospho-$p38^{MAPK}$ was immunoprecipitated from the protein lysates, to be used in an assay of ATF2 phosphorylation using exogenous ATF2 substrate. Figure 3.4 illustrates the typical western blot of $p38^{MAPK}$ immunoprecipitated BJAB cells, showing that ATF2 phosphorylation peaked at 60 minutes, and decreased afterward. BJAB cells showed a weak basal activation level of phospho ATF2 even without CpG-ODN stimulation, when compared with the untreated HeLa negative control cells which did not show any ATF2 phosphorylation production (Figure 3.4).

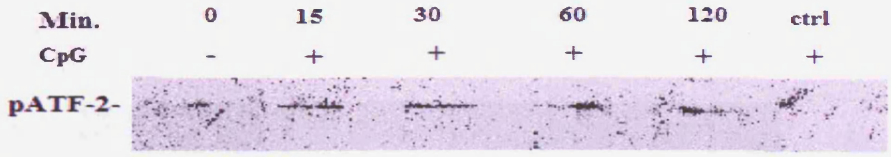

Figure 3.4. Activation of $p38^{MAPK}$-dependent phosphorylation of ATF2 and phosphorylation of $p38^{MAPK}$ in Burkitt's Lymphoma BJAB cells. BJAB cells ($5x10^6$cells/ml) were stimulated with 10103CpG-ODN (3μg/ml) for up to 120 minutes. Equal amounts of whole cell lysates (50μg/lane) were immunoprecipitated with agarose bead-bound anti-pp38 Abs. *In vitro* kinase assay was done at 30°C for 30 minutes using ATF-2 fusion protein as a substrate. Non-activated HeLa cell was used as a negative control in the last lane. This experiment was repeated in two independent times.

Figure 3.5 illustrates the band intensities of pATF-2 production in BJAB cells. Cells showed and increase in pATF2 production from the first 10 minutes of CpG-ODN activation with gradual increase to show the highest production after 60 minutes, then started to decline afterwards.

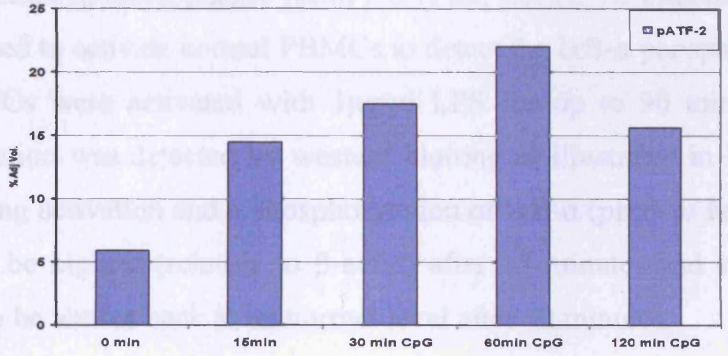

Figure 3.5. Activation of $p38^{MAPK}$-dependent phosphorylation of ATF2 and phosphorylation of $p38^{MAPK}$ in Burkitt's Lymphoma BJAB cells. BJAB cells ($5x10^6$cells/ml) were then stimulated with 10103CpG-ODN (3μg/ml) for up to 120 minutes. Band intensities of pATF-2 were quantified using a GS-710 densitometer.

3.3.3.3 PI3-kinase/AKT pathway:

The AKT pathway is considered a key determinant of biologic aggressiveness of tumours. To explore the significance of the PI3-kinase-Akt pathway in the CpG-ODN activated TLR9 positive cells, Burkitt's lymphoma BJAB cells were treated with 10103 CpG-ODN in a time-dependent manner and western blot analysis of phospho and total AKT were done. Blots in Figure 3.6 demonstrated increased phosphorylation of AKT in a time-dependent fashion that showed a maximal pAKT:total AKT ratio at 90 minutes. It also shows basal activation of pAKT in absence of CpG-ODN, which increased following CpG-ODN treatment.

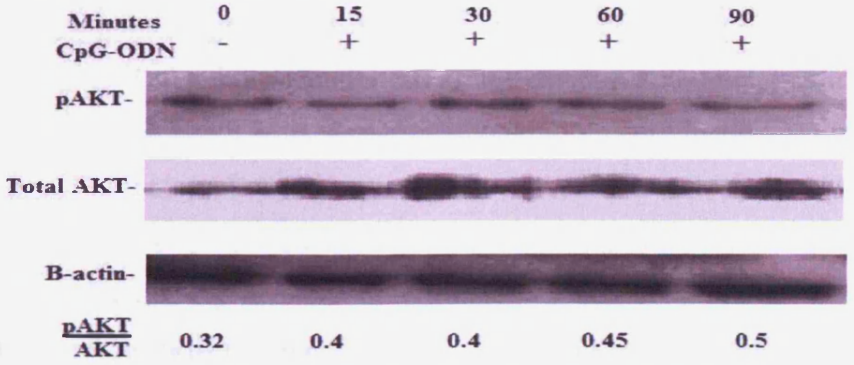

Figure 3.6. Activation of PI3K/AKT pathway by CpG-ODN in Burkitt's Lymphoma BJAB cells. BJAB cells ($5x10^6$cells/ml) were stimulated with CpG-ODN (3μg/ml) for up to 90 minutes. Equal amounts of whole cell lysates (50μl/lane) were subject to Western blotting using antibodies against the phosphorylation of AKT. Total AKT was determined for the same blot. β-actin in each sample was used as the equal loading control. This experiment was repeated in two independent times.

3.3.3.4 NF-κB/ IκB-α pathway:

A) IκB-α degradation:

Lipopolysaccharide (LPS), TLR4 agonist, is known to activate the IκB-α phosphorylation in macrophages (Kim CS *et al.*, 2001). To establish the technique, LPS was used to activate normal PBMCs to detect the IκB-α phosphorylation. In this study PBMCs were activated with 1μg/μl LPS for up to 90 minutes, and IκB-α phosphorylation was detected by western blotting as illustrated in Figure 3.7. Cells were showing activation and a phosphorylation of IκB-α (pIκB-α/ IκB-α), which was detected to be highest (relative to β-actin) after 15 minutes and started to decline afterward to be almost back to its normal level after 90 minutes.

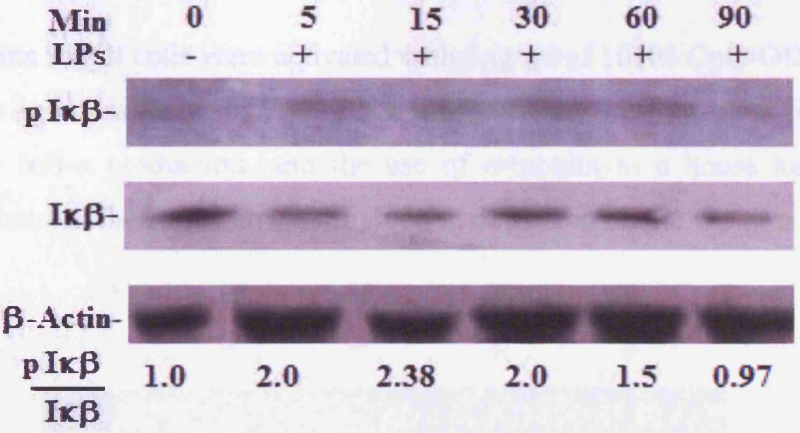

Figure 3.7. LPS induced IκB-α phosphorylation in PBMCs activated with 1μg/μl for LPS up to 90 minutes. Cells were lysed and blotted for pIκB-α and total IκB-α. β-actin was used as a house keeping protein loading control. This experiment was done only once.

To investigate the effect of TLR9 signalling on pIκB-α production, TLR9 positive Burkitt's Lymphoma Ramos and BJAB cell lines were activated with 3μg/ml 10103 CpG for up to 120 minutes and blotted for pIκB-α and total IκB-α. Figure 3.8 illustrates Ramos western blots showing activation and production of the pIκB-α and total IκB-α. β-actin as a house keeping gene was done to ensure the even loading of protein. Band intensity was quantified and the relative ratio of pIκB-α and total IκB-α signals to β-actin signal were determined. Ramos cells started to activate and phosphorylate the IκB-α in the first few minutes of activation to show a maximal pIκB-α/ IκB-α ratio at 15 minutes, declining afterward and returning back to normal after two hour.

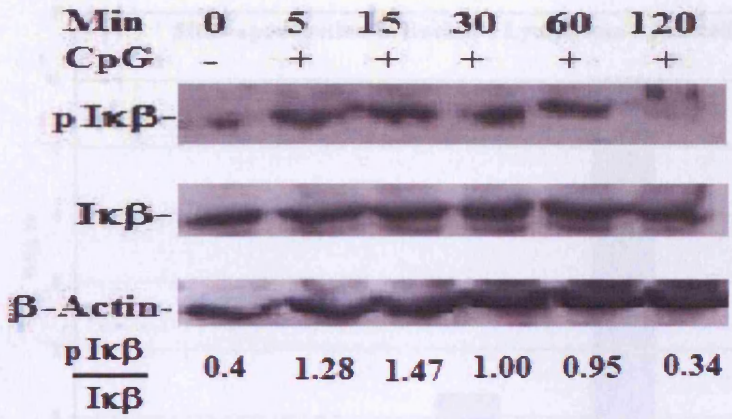

Figure 3.8. .CpG-ODN induced IκB-α phosphorylation in Ramos cells. Cells were activated with 3μg/ml 10103 CpG-ODN up to 120 minutes then lysed and blotted for pIκB-α and total IκB-α. β-actin was used as a house keeping protein loading control. This experiment was done only once

Burkitt's lymphoma BJAB cells were activated with 3μg/ml of 10103 CpG-ODN for up to 90 minutes in a similar way. Figure 3.9 illustrates the western blots for the pIκB-α and total IκB-α production, and the use of α-tubulin as a house keeping protein loading control. There was no clear induction of pIκB-α on the western blots.

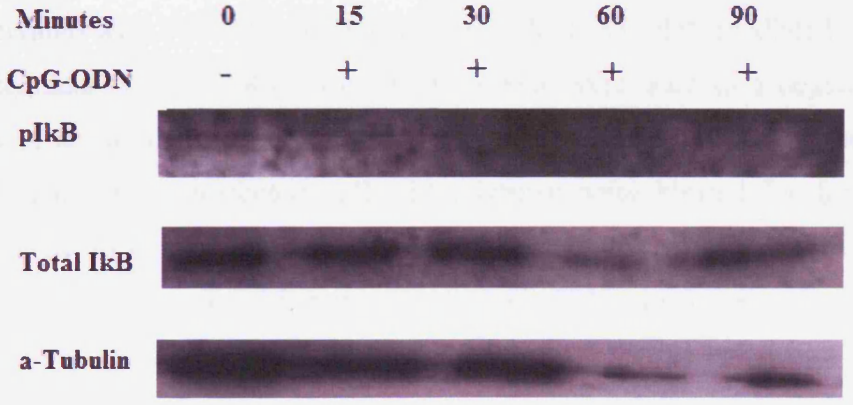

Figure 3.9. CpG-ODN induced IκB-α phosphorylation in BJAB cells. Cells were treated with 3μg/ml 10103 CpG-ODN up to 90 minutes then lysed and blotted for pIκB-α and total IκB-α. α-Tubulin was used as a house keeping gene and protein loading control. This experiment was repeated in two independent times.

However, Figure 3.10 illustrates the normalised band intensities for pIκB-α against the house keeping gene, α-tubulin. pIκB-α production showed low basal expression and a slight increase after 30 minutes of CpG-ODN activation, peaking after 60 minutes and declining afterwards.

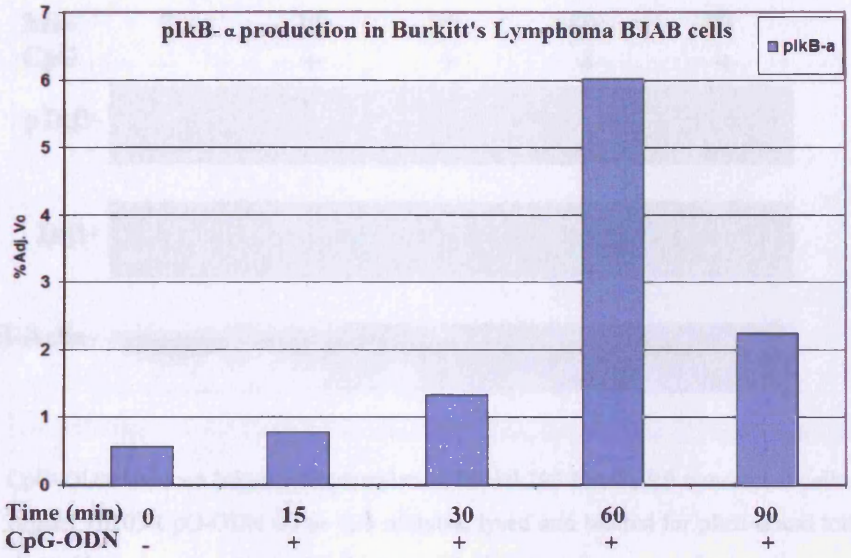

Figure 3.10. CpG-ODN induced IκB-α phosphorylation in BJAB cells. Band intensities of pIκB-α signals were normalised to α-tubulin house keeping protein loading control.

To determine whether transfected TLR9 is functional, and to demonstrate the specificity of CpG-ODN/TLR9 activation, TLR9 transfected Hek293 and HeLa cells were activated with 10103 CpG-ODN to detect the CpG-ODN mediated intracellular IκB-α degradation via TLR9. Mock transfectants were used as a negative control. Figure 3.11 shows the pIκB-α and total IκB-α bands produced upon the activation of Hek293 HA/TLR9 transfected cells. Membranes were blotted for β-actin house keeping gene to determine the protein loadings. Hek293 HA/TLR9 cells showed pIκB-α production after 15 minutes of CpG-ODN activation, which gradually increased over 60 to 90 minutes. pIκB-α level did not decline in the first 90 minutes, the latest time point determined in this assay. The total IκB-α degradation remained relatively constant (Figure 3.11). Hek293 pDisplay cells were treated with 10103 CpG-ODN and blotted the same way as Hek293 HA/TLR9, to determine if the effect is from TLR9 construct gene (Figure 3.12). CpG-ODN had no effect on the production of IκB-α phosphorylation in Hek293/pDisplay cells, as illustrated in Figures 3.12.

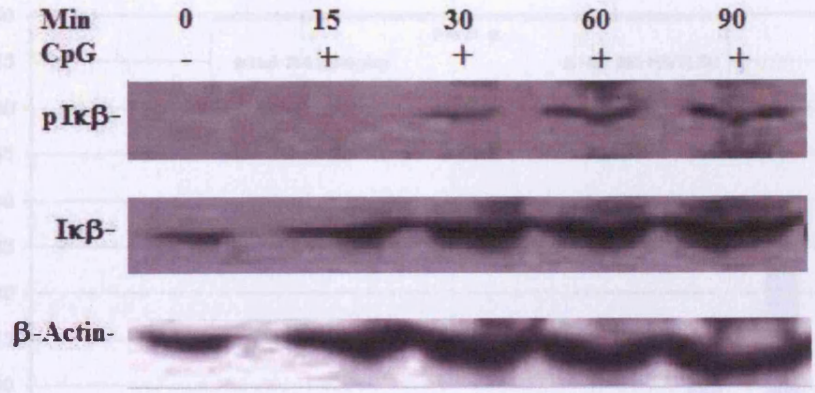

Figure 3.11. CpG-ODN induced IκB-α phosphorylation in Hek293 HA/TLR9 transfected cells. Cells were treated with 3μg/ml 10103 CpG-ODN up to 120 minutes, lysed and blotted for pIκB-α and total IκB-α. β-actin was used as a house keeping protein loading control. This experiment was done only once.

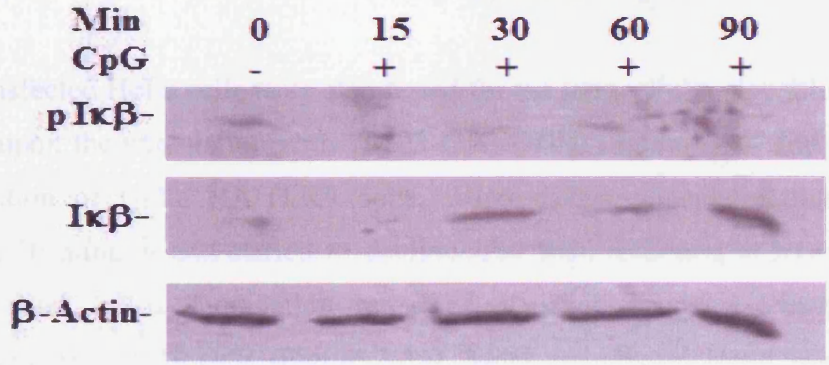

Figure 3.12. CpG-ODN does not induce IκB-α phosphorylation in Hek293 pDisplay mock transfected cells. Cells were treated with 3μg/ml 10103 CpG-ODN up to 120 minutes then lysed and blotted for pIκB-α and total IκB-α. β-actin was used as a house keeping gene and protein loading control. This experiment was done only once.

Figure 3.13 shows the normalised band intensities for pIκB-α against β-actin in Hek293 HA/TLR9 and Hek293 pDisplay cells. The pDisplay transfected Hek293 cells did not show any pIκB-α production upon 10103 CpG-ODN activation. In contrast, TLR9 transfected Hek293 (Hek293 HA/TLR9) cells showed an increase in pIκB-α production from the first 15 minutes showing a high levels of pIκB-α after 60 and 90 minutes (Figure 3.11). These data demonstrate that CpG-ODN induction of pIκB-α was mediated by TLR9.

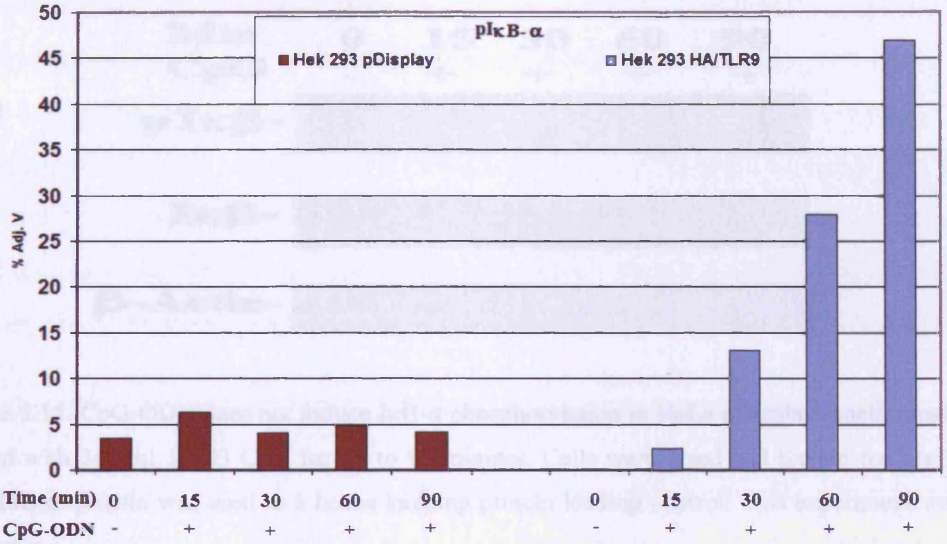

Figure 3.13. CpG-ODN induced IκB-α phosphorylation in Hek293 HA/TLR9 or Hek293 pDisplay cells. Cells were treated with 3μg/ml 10103 CpG-ODN for up to 90 minutes. Band intensities of pIκB-α signals were normalised to β-actin house keeping protein loading control.

TLR9 transfected HeLa cells were also tested for the intracellular signalling function of TLR9 upon the stimulation with 10103 CpG-ODN. Figures 3.14 and 3.16 show the activation of HeLa HA/TLR9 cells, where IκB-α phosphorylation was the highest in 30 minutes and started to decline after that, returning to baseline by 90 minutes. Total IκB-α degradation remained constant throughout in CpG-ODN treated HeLa HA/TLR9 cells (Figure 3.14). Mock transfected HeLa pDisplay was used as a negative control, to ensure the effect of TLR9 gene in this activation. Treatment of HeLa pDisplay with CpG-ODN did not induce pIκB-α and no pIκB-α production was seen, as indicated in Figure 3.15, and the total IκB-α production remained constant throughout. The presence of TLR9 construct gene in the HA-tagged/TLR9 construct rendered HeLa cells responsive to CpG-ODN activation.

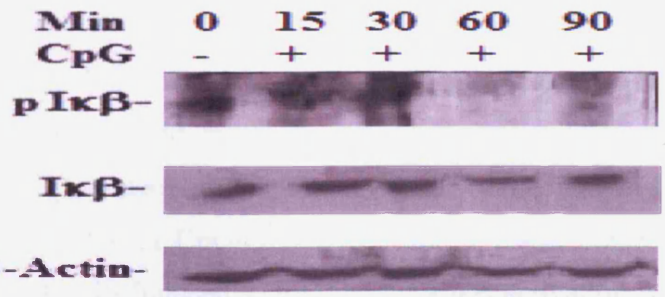

Figure 3.14. CpG-ODN induced IκB-α phosphorylation in HeLa HA/TLR9 transfected cells treated with 3μg/ml 10103 CpG for up to 90 minutes. Cells were lysed and blotted for pIκB-α and total IκB-α. β-actin was used as a house keeping protein loading control. This experiment was done only once.

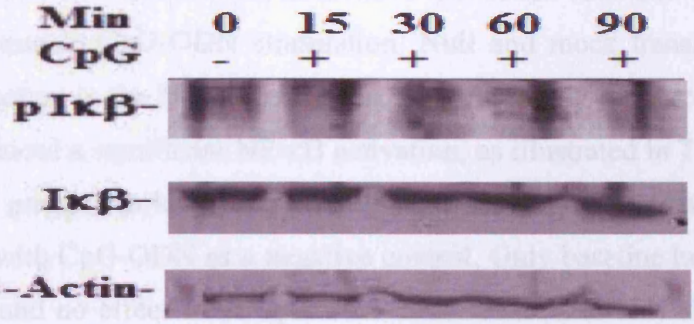

Figure 3.15. CpG-ODN does not induce IκB-α phosphorylation in HeLa pDisplay mock transfectants treated with 3μg/ml 10103 CpG for up to 90 minutes. Cells were lysed and blotted for pIκB-α and total IκB-α. β-actin was used as a house keeping protein loading control. This experiment was done only once.

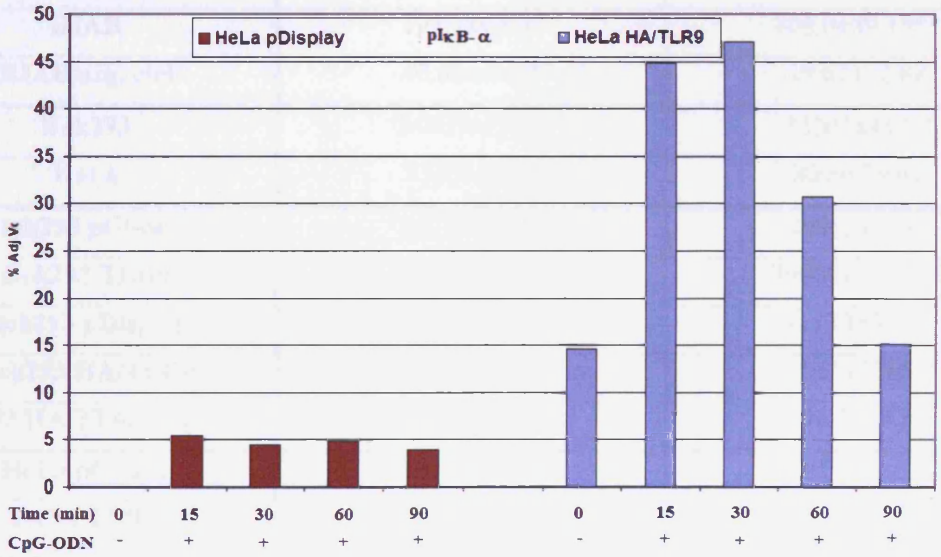

Figure 3.16. CpG-ODN induced IκB-α phosphorylation in HeLa cells transfected with HA/TLR9 and pDisplay blots activated with 3μg/ml 10103 CpG-ODN for up to 90 minutes. Band intensities of pIκB-α were normalised to β-actin house keeping protein.

B) NF-κB activation:

To determine the CpG-ODN mediated nuclear factor-κB (NF-κB) activation, PBMCs, tumour B-cells and transfected/non-transfected Hek293 and HeLa cells were transfected with a luciferase construct (3x-κB luc) containing 3 NF-κB binding regions, and activated with CpG-ODN. In Table 3.4 and Figure 3.17 the *ex vivo* PBMCs and B-CLL cells induced a significant NF-κB activation following treatment with CpG-ODN. In addition, TLR9 positive tumour B-cell lines (BJAB and RPMI) activated with 10103 CpG-ODN stimulated NF-κB activation. Untransfected, TLR9

transfected, and mock transfectants of Hek293 and HeLa cell lines were also tested for their response to CpG-ODN stimulation. Null and mock transfectants did not show any induction in the NF-κB activation, whereas TLR9 transfected Hek293 and HeLa cells induced a significant NF-κB activation, as illustrated in Table 3.4. For all cells tested, a group was left untransfected with the NF-κB construct gene resting and activated with CpG-ODN as a negative control. Only baseline luciferase activity was detected, and no effect from CpG-ODN was seen. (data only shown for BJAB and TLR9 transfected Hek293 and HeLa negative controls; Table 3.4).

NFκB production	Resting cells	Activated cells
PBMCs	368.7±56.70	772.7±55.15**
B-CLL	122.7±19.5	789.7±45.45**
RPMI	5086±188.2	104869±7369**
BJAB	197.7±9.905	703.0±39.15**
BJAB neg. ctrl	46.00±10.45	49.67±12.88
Hek293	34007±133.8	33205±410.7
HeLa	7766±102.0	8009±79.61
Hek293 pCl-neo	36735±2073	29813±1391
Hek293 TLR9	26037±351.6	39860±790.1**
Hek293 pDisplay	16336±132.5	11130±345.4
Hek293 HA/TLR9	38208±1056	73961±2766**
Hek293 HA/TLR9 neg. ctrl	187.5±2.887	176.5±39.84
HeLa pCl-neo	16264±1101	17776±815.3
HeLa TLR9	5665 ± 84.95	8465 ± 137.6***
HeLa pDisplay	2962±11.79	3162±44.29
HeLa HA/TLR9	3081 ± 64.41	3780 ± 41.62**
HeLa TLR9 neg. ctrl	103±2.45	98±4.65

Table 3.4. NF-κB activation in normal and tumour cells before and after the activation with 10103 CpG-ODN. Luciferase non-transfected cells were used as a negative control. Data represent the mean of luciferase activity RLU ± S.E.M of triplicates. This experiment was repeated in two independent experiments. * $P<0.05$, ** $P<0.005$, *** $P<0.001$ (compared to control non- activated cells).

From Table 3.4, *ex vivo* cells of PBMCs, B-CLL cells and RPMI and BJAB tumour B-cells showed a significant induction in the NF-κB activation after treatment with CpG-ODN. TLR9 transfected Hek293 and HeLa cells also showed an activation response for NF-κB upon stimulation with 10103 CpG-ODN (Table 3.4). Neither

untransfected or mock transfected Hek293 and HeLa cells showed an activation response for NF-κB (Table 3.4).

3.3.3.5 Effect of CpG-ODN on the induction of cytokines:

As CpG-ODN was known to stimulate the immune cells to release cytokines such as TNF-α, IL-6 and IL-10 (Wooldridge JE *et al.*, 1997; Smith JB *et al.*, 1998), I wanted to investigate the effect of CpG-ODN on the activation of the TLR9 positive cells and compare them with TLR9 negative cells. *Ex vivo* B-cells (normal PBMCs and B-CLL) and tumour B-cell lines (RPMI, LiLa and BJAB) were investigated for the release of IL-6, IL-10 and TNF-α cytokines. Table 3.5 shows the effect of CpG-ODN on the different B-cells. This Table also includes data from several cell lines (TH044, FC029, Ramos, U266 and Karpas) in which the cytokine assays were performed by Hélia Esteves, (BSc student, University of Leicester) and which were subsequently clarified as TLR9 positive or negative by me using RT-PCR (Chapter Two). *Ex vivo* B-cells (normal PBMCs, B-CLL, TH044 and FC029) were all found to express TLR9 and showed a significant induction of the three tested cytokines upon their activation with CpG-ODN. TLR9 expressing tumour B-cell lines (RPMI, Ramos, Lila and BJAB) showed CpG-ODN mediated cytokine induction, but in a variable way. RPMI 8226 cells showed a significant induction of TNF-α production, but not of IL-6 and IL-10. Ramos cell line upregulated synthesis of IL-10, but not IL-6 or TNF-α in the presence of CpG-ODN. Lila cells showed very low basal level expression of the three tested cytokines, but a highly significant CpG-ODN induction of IL-6 and IL-10, and a lesser upregulation of TNF-α production. BJAB cells showed a high basal level for IL-10 which was further induced by CpG-ODN, together with induction of IL-6 and TNF-α. In contrast, the TLR9 negative cell lines U266 and Karpas did not enhance cytokine induction in response to CpG-ODN. Although U266 showed a high basal level for IL-6, it did not enhance its induction after CpG-ODN activation. Karpas cells showed no cytokine expression of IL-6, IL-10 or TNF-α before or after CpG-ODN activation (Table 3.5).

TLR9 expression	Cells	CpG-ODN (μg/ml)	Cytokine release (pg/ml)		
			IL-6	IL-10	TNF-α
TLR9 positive	PBMCs	0	5.53±0.42	1.13±0.13	2.60±0.54
		3	802.8±21.95***	117.2±6.9**	7.84±0.00*
	B-CLL	0	19.60±0.96	0.09±0.05	0.51±0.003
		3	873.7±63.42**	676.1±21.25***	30.89±6.03*
	TH044#	0	38.73±1.61	1.00±0.00	1.00±0.00
		3	1226±2.25***	11.00±0.27***	25.00±0.41***
	FC029#	0	19.00±0.35	2.00±0.27	4.00±0.42
		3	553.0±14.87***	173.0±5.28***	187.0±8.04**
	RPMI	0	0.8372±0.00	19.84±1.03	1.76±0.76
		3	1.35±0.52	21.10±2.20	39.02±4.46*
	Ramos#	0	0.00±0.00	12.96±0.40	1.38±0.46
		3	0.00±0.00	107.78±2.45***	1.38±0.46
	LiLa	0	0.06±0.00	0.23±0.03	0.00±0.00
		3	170.8±5.73**	21.69±2.99**	3.99±0.81*
	BJAB	0	1.02±0.18	443.8±11.88	4.85±1.7
		3	13.41±1.11**	3240±72.72***	39.7±1.28**
TLR9 negative	U266#	0	1883.3±63.06	1.04±0.05	2.14±0.84
		3	1883.3±59.93	1.22±0.08	1.38±0.00
	Karpas#	0	0.00±0.00	0.00±0.00	1.38±0.46
		3	0.00±0.00	0.00±0.00	1.38±0.46

Table 3.5. Effect of CpG-ODN in mediating the induction of IL-6, IL-10 and TNF-α cytokines on B-cells. Cells ($1x10^5$cells/200μl/well) were stimulated with medium or 10103 CpG-ODN (3μg/ml) for 36 hours and supernatants were collected to determine the cytokine production. Cytokine release was assayed using Beadlyte® Human Multi-cytokine Beadmaster™ Kit (Milipore, UK). Data represent the mean concentration pg/ml ± S.E.M of triplicates. This experiment was done only once.* $P<0.05$, ** $P<0.005$, *** $P<0.001$ (compared to control non-activated cells). # Data derived from Helia Esteves, BSc student, University of Leicester.

TLR9 transfected Hek293 and HeLa cells were also tested for their response to CpG-ODN activation by the production of IL-6, IL-10 and TNF-α cytokines. Negative controls of mock transfected Hek293 and HeLa cells were also tested. Table 3.6 illustrates the effect of CpG-ODN on these cell lines. Hek293 transfected with either TLR9, HA/TLR9, pCl-neo or pDisplay constructs did not show any significant induction in IL-6, IL-10 and TNF-α production in response to CpG-ODN, although they showed a low basal expression for IL-6 cytokine which was not enhanced after CpG-ODN activation. HA/TLR9 transfected HeLa cells showed no basal expression for the tested cytokines, with no induction after CpG-ODN activation. Similar results were obtained with their mock transfected HeLa pDisplay cells (Table 3.6).

Cells	TLR9 expression	CpG-ODN (μg/ml)	Cytokine release (pg/ml)		
			IL-6	IL-10	TNF-a
Hek293 HA/TLR9	TLR9 positive	0	5.94±0.84	0.00±0.00	0.51±0.00
		3	5.53±0.42	0.032±0.03	0.51±0.00
Hek293 TLR9		0	2.33±0.85	0.00±0.00	0.34±0.17
		3	2.39±0.00	0.00±0.00	0.17±0.17
HeLa HA/TLR9		0	0.84±0.00	0.032±0.03	0.34±0.17
		3	0.84±0.00	0.155±0.06	0.34±0.17
Hek293 pDisplay	TLR9 negative	0	4.22±0.44	0.032±0.03	0.34±0.17
		3	3.32±0.47	0.0952±0.00	0.17±0.17
Hek293 pCl-neo		0	3.78±0.00	0.032±0.03	0.51±0.00
		3	3.78±0.00	0.00±0.00	0.34±0.17
HeLa pDisplay		0	0.84±0.00	0.00±0.00	0.34±0.17
		3	0.84±0.00	0.00±0.00	0.34±0.17

Table 3.6. Effect of CpG-ODN in mediating the induction of IL-6, IL-10 and TNF-α cytokines on TLR9 and mock trasnfected Hek293 and HeLa cells. Cells ($1x10^5$cells/200μl/well) were stimulated with medium or 10103 CpG-ODN (3μg/ml) for 36 hours and supernatants were collected to determine the cytokine production. Cytokine release in cell extracts was assayed using Beadlyte® Human Multi-cytokine Beadmaster™ Kit (Milipore, UK). Data represent the mean concentration pg/ml (fold induction from unstimulated control) ± S.E.M of triplicates. This experiment was done only once.

3.3.3.6 CpG-ODN mediated surface marker upregulation:

To determine the surface marker upregulation mediated by CpG-ODN activation, TLR9 positive cells were activated with the optimal dose and time course of 10103 CpG-ODN. Four relevant surface markers were tested for their upregulation upon CpG-ODN stimulation. The adhesion molecule CD54, the costimulatory molecules CD80 and CD86, and MHC class II are known to be expressed in B-lymphocytes, and their expression to be upregulated in CpG-ODN activated B-cells (Jahrsdorfer B *et al.*, 2001; Jahrsdorfer B *et al.*, 2005). Their upregulation would differ depending on the cell type and its responsiveness toward CpG-ODN activation. To investigate CpG-ODN mediated surface marker upregulation, I tested several *ex vivo* cells, tumour B-cell lines and non-haematological tumour cell lines. Different TLR9 positive cells showed variable surface marker upregulation levels after CpG-ODN activation, whereas TLR9 negative cells did not show any upregulation of the tested surface markers. This CpG-ODN activation response in the upregulation of the surface markers in normal and tumour cells is summarised in Table 3.7. *Ex vivo* cells from the PBMCs and B-CLL and the TLR9 positive tumour B-cells, Ramos, RPMI,

Raji, BJAB, 380 and Lila, showed a significant increase in the expression of at least one of those relevant surface markers. The degree of upregulation varied from one cell to another. TLR9 negative tumour cell lines HL-60 and U266 were not stimulated, and none of the tested surface markers was upregulated. TLR9 negative MCF-7, HeLa and Hek293 non-haematological cell lines did not show significant upregulation in surface markers upon their culture with CpG-ODN (Table 3.7).

From Table 3.7, CpG-ODN activated B-cells showed different responses toward the upregulation of the surface markers. The normal PBMCs showed an upregulation in the expression of all four surface markers upon the stimulation with 10103 CpG-ODN for three days. TLR9 expressing tumour B-cells showed different responses towards the activation of TLR9 (Table 3.7). *Ex vivo* B-CLL showed a significant upregulation in the four surface markers tested, with at least two fold increases after CpG-ODN activation. Burkitt's lymphoma cell line BJAB showed a highly significant upregulation in the surface markers tested, but to a lesser extent in the costimulatory CD80 molecule compared with the other surface markers tested. Ramos Burkitt's Lymphoma cell line showed an upregulation in all of the markers except CD80. Raji, BJAB and, to a less extent, Ramos Burkitt's Lymphoma cells showed high basal expression of the four surface markers. Upon stimulation with CpG-ODN, the surface marker's expression did not increase to a significant level in Raji cells except for the costimulatory molecule CD86 which showed a two fold upregulation.

Multiple myeloma RPMI 8226 cells showed an upregulation in all surface markers, with the greatest increase in CD54. Precursor B-ALL cell, 380, increased all surface markers while Lila upregulated CD54 and MHC II, but not costimulatory molecules CD80 and CD86 upon CpG-ODN treatment. HL-60 and U266, TLR9 negative cells, did not respond to CpG–ODN activation by upregulation of any of the surface markers tested (Table 3.7).

Non-haematological tumour cell lines (TLR9 negative cell lines), MCF-7, Hek293 and HeLa, did not show any response of the four surface markers (Table 3.7). Similarly, TLR9 transfected Hek293 and HeLa cell lines did not show a significant difference in expression of the surface markers upon CpG-ODN activation. Mock

transfected Hek293 cells (Table 3.7) and mock transfected HeLa cells (data not shown) were also tested for their response to CpG-ODN stimulation, and showed no upregulation of surface markers. Based on those results, TLR9 expression is a pre-request for CpG-ODN mediated surface marker upregulation, although TLR9 transfected Hek293 and HeLa cells did not upregulate the tested four surface markers suggesting that the TLR9 mediated response to CpG-ODN may be cell type specific.

Cells / Markers	Cell type	TLR9 expression	Resting Cells				Three days active cells			
			CD54	CD80	CD86	MHCII	CD54	CD80	CD86	MHCII
PBMCs	Normal *ex vivo*	+	51.1	4.57	7.62	15.20	206***	9.9***	79.1***	28***
B-CLL	Tumour *ex vivo* B-cells	+	177.8	5.19	12.99	352.8	474***	15***	58.8***	296***
RAMOS	Burkitt's Lymphoma	+	447.7	13.58	35.04	31.14	1475***	12.95	79.8***	112***
BJAB		+	712.3	78.26	494.57	772.8	1467***	114**	1050***	1046***
Raji		+	735.1	63.23	146.8	673.6	743.8	79.92	286***	550.3
380	Precursor B-ALL	+	79.25	5.58	122.1	596	564***	9.76**	179**	707**
Lila		+	63.02	5.92	101.89	183.2	245***	5.01	98.31	486***
RPMI	Multiple myeloma	+	557.9	6.765	81.374	11.155	1109**	12.6**	116.3*	21.3**
U266		-	635	13.01	18.18	54.22	578.3	18.33	20	33
HL60	Promyelocytic Leukemia	-	1072	96.86	561.11	463.1	889.2	64.28	389.9	307.9
MCF-7	Breast cancer adenocarcinoma	-	24.18	4.77	6.42	4.20	22.87	4.38	5.99	3.94
Hek293	Human embryo. Kidney	-	5.96	6.19	6.28	6.76	5.85	6.32	6.34	6.89
HeLa	Human cervical carcinoma	-	141.1	4.51	6.35	4.13	132.9	5.52	6.29	4.54
Hek293 TLR9	TLR9 Transf. Human embryon. Kidney	+	13.57	8.46	11.19	6.58	5.27	6.80	6.17	4.73
Hek293HA/TLR9		+	4.59	4.26	4.53	4.04	4.66	4.01	4.41	3.99
HeLa TLR9	TLR9 transf. Human cervical carcinoma	+	87.72	4.99	5.22	4.12	67.79	3.76	2.77	3.30
HeLa HA/TLR9		+	90.21	4.61	4.36	5.03	69.53	4.84	4.61	4.34
Hek293 pCI-neo	Mock transf. Human embryon. Kidney	-	6.10	5.46	6.54	5.45	6.26	4.33	5.01	5.75
HeK293 pDisplay		-	6.32	5.21	6.18	5.01	6.40	5.01	5.98	5.43

Table 3.7. CpG-ODN induced surface antigen upregulation in different tumour and normal cells. Data presents the mean of at least three independent experiments, and are expressed as mean MFI reading of surface markers. This experiment was repeated in two independent experiments.* $P<0.05$, ** $P<0.005$, *** $P<0.001$ (compared to control non-activated cells).

3.3.3.7 CpG-ODN mediated cellular proliferation:

In order to investigate the effect of CpG-ODN on cellular proliferation, DNA synthesis, an indicator of cell growth and cellular proliferation, was measured using a radioactive nucleotide ([methyl-3H] thymidine). Normal PBMCs were used as

control cells to detect the cellular proliferation after 10103 CpG-ODN stimulation. They showed a significant increase in their cellular proliferation after their treatment with CpG-ODN (Table 3.8). *Ex-vivo* B-CLL and TH044, and TLR9 positive tumour B-cell lines, Ramos, Raji, BJAB and RPMI, also showed a significant increase in cellular proliferation (Table 3.8).

TLR9 negative tumour cells of both haematological (Karpas and U266) and non-haematological cell lines (MCF-7, DU-145, HRT-18, WM1361A, Hek293 and HeLa) did not show any significant changes in the cellular proliferation (Table 3.8). TLR9 transfected Hek293 and HeLa cell lines, and their empty plasmid transfectants, were tested for their response to CpG-ODN stimulation to detect the functional effect of TLR9. TLR9 transfected HeLa cells did not show a significant increase in proliferation (Table 3.8), while TLR9 transfected Hek293 cells did increase cellular proliferation. Mock transfectants did not show any changes in the cellular proliferation (Table 3.8).

TLR9 expression	Cells	Cellular proliferation	
		Unstimulated cells	Activated cells
Control	Media	16±3	15±5
Positive	PBMCs	579.0±54.24	20929±371.3***
	B-CLL	87.50±43.62	1726±424.9***
	TH044	48.67±5.812	103.0±1.732**
	BJAB	70954 ± 9881	10125±5846**
	RAMOS	5515 ± 177.8	8751±618.1**
	RAJI	76784 ±3703	101424±2258*
	RPMI	33106 ±1829	61686±1881***
Negative	U266	35983 ±489.6	27079±897.6
	Karpas	8686 ± 274.0	8449±610.5
Negative	HeLa	65292±1597	62450±1469
	Hek293	112800 ±1244	93696 ±4263
	MCF-7	14863±786.5	14692±1557
	DU-145	3985±189.1	4614±348.3
	HRT-18	5081±658.1	5116±1276
	WM1361A	20531±3660	16714±2358
Positive	Hek293 TLR9	144261±11076	208265±1066*
	Hek293 HA/TLR9	190330±5954	243419±7555*
Negative	Hek293 pCl-neo	212502±6534	224821±7842
	Hek293 pDisplay	2301±40.51	1885±96.67
Positive	HeLa HA/TLR9	829.0±29.94	1072±50.65
Negative	HeLa pDisplay	666.0±56.11	824.0±38.04

Table 3.8. CpG-ODN induced cellular proliferation for normal and tumour cells, unstimulated or after activation with 10103 CpG-ODN for 3 days, and incorporated with [methyl-^{3}H] thymidine. Data present the mean of triplicate cultures ± SEM. This experiment was repeated in two independent experiments.* $P<0.05$, ** $P<0.005$, *** $P<0.001$ (compared to control non-activated cells).

3.4 Discussion:

In this Chapter, I wanted to check the CpG-ODN mediated immuno-stimulatory responses in haematological and non-haematological tumour cells and relate them to the expression of TLR9. To determine that, cells that express TLR9 at constitutively high levels (Chapter Two) were compared with the TLR9 negative cells in presence and absence of CpG-ODN, investigating their response to CpG-ODN activation. As previously stated, human tumour B-cells originate from different stages of differentiation which might render the cells to differ in their TLR9 expression and consequently in their response to CpG-ODN stimulation.

In the preliminary experiments, I determined that 3μg/ml 10103 CpG-ODN was the optimal dose to activate most of the TLR9 expressing cells, except Ramos cells which required 10-12μg/ml 10103 CpG-ODN concentrations (Table 3.1). In addition to that, the optimal activation time was found to be three days, when compared with the one day of stimulation as illustrated in Table 3.3.

As a control in this study and to demonstrate the role of TLR9 in cells' responsiveness to CpG-ODN, I have used TLR9 transfected Hek293 and HeLa cells. Mock transfected Hek293 and HeLa cells were used as a control for the TLR9 transfected ones. Again, I had to determine the optimal activating dose and time on the transfected Hek293 and HeLa cell lines, where 10103 CpG-ODN was used in different concentrations and times looking for the different CpG-ODN mediated immune responses. CpG-ODN activated TLR9 transfected Hek293 and HeLa did not show any effect on the upregulation of the relevant surface markers with 3μg/ml nor 10μg/ml 10103 CpG-ODN (Table 3.2). However, when tested for NF-κB activation mediated by CpG-ODN, 3μg/ml was sufficient to activate TLR9 transfected Hek293 and HeLa cells. In addition, 3μg/ml 10103 CpG-ODN induced increased cellular proliferation in TLR9 transfected Hek293, but not in TLR9 transfected HeLa cells. This may reflect the different levels of TLR9 expression observed in these cell lines (Chapter Two).

ODN 2137 is produced as a non-CpG control ODN. It was found to activate TLR9-positive cell lines, and to upregulate surface markers to almost the same level as the stimulatory 10103 ODN (Figure 3.3). This activating effect of the non-CpG ODN 2137 was also reported by other researchers and these ODN companies (Vollmer J *et al.*, 2004

and http://www.invivogen.com/family.php?ID=104&ID_cat=2&ID_sscat=9#groupe379 respectively). As 2137 ODN has an activating effect, I did not use it as a negative control for 10103 CpG-ODN, but used cells cultured in medium alone as a control, for the 10103 CpG-ODN mediated responses. As a conclusion of this part, three days of activation with 3μg/ml 10103 CpG-ODN treatments were considered the optimal conditions to induce TLR9 activation (with the exception of Ramos, 10-12μg/ml 10103 CpG-ODN for three days) for induction of upregulation of cell surface markers.

Akira S and colleagues in 2003 and 2004 indicated that TLR9 activation by CpG-ODN would undergo signalling cascades leading to a rapid activation of several mitogen-activated protein kinases, such as the extracellular signal-regulated kinases (ERK1/2), the $p38^{MAPK}$ protein kinase and phosphatidyltinositol 3-kinase (PI3-kinase)/AKT, in addition to IκB/NF-κB complex the down stream target of MAP Kinases. To study these CpG-ODN mediated immune responses, cells were tested for the production of the active protein kinases in each pathway in the presence and absence of CpG-ODN in a time dependent manner using a western blotting technique (except for $p38^{MAPK}$ by IP/WB) and NF-κB activation (using a luciferase assay).

BJAB Burkitt's lymphoma cell line was used as a model cell line in this study as it was previously found to express TLR9 constitutively and to respond to CpG-ODN 10103 in a similar way to normal B-cells. At the same time, other cells were tested for some signalling pathways and CpG-mediated responses to determine the CpG-ODN mediated responses in different normal and tumour cells. The downstream signalling molecules of MAPK kinases ERK1/2 and $p38^{MAPK}$ were detected in the activated BJAB cells. CpG-ODN activated TLR9 in BJAB cells and phosphorylation activity of ERK 1/2 and $p38^{MAPK}$ was detected, and cells showed significant pERK-1 activation after 60 minutes of CpG-ODN stimulation. pERK-2 also showed a high activation in 60 minutes, but it was higher at 120 minutes. Also, observations for phosphorylation of the activating transcription factor ATF-2, a $p38^{MAPK}$ target, was detected in the first 60 minutes of activation, and declined afterward, which would indicate that $p38^{MAPK}$ active form was produced within the first hour of activation. Furthermore, CpG-ODN treatment lead to the activation of PI3-kinase-AKT pathway in BJAB cells, and cells showed a significant level of pAKT in 90 minutes of activation. BJAB cells showed a significant basal activation level for pERK1/2 and pAKT products, but to a less extent for pATF-2

product. The basal levels of pERK1/2 declined directly upon the CpG-ODN stimulation, but returned to increase in a time manner response subsequently, whereas it increased gradually in AKT-1 activation. Moreover, ERK 1/2 and ATF-2 phosphorylation were only seen after one hour of CpG-ODN activation, whereas AKT phosphorylation was increasing and showed a high pAKT/AKT ratio at 90 minutes, the latest time point determined in this assay. As a result, PI3K/AKT pathway activation occurs in a longer time when compared with the other pathways.

As previously stated, the activation of TLR9 through CpG-ODN recruits MyD88-adaptor to induce the activation of MAPK and AKT pathways which induces the degradation of IκB-α complex and thus NF-κB pathways (Akira S. 2004). For that, detecting the activated parts of the subsequent pathway (pIκB-α and NF-κB activity respectively) indicates their activation with 10103 CpG-ODN. To detect IκB-α degradation, cells were tested using a western blotting technique in a time dependent manner in the presence or absence of 10103 CpG-ODN. Normal PBMCs treated with LPS, showed an activation and IκB-α phosphorylation in macrophages (Kim CS et al., 2001). In this work, LPS treated PBMCs showed a significant pIκB-α degradation in 15 minutes, which declined afterward indicating the efficiency of technique. pIκB-α degradation was then tested in tumour cell lines. Burkitt's lymphoma Ramos and BJAB cell lines treated with 10103 CpG-ODN showed a significant pIκB-α production. Ramos cell line was highly activating IκB-α degradation from the first minutes peaking the highest after 15 minutes, to decline after that. In contrast, BJAB cells needed a longer time to activate the IκB-α degradation, and showed a significant pIκB-α production after 60 minutes, declining towards normal after that, which was the same time as MAPK activated pathway results in BJAB cells.

To confirm the involvement of TLR9 in the CpG-ODN mediated downstream IκB-α degradation, TLR9 transfected Hek293 and HeLa cells were tested. Mock transfected Hek293 and HeLa cells were used as a TLR9 negative control cells. TLR9 transfected Hek293 and HeLa cells showed IκB-α degradation, leading to the production of pIκB-α that peaked at 15-30 minutes in HeLa HA/TLR9 cells and remained high after 90 minutes of CpG-ODN activation in Hek293 HA/TLR9, whereas the mock transfected cells (Hek293 pDisplay and HeLa pDisplay) did not show any activation process, as no pIκB-α was produced. These data indicate that CpG-ODN mediated pIκB-α production

is TLR9 dependent, and that the transfected TLR9 in Hek293 and HeLa cells was functional. Also, each cell line differs in its activation time, but all of the TLR9 positive cells tested were activated with CpG-ODN.

NF-κB activation results from CpG-ODN stimulation of IκB-α/ NF-κB pathway via TLR9 (Longo PG *et al.*, 2007). NF-κB activation prompts the synthesis of IκB and its activation is anti-apoptotic, so enhances cellular proliferation (Shishodia S *et al.*, 2005). Determining NF-κB activation indicates its involvement in the downstream signalling due to CpG-ODN activation via TLR9 and its influence on cellular proliferation. For that reason, cells were tested for the effect of CpG-ODN in activating NFκB pathway by transfecting them with 3xNFκB luciferase construct gene, to determine their luciferase activity in presence and absence of 10103 CpG-ODN. *Ex vivo* PBMCs and B-CLL cells, and tumour B-cells, BJAB and RPMI, showed a significant NF-κB activation on stimulation with CpG-ODN. A control group of the same cells were left without luciferase construct, did not enhance NF-κB activation. Untransfected, mock transfected and TLR9 transfected Hek293 and HeLa cells were also tested for their NF-κB activation in the same way. Un-transfected and Mock transfected Hek293 and HeLa cells were used as a negative control to ensure the involvement of TLR9 in this activation, and a control group of the same cells were left without luciferase construct. CpG-ODN treated untransfected and mock transfected Hek293 and HeLa cells did not activate NF-κB. In contrast, TLR9 transfected Hek293 and HeLa cells responded to CpG-ODN stimulation and showed NF-κB activation. These results were consistent with other studies (Takeshita F *et al.*, 2001; Ishii KJ *et al.*, 2002; Cornélie S *et al.*, 2004; Takeshita F *et al.*, 2004; Vollmer J *et al.*, 2004a), and indicate that CpG-ODN mediated activation of NF-κB is TLR9 dependent.

The observations of the IκB-α/NFκB activated pathway along with the activation of MAPK and AKT pathways, indicates that CpG-ODN induces a downstream signalling cascade via the activation of TLR9. In addition to that, each TLR9 positive cell line responds to this activation in slightly different times. These results are consistent with other studies done on CpG-ODN/TLR9 mediated responses (Hacker H *et al.*, 1998; Yi A *et al.*, 1998; Hacker H *et al.*, 1999; Hacker H *et al.*, 2000; Hemmi H *et al.*, 2000; Ishii KJ *et al.*, 2002 Yi AK *et al.*, 2002; Shishodia S *et al.*, 2005; Longo PG *et al.*, 2007).

Cytokine release results from the activation of TLR9 with CpG-ODN (Yi AK *et al.*, 2001; Yi AK *et al.*, 2002; Saegusa K *et al.*, 2007). Detecting their release would help in determining the functional responses of CpG-ODN via TLR9. TLR9 positive and negative cells were tested for their production of IL-6, IL-10 and TNF-α after 36 hours of stimulation with 10103 CpG-ODN or medium alone. The data indicate that *ex-vivo* cells (PBMCs, B-CLL, TH044 and FC029) expressed a low basal level of IL-6, that was significantly increased after CpG-ODN activation, whereas the TLR9 expressing B-cell lines (RPMI, Ramos, Lila and BJAB) did not express IL-6 cytokine in the resting stage, but significantly increased its release in Lila and BJAB cells after CpG-ODN activation, but not in Ramos and RPMI cell lines. In contrast, IL-10 basal level was relatively high in tumour B-cell lines (except for Lila), compared with the *ex vivo* cells, but upon the CpG-ODN stimulation most of them showed a significant increase in IL-10 release, except for RPMI cell line. *Ex-vivo* cells, PBMCs, B-CLL, TH044 and FC029, showed a low to negative basal expression of IL-10 that was significantly increased after CpG-ODN stimulation. Both *ex-vivo* cells and tumour B-cell lines showed a low basal expression of TNF-α that was mostly enhanced in the presence of CpG-ODN, except in Ramos cell line, which did not show any increase in TNF-α release. RPMI multiple myeloma cell line showed a small increase in the release of TNF-α, while it did not enhance the production of IL-6 and IL-10 after CpG-ODN activation. U266 and Karpas TLR9 negative multiple myeloma cell lines did not show any induction in the IL-6, IL-10 and TNF-α cytokines following culture with CpG-ODN. Although U266 cells expressed a high basal IL-6 level, consistent with previous observations of this cell line (Schwab G *et al.*, 1991), the expression was not augmented by the treatment with CpG-ODN.

To further determine the role of TLR9 in CpG-ODN mediated cytokine release, TLR9 transfected Hek293 and HeLa cells were tested. They showed no significant production or induction of IL-6, IL-10 and TNF-α cytokines in the absence or presence of CpG-ODN respectively. Furthermore, mock transfected Hek293 and HeLa, used as control cells, also did not show a basal cytokine expression nor an enhancement in the cytokine release after CpG-ODN treatment. Taken together with the data in U266 and Karpas (TLR9 negative multiple myeloma) cell lines, TLR9 is a pre-request for CpG-ODN mediated cytokine release. On the other hand, the lack of this response in TLR9 transfected Hek293 and HeLa cells might indicate cell type-specific differences in

cytokine responses between B-cells and epithelial cell lines. Published data on Hek293 and HeLa cells, mostly discussed IL-8 and MCP-1 cytokine release (Marchand P *et al.*, 2000; McFarlane SM *et al.*, 2002), which I did not test for.

To determine the functional effect of 10103 CpG-ODN in upregulating the relevant surface markers and cellular proliferation, *ex-vivo* cells and tumour (haematological and non-haematological) cells were tested for surface marker upregulation (CD54, CD80, CD86 and MHC II) and cellular proliferation in response to CpG-ODN stimulation. To rule out the effect of factors other than TLR9 in enhancing CpG-ODN function, TLR9 and mock transfected Hek293/HeLa cells were tested for their CpG-ODN mediated surface marker upregulation and cellular proliferation. CpG-ODN mediated responses towards the upregulation of the surface markers were variable depending on cell type. *Ex-vivo* B-cells (PBMCs and B-CLL) showed a highly significant upregulation on the four tested surface markers, whereas the tumour B-cell lines showed more variable results, although at least one surface marker upregulation was detected in TLR9 expressing cell lines, whilst TLR9 negative cell lines did not upregulate any of the surface markers in response to CpG-ODN. Almost all TLR9 expressing B-cells showed a significant upregulation in the adhesion molecule, CD54, except for Raji cells which only upregulated CD86 costimulatory molecule in response to CpG-ODN. CpG-ODN stimulation upregulated costimulatory molecules CD80 and/or CD86 in almost all the TLR9 expressing cells except for Lila cell line. MHC II was significantly upregulated in CpG-ODN stimulated tumour B-cell lines expressing TLR9, except Raji cell line. TLR9 negative tumour cells did not show any upregulation in the four surface markers although, two of them (HL-60 and U266) showed a high basal expression levels that was not upregulated after CpG-ODN activation.

These results were similar to the published data as they showed that normal B-cells, B-CLL cells, EBV–transformed cell lines and other cell lines representative of mature B-cell neoplasias (Burkitt's lymphoma and follicular lymphoma) expressed TLR9 and responded to CpG-ODN stimulation activating signalling pathway, secreting IL-6, IL-10 and TNF-α cytokines, activating NF-κB, upregulating CD54, CD80, CD86 and MHC II surface markers and induceding cellular proliferation (Krieg A *et al.*, 1995; Klinman D *et al.*, 1996; Decker T *et al.*, 2000a; Decker T *et al.*, 2000b; Hartmann, G *et al.*, 2000; Jahrsdorfer B *et al.*, 2001; Verthelyi *et al.*, 2001; Brouke E *et al.*, 2003; Leifer CA *et al.*,

2004; Takeshita F *et al.*, 2004; Henault M *et al.*, 2005; Jahrsdorfer B *et al.*, 2005; Grandjenette C *et al.*, 2007).

Jahrsdorfer B and colleagues (2005) found that most B-cell malignancies except plasmacytoma, isolated from bone marrow of patients with multiple myeloma, responded to CpG-ODN stimulation by upregulating surface markers and cellular proliferation. They also reported that B-CLL and marginal zone lymphoma showed the strongest activation upon stimulation with CpG-ODN whereas follicular lymphoma and mantle cell lymphoma showed an intermediate response. B-CLL cells also showed a strong response to CpG-ODN by increasing cellular proliferation and activating signalling pathways (Longo *et al.*, 2007). These results were consistent with mine, B-CLL showed significant responses to CpG-ODN activation while cells lacking the expressing of TLR9 (U266 and Karpas multiple myeloma) were unresponsive to CpG-ODN activation.

CpG-ODN stimulation of TLR9 negative non-haematological (MCF-7, Hek293 and HeLa) cells, had no effect on surface marker expression. In addition, TLR9 transfected or mock transfected Hek293 and HeLa cells did not show surface marker upregulation after CpG-ODN treatment. Taking the results together, CpG-ODN mediated surface marker upregulation is TLR9-dependent, but expression of TLR9 does not confer the ability to upregulates the surface markers tested, as demonstrated by TLR9 transfected Hek293 and HeLa cells. As with cytokine responses, this effect may be dependent on cell type and TLR9 transfected Hek293 and HeLa cells might respond to CpG-ODN activation by upregulating surface markers other than CD54, CD80, CD86 and MHC II.

To determine the other functional response of CpG-ODN, cellular proliferation, tumour cells were studied, according to their TLR9 expression. *Ex-vivo* (PBMCs, B-CLL and TH044) cells and TLR9 positive tumour B-cell lines showed a significant increase in cellular proliferation in response to CpG-ODN activation. On the other hand, TLR9 negative tumour B-cells, U266 and Karpas, did not show cellular proliferation in response to CpG-ODN. TLR9 negative non-haematological tumour cell lines, Hek293, HeLa, MCF-7, DU-145, HRT-18 and WM1361A, did not respond to CpG-ODN stimulation with enhanced cellular proliferation. To determine the role of TLR9 in CpG-ODN mediated cellular proliferation, TLR9 and mock transfected Hek293 and HeLa

cells were tested. TLR9 transfected Hek293 cells showed some increase in cellular proliferation when compared with their mock transfectants' response towards CpG-ODN mediated cellular proliferation. In contrast, TLR9 transfected HeLa cells did not show any changes in their cellular proliferation and same results were seen with the mock transfected HeLa cells. As TLR9 transfected HeLa cells did not express TLR9 to the same level as in TLR9 transfected Hek293 cells, it might be a reason why the TLR9 transfected HeLa cells did not show some increase in cellular proliferation. The response in cellular proliferation to CpG-ODN in TLR9 positive Hek293 cells, along with the activation of NF-κB pathway, further emphasizes that CpG-ODN activation is TLR9 dependent.

In this work, the cellular proliferation and NF-κB activation data from CpG-ODN activation via TLR9 indicate that NF-κB activation enhances and regulates cellular proliferation. This result is consistent with the reports indicating that NF-κB activation is anti-apoptotic and enhances cellular proliferation (Shishodia S *et al.*, 2005). At the end of this chapter, I have shown the different CpG-ODN mediated immune responses resulted from the activation of TLR9 in normal and tumour cells. However, major challenges remains; 'what are the biochemical and molecular events that connect the intracellular signalling pathways and the functional responses in CpG-ODN mediated responses?' Determining that could lead to the birth of new aspects in cancer therapy.

3.5 Conclusion:

This chapter demonstrates elemental insights into the role of TLR9 in CpG-ODN mediated responses in human tumour cells. Firstly, the expression of TLR9 is a prerequisite for CpG-ODN responsiveness. Results indicate that TLR9 positive haematological tumour B-cells are CpG-responsive cells, while TLR9 negative tumour B-cells and non-haematological tumour cells are not. Furthermore, TLR9 transfections in Hek293 and HeLa cells confer CpG reactivity to the cells that are otherwise non-responsive to cellular proliferation and NF-κB pathway activation, although these cells differed in cytokine responses and surface marker upregulation when compared with TLR9 positive B-cell lines.

The data in this chapter indicate that TLR9 recognizes CpG-ODN, mediating cellular activation and proliferation. CpG motif was recognized in this work as a potent adjuvant that led to the activation of ERK1/2, AKT, $p38^{MAPK}$ and IκB-α/NF-κB downstream intracellular pathways. TLR9 expressing B-cells were activated by CpG-ODN, and the active phosphorylated product of ERK1/2, ATF-2 ($p38^{MAPK}$ activation product), AKT and IκB-α were detected in BJAB Burkitt's lymphoma. NF-κB activation was also detected in CpG-ODN activated BJAB cells. The activation of these downstream signalling pathways by CpG-ODN suggested that they might be effectors in the TLR9 activating pathway during CpG-ODN stimulation. NF-κB downstream intracellular pathway was also tested in other cells to determine the CpG-ODN mediated stimulatory effect in TLR9 positive and negative cells. TLR9 expressing tumour B-cells were found to activate this pathway, while TLR9 negative cells did not.

TLR9 positive cells, also, showed a CpG-ODN mediated cytokine release, whereas TLR9 negative cells did not. The CpG motif was found to activate the cell and enhance the release of IL-6, IL-10 and TNF-α cytokines in *ex-vivo* cells and in some of the tumour B-cell lines. These cytokines were found to be CpG-ODN/TLR9 dependent to regulate the immune responses. IL-6, IL-10 and TNF-α release were increased in almost all TLR9 positive cells in response to CpG-ODN. TLR9 negative B-cell lines, U266 and Karpas, and non-haematological tumour cells did not respond to CpG-ODN and had no effect on cytokine release. However, CpG-ODN stimulation of TLR9 or mock transfected Hek293 and HeLa cells did not enhance IL-6, IL-10 and TNF-α cytokine release. This might indicate that these cytokines are not expressed in Hek293 and HeLa

cells, and I should look for the release of other cytokines after CpG-ODN activation. TNF-α was known for its role in the regulation of inflammatory responses by activating intracellular signalling and cellular proliferation (Han Y *et al.*, 1999), and data in this chapter were consistent with that. While TLR9 positive B-cells showed intracellular signalling, NF-κB pathway activation by inducing IκB-α phosphorylation and NF-κB translocation, increased CD54 and MHC II expression and cellular proliferation they also showed an increase in TNF-α release after CpG-ODN activation.

Human B-cell malignancies originate from different stages of cell differentiation which may affect expression of TLR9 and their sensitivity and responsiveness towards the CpG activation. TLR9 positive tumour B-cells recognized CpG motif and upregulated at least one of the four surface markers tested. The expression of adhesion molecule CD54 and the antigen-presenting molecule MHC II were significantly upregulated in almost all TLR9 positive tumour B-cells. The expression of the costimulatory molecules CD80 and /or CD86 was upregulated in most of the B-cells. The upregulation of the costimulatory molecules in the activated B-cells suggest that CpG-ODN would improve the cellular interactions of B cells and T cells by enhancing the upregulation and expression of the adhesion molecule CD54, and would increase the levels of the costimulatory molecules CD80 and CD86 and the antigen-presenting molecule MHC II needed to facilitate antigen presentation to naïve helper T cells. In this way, CpG-ODN might provide a rational immunotherapy for TLR9 positive B-cell malignancies.

The recognition of the CpG motif in the TLR9 positive cells was found to increase their cellular proliferation significantly. TLR9 negative cells did not induce any CpG-ODN mediated cellular responses, as no cytokine release, NF-κB activation, cellular proliferation or surface marker upregulation were indicated. Another fundamental insight of this work is that hTLR9 transfections in Hek293 and HeLa cells conferred CpG reactivity, leading to increase cellular proliferation, IκB-α degradation and NF-κB activation, but not to upregulation of the surface molecules or cytokine release as tested. This might be due to testing the wrong parameters, or to differences in responsiveness to CpG-ODN of different TLR9 positive cell types. These results indicate that the transfected TLR9 was capable of mediating CpG-ODN induced intracellular signalling, but that the effect of CpG-ODN stimulation in TLR9-transfected Hek293 and HeLa cells was distinct from the effects of CpG-ODN/TLR9 signalling in B-cells and cell lines

constitutively expressing TLR9. The conclusion of this chapter provides a clear evidence for the causative relationship between the expression of hTLR9 and the CpG-mediated response in human tumour cells.

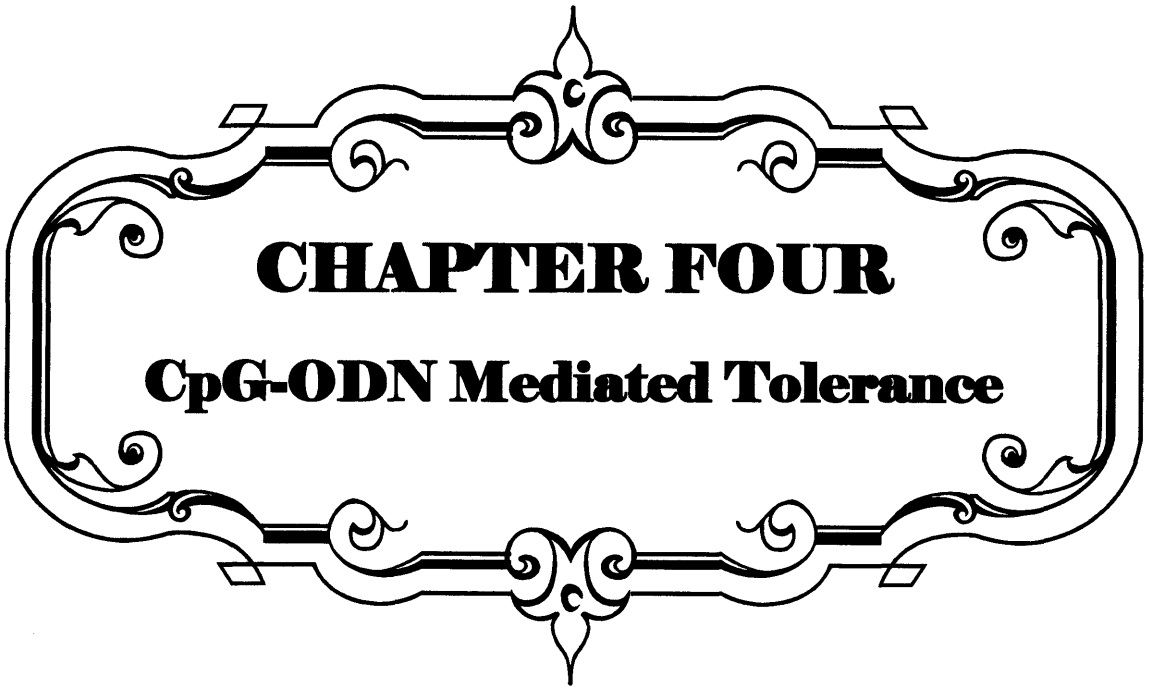

CHAPTER FOUR

CpG-ODN Mediated Tolerance

CHAPTER FOUR
CpG-ODN Mediated Tolerance

4.1 Introduction:

CpG oligodeoxynucleotide (ODN) mediated tolerance is a state of refractoriness towards a second stimulation by CpG-ODN after a preceding treatment with CpG-ODN. B-cells were found to express TLR9 and upon their activation with CpG-ODN, they rapidly increase levels of costimulatory molecules, produce cytokines, proliferate, and induce activation of transcription factor NF-κB. NF-κB plays a critical role in CpG DNA-mediated cellular proliferation and TNF-α cytokine production. TNF-α release stimulates the innate immune response, induces cytokine production such as IL-6, and induces tumour cell death (Klinman D M *et al.*, 1996 ; Yi AK *et al.*, 1998; Yi AK *et al.*, 2002; van Horssen R *et al.*, 2006; Wei L *et al.*, 2006). I wished to determine whether a non-activating dose of CpG-ODN could render the target cells unresponsive to a subsequent activating dose of CpG-ODN, as this could have important implications for the use of CpG-ODN in immunotherapy. Tolerance status has been demonstrated for Lipopolysaccharide (LPS) in TLR4 activation, a phenomena that has been called " endotoxin tolerance" (Wysocka M *et al.*, 2001; Sato S *et al.*, 2002).

CpG DNA /TLR9 tolerance has been studied in monocyte/macrophages of mouse (Crabtre. TD *et al.*, 2001; Yeo SJ *et al.*, 2003), but not previously in B-cells. The mechanisms that lead to 'endotoxin tolerance' and 'CpG DNA/TLR9 tolerance' and their immunological paralysis remain unclear and still under investigations. Most of the published studies were on 'endotoxin tolerance' induced by TLR2 and TLR4 agonists, LPS, suggesting an impaired expression and/or function of common signalling intermediates involved in LPS signalling including ERK, JNK, and p38 MAP Kinases and NF-κB pathways (Kraatz J *et al.*, 1999; Tominaga K *et al.*, 1999; Medvedev AE *et al.*, 2000; Dobrovolskaia MA *et al.*, 2003). Recent studies indicated the involvement of other signalling components, the IRAK and IκB, in the induction of 'endotoxin tolerance' (Dobrovolskaia MA *et al.*, 2003; Hatao F *et al.*, 2004; Kim YI *et al.*, 2008). The 'CpG-ODN/TLR9 tolerance' was studied in murine macrophages either as homotolerance (i.e. CpG-ODN is the tolerising and the challenge stimulus) or heterotolerance (i.e. in conjunction with LPS cross-tolerance), and the underlying

mechanisms were suggested to be an interaction of altered conditions at several steps of signal transduction and mainly in IRAK (Yeo SJ *et al.*, 2003; Hatao F *et al.*, 2004; Dalpke A.H *et al.*, 2005; Kim YI *et al.*, 2008).

As a result, the immunologic effects of CpG-ODN delivery are dose-dependent, and the appropriate dosage to regulate and initiate the innate and adaptive immune response are likely to be necessary for its immunotherapeutic uses. In *in vitro* studies on murine macrophages done by Wei L and colleagues, pretreatment with CpG-ODN significantly inhibited the activation of NF-κB, which also inhibited cellular proliferation (Wei L *et al.*, 2006). Additionally, several studies reported that CpG DNA pretreatment suppressed expression of TNF-α, IL-6, IL-10, and IL-12 in murine macrophage-like RAW264.7 cells in response to subsequent challenge by CpG DNA. Furthermore, they have stated that CpG DNA-mediated signalling activation, including ERK, p38 and NF-κB pathways, were greatly suppressed in RAW264.7 cells pretreated with CpG DNA (Crabtree TD *et al.*, 2001; Yeo SJ *et al.*, 2003; Dalpke AH *et al.*, 2005; Broad A *et al.*, 2007; Kim YI *et al.*, 2008).

In the last few years, a lot of effort has been put in to reveal the CpG DNA mediated responses in activating cells to mediate its therapeutic benefits. Yet, the effect of its suppressed activity and down-regulation of the immune system has received relatively little attention. It is still not clear whether previous exposure of tumour B-cells to a non-activating dose of CpG DNA induces suppressive response (tolerance) to subsequent stimulation with an activating dose. In the present study, I wanted to investigate whether CpG DNA has the ability to induce a refractory state in tumour B-lymphocytes via TLR9, and to what extent. For this purpose, I have used Burkitt's lymphoma BJAB tumour B-cells as a model system, and studied the effect of a non-activating dose of 10103 CpG-ODN on the downstream signalling for the induction of the transcription factor NF-κB and its role in CpG DNA-mediated cytokine production of TNF-α, IL-6 and IL-10 to subsequent challenge with CpG DNA in BJAB tumour B-cells. Furthermore, I have studied its effect on the levels of adhesion and costimulatory molecules and cellular proliferation. Finally, BJAB cell responses were compared with *ex vivo* B-cells and other transformed tumour B-cell line (RPMI) to demonstrate the consistency of these responses.

4.2 Materials and methods:

4.2.1 Materials:

- 10103 CpG ODN (Coley Pharmaceutical, Canada)
- Anti-CD54-PE (Beckman Coulter, UK)
- Anti-CD80-FITC (clone MAB104, Beckman Coulter, UK)
- CD86-PE (clone HA5.2B7, Beckman Coulter, UK)
- Anti-MHC II-FITC (monoclonal mouse anti-human HLA-DP DQ, Dako , UK)
- Anti-IgG1-PE (Beckman Coulter, UK)
- Anti-IgG1-FITC (Beckman Coulter, UK)
- [methyl-^{3}H] thymidine (GE Healthcare, UK, Ltd)
- Effectene Transfection Reagent (Qiagen, UK)
- Luciferase assay system (Promega, UK)
- Beadlyte® Human Muli-cytokine Beadmaster™ Kit (Milipore, UK)

4.2.2 Methods:

4.2.2.1 Tolerising effect of low dose of CpG-ODN:

As indicated in Chapter Three (section 3.3.1), 3μg/ml 10103 CpG-ODN was considered as an activating dose, for most of the tested TLR9 positive cells, whereas the low dose of 0.1μg/ml 10103 CpG-ODN showed little or no effect on the upregulation of their surface markers (Table 3.1). To test the effect of the non-activating dose of CpG-ODN on the *ex vivo* cells (PBMCs and CLL B-cells) and tumour B-cells (RPMI 8226 and BJAB), and to detect the response after the subsequent addition of an activating dose, cells were left one or three days in 0.1μg/ml 10103 CpG-ODN, before exposing the cells to the activating dose (3μg/ml 10103 CpG-ODN) for three days (optimum time). Tumour B-cells RPMI 8226 and BJAB were also pretreated for up to four weeks with 0.1μg/ml 10103 CpG-ODN and then activated for three days with 3μg/ml 10103 CpG-ODN to determine the duration of the tolerising effect. Finally, BJAB cells were treated with the low dose of 10103 CpG-ODN for one or three days, washed, and were then tested for the length of the time that they remained unresponsive to a subsequent activating dose of 3μg/ml 10103 CpG-ODN.

4.2.2.2 Effect of 0.1μg/ml 10103 CpG-ODN on NF-κB luciferase activity:

To determine the effect of the 0.1μg/ml 10103 CpG-ODN dose for a limited time on the activation of NF-κB, *ex vivo* cells (PBMCs and B-CLL) and tumour B-cell lines (RPMI 8226 and BJAB) were left for one and three days with 0.1μg/ml 10103 CpG-ODN before being transiently transfected with 3xNFκB.luc DNA construct gene using Effectene Transfection Reagent (Qiagen, UK) (as described in section 3.2.2.6). In addition, tumour B-cells (RPMI and BJAB) were left for up to four weeks with the non-activating dose and tested each week for its effect on the activation of NF-κB.

4.2.2.3 Effect of 0.1μg/ml 10103 CpG-ODN dose on cytokine release:

Ex vivo B-cells of PBMCs and B-CLL and tumour B-cells of Burkitt's lymphoma BJAB and multiple myeloma RPMI 8226 cell lines were left one and three days with 0.1μg/ml 10103 CpG-ODN before they were activated with the 3μg/ml 10103 CpG-ODN activating dose. Resting and 10103 CpG-ODN activated cells were cultured for 36 hours in triplicate wells, flat bottom 96 well plate, after which supernatants were collected and assayed for their cytokine release as described earlier in Chapter Three (section 3.2.2.7) using a multiplex cytokine assay, Beadlyte® Human Muli-cytokine Beadmaster™ Kit (Milipore, UK), for the measurement of the secretion of three cytokines (IL-6, IL-10 and TNF-α) by those cells.

4.2.2.4 Effect of low CpG dose on flow cytometric analysis of surface markers:

Flow cytometry was used to investigate the expression of the adhesion molecule CD54, costimulatory molecules CD80 and CD86 and Major Histocompatibility Complex (MHC) class II, and to detect if 0.1μg/ml 10103 CpG-ODN would affect their upregulation upon their subsequent activation with CpG ODN.

To determine the effect of the low dose of CpG-ODN for a limited time on the upregulation of the relevant surface markers, $5x10^5$ cells/ml were treated with the 0.1μg/ml 10103 CpG-ODN, cells were washed with PBS, and the pellet stained with the four surface marker monoclonal antibodies as described in section (3.2.2.8). Fluorescence values were brought together after live gating of 10,000 events were acquired using CellQuest software (BD Biosciences, UK).

4.2.2.5 Effect of low CpG dose on Cellular Proliferation:

A direct proliferation assay in which DNA synthesis was the indicator of cell growth was carried out using a radioactive nucleotide assay ([methyl-^{3}H] thymidine). The incorporation of ^{3}H-thymidine into replicating DNA was measured, which is directly proportional to the amount of cell division occurring in the culture. To determine the occurrence of CpG-ODN mediated tolerance phenomena, cells were pretreated with the low dose CpG-ODN for a limited time before exposing the cells to an activating dose and measuring their proliferative response. $5x10^6$ cells/well in triplicates, flat bottom 96 well plate, of tumour B-cell lines (RPMI and BJAB) and *ex-vivo* cells (PBMC and B-CLL) were pretreated with the low dose of 0.1μg/ml 10103 CpG-ODN for one and three days. In addition, tumour B-cells (RPMI and BJAB) were left for up to four weeks with the low dose and tested each week for their proliferative responsiveness to a subsequent activating dose of CpG-ODN. A control group of the same cells were left untreated with 0.1 μg/ml 10103 CpG-ODN. [Methyl-^{3}H] thymidine (1μCi/well) (GE Healthcare, UK, Ltd) was added overnight and cells were harvested and read as described in section (3.2.2.9). The incorporation of [^{3}H] thymidine in cellular DNA was measured using β-counter (1450 Microbeta plus liquid scintillation counter - Wallac, Finland).

4.2.2.6 Time-dependent response of CpG-ODN to re-activate pretreated BJAB cells.

To determine the effect of pre-treatment on the length of refractory period, BJAB cell lines were pretreated with the low dose (0.1 μg/ml) of 10103 CpG-ODN for one and three days before washing them with fresh media and then investigated for the time that they needed to return back to be responsive to the activating dose of 3μg/ml 10103 CpG-ODN and activate NF-κB production.

4.2.2.7 Statistical analysis:

Each experiment was done in triplicates, except for the FACS results. Data were analysed using Student's paired t-test using GraphPad prism 4 software version 4.03. Data points represent the mean of at least three parallel samples plus/minus S.E.M. Results were considered significant when p value was less than 0.05, and very significant when p value was less than 0.001.

4.3 Results:

As was previously determined (Chapter Three, Table 3.1), 0.1μg/ml of 10103 CpG-ODN was found to be a non-activating dose for many cell lines when tested for its effect on upregulating the surface marker CD54, CD80, CD86 and MHC II. Burkitt's lymphoma BJAB cell line was found to express TLR9 and respond to CpG-ODN activation in a highly sensitive way. 0.1μg/ml 10103 CpG-ODN did not upregulate the four surface markers' expression in BJAB cell line (data not shown) suggesting that it might be a non-activating dose. In this work I wanted to investigate whether pre-exposure to low dose (0.1μg/ml) of 10103 CpG-ODN would induce hypo-responsiveness in Burkitt's lymphoma BJAB cells in response to subsequent activating dose (3μg/ml) 10103 CpG-ODN challenge, and to compare its response with that of another TLR9 positive tumour B-cells (RPMI multiple myeloma) and normal PBMCs and B-CLL *ex vivo* B cells to demonstrate the consistency of this effect. Cells were pretreated with the proposed non-activating dose of 10103 CpG-ODN (0.1μg/ml) for a limited time, and then tested for their responsiveness to the subsequent activating dose of 10103 CpG-ODN (3μg/ml), by activating the transcription factor NF-κB, enhancing cytokine release, upregulating the relevant surface markers, and increasing cellular proliferation.

4.3.1 Effect of 0.1μg/ml of 10103 CpG-ODN pretreatment on CpG-mediated immune responses:

As previously demonstrated (Chapter Three), TLR9 expressing B-cells showed significant CpG mediated immune responses to stimulation with optimal doses of CpG-ODN. In this work I wanted to determine the effect of pretreatment with low doses of CpG-ODN (0.1μg/ml of 10103 CpG-ODN) on B-cells, and to what extent it will affect the CpG-ODN mediated responses to a subsequent activating dose.

4.3.1.1 CpG-ODN mediated response of Burkitt's lymphoma BJAB B-cells pretreated with 0.1μg/ml of 10103 CpG-ODN:

Burkitt's lymphoma BJAB cell line was used as the main cell line in my studies to determine their CpG-ODN functional and molecular mediated immune responses. BJAB cells were found to respond to 3μg/ml of 10103 CpG-ODN by activating the downstream signalling pathways (ERK, p38 ^{MAPK}, AKT pathways and IκB-NF-κB pathway), by releasing cytokines, upregulating surface marker expression and

increasing cellular proliferation (Chapter Three). BJAB cells were left for up to three weeks in 0.1μg/ml 10103 CpG-ODN before activating them with 3μg/ml 10103 CpG-ODN to study the short term and long term effects of low dose CpG-ODN.

A) Effect on CpG-ODN mediated downstream signalling:

Table 4.1 illustrates the effect of 0.1μg/ml 10103 CpG-ODN pretreatment of BJAB cells on the activation of the transcription factor NF-κB. Control BJAB cells (cultured in medium alone) showed a highly significant increase in NF-κB activity after CpG-ODN activation. Additionally, BJAB cells were tested for the effect of short term (one, two and three days) and long term (two and three weeks) pretreatment with 0.1μg/ml CpG-ODN and showed an obvious inhibition of NF-κB activity following subsequent exposure to an activating dose of CpG-ODN (3μg/ml). 0.1μg/ml 10103 CpG-ODN was found to be a non-activating dose, and cells did not increase the basal activation level of NF-κB. As a result, BJAB cells pretreated with the non-activating (0.1μg/ml) dose dramatically inhibited NF-κB activation to a subsequent activating dose (3μg/ml) in a short or long term assay.

BJAB NF-κB activation.		Resting	Active
Control	Medium	197.2±10.10	702.7±38.90**
Short term	One day	207.2 ±10.79	249.2 ±3.928
	Two days	260.7 ±31.71	204.7±18.85
	Three days	152±9.849	238.7±37.37
Long term	Two Week	127.7±5.696	193±30.24
	Three weeks	270.1 ± 4.816	254.7 ± 7.351

Table 4.1. Effect of the non-activating dose of 0.1μg/ml 10103 CpG-ODN on NF-κB activation in Burkitt's lymphoma BJAB cells pretreated for up to three weeks followed by a subsequent activating dose of 3μg/ml 10103 CpG-ODN. Control Burkitt's lymphoma BJAB cells were left untreated (medium alone) before their activation for 18 hours. Data represent the mean luciferase activity RLU ± S.E.M of triplicates. This experiment was done only once. ** $P<0.005$ (compared to control non-active cells).

To determine the effect of pretreatment with 0.1μg/ml 10103 CpG-ODN on the ability of BJAB cell line to release cytokines, cells were left with the 0.1μg/ml 10103 CpG-ODN for one and three days before their subsequent activation with 3μg/ml 10103 CpG-ODN for 36 hours. As Table 4.2 illustrates, the control group of untreated BJAB cells showed a highly significant release in IL-6, IL-10 and

TNF-α cytokines after CpG-ODN activation (3μg/ml). The basal expression level of the cytokines in the control cells was low except for IL-10, which also showed the highest induction after the subsequent activation. The basal expression level of three cytokines did not change upon their pretreatment with 0.1μg/ml 10103 CpG-ODN. On the other hand, 0.1μg/ml 10103 CpG-ODN did not induce a complete inhibition of cytokine release in pretreated BJAB cells, and cells still showed some induction of IL-6, IL-10 and TNF-α release, although this was reduced compared with the responses of control resting and CpG-ODN activated cells for IL-6 and TNF-α production (Table 4.2).

Cells	Time	CpG-ODN (μg/ml)	Cytokine release (pg/ml)		
			IL-6	IL-10	TNF-α
BJAB	Control	0	1.020±0.1823	443.8±11.88	4.845±1.7
		3	13.41±1.1**	3240±72.7***	39.70±1.28**
	One day	0.1	1.353±0.52	293.7±11.21	3.147±0.00
		3	7.923±2.07*	2699±264.6*	23.92±4.69**
	Three days	0.1	1.868±0.52	375.0±14.57	2.602±0.545
		3	5.527±0.42*	3393±186.3**	18.41±3.21*

Table 4.2. Effect of 0.1μg/ml 10103 CpG-ODN on the CpG-ODN mediated induction of IL-6, IL-10 and TNF-α cytokines in Burkitt's Lymphoma BJAB cells. BJAB cells ($1x10^5$cells/200μl/well) were pretreated with medium alone or with 0.1μg/ml 10103 CpG-ODN for one and three days before their subsequent activation with 3μg/ml 10103 CpG-ODN for 36 hours, and supernatants were collected to determine the cytokine production. Cytokine release in cell supernates was assayed using Beadlyte® Human Multi-cytokine Beadmaster™ Kit (Milipore, UK). Data represent the mean concentration pg/ml ± S.E.M of triplicates. This experiment was done only once. * $P<0.05$, ** $P<0.005$, *** $P<0.001$ (compared to its non-activated cells).

B) Effect on CpG-ODN mediated surface marker upregulation and cellular proliferation:

In this work I wanted to determine the effect of 0.1μg/ml 10103 CpG-ODN on the subsequent ability of CpG-ODN to upregulate surface marker expression and cellular proliferation in Burkitt's lymphoma BJAB cell line. BJAB cells were tested for their short term (one and three days) and long term (one, two and three weeks) effects.

Figure 4.1 shows the effect of 0.1μg/ml of 10103 CpG-ODN pretreatment on the surface markers CD54, CD80, CD86 and MHC II upregulation in BJAB cells. BJAB control cells pretreated with medium alone showed a significant upregulation in the adhesion molecule CD54, costimulatory molecules CD86, MHC II and to a lesser extent CD80 surface markers in response to CpG-ODN subsequent activation. 0.1μg/ml 10103 CpG-ODN did not show a significant increase in the basal CD54, CD80 and CD86 expressions over the three weeks of pretreatment, indicating that it is a non-activating dose for them (data not shown).

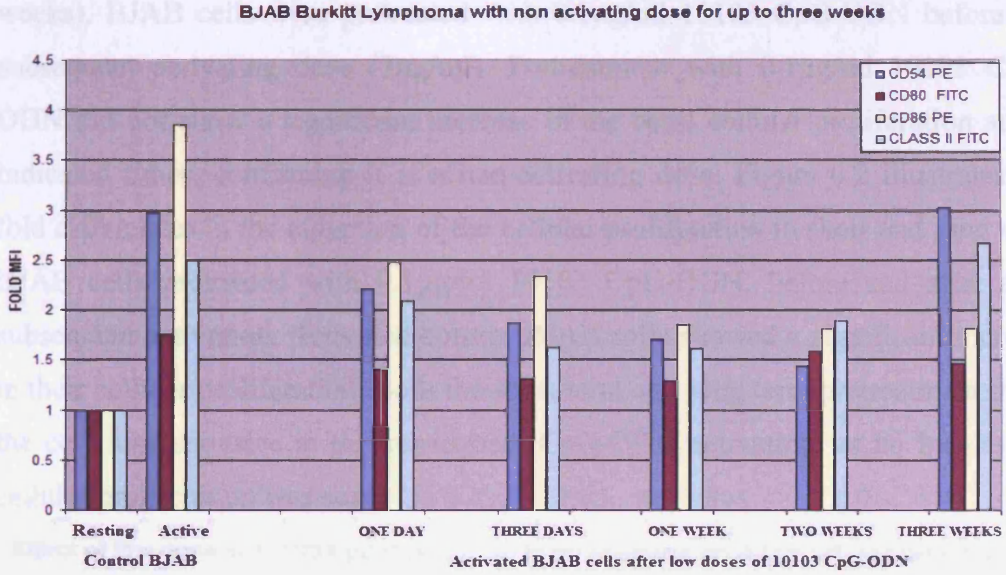

Figure 4.1. Fold changes in the effect of 0.1μg/ml 10103 CpG-ODN on the upregulation of adhesion molecule CD54, costimulatory molecules CD80, CD86, and MHC II expression in pretreated BJAB Burkitt's lymphoma up to three weeks, followed by a subsequent activating dose of 3μg/ml 10103 CpG-ODN for three days. Control BJAB Burkitt's lymphoma was left untreated before their activation for three days. Data represent the fold induction from unstimulated control of MFI. This experiment was done only once.

The short term (less than a week) changes in the surface marker upregulation showed a reduced expression level in all of the surface markers, but to a lesser extent for CD80 than for the other markers, after the subsequent activation. The long term effect of one and two weeks were still showing a reduction in CD54, CD86 and MHC II expression after CpG-ODN activation, but their upregulation returned towards normal after three weeks of pretreatment for CD54 and MHC II expression, although CD86 upregulation remained reduced even in the three weeks pretreated cells compared with the activated control BJAB cells. CD80 expression

did not show a significant short term and long term effect compared with the activated control cells, although it was also the surface marker that showed the least response to CpG-ODN in control BJAB cells.

To determine the influence of the low dose of CpG-ODN on BJAB proliferative responsiveness to a subsequent activating dose, CpG-ODN mediated cellular proliferation was investigated. Cells were studied for their cellular proliferation response in short term (one and three days) and long term effect (one and three weeks). BJAB cells were pretreated with 0.1μg/ml 10103 CpG-ODN before the subsequent activating dose (3μg/ml). Pretreatment with 0.1μg/ml 10103 CpG-ODN did not show a significant increase in the basal cellular proliferation at the indicated times, confirming it is a non-activating dose. Figure 4.2 illustrates the fold differences in the induction of the cellular proliferation in short and long term BJAB cells pretreated with 0.1μg/ml 10103 CpG-ODN, before and after their subsequent activation. Activated control BJAB cells showed a significant increase in their cellular proliferation. Both the short term and long term pretreatment made the cells unresponsive to the subsequent CpG-ODN activation, as no increase in cellular proliferation was seen.

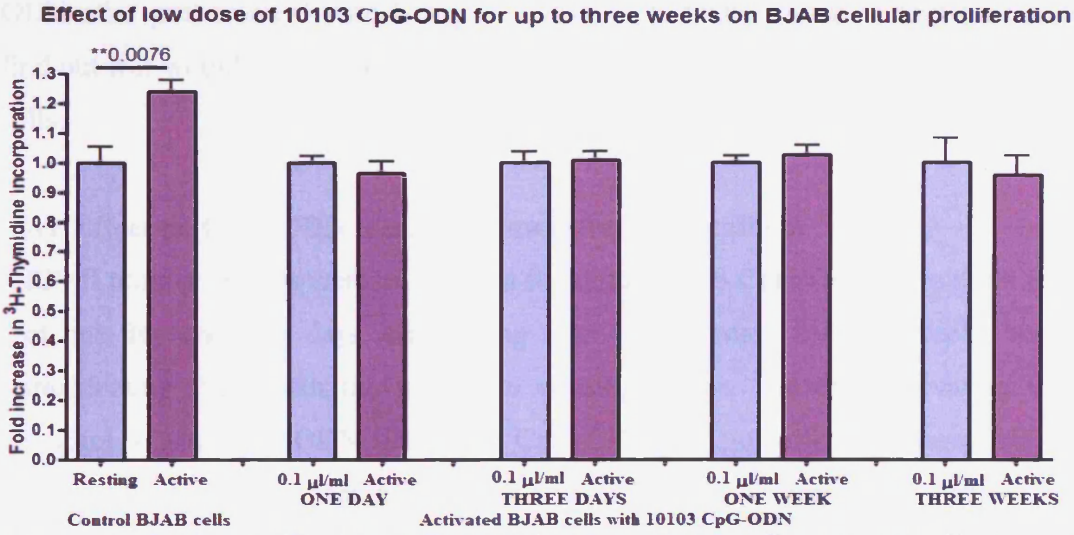

Figure 4.2. Cellular proliferation in Burkitt's lymphoma BJAB cells pretreated with the non-activating dose of 0.1μg/ml 10103 CpG-ODN for up to three weeks, followed by a subsequent activating dose of 3μg/ml 10103 CpG-ODN for 3 days. Control Burkitt's lymphoma BJAB cells were left untreated (resting) before their activation for three days. Resting or non-activating dose: blue bar, three days activated cells: purple bars. Basal count in resting cells is (90270±4934 cpm), and it did not change over the time. Data represent the mean (fold induction from unstimulated control) ^{3}H-thymidine incorporation ± S.E.M of triplicates. This experiment was repeated in two independent times.

As a conclusion, the non-activating dose 0.1μg/ml 10103 CpG-ODN induced a hyporesponsive state in Burkitt's lymphoma BJAB cells for periods of up to three weeks in some CpG-ODN mediated responses. To evaluate the tolerising effect of low doses of CpG-ODN further, another tumour B-cell line (RPMI cells) and normal PBMCs and tumour *ex vivo* B-cells were studied for the same effects.

4.3.1.2 CpG-ODN mediated response on RPMI multiple myeloma cells pretreated with 0.1μg/ml of 10103 CpG-ODN:

I wanted to investigate the tolerising effect of low doses of CpG-ODN on multiple myeloma RPMI 8226, another TLR9 positive tumour B-cell line. As transformed B-cell lines can grow for longer time in the tissue culture, RPMI 8226 was tested for the short and long term effects of the pretreatment with 0.1μg/ml 10103 CpG-ODN on CpG-ODN mediated responses after the subsequent activation.

Effect on Multiple myeloma RPMI 8226 tumour B-cells:

Multiple Myeloma RPMI 8226 cell line was studied to detect any changes in the CpG-ODN mediated NF-κB activation, cytokine release, surface marker upregulation and cellular proliferation to the activating dose of 3μg/ml 10103 CpG-ODN after pretreatment with 0.1μg/ml 10103 CpG-ODN for up to four weeks, to find out if it would induce a hyporesponsiveness state, as was demonstrated in BJAB cells.

A) Effect on CpG-ODN mediated downstream signalling:

RPMI tumour B-cells were cultured in 0.1μg/ml 10103 CpG-ODN for a short term of one day and four days, and a long term of one week and two weeks before transfecting them with the luciferase construct gene, and then activating with 3μg/ml 10103 CpG-ODN. 0.1μg/ml CpG-ODN did not affect the basal NF-κB activation, indicating that it is a non-activating dose. Figure 4.3 illustrates the effect of 0.1μg/ml 10103 CpG-ODN pretreatment of RPMI tumour B-cells on the activation of the transcription factor NF-κB after a subsequent activation dose of CpG-ODN. The control (untreated) cells were done in parallel at each time interval, and the results are expressed as the mean fold increase for each time point presented. Control RPMI cells showed a significant increase in NF-κB activity in response to 3μg/ml 10103 CpG-ODN, while RPMI cells pretreated with 0.1μg/ml

10103 CpG-ODN for one and four days did not show any activation for the transcription factor NF-κB after the subsequent CpG-ODN activation. In contrast, pretreatment of RPMI cells with 0.1μg/ml 10103 CpG-ODN for one and two weeks had no effect on the subsequent ability of CpG-ODN to induce NF-κB activation.

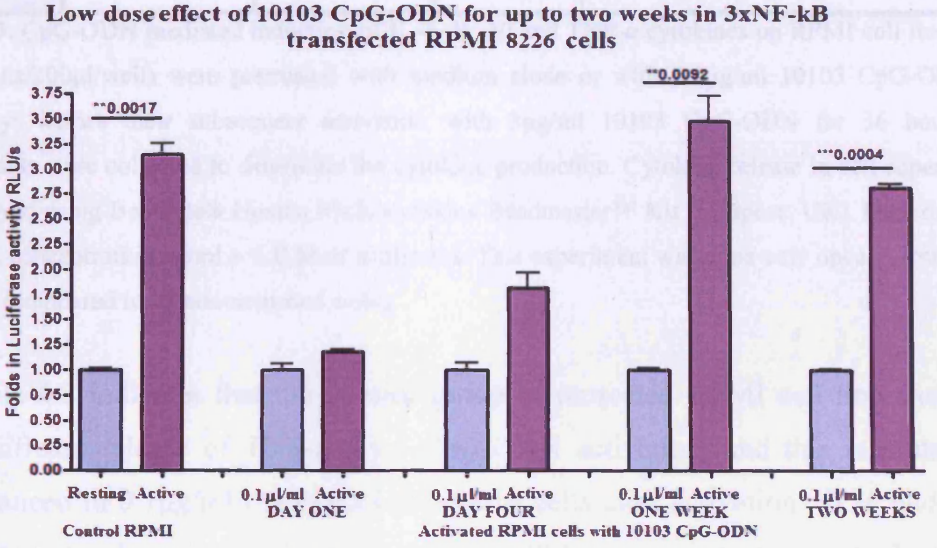

Figure 4.3. NF-κB activation in multiple myeloma RPMI 8226 cells pretreated with 0.1μg/ml 10103 CpG-ODN for up to two weeks, followed by a subsequent activating dose of 3μg/ml 10103 CpG-ODN. Control multiple myeloma RPMI 8226 cells were left untreated (medium alone) before their activation for 18 hours. Resting or non-activating dose: blue bar, 18 hours activated cells: purple bars. Basal activity in resting cells is (1402±33.2 RLU/s), and it did not change over the time. Data represent the mean fold induction, from unstimulated control, in luciferase activity RLU± S.E.M of triplicates. This experiment was repeated in two independent times.

The effect of CpG-ODN mediated cytokine release was also determined for RPMI tumour B-cell lines pretreated with 0.1μg/ml 10103 CpG-ODN. RPMI cells were pretreated for three days with the 0.1μg/ml 10103 CpG-ODN, before their subsequent activation with 3μg/ml 10103 CpG-ODN for 36 hours. Table 4.3 illustrates the effect of 0.1μg/ml 10103 CpG-ODN pretreatment on the release of IL-6, IL-10 and TNF-α before and after the subsequent activation on RPMI cell lines.

Cells	Time	CpG-ODN (μg/ml)	Cytokine release (pg/ml)		
			IL-6	IL-10	TNF-a
RPMI	Control	0	0.84±0.00	19.84±1.025	1.76±0.76
		3	1.35±0.52	21.10±2.21	39.02±4.46*
	Three day	0.1	0.56±0.28	13.38±0.348	0.34±0.17
		3	0.84±0.00	39.80±1.88**	154.8±21.35*

Table 4.3. CpG-ODN mediated induction of IL-6, IL-10 and TNF-α cytokines on RPMI cell line. Cells ($1x10^5$cells/200μl/well) were pretreated with medium alone or with 0.1μg/ml 10103 CpG-ODN for three days before their subsequent activation with 3μg/ml 10103 CpG-ODN for 36 hours and supernatants were collected to determine the cytokine production. Cytokine release in cell supernatants was assayed using Beadlyte® Human Multi-cytokine Beadmaster™ Kit (Milipore, UK). Data represent the mean concentration pg/ml ± S.E.M of triplicates. This experiment was done only once. * $P<0.05$, ** $P<0.005$ (compared to its non-activated cells).

Table 4.3 indicates that the control group of untreated RPMI cell line showed a significant release of TNF-α after CpG-ODN activation, and this response was enhanced in 0.1μg/ml CpG-ODN pretreated cells after activation. IL-6 and IL-10 were not released in activated control RPMI cells, but 0.1μg/ml CpG-ODN pretreated RPMI cells enhanced IL-10 release after the subsequent CpG-ODN activation. 0.1μg/ml 10103 CpG-ODN did not enhance basal cytokine release in RPMI after three days, indicating that it is a non-activating dose.

B) Effect on CpG-ODN mediated surface marker upregulation and cellular proliferation:

RPMI tumour B-cell line pretreated with medium alone showed an upregulation in the adhesion molecule CD54, costimulatory molecules CD80 and CD86 and MHC II expression. RPMI cells were cultured for up to four weeks with 0.1μg/ml of 10103 CpG-ODN, to study its effect on the upregulation of the surface markers after their subsequent treatment with an activating dose of CpG-ODN. Cells were studied for a short term effect (less than a week) and a long term effect (one to four weeks) and 0.1μg/ml of 10103 CpG-ODN had no effect on basal surface markers expression by the RPMI cells over this time period.

Figure 4.4 illustrates the changes in the expression of the adhesion molecule CD54, costimulatory molecules CD80 and CD86, and MHC II in medium (control) and 0.1μg/ml 10103 CpG-ODN pretreated RPMI cells before and after their

activation with 3μg/ml 10103 CpG-ODN. The short term response (less than one week) was not clearly inhibiting the expression of the four surface markers. However, RPMI cells showed a clear inhibition on the upregulation of the surface markers in the long term response compared to control cells. At two and three weeks, CD54 and CD86 upregulation was inhibited after pretreatment with 0.1μg/ml 10103 CpG-ODN, whereas CD80 and MHC II expression in the activated cells, were only inhibited after one week of pretreatment.

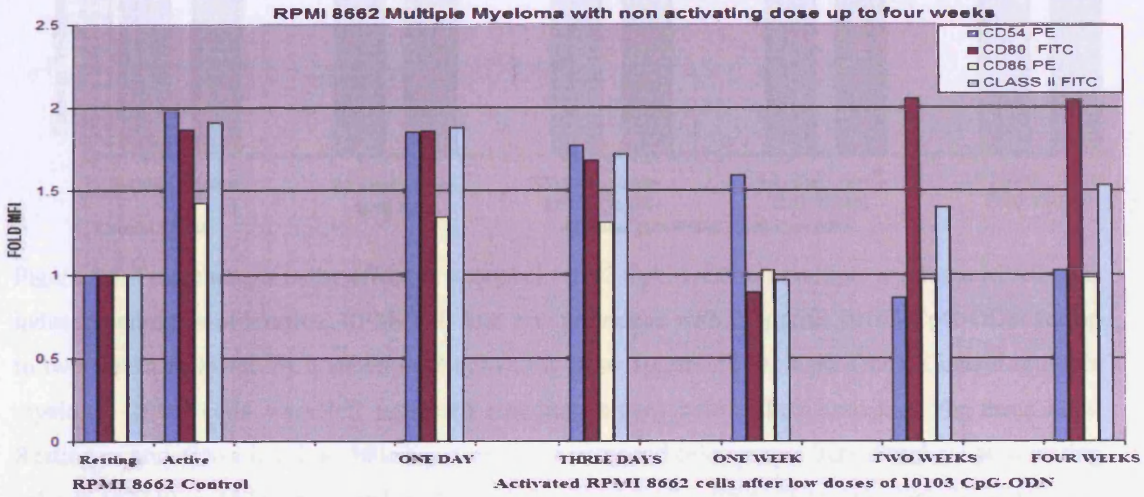

Figure 4.4. The effect of 0.1μg/ml 10103 CpG-ODN on the expression of the adhesion molecule CD54, costimulatory molecules CD80 and CD86, and MHC II expression on Multiple Myeloma RPMI cells pretreated with 0.1μg/ml 10103 CpG-ODN for up to four weeks, followed by a subsequent activation with 3μg/ml 10103 CpG-ODN for three days. Control Multiple Myeloma RPMI cells were left not treated (medium alone) before their three days of activation with 3μg/ml 10103 CpG-ODN. Data represents fold induction of MFI from unstimulated control. This experiment was repeated in two independent times.

To determine the effect of 0.1μg/ml 10103 CpG-ODN on the ability of multiple myeloma RPMI cell line to proliferate, cells were left in 0.1μg/ml 10103 CpG-ODN to study its short term effect (one and three days) and long term effect (one and two weeks), before their subsequent activation with 3μg/ml 10103 CpG-ODN for another three days. Control RPMI cells were pretreated with medium alone before their activation with 3μg/ml 10103 CpG-ODN, and cells showed a significant increase in cellular proliferation. 0.1μg/ml 10103 CpG-ODN did not show an activating response at any of the indicated times, indicating that it is a non-activating dose. From Figure 4.5, the short term effect of 0.1μg/ml 10103 CpG-ODN for one and three days was to inhibit the subsequent CpG-ODN

induced cellular proliferation. In the long term effect, the one week pretreated cells were partially inhibited, whereas it did not inhibit the subsequent CpG-ODN induced cellular proliferation after two weeks of pretreatment.

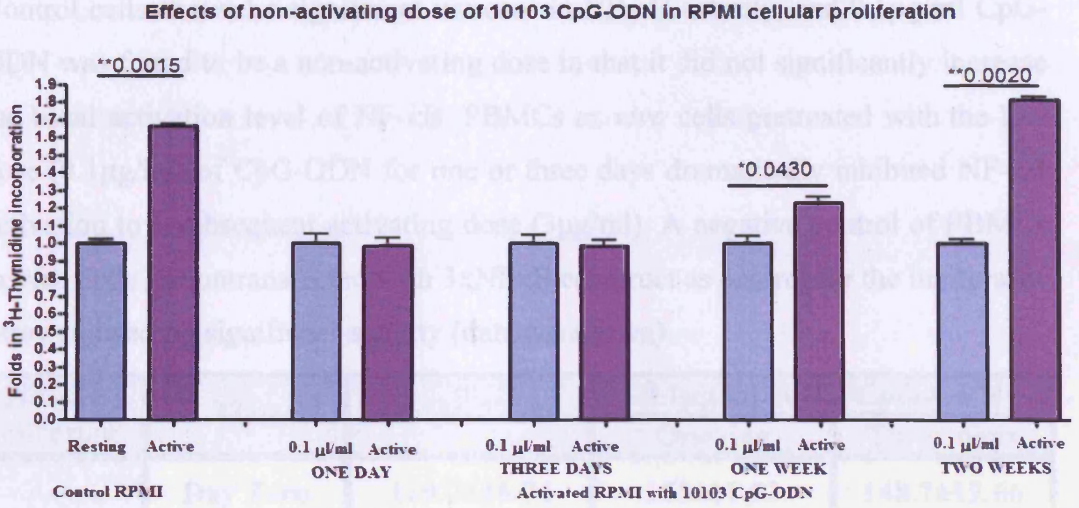

Figure 4.5. Fold changes in the effect of 0.1µg/ml 10103 CpG-ODN on multiple myeloma RPMI cells induced cellular proliferation. RPMI cell line was pretreated with 0.1µg/ml 10103 CpG-ODN for up to two weeks followed by a subsequent activating dose 3µg/ml 10103 CpG-ODN. Control multiple myeloma RPMI cells were left untreated (medium alone) before their activation for three days. Resting or non-activating dose: blue bar, three days activated cells: purple bars. Basal count in resting cells is (43730 ± 1833 cpm), and it did not change over the time. Data represent the mean fold induction, from unstimulated control, in ^{3}H-Thymidine incorporation ± S.E.M of triplicates. This experiment was repeated in two independent times.

4.3.1.3 CpG-ODN mediated response on *ex vivo* cells pretreated with 0.1µg/ml of 10103 CpG-ODN:

Normal PBMCs and B-CLL cells were used as *ex vivo* cells, to determine their response towards CpG-ODN sensitivity. Cells were pretreated with a low dose of 0.1µg/ml 10103 CpG-ODN for one and three days, and then tested for their CpG-ODN mediated response upon the subsequent activation with 3µg/ml 10103 CpG-ODN.

1. Effect on *ex vivo* normal PBMCs:

Normal PBMCs were studied as a normal B-lymphocyte control, and cells were pretreated with 0.1µg/ml 10103 CpG-ODN for 24 hours and 72 hours before their activation with 3µg/ml 10103 CpG-ODN. Cells were studied for their response towards the downstream signalling NF-κB activation and cytokine release, in addition to upregulating surface markers and cellular proliferation.

A) Effect on CpG-ODN mediated downstream signalling:

Table 4.4 illustrates the effect of 0.1μg/ml CpG-ODN pretreatment of PBMCs on the activation of the transcription factor NF-κB in response to 3μg/ml CpG-ODN. Control cells showed a significant increase in NF-κB activity, and 0.1μg/ml CpG-ODN was found to be a non-activating dose in that it did not significantly increase the basal activation level of NF-κB. PBMCs *ex vivo* cells pretreated with the low dose (0.1μg/ml) of CpG-ODN for one or three days dramatically inhibited NF-κB activation to a subsequent activating dose (3μg/ml). A negative control of PBMCs *ex vivo* cells left untransfected with 3xNFκB construct as control for the luciferase assay showed no significant activity (data not shown).

NF-κB activation	Time	Control cells	0.1μg/ml 10103 CpG-ODN	
			One day	Three days
PBMCs	Day Zero	119.7±16.74	155±11.53	148.7±12.66
	Day Three (3μg/ml CpG)	414.7±34.82**	152±14.11	176.7±12.9

Table 4.5. NF-κB activation in PBMCs pretreated with 0.1μg/ml 10103 CpG-ODN for one day or three days, followed by a subsequent activating dose of 3μg/ml 10103 CpG-ODN. Control PBMCs cells were left untreated (medium alone) before their activation for three days. Data represent the mean luciferase activity RLU ± S.E.M of triplicates. This experiment was repeated in two independent times. ** $P<0.005$ (compared to control unactivated cells).

To determine the effect of 0.1μg/ml 10103 CpG-ODN pretreatment on the ability of PBMCs to release cytokines, cells were left with CpG-ODN for one or three days before their subsequent activation with 3μg/ml CpG-ODN for 36 hours.

Cells	Time	CpG-ODN (μg/ml)	Cytokine release (pg/ml)		
			IL-6	IL-10	TNF-α
PBMCs	Control	0	5.527±0.42	1.125±0.13	2.602±0.54
		3	802.8±21.95***	117.2±6.9**	7.836±0.00*
	One day	0.1	16.72±0.00	2.840±0.38	2.602±0.54
		3	806.5±55.35**	132.5±4.9**	9.304±1.47*
	Three days	0.1	168.6±14.83	28.96±1.98	159.3±17.07
		3	976.4±33.69***	62.83±4.73*	20.23±1.66*

Table 4.4. CpG-ODN mediated induction of IL-6, IL-10 and TNF-α cytokines on *ex-vivo* PBMCs. Cells ($1x10^5$cells/200μl/well) were pretreated with medium alone or with 0.1μg/ml 10103 CpG-ODN for one or three days before their subsequent activation with 3μg/ml 10103 CpG-ODN for 36 hours, and supernatants were collected to determine the cytokine production. Cytokine release in cell supernatants was assayed using Beadlyte® Human Multi-cytokine Beadmaster™ Kit (Milipore, UK). Data represent the mean concentration pg/ml ± S.E.M of triplicates. This experiment was done only once. * $P<0.05$, ** $P<0.005$, *** $P<0.001$ (compared to its non-activated cells).

As Table 4.4 illustrates, the control group of PBMCs showed a highly significant release of IL-6 and IL-10, with less but still significant release of TNF-α following activation with 3μg/ml CpG-ODN. 0.1μg/ml 10103 CpG-ODN induced cytokine release on its own, mostly on day three, indicating that it is an activating dose for these cells. Furthermore, it inhibited the subsequent TNF-α cytokine response to 3μg/ml CpG-ODN, and possibly for IL-10 release, on day three.

B) Effect on CpG-ODN mediated surface marker upregulation and cellular proliferation:

Control PBMCs (medium alone) activated with 3μg/ml 10103 CpG-ODN showed a significant upregulation of the adhesion molecule CD54 and costimulatory molecule CD86, and to a lesser extent of CD80 and MHC II expression. 0.1μg/ml of 10103 CpG-ODN pretreatment for one or three days did not significantly increase the basal expression level of those molecules, indicating that it is a non-activating dose.

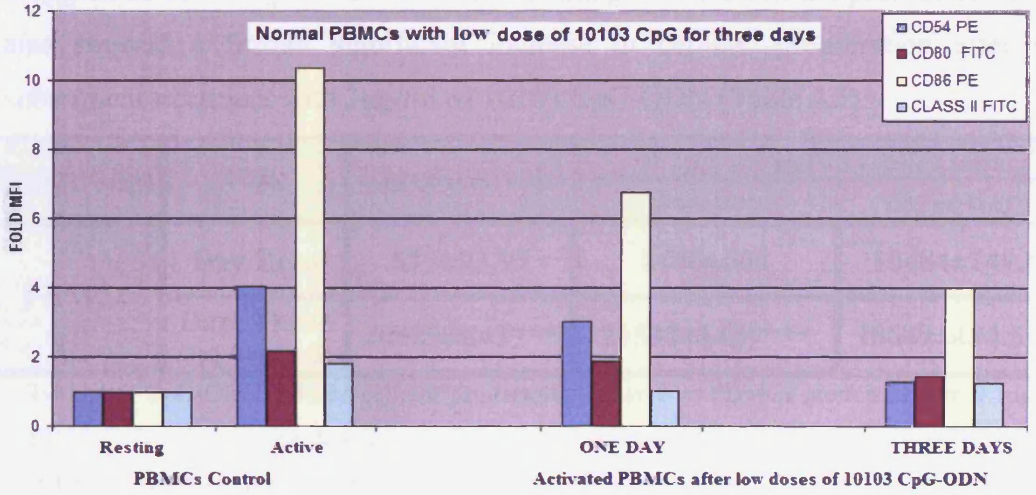

Figure 4.6. Adhesion molecule CD54 (purple bar), costimulatory molecules CD80 (red bar), CD86 (cream bar), and MHC II (blue bar) expression on PBMCs pretreated with the non-activating dose of 0.1μg/ml 10103 CpG-ODN for one day or three days, followed by a subsequent activating dose of 3μg/ml 10103 CpG-ODN for further 3 days. Control PBMCs were left not treated (resting) before their activation for three days. Data represent the fold induction from unstimulated control of MFI ± S.E.M of triplicates. This experiment was repeated in two independent times.

Figure 4.6 shows a substantial decrease in the upregulation of the surface markers (except for CD80) on PBMCs pretreated with 0.1μg/ml 10103 CpG-ODN in response to the subsequent 3μg/ml CpG-ODN stimulation. This inhibitory effect

induced by 0.1μg/ml of 10103 CpG-ODN pretreatment was time-dependent. PBMCs pretreated with CpG-ODN for three days showed a reduction in the expression levels of all the surface markers after the subsequent CpG-ODN challenge compared with the control cells, with partial inhibition seen in cells pretreated with 0.1μg/ml of 10103 CpG-ODN for one day.

To determine the effect of pretreatment with 0.1μg/ml 10103 CpG-ODN on the ability of PBMCs to proliferate, cells were left with the 0.1μg/ml 10103 CpG-ODN for one or three days before their subsequent activation with 3μg/ml 10103 CpG-ODN for three days. Table 4.5 illustrates the effect of 0.1μg/ml 10103 CpG-ODN on the subsequent CpG-ODN activation in inducing cellular proliferation. Control PBMCs were pretreated with medium alone before their activation with 3μg/ml 10103 CpG-ODN, and cells showed a highly significant induction in their cellular proliferation. The basal cellular proliferation level was significantly increased after one and three days of 0.1μg/ml 10103 CpG-ODN pretreatment, indicating that 0.1μg/ml of 10103 CpG-ODN was an activating dose for cellular proliferation, and also showed a further significant increase in cellular proliferation after the subsequent treatment with 3μg/ml of 10103 CpG-ODN (Table 4.5).

Proliferation	Time	Untreated cells	0.1μg/ml 10103 CpG-ODN	
			One day	Three days
PBMCs	Day Zero	579±93.95	2480±500	10484±749.6
	Day Three (3μg/ml CpG)	20929±643***	21532±1439***	18649±484.5**

Table 4.5. CpG-ODN induced cellular proliferation of *ex vivo* PBMCs pretreated with 0.1μg/ml 10103 CpG-ODN for one day or three days, followed by a subsequent activating dose of 3μg/ml 10103 CpG-ODN then incorporated with [methyl-^{3}H] thymidine. Control PBMCs were left untreated before their activation for three days. Data represent the mean ^{3}H-Thymidine incorporation (cpm) ± S.E.M of triplicates. This experiment was repeated in two independent times. ** $P<0.005$, *** $P<0.001$ (compared to its non-activated cells).

2. Effect on *ex vivo* B-CLL cells:

B-CLL cells were pretreated with 0.1μg/ml 10103 CpG-ODN for one or three days before their activation with 3μg/ml 10103 CpG-ODN. Cells were studied for their response towards the downstream signalling NF-κB activation and cytokine release, in addition to upregulating surface markers and cellular proliferation.

A) Effect on CpG-ODN mediated downstream signalling:

Table 4.6 illustrates the effect of 0.1μg/ml 10103 CpG-ODN pretreatment of B-CLL cells on the activation of the transcription factor NF-κB. Control cells showed a significant increase in NF-κB activity, while B-CLL cells pretreated with 0.1μg/ml 10103 CpG-ODN for one or three days did not show any activation in the transcription factor NF-κB after the subsequent 3μg/ml 10103 CpG-ODN activation. The basal activity of NF-κB in the pretreated B-CLL cells did not change after one day or three days of pretreatment with 0.1μg/ml 10103 CpG-ODN, indicating that it is a non-activating dose for B-CLL cells. A negative control of B-CLL cells left untransfected with 3xNFκB construct were used as a control for the luciferase assay (data not shown).

NF-κB activation	Time	Control cells	0.1μg/ml 10103 CpG-ODN	
			One day	Three days
B-CLL	Day Zero	122.7±19.50	123.7±5.686	183±12.53
	Day Three (3μg/ml CpG)	789.7±45.45**	193.7±52.01	212.7±4.726

Table 4.6. NF-κB activation in B-CLL pretreated with 0.1μg/ml 10103 CpG-ODN for one day or three days followed by a subsequent activating dose of 3μg/ml 10103 CpG-ODN. Control B-CLL cells were left untreated (medium alone) before their activation with 3μg/ml 10103 CpG-ODN for three days. Data represent the mean luciferase activity RLU ± S.E.M of triplicates. This experiment was repeated in two independent times. ** $P<0.005$ (compared to its non-activated cells).

To determine the effect of pretreatment with 0.1μg/ml 10103 CpG-ODN on the ability of B-CLL cells to release cytokines, the *ex vivo* cells were left with the 0.1μg/ml 10103 CpG-ODN for one or three days before their subsequent activation with 3μg/ml 10103 CpG-ODN for 36 hours.

Table 4.7 indicates that the control group of untreated B-CLLs showed a highly significant release of IL-6 and IL-10, with significant induction of TNF-α. 0.1μg/ml 10103 CpG-ODN was found to be a non-activating dose for IL-6, IL-10 and TNF-α in B-CLL cells when left for one or three days before their activation with 3μg/ml 10103 CpG-ODN. On the other hand, 0.1μg/ml 10103 CpG-ODN induced a partial inhibition of IL-6 and marked inhibition of IL-10 release in pretreated B-CLL cells subsequently exposed to 3μg/ml 10103 CpG-ODN while

TNF-α release was enhanced with the subsequent challenge with CpG-ODN after three days pretreatment with low dose CpG-ODN, compared with the responses of control cells (Table 4.7).

Cells	Time	CpG-ODN (μg/ml)	Cytokine release (pg/ml)		
			IL-6	IL-10	TNF-a
B-CLL	Control	0	19.60±0.96	0.089±0.050	0.51±0.003
		3	873.7±63.42**	676.1±21.25***	30.89±6.031*
	One day	0.1	24.73±1.94	0.23±0.029	1.40±0.89
		3	325.2±25.09**	246.3±8.529**	10.18±1.29*
	Three days	0.1	24.37±1.1	0.90±0.055	14.48±3.33
		3	540.8±18.49***	44.87±2.973*	233.8±18.79*

Table 4.7. CpG-ODN mediated induction of IL-6, IL-10 and TNF-α on *ex-vivo* B-CLL. Cells ($1x10^5$cells/200μl/well) were pretreated with medium alone or with 0.1μg/ml 10103 CpG-ODN for one or three days before their subsequent activation with 3μg/ml 10103 CpG-ODN for 36 hours, and supernatants were collected to determine the cytokine production. Cytokine release in cell supernatants was assayed using Beadlyte® Human Multi-cytokine Beadmaster™ Kit (Milipore, UK). Data represent the mean concentration pg/ml ± S.E.M of triplicates. This experiment was done only once. * $P<0.05$, ** $P<0.005$, *** $P<0.001$ (compared to its non-activated cells).

B) Effect on CpG-ODN mediated surface marker upregulation and cellular proliferation:

Figure 4.7 illustrates the changes in median fluorescence intensities for the expression of the surface markers on the control, one and three days pretreated B-CLL *ex vivo* cells. Control B-CLL cells (medium alone) showed an upregulation in the adhesion molecule CD54, costimulatory molecules CD80 and CD86 and MHC II surface markers. 0.1μg/ml of 10103 CpG-ODN pretreatment for one and three days did not clearly increase the basal expression level of those molecules whereas, after the subsequent activating dose of CpG-ODN, CD54 upregulation was reduced tolerising one and three days pretreatment, while CD86 expression was enhanced after one day. B-CLL cells treated with 0.1μg/ml 10103 CpG-ODN for three days, however, showed a decrease in the expression of CD80, CD86 and MHC II after the subsequent activation.

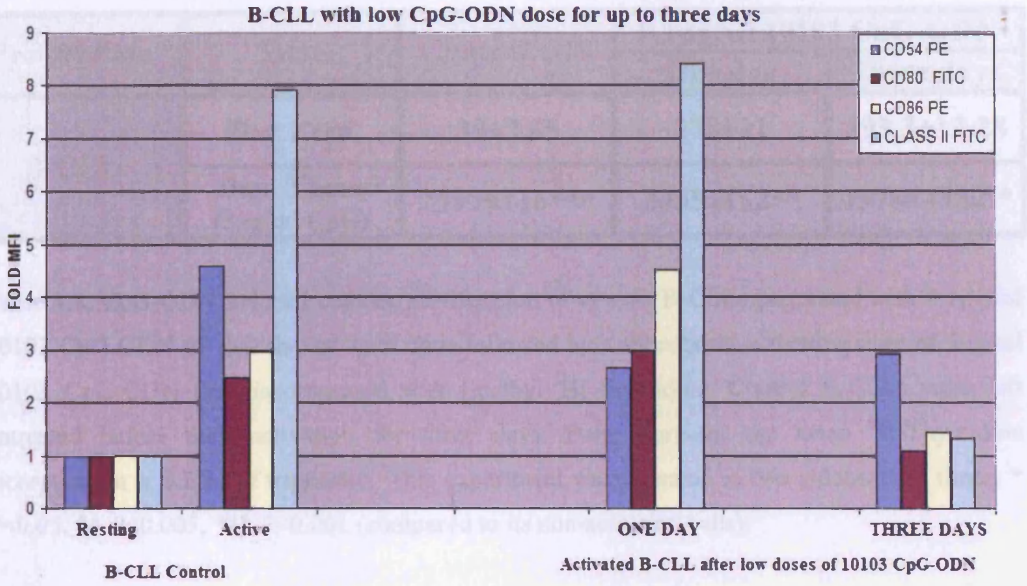

Figure 4.7. Adhesion molecule CD54 (purple bar), costimulatory molecules CD80 (red bar), CD86 (cream bar) and MHC II (blue bar) expression on B-CLL pretreated with 0.1μg/ml 10103 CpG-ODN for one day or three days, followed by a subsequent activating dose of 3μg/ml 10103 CpG-ODN for three days. Control B-CLL was left untreated (medium alone) before their activation for three days. Data represent the fold induction from unstimulated control of MFI. This experiment was done only once.

To determine the effect of pretreatment with 0.1μg/ml 10103 CpG-ODN on the ability of *ex vivo* B-CLL to proliferate, cells were left with the 0.1μg/ml 10103 CpG-ODN for one or three days before their subsequent activation with 3μg/ml 10103 CpG-ODN for three days. The effect of 0.1μg/ml 10103 CpG-ODN for one and three days on the subsequent CpG-ODN activation in inducing cellular proliferation is presented in Table 4.8. 0.1μg/ml CpG-ODN enhanced cellular proliferation in pretreated cells before and after 3μg/ml CpG-ODN activation, suggesting that 0.1μg/ml is an activating dose. Control B-CLL cells were pretreated with medium alone before their activation with 3μg/ml 10103 CpG-ODN, and showed a highly significant increase in their cellular proliferation. 0.1μg/ml CpG-ODN pretreatment for three days showed a partial inhibition of the cellular proliferation to subsequent activating dose of CpG-ODN. The effect of pretreatment with 0.1μg/ml CpG-ODN on B-CLL cells shows a dose dependent increase in cellular proliferation, indicating (suboptimal) activation.

Proliferation	Time	Control cells	0.1μg/ml 10103 CpG-ODN	
			One day	Three days
B-CLL	Day Zero	39±2.65	278±21	393.3±13.28
	Day Three (3μg/ml CpG)	2597±116***	2055±152**	1376±145.5*

Table 4.8. CpG-ODN induced cellular proliferation of *ex vivo* B-CLLs pretreated with 0.1μg/ml 10103 CpG-ODN for one day or three days followed by a subsequent activating dose of 3μg/ml 10103 CpG-ODN then incorporated with [methyl-^{3}H] thymidine. Control B-CLLs were left untreated before their activation for three days. Data represent the mean ^{3}H-Thymidine incorporation ± S.E.M of triplicates. This experiment was repeated in two independent times. * $P<0.05$, ** $P<0.005$, *** $P<0.001$ (compared to its non-activated cells).

4.3.2 Time-dependent response of CpG-ODN to re-activate 0.1μg/ml 10103 CpG-ODN pretreated BJAB Burkitt's lymphoma tumour B-cells.

The different 0.1μg/ml 10103 CpG-ODN pre-treated B-cells tested showed variable hyporesponsiveness to the CpG-ODN challenges with respect to different parameters of CpG-ODN mediated responses. NF-κB activation was one of those parameters that was clearly inhibited when the cells were pretreated with 0.1μg/ml CpG-ODN. For that, I further investigated whether the suppressed NF-κB activation in BJAB cells pre-exposed to CpG-ODN would remain hyporesponsive if the cells were exposed to a low dose of CpG-ODN for a limited time (one day or three days), washed and then retained in medium in absence of CpG-ODN before subsequently stimulating them with CpG-ODN.

Figure 4.8 illustrates the changes in the CpG-ODN mediated NF-κB activation in BJAB cells after being left for one day or three days with 0.1μg/ml 10103 CpG-ODN before washing the cells, and the time required for the cells to become responsive again. Control cells showed a significant NF-κB activation after CpG-ODN stimulation. BJAB cells pretreated for one day before activation with 3μg/ml 10103 CpG-ODN showed a significant inhibition in NF-κB activity. BJAB cells pretreated for one day and then washed to get rid of CpG-ODN and kept in fresh medium for one further day before activating them with 3μg/ml 10103 CpG-ODN, however, mediated significant NF-κB activation, but not to the same extent as the control cells, indicating that cells rapidly became responsive to a subsequent activity dose of CpG-ODN.

The above observations indicate that one day of pretreatment was not enough to keep BJAB cells hyporesponsive to the subsequent activating dose of CpG-ODN. Cells were therefore left for three days with the non-activating dose before washings to determine the duration of hyporesponsiveness to the subsequent CpG-ODN stimulation. From Figure 4.8, three days of pretreatment induced a hyporesponsive state towards the CpG-ODN mediated NF-κB activation, which lasted up to two weeks after removal of the cells from exposure to CpG-ODN. This indicates that in BJAB cell line, the non-activating dose (0.1μg/ml 10103 CpG-ODN) can affect cell responsiveness even after removing it for more than one week.

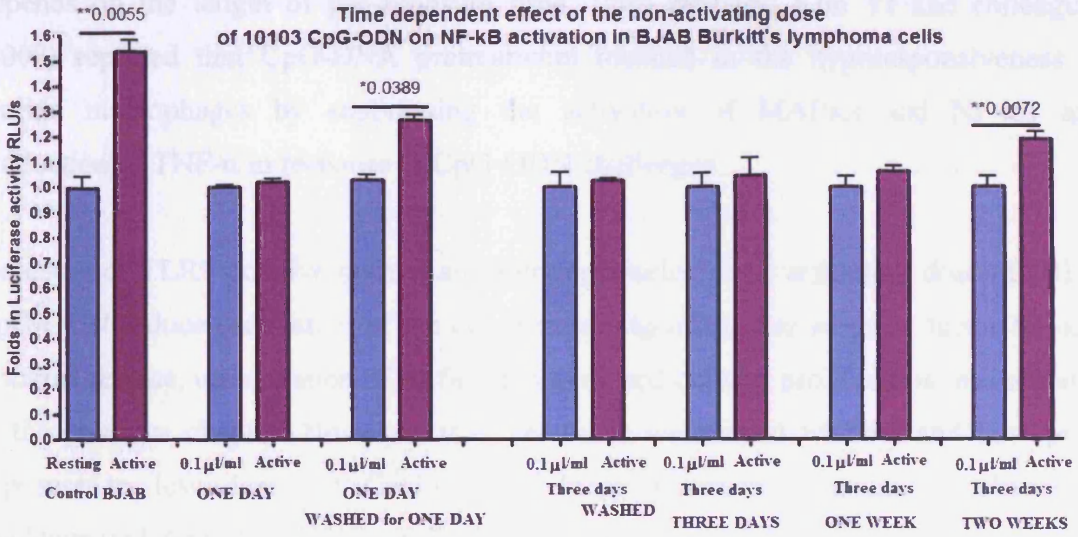

Figure 4.8. Fold changes in the NF-κB activity for control cells (medium alone), one day (0.1μg/ml 10103 CpG-ODN) pretreated cells, and one day of pretreatment before cells were washed and left for another day in fresh medium. In addition, another set of cells pretreated with 0.1μg/ml 10103 CpG-ODN for three days then washed and left for three days, one or two weeks in fresh medium. NF-κB activity was determined before and after their subsequent activation with 3μg/ml 10103 CpG-ODN for 18 hours. Resting or non-activating dose: blue bar, 18 hours activated cells: purple bars. Basal activity in resting cells is (651±27.9 RLU/s), and it did not change over the time. Data represent the mean fold induction, from unstimulated control, in luciferase activity RLU± S.E.M of triplicates. This experiment was done only once.

4.4 Discussion:

In recent years, a lot of effort has been made to uncover the mechanism of CpG DNA mediated innate cell activation, and its beneficial effects and therapeutic uses. However, we still need to understand the mechanisms where by the CpG-ODN mediated response can be regulated and how the immune system would respond towards that. It has previously been demonstrated that LPS pretreatment significantly suppresses the NF-κB activation, and IL-6, IL-10, IL-12, and TNF-α production in response to CpG DNA or LPS stimulation in murine macrophage-like cell RAW264.7 pretreated with CpG DNA (Yeo SJ 2003; Hatao F *et al.*, 2004; Dalpke AH *et al.*, 2005; Wei L *et al.*, 2006; Broad A *et al.*, 2007), however, Crabtree TD and colleagues (2001) indicated that this response depends on the length of pre-exposure time. Very recently, Kim YI and colleagues (2008) reported that CpG-DNA pretreatment resulted in the hyporesponsiveness of murine macrophages by suppressing the activation of MAPKs and NF-κB and production of TNF-α in response to CpG-ODN challenges.

Exposure of TLR9 positive normal and tumour B-cells to the activating dose of 10103 CpG-ODN induces activation of the downstream signalling transcription factor NF-κB, cytokine release, upregulation of surface markers, and cellular proliferation, as indicated in the previous chapter. However, it is yet to be understood whether and how prior exposure to low doses of CpG-ODN induces hyporesponsiveness to subsequent challenge with CpG-ODN in normal and malignant B-cells, as indicated with CpG-ODN or LPS studies in murine macrophages (Crabtree TD *et al.*, 2001; Yeo SJ 2003; Hatao F *et al.*, 2004; Wei L *et al.*, 2006; Kim YI *et al.*, 2008).

In the present study, I have used Burkitt's lymphoma BJAB cell line as the main model of this study, and investigated whether CpG-ODN has the ability to induce a refractory state in B-lymphocytes to a subsequent activating dose of CpG-ODN. Different *ex vivo* B-cells and tumour B-cell lines were studied as supporting models to determine whether CpG-ODN mediated responses are altered in *ex vivo* cells and cell lines pre-exposed to low doses of CpG-ODN. In addition, I investigated the time needed for BJAB B-cells to regain their responsiveness after pretreatment with the low doses of CpG-ODN. Tumour B-cell lines (BJAB and RPMI) that can grow continuously in tissue culture were used in this study for longer duration, up to four weeks, to determine the duration of the

tolerising effect. RPMI cells regained some its responses within four weeks, whereas BJAB cells regained responsiveness within three weeks.

Burkitt's lymphoma BJAB B-lymphocytes express TLR9 and respond to CpG-ODN activation. It was therefore considered a good model to study the effect of low doses of CpG-ODN pretreatment on the subsequent CpG-ODN activation, and its ability to maintain the cells refractory to CpG-ODN challenges. BJAB cells were studied for their downstream signalling (NF-κB) and extracellular CpG-ODN mediated responses (cytokine release, surface marker upregulation and cellular proliferation) following treatment with low doses of CpG-ODN before their activation with optimal doses of CpG-ODN. To determine the extent of this effect, it has been also tested on *ex vivo* B-cells (PBMCs and B-CLL) and the tumour multiple myeloma cell line (RPMI).

0.1μg/ml 10103 CpG-ODN was a non-activating dose for all of the studied CpG-ODN mediated responses in BJAB and RPMI tumour B-cell lines and for some responses in *ex vivo* PBMCs and B-CLL cells, but inhibition levels vary depending on responses and periods of pretreatment.

In BJAB cells, the non-activating dose (0.1μg/ml) did induce some refractory status for IL-6 release, but not for IL-10. TNF-α release after activating the pretreated cells was relatively less than that in the activated control cells. This attenuation of responsiveness was also induced in the activation of the transcription factor NF-κB, and cells showed an inhibition in CpG-ODN mediated NF-κB activation after pretreatment with low dose CpG-ODN. These observations suggest that IL-6 production might be dependent on NF-κB activation, whilst IL-10 and TNF-α production are independent. 0.1μg/ml 10103 CpG-ODN, also, induced a refractory state in BJAB cells that attenuated the upregulation of CD86 surface marker after a week of pretreatment which was maintained for another two weeks. As a result, CpG-ODN mediated CD86 upregulation is CpG-ODN long-term dose dependent. In contrast, MHC II upregulation showed the least induction after three days of pretreatment, which gradually returned to show an activation level after three weeks of pretreatment. This indicates that attenuation of CpG-ODN mediated MHC II upregulation is a short term effect. In contrast, CD54 upregulation showed the most inhibitory effect after two weeks of 0.1μg/ml CpG-ODN pretreatment and returned to its control level after three weeks of pretreatment followed

by 3μg/ml CpG-ODN activation. Finally, three weeks of non-activating doses of 10103 CpG-ODN were sufficient to keep the BJAB cells hyporesponsive in regard to the cellular proliferation and NF-κB activation in response to subsequent CpG DNA challenge.

In conclusion, pretreatment with the non-activating dose induced a time-dependent refractory state for NF-κB activation, cellular proliferation and CD54, CD86 and MHC II surface marker upregulation following CpG-ODN challenge in BJAB cells. With regard to cytokine release, IL-10 was CpG-ODN pretreatment-independent, while IL-6 release was attenuated by CpG-ODN pretreatment, and TNF-α release was partially decreased. This would demonstrate that BJAB pretreated with 0.1μg/ml 10103 CpG-ODN induces suppressive responses to subsequent stimulation with CpG DNA. These results are consistent with studies done on murine macrophages RAW264.7 cells pre-exposed to CpG-ODN before their subsequent LPS challenge. They have shown that pre-exposure to CpG-ODN elicited IL-10 production, reduced TNF-α release and inhibited the activation of NF-κB (Crabtree TD *et al.*, 2001; Yeo SJ 2003; Hatao F *et al.*, 2004; Wei L *et al.*, 2006; Broad A *et al.*, 2007; Kim YI *et al.*, 2008).

CpG-ODN mediated downstream NF-κB signalling in RPMI cells, showed a short term refractory state in cells left for less than a week in 0.1μg/ml 10103 CpG-ODN, but it gained responsiveness to CpG-ODN challenge after one week. This indicates that NF-κB tolerance in RPMI cells is a short term (less than a week) response. Control RPMI cells responded to CpG-ODN activation by releasing TNF-α, but not IL-6 or IL-10. Pretreatment with 0.1μg/ml 10103 CpG-ODN did not induce a refractory state in RPMI cells for CpG-ODN mediated TNF-α release, but it enhanced its activity. It also activated IL-10 release with no effect on IL-6. This is relatively consistent with Crabtree TD *et al.*, (2001) and Dalpke AH *et al.*, (2005) results where they showed that CpG-DNA pretreatment enhanced TNF-α release to subsequent LPS challenge in murine macrophage-like cell RAW264.7.

CpG-ODN mediated surface marker upregulation in RPMI cell line for CD54, CD80, and MHC II expression and to a lesser extent for CD86 expression. 0.1μg/ml 10103 CpG-ODN did not induce a refractory state in the short term effect (less than a week) and cells were responsive to the subsequent CpG activation by upregulating surface

markers to almost the same level as in control cells in response to CpG-ODN activation. Whereas for longer periods, they showed a hyporesponsiveness to the subsequent CpG activation in all tested surface markers, but this effect was variable depending on the surface marker and time. One week in 0.1μg/ml 10103 CpG-ODN induced a complete refractory state for the upregulation of CD80, CD86 and MHCII, while it reduced CD54 upregulation compared with the non-activated control cells. In contrast, two and four weeks in 0.1μg/ml 10103 CpG-ODN induced a complete refractory state in CD54 upregulation, so inhibition of CD54 expression is a time-dependent response and requires longer exposure time to affect its expression. CD80 and MHC II upregulation was completely inhibited in activated RPMI cell line after a week in 0.1μg/ml 10103 CpG-ODN, but this effect was transient, and cells showed a significant activation after two and four weeks in 0.1μg/ml CpG suggesting that cells were able to regain its responsiveness and upregulate CD80 and MHC II in a short period.

RPMI cells pretreated with 0.1μg/ml 10103 CpG-ODN showed a refractory status in less than a week in CpG-ODN induced cellular proliferation, but it retained its responsiveness afterward, suggesting that RPMI response to the low doses of CpG-ODN is time dependent. The same time dependent effect was noticed for CpG-ODN mediated NF-κB activation in RPMI cells. Cells went into the refractory state in less than a week, but regained their activity gradually afterward. As a conclusion, CpG-ODN mediated cellular proliferation and NF-κB activation are time dependent and transient in RPMI cells pretreated with 0.1μg/ml 10103 CpG-ODN. Furthermore, cellular proliferation is NF-κB-dependent, consistent with Lin A *et al.*, (2003) and Shishodia S *et al.*, (2005) findings. This demonstrates that, RPMI tumour B-cell line pretreated with 0.1μg/ml 10103 CpG-ODN induces transient suppressive responses in NF-κB activation, surface marker upregulation and cellular proliferation, to subsequent stimulation with CpG-ODN. These results are consistent with Crabtree TD and colleagues (2001) who indicated that CpG-ODN responsiveness depends on the length of pre-exposure time to CpG-ODN.

Comparing BJAB Burkitt's lymphoma cell line with RPMI multiple myeloma cell line, 0.1μg/ml 10103 CpG-ODN induced a refractory state in NF-κB activation and cellular proliferation in both cell lines, but it was transient and time dependent in RPMI cells. In addition to that, low doses of CpG-ODN did not induce a hyporesponsiveness state for

all tested cytokines in both cell lines, with inhibition of IL-6 and TNF-α in BJAB cells, but enhanced IL-10 and TNF-α release in RPMI cells. Finally, both cell lines pretreated with 0.1μg/ml 10103 CpG-ODN showed partial tolerance on the long term period for the upregulation of surface markers, but in BJAB cells showed a transient response, suggesting that this response is cell line specific, dose and time dependent, consistent with Crabtree TD *et al.*, (2001) and Wei L *et al.*, (2006) publications.

To study the tolerising effect of 0.1μg/ml 10103 CpG-ODN on *ex vivo* cells, normal PBMCs and B-CLL cells were studied. *Ex vivo* PBMCs and B-CLL B-cells were tested only for a short term effect (24 and 72 hours), as they can not grow for long times in tissue culture. Normal *ex vivo* PBMCs control cells responded to CpG-ODN activation (3μg/ml) by activating NF-κB, releasing IL-6, IL-10 and TNF-α cytokines, upregulating surface markers (mostly CD54 and CD86) and enhancing cellular proliferation. 0.1μg/ml 10103 CpG-ODN was a non-activating dose for some responses, such as NF-κB activation, but it showed an activation response in cellular proliferation before and after the subsequent CpG-ODN challenges. Pretreatment of PBMCs with 0.1μg/ml 10103 CpG-ODN for one and three days showed a complete inhibition in NF-κB activation while no clear tolerance on cellular proliferation and cytokine release in response to subsequent CpG-ODN activation, but it induced an apparent reduction in CD54 and CD86 expression after three days. Some of these results were consistent with publications in CpG-ODN or LPS pretreated murine macrophages, showing an inhibition in NF-κB activation in response to subsequent CpG-ODN or LPS challenges (Crabtree TD *et al.*, 2001; Yeo SJ *et al.*, 2003; Hatao F *et al.*, 2004; Dalpke AH *et al.*, 2005).

Ex vivo B-CLL cells responded to 3μg/ml CpG-ODN activation by activating NF-κB, releasing IL-6, IL-10 and TNF-α cytokines, upregulating surface markers (mostly CD54 and MHC II) and enhancing cellular proliferation. 0.1μg/ml 10103 CpG-ODN was a non-activating dose for some responses, such as NF-κB activation, but it showed an activation response in cellular proliferation before and after the subsequent CpG-ODN challenges. Pretreatment of B-CLL cells with 0.1μg/ml 10103 CpG-ODN for one and three days, showed a tolerising effect in NF-κB activation and IL-10 release with partial inhibition on cellular proliferation, surface markers upregulation (more in CD54 and CD86 expression) and IL-6 release, but enhanced TNF-α release in response to CpG-

ODN subsequent activation, especially three days of pretreatment, consistent with publications showing that murine macrophage-like cell RAW264.7 pretreatment with CpG-ODN resulted in enhancement of TNF-α release, suppression of IL-10 release and inhibition of NF-κB activation to subsequent LPS or CpG-ODN challenges (Crabtree TD *et al.*, 2001; Yeo SJ *et al.*, 2003; Hatao F *et al.*, 2004; Dalpke AH *et al.*, 2005).

In conclusion, pretreatment with 0.1μg/ml 10103 CpG-ODN induced a refractory state in *ex vivo* cells (PBMCs and B-CLL), after three days, that rendered the cells hyporesponsive to CpG-ODN mediated NF-κB activation, while no clear tolerising effect on cellular proliferation, but a partial tolerising effect on IL-10 was seen in PBMCs while it was strongly inhibited in B-CLL after the subsequent CpG-ODN activation. On the other hand, CpG-ODN mediated TNF-α release was significantly decreased after three days of pretreatment in PBMCs, whereas it was significantly activated in B-CLL cells. This might explain the involvement of TNF-α cytokine in tumour cells more than normal cells, although the study was done on one *ex vivo* tumour cell, which might not be indicative to all *ex vivo* tumour cells. Finally, CD54 adhesion molecule upregulation was clearly inhibited after the subsequent activation in PBMCs and B-CLL cells pretreated for three days in 0.1μg/ml 10103 CpG-ODN. As a result, *ex vivo* B-cells were almost responding in the same way with some exceptions which might be related for being normal or tumour cells. These results are supported with Crabtree TD *et al.*, (2001) and Yeo *et al.*, SJ (2003) publications, showing that CpG-ODN hyporesponsiveness depends on the length of pre-exposure time.

Determining the tolerising effects of low doses of CpG-ODN in *ex vivo* B-cells was helpful to a certain extent, in that it gave an idea about the responses in *ex vivo* normal and tumour B-cells. However, the growth time limitations of these cells and sample size limitations (one from each) could not make it a complete model for comparison with BJAB or RPMI cell lines.

As Burkitt's lymphoma BJAB cell line pretreated with 0.1μg/ml 10103 CpG-ODN induced suppressive responses (such as in NF-κB and cellular proliferation) to subsequent stimulation with CpG-ODN, I wanted to determine the time needed for BJAB cells to regain its responsiveness after removing the low dose effect. In this part, NF-κB activity was studied in BJAB cells pretreated with 0.1μg/ml 10103 CpG-ODN

for one and three days before washing and maintaining them in fresh medium for up to a further two weeks. One day of pretreatment was not enough to keep BJAB cells hyporesponsive to the subsequent activating dose of CpG-ODN, while the suppressive response to NF-κB activation was completely established in three days and lasted up to two weeks after removal of the cells from exposure to CpG-ODN. This type of hyporesponsiveness in BJAB B-cell line does not reflect a global deactivation of B-cell function, but it might indicate that NF-κB activation was only partially deactivated for a limited time in BJAB cells.

As a summary for this chapter, low doses of CpG-ODN can induce a tolerising effect on TLR9 positive *ex vivo* cells (PBMCs and B-CLL) and tumour B-cell lines (BJAB and RPMI) with respect to NF-κB activation and surface markers upregulation, when pretreated with 0.1μg/ml 10103 CpG-ODN before their subsequent CpG-ODN activation. Also, a variable effect on cytokine release was induced in the pretreated cells after their activation, with inhibition of some cytokines (e.g. IL-6) in some cells (B-CLL and BJAB), but not consistent for all cell lines tested. In addition, no clear effect on cellular proliferation was induced in the pretreated cells after the subsequent activation. The studied responses that were not activated with 0.1μg/ml CpG-ODN pretreatment, such as NF-κB activation, showed a tolerance status towards the subsequent CpG-ODN challenges, whilst the responses activated with 0.1μg/ml CpG-ODN, such as cellular proliferation in *ex vivo* B-cells, did not. Finally washed and then 3μg/ml CpG-ODN activated BJAB cell line, established a stable refractory state after three days of pretreatment with 0.1μg/ml CpG-ODN that lasted at least one week before it regained its responsiveness to NF-κB activation. This indicates that well-timed addition or deletion of CpG-ODN low doses in BJAB cells, prior to their subsequent CpG-ODN activation, might have enough effect to be useful as a new therapeutic modality in the treatment of Burkitt's lymphoma at least, but it might also be a time dependent effect.

Although there are no publications for the effect of CpG-ODN pretreatment on the normal and tumour human B-cell's responsiveness, and I was limited to a small group of cells, only two tumour B-cell lines (BJAB and RPMI), one tumour *ex vivo* B-cells (B-CLL) and normal PBMCs, the results in this work were relatively consistent with other publications on murine macrophages (Crabtree TD *et al.*, 2001; Yeo SJ 2003; Hatao F *et al.*, 2004; Wei L *et al.*, 2006; Kim YI *et al.*, 2008). Wei and colleagues found that

macrophage pretreatment with CpG-ODN would significantly inhibit NF-κB and cellular proliferation (Wei L *et al.*, 2006). NF-κB activation was found to be anti-apoptotic so it would enhance cellular proliferation (Lin A *et al.*, 2003; Shishodia S *et al.*, 2005). This activation prompts the synthesis of IκB and anti-apoptosis factors such as IAP family (e.g.; survivin) (Lin A *et al.*, 2003). NF-κB activation is also known to stimulate TNF-α release which in turn stimulates innate immunity and induces cytokines (van Horssen R *et al.*, 2006). The results in this work were consistent with these facts. Cell lines going into a refractory state inducing an inhibition in NF-κB activation also induced relatively a hyporesponsive state towards CpG-ODN mediated cellular proliferation for the same period of time. Also the response was mostly depending on cell type and its differentiation. TNF-α release was affected in pretreated cells before their subsequent CpG-ODN activation, enhanced in RPMI cell line and *ex vivo* B-CLL while reduced in BJAB cell line and *ex vivo* PBMCs cells. Furthermore, the release of IL-6, IL-10 and TNF-α showed some refractory responses in this study, which has been seen in murine macrophages in previous studies (Crabtree TD *et al.*, 2001; Yeo SJ 2003; Hatao F *et al.*, 2004; Dalpke AH *et al.*, 2005; Wei L *et al.*, 2006; Kim YI *et al.*, 2008), suggesting that cytokine release might be NF-κB–dependent. Finally, CpG-ODN-induced hyporesponsiveness in pretreated cells is cell line specific, also, dose and time dependent, which is consistent with Crabtree TD *et al.*, (2001) and Wei L *et al.*, (2006) findings. As a conclusion, pretreatment with low doses of CpG-ODN suppresses at least some responses to subsequent challenges, with the activating dose of CpG-ODN rendering the tumour cells refractory to the effect of CpG-ODN.

Finally, the mechanisms underlying tolerance induction and cellular hyporesponsiveness are expected to be due to altered conditions at several steps of signal transduction, however, this is still incompletely known. Further studies are required to address the mechanisms involved in CpG-ODN hyporesponsiveness in B-cells, and their cross-tolerance with other TLR ligands, as previous studies were done on murine macrophages. Yeo SJ and colleagues (2003) indicated that CpG-ODN mediated tolerance of murine macrophages might be due to dysregulation of IRAK expression, also Kim YI and colleagues (2008) recently reported that CpG-ODN pretreatment in murine macrophages suppressed expression of IRAK-1, which was responsible for hyporesponsiveness to CpG-ODN. On the other hand, Wei L *et al.*, (2006) suggested that macrophage pretreatment with CpG-ODN might lead to the suppression of a step(s)

in the TLR9- signalling pathway, which is possibly through the reduction of intracellular TLR9 expression. However, it is crucial to understand the mechanisms that lead to this tolerance in normal and tumour B-cells.

The effect of low CpG-ODN doses on the upregulation of surface markers after the subsequent CpG-ODN activation has not been studied previously. Most of the reports studying the hyporesponsiveness of cells were looking for the intracellular signalling effect, but not surface marker upregulation. This study is considered to be the first to determine the refractory state induced for the intracellular signalling, cytokine release, surface marker upregulation and cellular proliferation in human tumour B-cells and normal PBMCs pretreated with low CpG-ODN after their subsequent CpG-ODN activation, and therefore presents novel findings.

4.5 Conclusion:

The present study attempts to address questions of whether low doses of CpG DNA can induce hyporesponsiveness in B-cells in response to the subsequent challenge with CpG DNA and the duration of this response. In contrast to the ability of CpG DNA to induce strong innate immune responses, this study has shown that B-cells previously exposed to low doses of CpG DNA can induce a refractory state that leads to hyporesponsiveness towards CpG-ODN mediated downstream signalling of NF-κB activation, cytokine release, surface marker upregulation and/or cellular proliferation when subsequently stimulated with CpG DNA. In summary, the present study demonstrates that normal and tumour B-cells respond in a unique way to the subsequent CpG challenges after their pretreatment with 0.1μg/ml 10103 CpG-ODN. Cells went through a hyporesponsiveness state (e.g. in cytokine release and surface marker upregulation) after their exposure to the low doses of CpG DNA, but in different times for different responses, and also different cells responded in different ways as indicated in this study. This CpG DNA-mediated refractory status in B-cells may, at least partially, involve desensitization of the downstream signalling pathways by inhibiting of the transcription factor NF-κB activation and thus cellular proliferation.

As a conclusion for this chapter, CpG-ODN pretreatment greatly attenuates the activation of the transcription factor NF-κB, but the degree and length of suppression is different for each cell line, and is also dependent on the time of the subsequent CpG-ODN stimuli. Furthermore, NF-κB and TNF-α plays a critical role in CpG-ODN mediated response. Finally, incorrect CpG-ODN dose could influence CpG-ODN mediated responses, which in turn might affect tumour immunotherapy.

Finally, the understanding of the mechanisms involved in tolerance induction and cellular hyporesponsiveness in those cells is still incomplete. Therefore, major challenges remain to be elucidated to determine the underlying mechanisms involved in the regulation of the hyporesponsiveness state towards the CpG-ODN mediated responses in *ex vivo* B-cells and tumour B-cell lines.

CHAPTER FIVE

Molecular Mechanisms of CpG-ODN /TLR9 Mediated Responses

CHAPTER FIVE
Molecular Mechanisms of CpG-ODN/TLR9 Mediated Responses

5.1 Introduction:

The molecular mechanism by which CpG-ODN mediates immune responses is still under investigation. The CpG-ODN induced immune response in B-lymphocytes is mediated via TLR9. Burkitt's lymphoma BJAB cells are TLR9 positive B-cells which showed a response to the CpG-ODN activation. In this study, I wanted to characterize the molecular mechanism by which CpG-ODN activates TLR9 in BJAB cells. Nejad A *et al.*, (2002) indicated that upon the presence of CpG ODN, it will be endocytosed to the endosome to be recognized by TLR9 in the cell. TLR9 then will initiate a signalling cascade by recruiting the myeloid differentiation factor 88 (MyD88), an adapter molecule, through an interaction between Toll/IL-1 receptor (TIR) domains of both molecules, which would initiate a signalling pathway that starts with the recruitment of IL-1 receptor–associated kinases (IRAKs) and tumour necrosis factor-alpha receptor associated factor 6 (TRAF6) (Wesche *et al.*, 1997; Hacker H *et al.*, 2000; Nejad A *et al.*, 2002).

The MyD88-mediated signalling pathway is essential for CpG-ODN induced NF-κB, phosphatidylinositol 3-kinase (PI3K)/AKT and mitogen-activated protein kinases (MAPKs) pathways. Three major MAPK pathways have been identified in this activation, the extracellular signal-regulated kinase (MEK/ERK) which is the classical MAP kinase that regulates the cellular proliferation and differentiation, c-Jun N-terminal Kinase (JNK) which is also known as stress-activated protein kinases (SAPK/JNK), and $p38^{MAPK}$ pathway. JNK and $p38^{MAPK}$ signalling pathways are responsive to stress stimuli and are involved in cell differentiation and apoptosis (Hacker H *et al.*, 2000; Hemmi H *et al.*, 2000). The PI3K-AKT signalling pathway normally regulates cellular proliferation, survival and growth through multiple downstream targets in normal and cancer cells. In normal B-cells, CpG-ODN induced NF-κB activation and MAP kinases and PI3K/AKT were found to initiate the up-regulation of costimulatory molecules, cellular proliferation and the secretion of proinflammatory cytokines, such as TNF-α and IL-6 and IL-10 (Yi AK *et al.*, 1998; Chu W *et al.*, 2000; Peng SL 2005).

The CpG-ODN induced response is a complex response, as it was found to require both TLR9 dependent and independent pathways. Chu W *et al.*, 2000 found that CpG-ODN can activate DNA protein kinases (DNA-PK), which phosphorylates IκB kinases leading to the activation of NF-κB which plays a central role in regulating the expression of genes that encode for the pro- inflammatory cytokines and chemokines production in the immune cells (Chu W *et al.*, 2000). Dragoi *et al.*, (2005) reported that DNA-PK is required in the CpG-ODN induction of PI3K/AKT pathway. On the other hand, they found that the activation and phosphorylation of AKT in response to CpG-ODN is a TLR9 independent mechanism and it mostly involves the DNA-dependent protein kinase (Dragoi *et al.*, 2005), but this is not conclusive as recent study indicated that it is TLR9-dependent (Sester *et al.*, 2006).

In this work, TLR9 positive BJAB cell line, which exhibits a significant response to CpG-ODN activation, was investigated for its responsiveness towards CpG-ODN mediated signalling pathways, and to determine the molecular mechanisms that would lead to this CpG-ODN induced activation by the use of selective inhibitors of NF-κB, AKT and MAPK signalling pathways. CpG-ODN stimulation of BJAB cells showed an upregulation of the relevant surface markers, increase in cellular proliferation, NF-κB activation and cytokine release. For therapeutic/pathologic intentions, detecting the biochemical and molecular activations in BJAB cells would help in determining the best immunotherapeutic approaches. To establish that, BJAB cells were pre-treated with signalling pathway inhibitors and stimulated with media alone or 10103 CpG-ODN.

Curcumin, derived from turmeric roots (*Curcuma longa*), is pharmacologically safe agent known as a potent anti-tumour agent that exhibits anti-inflammatory and anti-oxidant properties. Curcumin has been found to generally affect NF-κB activation in normal and tumour cells, and to suppress a number of cellular responses in tumour cells (Figure 5.1) (Singh S *et al.*, 1995; Shishodia Sh *et al.*, 2005; Shakibaei *et al.*, 2007).

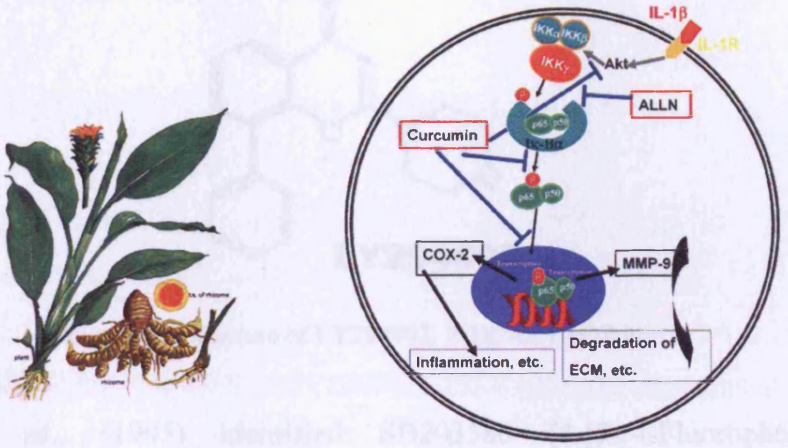

Figure 5.1. Turmeric plant and roots (*Curcuma longa*) (left). Effect of Curcumin on NF-κB activation (right). (Shakibaei *et al.*, 2007).

Favata MF *et al.*, (1998) identified a potent and specific inhibitor of the MAPK cascade that selectively inhibited ERK1 and ERK2 activation. They have identified U0126 (Figure 5.2) which blocks the phosphorylation and activation of ERK. 30μM of U0126 was recommended by Li J *et al.*, (2002) for the optimal inhibitory effect, and was the dose used in the following experiments.

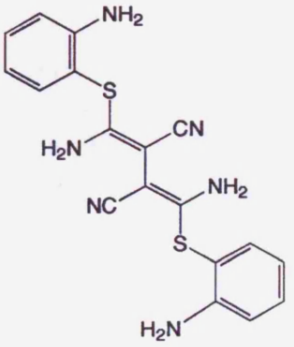

U0126

Figure 5.2.Structure of U0126, MEK/ERK inhibitor.

Scheid and Duronio (1996) identified LY294002 (Figure 5.3) as a potent and specific cell-permeant inhibitor of phosphatidylinositol 3-kinases (PI3-K). This inhibitor was found to act as antiproliferative agent and further substantiate a role for (PI3K)/AKT in cell proliferation. It also competitively inhibits ATP binding to the catalytic subunit of PI 3-kinases. Chiu D *et al.*, (2005) recommended the use of 50μM LY294002 for the optimal inhibitory effect in B-cells, and I have used this dose in the following experiments.

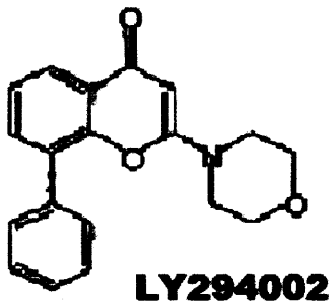

Figure 5.3.Structure of LY294002, PI3K/AKT inhibitor.

Cuenda A *et al.*, (1995) identified SB203580 (4-[5-(4-Fluorophenyl)-2-[4-(methylsulfonyl) phenyl]-1H-imidazol-4-yl] pyridine) as a highly selective and cell permeable inhibitor of p38 mitogen activated protein kinase (Figure 5.4). 10μM was recommended to exhibit the optimal inhibitory effect for SB203580 (Chang JH *et al.*, 2006), which I also used in my experiments.

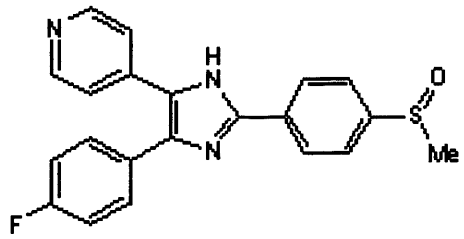

Figure 5.4. Structure of SB203580, $p38^{MAPK}$ inhibitor.

The aims of this work were to determine the intracellular molecular mechanisms that led to the CpG-ODN mediated responses, by studying the different signalling pathways involved in the activation of TLR9 by CpG-ODN. Also, to evaluate the effects of these pathways on different functional responses to CpG-ODN, using a panel of inhibitors specific for the different intracellular signalling pathways.

5.2 Materials and methods:

5.2.1 Materials:

- 10103 CpG ODN (Coley Pharmaceutical, Canada)
- Anti-CD54-PE (Beckman Coulter, UK)
- Anti-CD80-FITC (clone MAB104, Beckman Coulter, UK)
- Anti-CD86-PE (clone HA5.2B7, Beckman Coulter, UK)
- Anti-MHC II-FITC (monoclonal mouse anti-human HLA-DP DQ, Dako , UK)
- Anti-IgG1-PE (Beckman Coulter, UK)
- Anti-IgG1-FITC (Beckman Coulter, UK).
- Rabbit polyclonal anti- p-IκB-α (Ser 32)-R Santa Cruz Biotechnologies, Santa Cruz, USA)
- Peroxidase-labelled anti-mouse IgG (NIF824, Amersham Biosciences, Little Chalfont, UK).
- Peroxidase labelled anti-rabbit Ab (NIF824, Amersham Biosciences, Little Chalfont, UK)
- β-actin/HRP antibody (Santa Cruz Biotechnologies, Santa Cruz, USA)
- α-tubulin/HRP antibody (Santa Cruz Biotechnologies, Santa Cruz, USA)
- Mouse polyclonal anti- p-ERK (E-4) (Santa Cruz Biotechnologies, Santa Cruz, USA)
- Rabbit polyclonal affinity purified anti-ERK of rat origin (sc-94 Santa Cruz Biotechnologies, Santa Cruz, USA)
- Rabbit monoclonal AKT/PKB [pS473] (BioSource™ , Invitrogen, UK)
- Goat polyclonal affinity purified antibody to Akt1 of human origin (C-20) (sc-1618 Santa Cruz Biotechnologies, Santa Cruz, USA)
- A non radioactive p38 MAP Kinase assay kit purchased from (New England BioLab, UK)
- MEK/ERK inhibitor U0126 (Promega, UK).
- PI3 Kinase/AKT Inhibitor LY 294002 (Promega, UK).
- p38 mitogen activated protein kinase inhibitor SB203580 (Promega, UK).
- Curcumin (Sigma, UK).
- Beadlyte® Human Multi-cytokine Beadmaster™ Kit (Milipore, UK)
- [methyl-^{3}H] thymidine (GE Healthcare, UK, Ltd)

5.2.2 Methods:

TLR9 positive Burkitt's lymphoma BJAB cells were treated with different inhibitors to determine the signalling pathway in response to CpG-ODN which should activate TLR9 signalling pathway. The pharmaceutical inhibitors used in this study were 30μM U0126 (MEK inhibitor), 50μM LY 294002 (PI3 Kinase Inhibitor), 10μM SB203580 (p38 activity inhibitor) (all from Promega, UK) and 10, 25 and 50μM Curcumin (Sigma, UK) used 30-60 minutes before CpG-ODN activation. The U0126 and LY294002 inhibitors were kind gifts from Prof. M. Manson, Department of Biochemistry, University of Leicester. SB203580 and Curcumin are kind gifts from Dr. Raj Patel, Department of Biochemistry, and Prof. Andreas Gescher, Department of Cancer Studies and Molecular Medicine, University of Leicester, respectively.

BJAB Cells were divided into four groups: cells pre-treated with the inhibitors, but without CpG-ODN, cells activated with 3μg/ml 10103 CpG-ODN, but without pretreatment with inhibitor, cells pre-treated with inhibitors prior the activation with CpG-ODN, and a control group of cells left in medium alone. Initially, to test the specificity of U0126, LY294002 and SB203580 inhibitors, cells were studied for the inhibitory effect on the specific signalling pathway in response to CpG-ODN activation. After that, cells were studied for their response in upregulating the relevant surface markers, cellular proliferation, NF-κB activation and cytokine release in the presence or absence of the selective inhibitors.

5.2.2.1 Cell viability:

Pretreated BJAB cells with the signalling inhibitors were tested for their viability before and after the activation by counting the number of viable cells, after mixing 20μl of cells with 20μl of trypan blue (Fischer Scientific, UK). Percentage of the viable cells (excluding trypan blue) was calculated from the total number of cells.

5.2.2.2 Curcumin optimal effective concentration:

Curcumin (Sigma, UK) was tested for the the optimal effective concentration to inhibit the CpG-ODN mediated responses. NF-κB activation was the tested response using 10μM, 25μM and 50μM concentrations dissolved in dimethyl sulfoxide (DMSO). For that, 0.1% DMSO (used to dissolve the 50μM Curcumin) was also tested for its effect on the cell viability and effectivness. 3xNF-κB luc transfected

BJAB cells were left growing in the different concentrations of Curcumin or in 0.1% DMSO for 30-60 minute before their activation with 3μg/ml 10103 CpG-ODN overnight. NF-κB luciferase activity was measured as indicated in section (5.2.2.5).

5.2.2.3 Western blot analysis:

CpG-ODN activation of cells via TLR9 mediates several signalling pathways. To determine the involvement of MAPK and/or AKT pathways in CpG-ODN/TLR9 signalling cascades, BJAB, Burkitt's lymphoma B-cells ($5x10^6$cells/ml) were activated with 3μg/ml 10103 CpG-ODN for up to 120 minutes in the presence or absence of the inhibitors; 30μM U0126 (MEK inhibitor), 50μM LY 294002 (PI3 Kinase /AKT Inhibitor) or 10μM SB203580 (p38 activity inhibitor) added 30-60 minutes prior to the addition of CpG-ODN.

5.2.2.3.1 Preparation of cell lysate.

To determine the effect of U0126 and LY294002 inhibitors in response to CpG-ODN activation, treated cells for each time interval, were centrifuged and washed with PBS and then pellets were lysed and prepared as described in section (3.2.2.4-A). SB203580 inhibited cells were studied for their effect by IP/WB using a non radioactive p38 MAP Kinase assay kit (New England BioLab, UK) as discussed in section (5.2.2.2).

5.2.2.3.2 Gel Electrophoresis procedure.

After lysing the cells, the samples were centrifuged at 14,000rpm for 10 min /4°C and supernatants collected in a new tube. 20μl of the lysed cells were suspended in 20μl 2x loading dye with β-ME (reduced) (BioRad, Hercules, USA) and boiled for 5 minute/95°C. 25μl protein of each time period was loaded on precast 12% SDS-PAGE gels (Ready gel Tris-HCL gels, BioRad, Hercules, USA) and submitted to electrophoresis as described in section (3.2.2.4-B).

5.2.2.3.3 Immunoblotting procedure.

The membrane blots were washed in 1X PBS – 0.1% Tween 20 for 10 minutes and then blocked in 5% non-fat powdered milk in 1X PBS – 0.1% Tween 20 for 1 hour. The membranes were washed in 1X PBS – 0.1% Tween 20 three times for 10 minutes each time and then blotted with the specific antibody relevant to the

signalling pathway under investigation in 1X PBS – 0.1% Tween 20/overnight. For ERK 1/2 inhibitor U0126, blots were stained with 1:1000 mouse polyclonal anti-p-ERK (Santa Cruz Biotechnologies, Santa Cruz, USA). This primary monoclonal antibody epitope corresponds to a sequence containing phosphorylated Tyr 204 of ERK of human origin. The membrane with AKT inhibitor LY294002 lysates was blotted with 1:1000 rabbit monoclonal AKT/PKB [pS473]. The membranes were then washed in 1X PBS – 0.1% Tween 20 three times for 10 minutes each time followed by secondary antibody staining as described in section (3.2.2.4-C). Membranes were washed in 1X PBS – 0.1% Tween 20 three times, 10 minutes each time. The protein bands were visualized by Chemiluminescence ECL Blotting detection kit and exposed to Hyperfilm™ ECL Western (Amersham Biosciences, Little Chalfont, UK) for 1 minute to get bands at 42 and 44 kDa for pERK 1/2 and 60 kDa for pAKT-1.

5.2.2.3.4 Stripping and membrane re-blotting procedure.

After investigating the presence of the phosphorylated active part of ERK1/2 or AKT resulting from the activation by CPG-ODN in presence or absence of each inhibitor, the membranes were tested for the total ERK1/2 and AKT-1 proteins. The membranes were washed for 10 minutes in 1X PBS – 0.1% Tween 20 and stripped with 0.15M Glycine (pH 2.2) and 1% SDS in 1X PBS – 0.1% Tween 20 for 10 minutes three times. To stain the membranes for the total proteins of each, they were blocked with 5% non-fat powdered milk in 1X PBS – 0.1% Tween 20 for 1 hour before blotting for ERK or AKT-1 as described in section (3.2.2.4-D). ERK 1/2 blots showed 42/44kDa bands while 60kDa bands for AKT-1 blots were visualized within 1 minute after the exposure to the ECL.

5.2.2.3.5 Loading control determination procedure.

To ensure that each well was loaded with an equal concentration of protein, blots were stained for a house keeping protein (α-tubulin for ERK blots and β-actin for AKT blots) as described in section (3.2.2.4-E).

5.2.2.4 Effect of SB203580 inhibitor on P38 MAP Kinase activation upon TLR9 stimulation.

A non-radioactive p38 MAP Kinase assay kit (New England BioLab, UK) was used to detect $p38^{MAPK}$ activation product, ATF-2, in BJAB cells in the presence or absence of 10μM of SB203580 inhibitor of p38 mitogen activated protein kinase. The same four groups of BJAB cells were prepared and tested for $p38^{MAPK}$ pathway activation as described in section (3.2.2.5).

5.2.2.4.1 Preparation of cell lysate.

BJAB, Burkitt's Lymphoma B-cells ($5x10^6$cells/ml), were activated with 3μg/ml 10103 CpG-ODN for up to 120 minutes in the presence or absence of SB203580 inhibitor. To determine the involvement of $p38^{MAPK}$ pathway in response to CpG-ODN activation, cells were pretreated with the SB203580 inhibitor 30-60 minutes prior to CpG-ODN activation. Treated cells for each time interval, were centrifuged and washed with PBS, and then pellets were lysed for 30 minutes/ice with lysis buffer and lysates were prepared as described in section (3.2.2.5-A).

5.2.2.4.2 Immunoprecipitation/Western blotting procedure.

Lysed and sonicated cell preparation with 100μg protein concentration were immunoprecipitated using 20μl bead slurry immobilized phospho-$p38^{MAPK}$ (Thr180/tyr184) monoclonal antibody. Cell lysate/immobilized antibody was prepared, immunoprecipitated, submitted to electrophoresis and stained as described in section (5.2.2.5-B). ATF-2 protein bands were visualized by Chemiluminescence ECL Blotting detection kit and exposed to Hyperfilm™ ECL Western (Amersham Biosciences, Little Chalfont, UK) for 1 min to get the images of a band at 38 kDa.

5.2.2.5 NF-κB luciferase assay:

To determine the effect of the inhibitors (30μM UO126, 50μM LY294002 ,10μM SB203580 and 25μM Curcumin) on the activation of NF-κB transcription factor in response to CpG-ODN stimulation, plasmid DNA of NF-κB luciferase reporter construct was transiently transfected, as described in section (3.2.2.6), in the four groups of the Burkitt's lymphoma BJAB cells. After 24 hours of transfection, cells were washed and fresh media was added. Two groups were pre-treated with the

inhibitors for 60 minutes before activating one of them with 3μg/ml 10103 CpG/ODN for another 18 hours. Another one from the other two groups was also activated with 3μg/ml 10103 CpG/ODN for another 18 hours. Non activated groups were used as a control for the activated cells. Afterward, cells from all groups were washed with PBS and pellet was dissolved in 150μl of 1X reporter lysis buffer (Promega, UK). The luciferase assay protocol was done as described in section (3.2.2.6) and twenty microliters of lysate was used for assay with 100μl of luciferase assay system (Promega, UK). The luciferase activity was measured using the Sirius luminometer which measures standard glow (Berthold Detection Systems, Germany) and normalized with the protein concentration measured using Lowry method. Results were analyzed using GraphPad software.

5.2.2.6 Cytokine release assay:

To determine effect of the pharmacological inhibitors (30μM UO126, 50μM LY294002, 10μM SB203580 and 25μM Curcumin) on the production of cytokines in response to CpG-ODN activation, the four BJAB groups of cells (section 5.2.2) were investigated for their response on the release of the three cytokines IL-6, IL-10 and TNF-α. In a flat bottom 96 well plate, cell supernatants of the four groups of cells were incubated for 36 hours with or without CpG-ODN and assayed for their cytokine release. Cytokine assay was done according to the manufacturer's instructions as described in section (3.2.2.7) using Luminex® 100 instrument.

5.2.2.7 Flow cytometry:

To determine effect of the signalling pharmacological inhibitors (30μM UO126, 50μM LY294002, 10μM SB203580 and 25μM Curcumin) on the upregulation of the relevant surface markers in response to CpG-ODN activation, the four BJAB groups of cells were investigated for their response on the cell surface expression of the adhesion molecules CD54, costimulatory molecules CD80 and CD86, and Major Histocompatibility Complex (MHC) class II using flow cytometry technique after three days of activation with 3μg/ml 10103 CpG-ODN. In each group of the Burkitt's lymphoma BJAB cell line, $5x10^5$ cells /ml was washed with PBS and the pellet was stained with CD54-PE, CD80-FITC, CD86-PE and MHC II-FITC antibodies. IgG1-PE and IgG1-FITC antibody stains were used as isotype controls for PE and FITC conjugates. Flow cytometry technique was done as described in

section (3.2.2.3). Live gated cells (of 199 threshold or more) were read by the FACS-Calibur and analyzed using Cell Quest Pro software (Becton-Dickinson Ltd, UK).

Fluorescence values were brought together after gating on a combination of forward scatter (FSC) and side-scatter (SSC) features. Data of 10,000 events were acquired using CellQuest software (BD Biosciences, UK). The signals were acquired in a linear mode for FSC and SSC characteristics, and in a logarithmic mode for fluorescence intensities. Measurements included percentage of total population, and median in addition to mean channel fluorescence intensity (MFI) in energy channels.

5.2.2.8 Cellular proliferation:

To determine effect of the signalling pharmacological inhibitors (30μM UO126 MEK inhibitor, 50μM LY294002, 10μM SB203580 and 25μM Curcumin) on cellular proliferation in response to CpG-ODN activation, the four BJAB groups of cells (section 5.2.2) were investigated for their response in the cellular proliferation by measuring the incorporation of [methyl-^{3}H] thymidine into DNA, which is directly proportional to the amount of cell division occurring in the culture, after three days of activation with 3μg/ml 10103 CpG-ODN. The technique used or the determination of cellular proliferation was described previously in section (3.2.2.4).

5.2.2.9 Statistics:

Each experiment was done in triplicates with the exception of WB and flow cytometry, which was done mostly two times. Data were analysed using Student's paired t-test using GraphPad prism 4 software version 4.03. Data points represent the mean of at least three parallel samples plus/minus S.E.M. Results were considered significant when p value was less than 0.05, and very significant when p value was less than 0.001.

5.3 Results:

BJAB Burkitt's Lymphoma B cells showed TLR9 activation in response to CpG-ODN stimulation by inducing cellular proliferation, surface marker upregulation, TNF-α, IL-6 and IL-10 release, and by activating ERK1/2, $p38^{MAPK}$, AKT and NF-κB intracellular signalling pathways (Chapter Three). The biochemical mechanism by which CpG-ODN activates the immune system is still not clear. In the current study, I wanted to determine the effects of inhibiting specific signalling pathways on NF-κB activation, cytokine secretion, surface marker upregulation and cellular proliferation following the activation of TLR9 with CpG-ODN. Although several signalling pathways in TLR9 expressing cells have been implicated in the activation of TLR9 with CpG-ODN, it is still not clearly known in the TLR9 positive Burkitt's lymphoma BJAB B-cell lines which pathways mediate the cellular responses to the CpG-ODN activation. To clarify that, BJAB cells were tested for their response to CpG-ODN in the presence of selective inhibitors of the signalling pathways that have been identified in CpG-ODN/TLR9 activation. Cells were pretreated for 30-60 minutes with the pharmacological inhibitors prior to their activation with 3μg/ml 10103 CpG-ODN. After verifying the outcome of those inhibitors on the signalling pathways, they were studied for their effect on CpG-ODN mediated cellular responses. The cellular events determined in this study were to investigate the effects of the inhibitors on the activation of ERK1/2, $p38^{MAPK}$, AKT and NF-κB, also on the release of cytokines (IL-6, IL-10 and TNF-α), surface marker upregulation and cellular proliferation.

The inhibitors used in this study were U0126, MEK/ERK inhibitor (Favata, MF *et al.*, 1998; Li J *et al.*, 2002); SB203580, $p38^{MAPK}$ inhibitor (Chang JH *et al.*, 2006); and LY294002, PI3K/AKT inhibitor (Scheid and Duronio 1996). Curcumin was used as an inhibitor of NF-κB activation (Singh S *et al.*, 1995; Shishodia Sh *et al.*, 2005; Shakibaei *et al.*, 2007). The optimal inhibitory concentrations on the above mentioned signalling pathways for U0126, LY294002 and SB203580 were used, as recommended by other researchers (Li J *et al.*, 2002; Chiu D *et al.*, 2005; Chang JH *et al.*, 2006 respectively). Cells were also tested for their viability with the inhibitors after three days of activation, and no significant decline in cell viability were seen compared with the activated control cells in the absence of inhibitors (data not shown). However, Curcumin was tested for the optimal effective concentration to inhibit NF-κB activation, using 10μM, 25μM and 50μM concentrations dissolved in dimethyl sulfoxide (DMSO). 0.1% DMSO, used to

dissolve the 50μM Curcumin, was also tested for its effect on the cell viability and inhibitory effects. BJAB cells growing in the different concentrations of Curcumin or in 0.1% DMSO for four days showed equivalent viabilities as the non-treated control cells (data not shown). Figure 5.5 shows the effect of the different concentrations of Curcumin in one of the tested CpG-ODN mediated responses in BJAB cells, NF-κB activation, for the determination of the optimal inhibitory concentration of Curcumin. 25μM had the optimal inhibitory effect on the activation of NF-κB, while 0.1% DMSO did not show any inhibitory effects, indicating that the inhibitory effect is from the Curcumin and not DMSO.

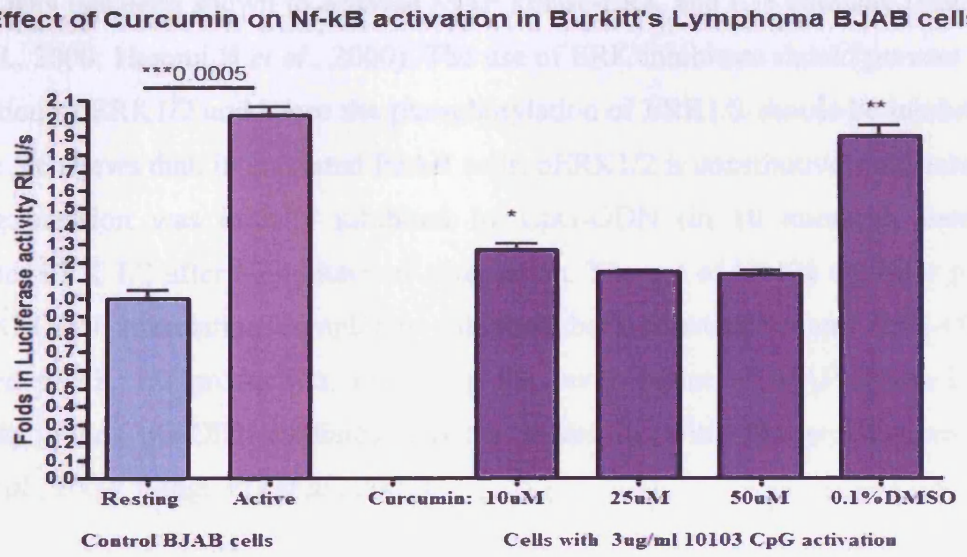

Figure 5.5. Effect of different Curcumin concentrations and DMSO on the CpG-ODN mediated activation of transcription factor NF-κB on BJAB Burkitt's Lymphoma. BJAB cells were transiently transfected with NF-κB-luciferase construct using Effectene Transfection Reagent. Transfected cells were pooled and washed with culture media. Cells (10^5 cells/200μl/well) were stimulated with medium (control-blue bar) or with 10103 CpG-ODN (3μg/ml) (pink bar and purple bar for Curcumin treated) for 18 hours in the presence 10μM, 25μM and 50μM of Curcumin or 0.1%DMSO. NF-κB-luciferase activities in cell extracts were analyzed using Single-Luciferase Reporter Assay System and normalized using the concentration of the protein detected by Lowry method. Data represent the fold induction of the luciferase activity over control cells ± S.E.M of triplicates. This experiment was repeated in two independent times. *P<0.05 (compared to control non-activated cells).

5.3.1 The effect of inhibitors on the TLR9 signalling pathways:

Activation of the ERK, $p38^{MAPK}$ and AKT kinases is important in mediating many B-lymphocyte functions, including cellular proliferation, activation of various transcription factors such as NF-κB and production of different cytokines such as

TNF-α, IL-6 and IL-10. Therefore, I sought to examine whether the CpG-ODN mediated response via these signalling pathways was affected by the presence of the pharmacological inhibitors. To ensure effect of the inhibitors, cells were stimulated with media or CpG ODN in the presence or absence of 30μM U0126 inhibitor, 10μM SB203580 or 50μM LY294002 for 30-60 minutes. Phosphorylation of ERK1/2, ATF-2 and AKT was analyzed by Western blot.

5.3.1.1 Effect of selective inhibitors of ERK1/2 and p38 on CpG ODN-induced MAPK signalling activation:

CpG-ODN has been shown to activate MAP kinase-ERK and p38 pathway (Hacker H *et al.*, 2000; Hemmi H *et al.*, 2000). The use of ERK inhibitors should prevent the activation of ERK1/2 and hence the phosphorylation of ERK1/2 should be inhibited. Figure 5.6 shows that, in untreated BJAB cells, pERK1/2 is constitutively expressed. This expression was initially inhibited by CpG-ODN (in 10 minutes), then it activates ERK 1/2 after 60 minutes of stimulation. The use of U0126 inhibitor prior to CpG-ODN stimulation completely inhibited both constitutive and CpG-ODN induced pERK 1/2 production, indicating the involvement of MAP kinase-ERK pathway in the CpG-ODN mediated response, in keeping with other publications (Yi AK *et al.*, 2002; Longo PG *et al.*, 2007).

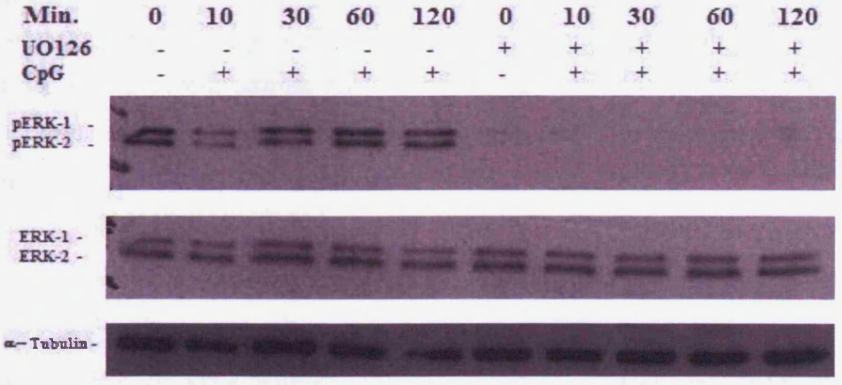

Figure 5.6. Effect of U0126 inhibitor. Burkitt's lymphoma BJAB cells ($5x10^6$cells/ml) were left untreated or pretreated with U0126 (30μM) for 30 minutes. Cells were then stimulated with CpG-ODN (3μg/ml) for up to 120 minutes. Equal amounts of whole cell lysates (30μl/lane) were subject to Western blotting using antibodies against the phosphorylation of ERK1/2. Total ERK1/2 was determined from the same blot. α-tubulin in each sample was used as the equal protein loading control. This experiment was repeated in two independent times.

SB203580 inhibitor does not prevent phosphorylation of p38, but rather blocks its kinase activity, and hence inhibits downstream targets such as the phosphorylation of ATF-2. CpG-ODN mediated response was found to activate p38 kinase in BJAB cells in the absence of SB203580 activity, and ATF-2 phosphorylation was induced. Figure 5.7 illustrate that the presence of SB203580 inhibited the pATF-2 activation resulting from CpG-ODN mediated $p38^{MAPK}$ activation. IP/WB of ATF-2 phosphorylated bands resulting from CpG-ODN activation in presence of SB203580 inhibitor were substantially inhibited compared with those produced in the absence of the inhibitor (Figure 5.7). A basal activation level was seen in absence of the inhibitor and CpG-ODN, but reduced in its presence. CpG-ODN-induced ATF-2 phosphorylation showed the highest activation after 60 minutes of stimulation in absence of inhibitor, however, pre-treatment with p38 inhibitor showed a maximal inhibitory effect (Figure 5.7).

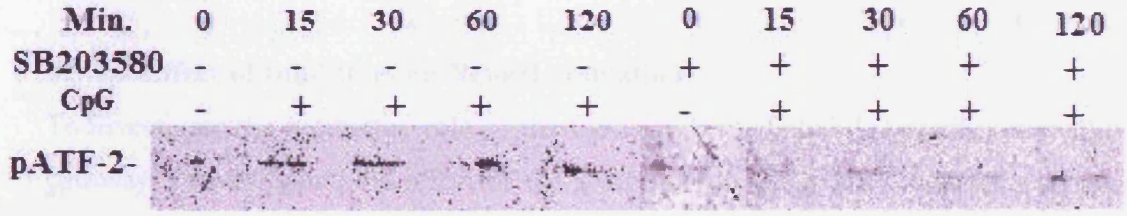

Figure 5.7. CpG-ODN induced ATF-2 is inhibited by SB203580. Burkitt's lymphoma BJAB cells ($5x10^6$cells/ml) were pretreated with SB203580 (10μM) for 30 minutes. Cells were then stimulated with CpG-ODN (3μg/ml) for up to 120 minutes. Equal amounts of whole cell lysates (50μg/lane) were immunoprecipitated with agarose bead-bound anti-pp38 Abs. In vitro kinase assays were done at 30°C for 30 minutes using ATF-2 fusion protein as a substrate. This experiment was repeated in two independent times.

5.3.1.2 Effect of selective PI3K/AKT inhibitor on CpG ODN-induced PI3K/AKT signalling activation:

PI3K/AKT pathway was found to be activated in the presence of CpG-ODN stimulation. This pathway can be inhibited with 50μM LY294002. Figure 5.8 shows the CpG-ODN mediated response activating PI3K/AKT pathway, as evidenced by the increase in phospho-AKT production seen at 90 minutes in BJAB cells. Basal activation was seen at time zero in the absence of inhibitor and CpG-ODN, but it was not in the presence of the inhibitor and using LY294002 inhibitor showed a clear inhibition of the pAKT product.

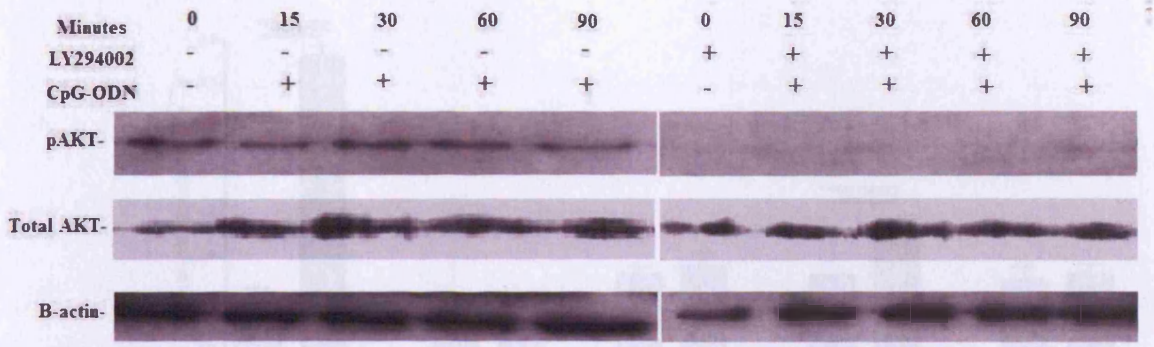

Figure 5.8. Effect of LY294002 inhibitor on CpG-ODN activation. Burkitt's lymphoma BJAB cells ($5x10^6$cells/ml) were pretreated with LY294002 (50μM) for 30 minutes. Cells were then stimulated with CpG-ODN (3μg/ml) for up to 120 minutes. Equal amounts of whole cell lysates (30μl/lane) were subject to Western blotting using antibodies against the phosphorylated form of AKT. Total AKT was determined from the same blot. House keeping gene β-actin for each sample was done to ensure equal protein loadings. This experiment was repeated in two independent times.

The experiments presented above demonstrate the inhibition of the respective intracellular signalling pathways by the selective chemical inhibitors used.

5.3.1.3 Effect of inhibitors on NF-κB activation:

To investigate the regulatory role of the CpG-ODN mediated downstream signalling pathway, I investigated the effect of the inhibitors on CpG-ODN induced activation of the transcription factor NF-κB. Cells were transfected with 3xNF-κB luciferase construct and stimulated with media or CpG-ODN for 18 hours in the presence or absence of 30μM U0126, 10μM SB203580, 50μM LY294002 and 25μM Curcumin (60 minutes pretreatment). NF-κB activation in the presence of inhibitors was compared with control BJAB cells (not inhibited). Figure 5.9 illustrates fold changes in the luciferase activity for BJAB pretreated cells with the inhibitors prior to their CpG-ODN activation. In the absence of CpG-ODN, Curcumin, U0126, LY294002 and SB203580 pretreated cells did not show a significant difference in NF-κB activation from resting BJAB cells. CpG-ODN activation induced a significant increase in NF-κB activity in the absence of inhibitors. Pretreatment with U0126, SB203580 and Curcumin markedly inhibited CpG-ODN-induced NF-κB activation, compared to levels that were not significantly different to those of resting, non inhibited BJAB cells. However, LY294002 pretreated and CpG-ODN activated cells showed a significant increase in NF-κB activation over their respective control BJAB cells, although this activation was less than that of the CpG-ODN activated but not inhibited control BJAB cells.

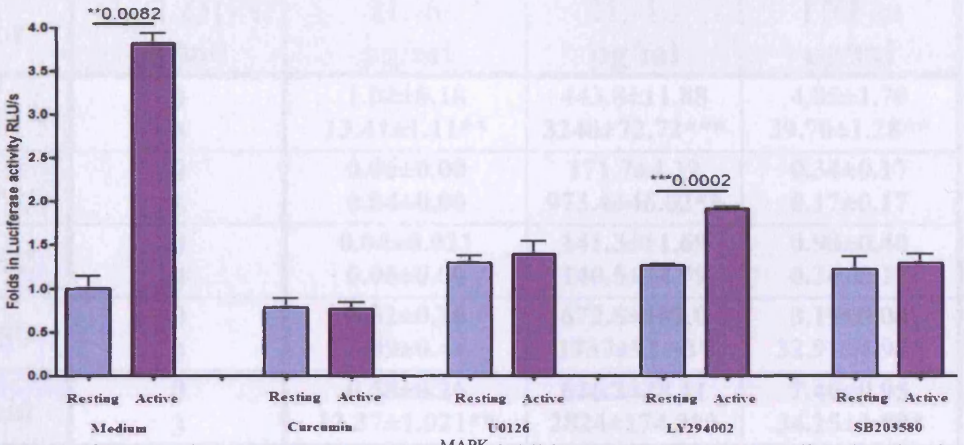

Figure 5.9. Effect of Curcumin and ERK, AKT, $p38^{MAPK}$ inhibitors on CpG-ODN mediated activation of transcription factor NF-κB in BJAB Burkitt's Lymphoma cells. BJAB cells were transiently transfected with NF-κB-luciferase construct using Effectene Transfection Reagent. Transfected cells were pooled and washed with culture media. Cells ($1x10^5$cells/200µl/well) were stimulated with medium (control-blue bar) or with 10103 CpG-ODN (3µg/ml)(purple bar) for 18 hours in the presence or absence of 25µM Curcumin (NF-κB inhibitor), 30µM U0126 (ERK inhibitor), 50µM LY294002 (AKT inhibitor) or 10µM SB203580 (p38 inhibitor). NF-κB-luciferase activities in cell extracts were analyzed using Single-Luciferase Reporter Assay System and normalized using the concentration of the protein detected by Lowry method. Data represent the fold induction of the luciferase activity over control cells ± S.E.M of triplicates. ** $P<0.005$, *** $P<0.001$. This experiment was repeated in two independent times.

5.3.2 Selective effect of inhibitors on the release of cytokines:

In Chapter Three (Section 3.3.3.3), CpG-ODN activation induced production of IL-6, IL-10 and TNF-α cytokines in BJAB Burkitt's Lymphoma cells. In the present study, I wanted to investigate the effect of the inhibitors on CpG-ODN induced cytokine release by BJAB cells. This would help to specify the involvement of the different CpG-ODN/TLR9 signalling pathways in the induction of cytokines. 30-60 minutes pretreated BJAB cells were stimulated with media or CpG-ODN for 36 hours in the presence or absence of 30µM U0126 MEK inhibitor, 10µM SB203580 $p38^{MAPK}$ inhibitor, 50µM LY294002 AKT inhibitor and 25µM Curcumin NF-κB inhibitor. Cytokine release in the presence of inhibitors was compared with control BJAB cells (not inhibited). Supernatants were measured for the cytokine release, and results are shown in Table 5.2.

Inhibitor	CpG-ODN (μg/ml)	IL-6 pg/ml	IL-10 pg/ml	TNF-α pg/ml
Medium	0	1.02±0.18	443.8±11.88	4.85±1.70
	3	13.41±1.11**	3240±72.72***	39.70±1.28**
U0126	0	0.06±0.00	171.7±4.32	0.34±0.17
	3	0.84±0.00	973.4±46.02**	0.17±0.17
LY294002	0	0.04±0.021	141.3±11.69	0.90±0.40
	3	0.06±0.00	140.5±14.99	0.34±0.17
SB203580	0	0.32±0.26	672.8±102.0	3.19±0.00
	3	3.09±0.44	1937±93.68*	32.91±4.94*
Curcumin	0	0.58±0.26	626.2±28.11	7.46±0.95
	3	12.37±1.021**	2824±174.3**	34.25±2.88*

Table 5.2. Effect of Curcumin and ERK, AKT or $p38^{MAPK}$ inhibitors on CpG-ODN mediated induction of IL-6, IL-10 and TNF-α cytokines by BJAB Burkitt's Lymphoma. Cells ($1x10^5$cells/200μl/well) were stimulated with medium or 10103 CpG-ODN (3μg/ml) for 36 hours in the presence or absence of Curcumin (25μM), U0126 (30μM), LY294002 (50μM) or SB203580 (10μM). Cytokine release in cell extracts was assayed using Beadlyte® Human Multi-cytokine Beadmaster™ Kit (Milipore, UK). Data represent the mean concentration pg/ml ± S.E.M of triplicates. This experiment was done only once. *P<0.05, ** P<0.005, *** P<0.001 (compared to control non-activated cells).

As shown in Table 5.2, non-inhibited control BJAB cells showed a significant increase in the release of IL-6, IL-10 and TNF-α cytokines in response to CpG-ODN activation, but this was significantly changed upon the pretreatment with the inhibitors. CpG-ODN induced IL-6 production in BJAB cells was completely inhibited in the presence of the MAPK (U0126 and SB203580) and AKT (LY294002) signalling inhibitors as illustrated in Table 5.2. No significant difference was detected with the activated pretreated cells with Curcumin compared with the active control BJAB cells. The basal level of IL-6 release was significantly (P<0.05) inhibited in BJAB cells pretreated with U0126, SB203580 and LY294002, but not with Curcumin. This indicates that CpG-ODN-mediated production of IL-6 in BJAB cells is regulated through MAPK and PI3K/AKT pathways, and it is regulated before and independent of the NF-κB activation. Such results were seen in previous works, but using macrophage-like cell line RAW264.7 and a murine B lymphoma cell line WEHI-231 (Yi AK *et al.*, 2002; Yi AK *et al.*, 2003).

CpG-ODN induced IL-10 production in BJAB cells was completely inhibited by LY294002 inhibitor, and the basal IL-10 level was greatly reduced in the presence of LY294002 (Table 5.2). Furthermore, the basal level of IL-10 was reduced in BJAB cells pretreated with U0126, whereas it was increased in Curcumin pretreated cells

with no significant effect in SB203580 pretreated cells. However, CpG-ODN significantly enhanced IL-10 release in the cells pretreated cells with U0126, SB203580 and Curcumin, although the response in U0126 and SB203580 treated cells were lower than in control (uninhibited) cells. Yi AK *et al.*, and other researchers indicated such effects, but in mouse peritoneal macrophages, murine B lymphoma cell line WEHI-231 and macrophage-like cell line RAW264.7 (Yi AK *et al.*, 2002; Yi AK *et al.*, 2003; Saegusa K *et al.*, 2007). This indicates that CpG-ODN-mediated production of IL-10 in BJAB cells is largely MAPK and NF-κB – independent, while it is PI3K/AKT-dependent.

TNF-α basal release in BJAB cells was not significantly affected after their pretreatment with the four signalling inhibitors compared with non-activated control cells. CpG-ODN induced TNF-α production in BJAB cells was completely inhibited by U0126 and LY294002 inhibitors (Table 5.2), but was unaffected in cells pretreated with SB203580 and Curcumin. This indicates that CpG-ODN-mediated production of TNF-α in BJAB cells is regulated though ERK-dependent pathway in addition to AKT-dependent pathway, and it is p38 and NF-κB -independent. Studying the effect of those inhibitors on TNF-α production was also done by other researchers, but in a murine B lymphoma cell line WEHI-231, mouse peritoneal macrophages and macrophage-like cell line RAW264.7 (Yi AK *et al.*, 2002; Yi AK *et al.*, 2003; Saegusa K *et al.*, 2007).

5.3.3 Effect of Inhibitors on CpG-ODN mediated upregulation of surface markers:

To determine the involvement of MAPK, AKT and NF-κB pathways in the CpG-ODN induced upregulation of the surface markers, inhibitors for those pathways were used. BJAB cells were incubated for 30-60 minutes with optimal concentration of the inhibitors (25μM Curcumin, 30μM U0126, 10μM SB203580 and 50μM LY294002) before their activation with 3μg/ml 10103 CpG-ODN for another three days. Surface marker upregulation in the presence of inhibitors was compared with control BJAB cells (not inhibited). BJAB cells responded to CpG-ODN activation, by upregulating CD54, CD86 and MHCII, and to a lesser extent CD80 expression (Chapter Three). In this work I wanted to investigate the effect of the different proposed signalling pathways (ERK, $p38^{MAPK}$, AKT and NF-κB pathways) on the upregulation of the

surface marker. As the concentrations of the inhibitors used did not induce cell death, they were used to study this effect. To achieve that, the signalling inhibitors (U0126, SB203580, LY294002 and Curcumin respectively) were used, and BJAB cells were treated with the inhibitors 30-60 minutes prior to CpG-ODN activation for three days. A positive control of BJAB cells were left without inhibitor and activated with 10103 CpG-ODN. Median fluorescence intensity (MFI) for each surface marker was determined. MFI of the CpG-ODN activation in the inhibited cells was compared with the CpG-ODN activated control cells. Furthermore, non-activated inhibited cells were used as control for each inhibitory group to indicate the effect of the inhibitors alone on the surface markers.

Figure 5.10 summarises the effect of the signalling inhibitors on the upregulation of the adhesion molecule CD54, costimulatory molecules CD80 and CD86 and MHC class II in BJAB cells. The MFI readings of the inhibited cells before and after CpG-ODN stimulation are compared with the non-inhibited control groups, and results are shown as a fold induction in each studied surface marker. Each inhibitor showed a different response towards the CpG-ODN induction of surface marker upregulation, as discussed in the following sections.

5.3.3.1 The effect of Curcumin (NF-κB inhibitor) on surface markers:

Figure 5.10-A shows that inhibition of BJAB cells with Curcumin for three days had little effect on basal surface marker expression. However, CpG-ODN activated, Curcumin pretreated cells, showed reduced upregulation of CD54 and MHC II, but had no clear effect on the upregulation of costimulatory molecules CD80 and CD86, compared with the control non-inhibited BJAB cells.

5.3.3.2 The effect of U0126 inhibitor on the surface markers:

Figure 5.10-B shows that U0126 strongly inhibited the basal expression of all of the tested surface markers, and completely blocked CpG-ODN induced upregulation of these markers in BJAB cells.

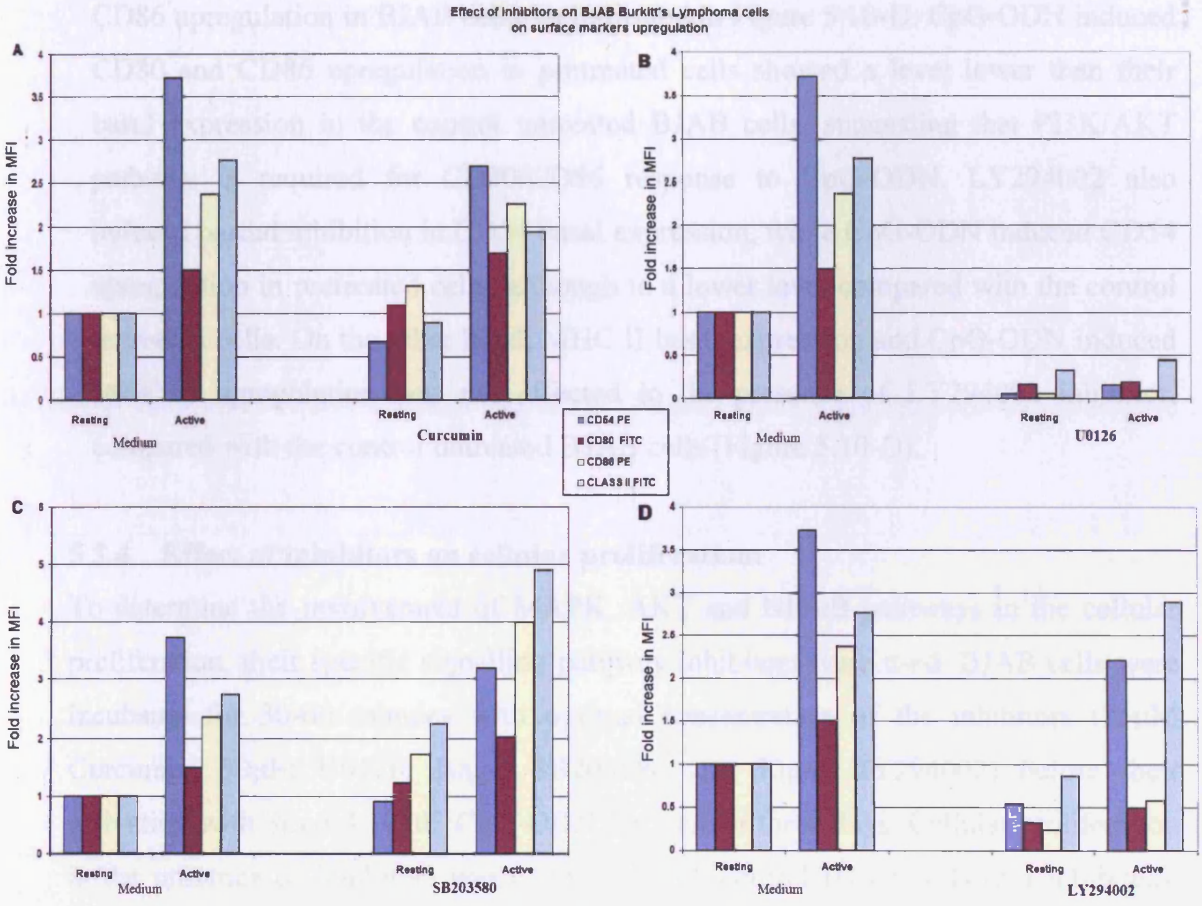

Figure 5.10. Effect of inhibition of ERK, p38, AKT and NF-κB on CpG-ODN induced surface marker upregulation. BJAB Burkitt's Lymphoma cells ($2x10^5$cells/ml) were pretreated with media (control group), (A) Curcumin (25μM), (B) U0126 (30μM), (C) SB203580 (10μM) and (D) LY294002 (50μM) for 30-60 minutes. Cells were then stimulated with medium or 10103CpG-ODN (3μg/ml) for three days. Surface expression of the adhesion molecule CD54 (purple bar), costimulatory molecules CD80 (red bar) and CD86 (creamy bar) and MHC II molecule (blue bar) was investigated using monoclonal antibody staining and flow cytometry. Data represents the fold induction in MFI over control. This experiment was done only once.

5.3.3.3 The effect of SB203580 inhibitor on the surface markers:

Figure 5.10-C indicates that SB203580 pretreatment did not affect the basal expression level of CD54 and CD80, but it increased CD86 and MHC II expression. In CpG-ODN activated cells, SB203580 had little effect on CD54 and CD80 upregulation while it enhanced CD86 and MHC II upregulation compared with the CpG-ODN activated control untreated BJAB cells.

5.3.3.4 Effect of LY294002 inhibitor on the surface markers:

Pretreatment with LY294002 inhibited the basal expression of the costimulatory molecules, CD80 and CD86, and almost blocked CpG-ODN induced CD80 and

CD86 upregulation in BJAB cells, as indicated in Figure 5.10-D. CpG-ODN induced CD80 and CD86 upregulation in pretreated cells showed a level lower than their basal expression in the control untreated BJAB cells, suggesting that PI3K/AKT pathway is required for CD80/CD86 response to CpG-ODN. LY294002 also induced partial inhibition in CD54 basal expression, while CpG-ODN induced CD54 upregulation in pretreated cells, although to a lower level compared with the control untreated cells. On the other hand, MHC II basal expression and CpG-ODN induced MHC II upregulation was not affected in the presence of LY294002 inhibitor, compared with the control untreated BJAB cells (Figure 5.10-D).

5.3.4 Effect of inhibitors on cellular proliferation:

To determine the involvement of MAPK, AKT and NF-κB pathways in the cellular proliferation, their specific signalling pathway inhibitors were used. BJAB cells were incubated for 30-60 minutes with optimal concentration of the inhibitors (25μM Curcumin, 30μM U0126, 10μM SB203580 and 50μM LY294002) before their activation with 3μg/ml 10103 CpG-ODN for another three days. Cellular proliferation in the presence of inhibitors was compared with control BJAB cells (not inhibited). BJAB cells showed an inhibition in their proliferation after CpG-ODN activation. Experiments carried out previously for CpG-ODN mediates cellular proliferation in BJAB cells (section 3.3.7), showed an increase in cellular proliferation after CpG-ODN activation. Control BJAB cells used in here showed a decrease in cellular proliferation after CpG-ODN stimulation (Figure 5.11), which made it more difficult to interpret when it previously enhanced. Curcumin and SB203580 did not significantly reduce the basal cellular proliferation level in BJAB cells, but CpG-ODN activated Curcumin or SB203580 pretreated cells did not show significant changes in cellular proliferation before and after CpG-ODN activation. LY294002 showed most potent inhibition of basal cellular proliferation, but cells still responded to CpG-ODN activation with a small but significant increase in cellular proliferation, whereas U0126 inhibited basal proliferation, and CpG-ODN was associated with a significant further reduction in cellular proliferation.

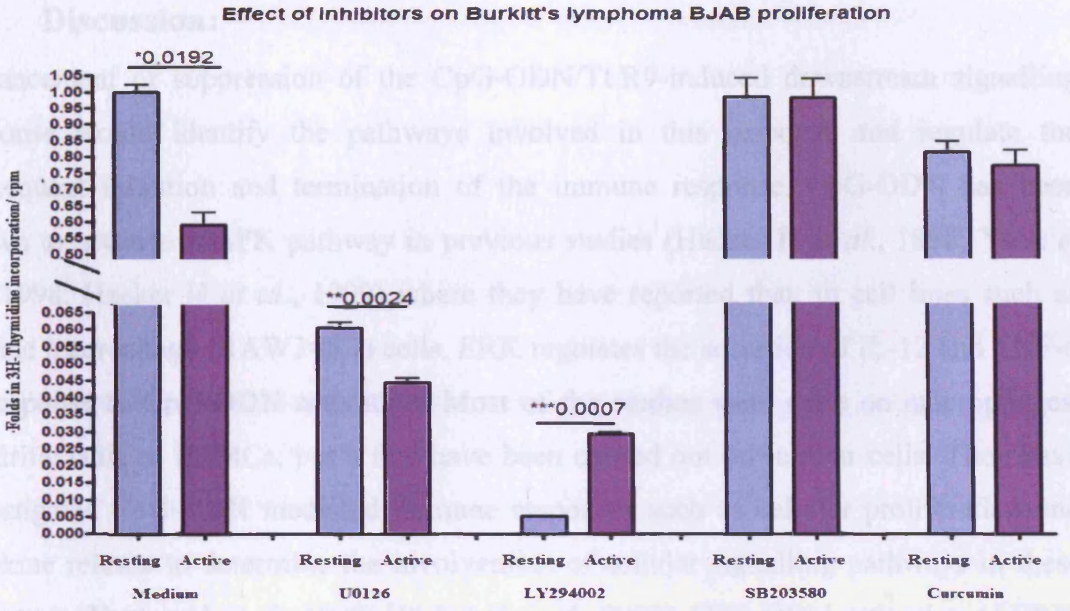

Figure 5.11. Effect of ERK, AKT, $p38^{MAPK}$ inhibitors or Curcumin on the CpG-ODN mediated cellular proliferation of BJAB Burkitt's Lymphoma. BJAB cells (10^5cells/200µl/well) were cultured with medium (control-blue bar) or with 10103 CpG-ODN (3µg/ml)(purple bar) for three days in the presence or absence of U0126 (30µM), LY294002 (50µM), SB203580 (10µM) or Curcumin (25µM). Cellular proliferation was determined by measuring the counts per minute (CPM) of the incorporation of [methyl-^{3}H] thymidine into DNA. Basal count in resting cells is (162592±3440 cpm). Data represent the fold induction of CPM compared with non-stimulated BJAB cells without inhibition ± S.E.M of triplicates. * P<0.05, ** P<0.005, *** P<0.001. This experiment was repeated in two independent times.

5.4 Discussion:

Enhancement or suppression of the CpG-ODN/TLR9-induced downstream signalling response would identify the pathways involved in this response and regulate the subsequent initiation and termination of the immune response. CpG-ODN has been shown to activate MAPK pathway in previous studies (Hacker H *et al.*, 1998; Yi A *et al.*, 1998; Hacker H *et al.*, 1999) where they have reported that, in cell lines such as murine macrophage (RAW246.7) cells, ERK regulates the secretion of IL-12 and TNF-α in response to CpG-ODN activation. Most of the studies were done on macrophages, dendritic cells or PBMCs, but a few have been carried out on tumour cells. They have investigated CpG-ODN mediated immune responses such as cellular proliferation and cytokine release to determine the involvement of cellular signalling pathways in these responses (Hacker H *et al.*, 1999; Häcker G *et al.*, 2002). CpG-ODN activation of ERK, $p38^{MAK}$, PI3K/AKT and NF-κB signalling pathways is important in mediating a broad array of cellular responses, including cellular proliferation, surface marker upregulation, NF-κB activation and cytokine release. BJAB Burkitt's Lymphoma cells express TLR9 and respond to CpG-ODN activation by activating signalling (ERK1/2, $p38^{MAPK}$, AKT and NF-κB) downstream pathways, upregulating CD54, CD80, CD86 and MHC II surface markers, and increasing cellular proliferation and IL-6, IL-10 and TNF-α cytokine production (Chapter Three). A few studies have included BJAB cells as control cells (Longo PG *et al.*, 2007), but none was done studying all those CpG-ODN mediated responses. For that reason, I wanted to investigate the molecular mechanisms resulting from CpG-ODN activation via TLR9 in BJAB cells as a model of B-cell activation, and to evaluate its effect on ERK, $p38^{MAPK}$, NF-κB and PI3K/AKT pathways. To achieve that, I have used a variety of signalling inhibitors known for their specificity towards those pathways. Investigating the involvement of the kinases in the CpG-ODN induced responses helps to understand the cellular responses occurring via TLR9 stimulation.

Studying the activation pattern of signalling molecules, Burkitt's lymphoma BJAB cells showed a CpG-ODN induced signalling response by the activation of ERK, $p38^{MAPK}$, and PI3K/AKT pathways. p38 phosphorylation was detected by the determination of pATF-2 activation product of phosph-p38 kinase. The time required for the activation and phosphorylation of MAPK pathways (ERK and $p38^{MAPK}$) was 60 minutes (section 3.3.3.2), whereas it was high after 90 minutes for PI3K/AKT (section 3.3.3.3). The active products of the downstream signalling indicate that CpG-ODN stimulates the

induction of the MAPK/ERK pathway and PI3K/AKT pathway. Such results were seen in previous works, but in different cell types such as murine macrophages (Hacker H *et al.*, 2000; Hemmi H *et al.*, 2000; Yi AK *et al.*, 2002 ; Longo PG *et al.*, 2007).

Initially, I wanted to determine whether the inhibitors were toxic to the cells over the time periods to be used. Resting and CpG-ODN activated BJAB cells were viable in the presence of the inhibitors compared with control untreated cells, indicating that the inhibitors did not have a toxic effect on cells. Curcumin is one of the inhibitors used in this work and it has been known to inhibit NF-κB activation (Singh S *et al.*, 1995; Shishodia Sh *et al.*, 2005; Shakibaei *et al.*, 2007). The effect of the different tested concentrations of Curcumin on the cell viability was not significant. As a conclusion, the inhibitors used in this study did not exhibit a toxic effect on BJAB cells at the concentrations used. Therefore, the inhibitory effect on the cellular immune responses was due to their inhibitory effects on intracellular signalling.

Several reports studied CpG-ODN mediated immune responses via TLR9 activation (Klinman DM *et al.*, 1996; Decker T *et al.*, 2000a; Decker T *et al.*, 2000b; Jahrsdorfer B *et al.*, 2001; Jahrsdorfer B *et al.*, 2005; Grandjenette C *et al.*, 2007), while other reports discussed CpG-ODN mediated signalling via TLR9 activation in different cell lines (Hacker H *et al.*, 1998; Hacker H *et al.*, 1999; Hacker H *et al.*, 2000; Yi AK *et al.*, 2002; Yi AK *et al.*, 2003; Saegusa K *et al.*, 2007). In this work, I wanted to determine the molecular mechanisms associated with the different CpG-ODN mediated responses in BJAB cells, and to evaluate the effects of the signalling pathways on different functional responses to CpG-ODN.

To investigate the functional role of ERK, $p38^{MAPK}$ and PI3K in BJAB cells upon stimulation with CpG-ODN, the signalling inhibitors U0126, SB203580, and LY294002 respectively were used. U0126, a potent inhibitor of ERK 1/2 (Favata, MF *et al.*, 1998), completely inhibited ERK1 and ERK2 phosphorylation in basal and CpG-ODN activated cells, and that was consistent with other publications using murine macrophages (Yi AK *et al.*, 2002). SB203580 is an inhibitor of p38 mitogen activated protein kinase (Cuenda A *et al.*, 1995). Phosphorylated ATF-2, a product of this activation, was inhibited when cells were pre-treated with SB203580. pATF-2 activity was the highest in 60 minutes without inhibitors, while it was completely inhibited in the

presence of SB203580. LY294002 is a potent and specific cell inhibitor of phosphatidylinositol 3-kinases (PI3-K) (Scheid MP *et al.*, 1996), and AKT phosphorylation was clearly inhibited in the presence of the inhibitor. Recently, Saegusa K. and colleagues reported similar results when murine macrophages were activated with CpG-ODN after LY294002 pretreatment (Saegusa K *et al.*, 2007).

BJAB cells have not been tested before for the effect of such inhibitors prior to CpG-ODN activation, but some studies reported the effect of the inhibitors on other B cells or macrophages. Lim EJ and colleagues (2007) indicated that SB203580, but not U0126, inhibited CpG-ODN induced NF-κB activation in RAW264.7 (Lim EJ *et al.*, 2007). Furthermore, the effect of LY294002 inhibitor on CpG-ODN induction of NF-κB activation on BJAB cells has not been investigated before, but studies on PI3K/AKT pathway using LY294002 inhibitors showed inhibitory effects on the activation of NF-κB and this effect depended on the cell type (Hazeki K *et al.*, 2007). For that, and after determining the involvement of the signalling pathways in the CpG-ODN activation, I wanted to investigate the effect of those kinases and their signalling pathways on the cellular response. So, BJAB cells were activated with 3μg/ml 10103 CpG-ODN in the presence or absence of the pharmacological inhibitors. These signalling inhibitors were tested for their effects on the activation of the transcription factor NF-κB, cytokine release, the upregulation of the relevant cell surface molecules, and on cellular proliferation. Surprisingly, Burkitt's lymphoma BJAB cells showed a decrease in cellular proliferation in response to CpG-ODN in this study, although in earlier experiments it was increased. No clear reason for this difference in response, although other CpG-ODN responses remained consistent.

NF-κB activation was significantly inhibited upon CpG-ODN activation in Curcumin pretreated BJAB cells to be the same as the basal level of the non-activated cells after inhibition. The suppression of CpG-ODN mediated NF-κB activation in Curcumin pretreated cells was associated with the inhibition of the CpG-ODN mediated cellular proliferation. However, cytokine release (IL-6, IL-10, and TNF-α) was not significantly affected upon the pre-treatment of the cells with Curcumin. Studying the effect of the inhibitors on the upregulation of the surface markers, Curcumin showed a small reduction in the basal expression of CD54 and MHC II molecules, and CpG-ODN mediated upregulation of CD54 and MHC II were partially inhibited compared with the

CpG-ODN activated non-inhibited control BJAB cells. No clear effect were seen in the costimulatory molecules CD80 and CD86. As a result, Curcumin is mainly working on the transcription factor NF-κB (Singh S *et al.*, 1995; Shishodia Sh *et al.*, 2005; Shakibaei *et al.*, 2007), leading to the inhibition of cellular proliferation, but not on the induction of the cytokines, and had variable effects on CpG-ODN induced surface marker upregulation.

The CpG-ODN induced NF-κB activation and IL-6 and TNF-α cytokine release was completely suppressed by U0126, although the IL-10 response was only partially suppressed. As NF-κB inhibition by Curcumin did not affect cytokine release, this implies that CpG-ODN induction of IL-6 and TNF-α was dependent on MEK/ERK, but independent of NF-κB. Inhibition of the CpG-ODN mediated ERK activation by U0126 completely blocked the basal expression level of all the surface markers tested, and completely inhibited their upregulation after the activation with CpG-ODN. The inhibition of ERK activation also led to a decrease in their cellular proliferative activity by both significantly reducing the basal level of cellular incorporation to the H^3-thymidine, and inhibiting the proliferative response to CpG-ODN. The data in this work showed that, CpG-ODN induced changes in the expression of the relevant surface markers, cellular proliferation, and cytokine release are associated with the activation of ERK kinase, whilst the CpG-ODN induced transcription factor NF-κB may regulate the cellular proliferative activity.

SB203580, $p38^{MAPK}$ inhibitor, showed no effect on NF-κB activation and proliferation in absence of CpG-ODN, but inhibited CpG-ODN mediated proliferative response and NF-κB activation. It also showed a significant inhibition in the release of IL-6 before and after CpG-ODN activation. While SB203580 enhanced the basal release of IL-10, no effect was seen on TNF-α basal release, but the presence of CpG-ODN significantly induced IL-10 and TNF-α release, although CpG-ODN induced IL-10 release in SB203580 pretreated cells was significantly less than IL-10 release in the activated control (untreated) cells. Thus, whilst CpG-ODN induced IL-6 production (and to a lesser extent IL-10 production) depended on MEK/ERK and $p38^{MAPK}$ pathways, CpG-ODN induced TNF-α production was dependent only on MEK/ERK signalling. The pre-treatment of BJAB cells with SB203580 inhibited the upregulation of CD54 molecule induced by CpG-ODN stimulated $p38^{MAPK}$ activation, but it did not affect the

upregulation of the costimulatory molecules CD80 and CD86 and MHC II, although the presence of the inhibitor in the absence of CpG-ODN increased CD86 and MHC II basal expression levels. As a result, the inhibitory effect of SB203580 works on most levels of CpG-ODN mediated responses, except the induction of costimulatory CD80 and CD86, indicating that $p38^{MAPK}$ pathway is involved in the TLR9 signalling pathway, and is involved in the response to CpG-ODN in relation to surface marker upregulation, cellular proliferation and cytokine synthesis.

The use of LY294002 inhibitor strongly inhibited basal cellular proliferation, but cells was still able to respond to CpG-ODN (weak response), and this is correlated with the effect of the inhibitor on the activation of the transcription factor NF-κB, in that LY294002 did not completely inhibit the activation of NF-κB. On the other hand, PI3K/AKT pathway is clearly involved in the production of IL-6, IL-10 and TNF-α cytokines. LY294002 showed a clear inhibition in the CpG-ODN mediated IL-6, IL-10 and TNF-α cytokine release. It also showed a complete inhibition in their basal induction in the absence of CpG-ODN. LY294002 showed a reduction in the basal expression levels of CD54, CD80 and CD86, and a clear inhibition in the CpG-ODN induced CD80 and CD86 upregulation. This appears to indicate that the costimulatory molecules are regulated by PI3K/AKT pathway, but not MAPK pathway.

This study indicates that, ERK, $p38^{MAPK}$, PI3K/AKT and NF-κB pathways all involved in TLR9 signalling in response to CpG-ODN in BJAB cells, but that different signalling pathways mediate different cellular responses to CpG-ODN as summarised in Table 5.5. In CpG-ODN activated BJAB cells, MAPK pathways (ERK and $p38^{MAPK}$), but not PI3K/ AKT pathway, mediates CD54 and MHC II upregulation, NF-κB activation, cellular proliferation, and suppresses IL-10 synthesis. ERK and p38 MAPK pathways are similar to PI3K/AKT pathway by enhancing IL-6 and TNF-α (in ERK only) cytokine release, but PI3K/AKT pathway also enhances IL-10 cytokine release. NF-κB pathway enhances cellular proliferation, IL-6 release and CD54 and MHC II upregulation in CpG-ODN activated BJAB cells.

In addition to that, the activation of CpG-ODN mediated ERK and $p38^{MAPK}$ induced downstream NF-κB activation, as was demonstrated by the loss of CpG-ODN induction of NF-κB activation in the presence of U0126 and SB203580 inhibitors respectively.

Furthermore, the inhibition of NF-κB activation demonstrates its importance in cellular proliferation. U0126 exhibited a great inhibitory effect on the tumour cells while SB203580 was sufficient to inhibit further proliferation.

Inhibitors	Pathway	Surface marker upregulation (Inhibition)	NF-κB	Cellular proliferation	Cytokine release (Inhibition)
Medium	Control	None	Activated	Proliferates	None
U0126	ERK	CD54, CD80, CD86 & MHC II	Inhibited	Inhibited	IL-6 and TNF-α
LY294002	PI3K/AKT	CD80 and CD86	Activated	Partial inhibition	IL-6, IL-10 & TNF-α
SB203580	P38	Partial inhibition for CD54	Inhibited	Inhibited	IL-6 & reduced IL-10
Curcumin	NF-κB	Partial inhibition for CD54 and MHC II	Inhibited	Inhibited	No effect

Table 5.5. Effect of the signalling inhibitors on CpG-ODN/TLR9 mediated responses.

In conclusion, this study indicates that CpG-ODN activates the ERK and p38 MAPK pathways, and they differentially regulate NF-κB pathway, IL-6 release, cellular proliferation and CD54 upregulation. Furthermore, CpG-ODN activates PI3K/AKT pathway and this pathway differentially regulates the upregulation of costimulatory molecules CD80 and CD86 and IL-6, IL-10 and TNF-α production BJAB cells.

The results of the current study support previous observations where $p38^{MAPK}$ activity induced by CpG DNA at least partly contributes to the production of IL-6, whereas ERK activation by CpG DNA promotes the IL-6 and TNF-α production, but suppresses IL-10 production in the cells (Yi AK *et al.*, 2001; Yi AK *et al.*, 2002). Furthermore, PI3K/AKT pathway negatively regulates IL-6 and TNF-α release by enhancing IL-10 production (Yi AK *et al.*, 2002; Saegusa K *et al.*, 2007). Yi AK and colleagues (2001) indicated that NF-κB and ERK activation induces TNF-α release. My data supports this finding, in that U0126 (ERK inhibitor) was associated with inhibition of both CpG-ODN induced NF-κB and TNF-α production.

Finally, studying the involvement of the different CpG-ODN mediated signalling pathways clarified the molecular mechanisms resulting in CpG-ODN mediated immune responses in BJAB Burkitt's Lymphoma cells. Figure 5.12 represents the different signalling pathways involved in CpG-ODN activation, and the sites of action for the inhibitors.

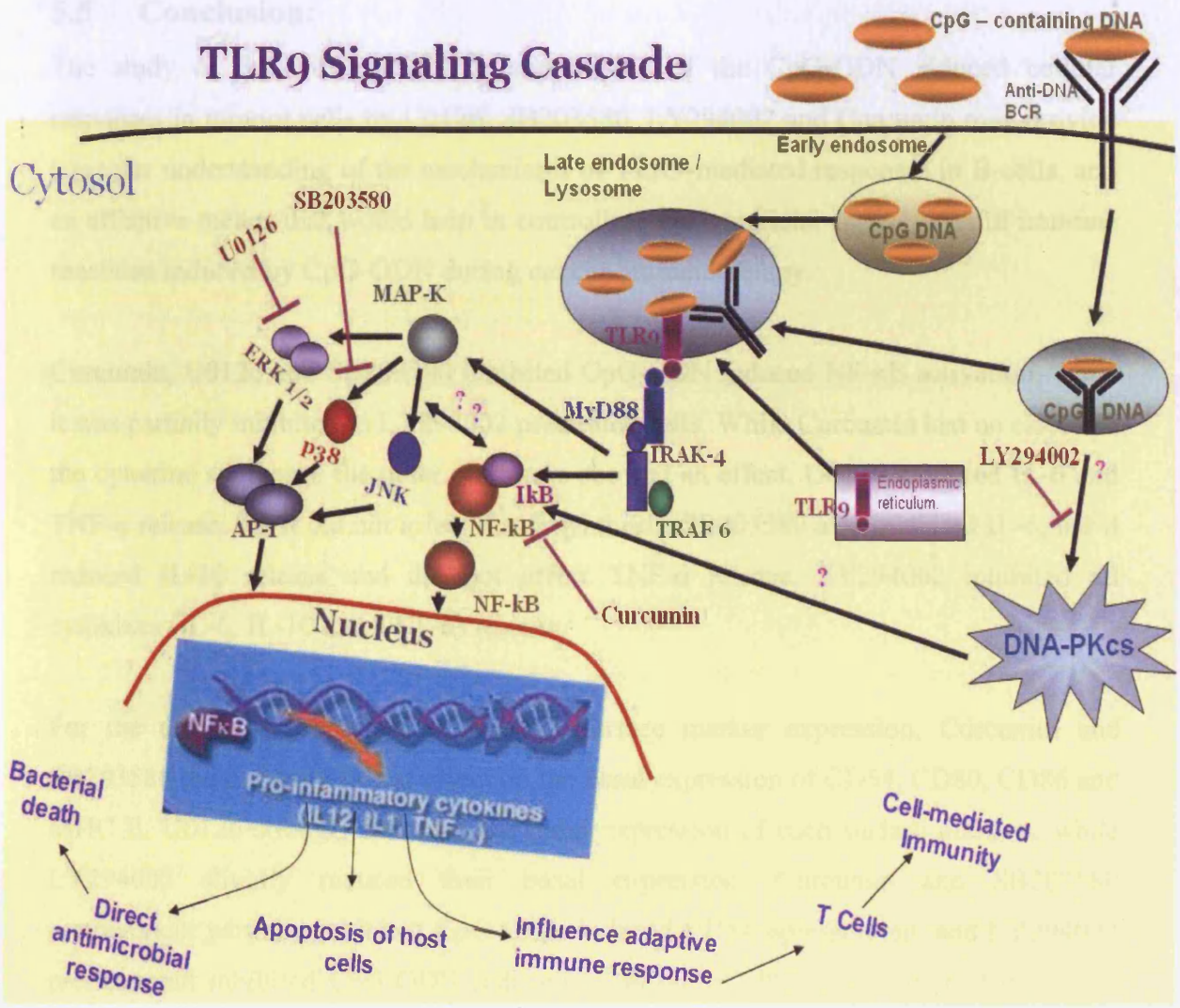

Figure 5.12. The different signalling (MEK/ERK, $p38^{MAPK}$, PI3K/AKT and NF-κB) pathways involved in TLR9 activation by CpG-ODN, and the targets of the signalling inhibitors (U0126, SB203580, LY294002 and Curcumin respectively).

5.5 Conclusion:

The study of the enhancement or suppression of the CpG-ODN induced cellular responses in tumour cells by U0126, SB203580, LY294002 and Curcumin may provide a greater understanding of the mechanisms of TLR9-mediated responses in B-cells, and an effective means that would help in controlling the beneficial and/or harmful immune reactions induced by CpG-ODN during cancer immunotherapy.

Curcumin, U0126 and SB203580 inhibited CpG-ODN induced NF-κB activation, while it was partially inhibited in LY294002 pretreated cells. While Curcumin had no effect on the cytokine synthesis, the other inhibitors showed an effect. U0126 inhibited IL-6 and TNF-α release, but it did not affect IL-10 synthesis. SB203580 also inhibited IL-6, but it reduced IL-10 release and did not affect TNF-α release. LY294002 inhibited all cytokines (IL-6, IL-10 and TNF-α) release.

For the effect of the inhibitors on the surface marker expression, Curcumin and SB203580 did not have a clear effect on the basal expression of CD54, CD80, CD86 and MHC II. U0126 strongly inhibited the basal expression of each surface markers, while LY294002 slightly reduced their basal expression. Curcumin and SB203580 pretreatment partially inhibited CpG-ODN induced CD54 upregulation, and LY294002 pretreatment inhibited CpG-ODN induced CD80 and CD86 upregulation. U0126 is a potent inhibitor that strongly inhibited CpG-ODN induced CD54, CD80, CD86 and MHC II upregulation.

Finally, Curcumin and SB203580 inhibited the effect of CpG-ODN on cellular proliferation without significantly affecting basal proliferation. U0126 strongly inhibited the basal cellular proliferation, and a significant further reduction was enhanced with CpG-ODN activation, while LY294002 profoundly inhibited basal cellular proliferation, although LY294002 pretreated cells still respond (weakly) to CpG-ODN stimulation.

As a conclusion, this work demonstrated the involvement of ERK, $p38^{MAPK}$, PI3K/AKT and NF-κB signalling pathways upon the activation of TLR9 with CpG-ODN. MEK/ERK pathway has an important role for basal expression and CpG-ODN induced surface marker CD54, CD80, CD86 and MHC II upregulation, also in the activation of NF-κB and cellular proliferation. ERK pathway enhances IL-6 and TNF-α release, and

partially supports CpG-ODN induction of IL-10. These findings were investigated by the use of ERK inhibitor, U0126, which completely inhibited the upregulation of those surface markers and completely inhibited the NF-κB activity.

This study also showed that $p38^{MAPK}$ is important for the upregulation of CD54. Transcription factor NF-κB and hence cellular proliferation were also found to be dependent on $p38^{MAPK}$ pathway. $p38^{MAPK}$ pathway is also involved in the CpG-ODN induction of IL-6 and IL-10 but not TNF-α cytokines. These conclusions were emphasized after treating the cells with SB203580, a potent $p38^{MAPK}$ inhibitor.

PI3K/AKT pathway showed an important involvement in the upregulation of the costimulatory molecules CD80 and CD86, but not the adhesion molecule CD54 nor MHC II. It is also involved in the production of IL-6, IL-10 and TNF-α cytokines. Finally, PI3K/AKT pathway is partially involved in the activation of NF-κB activation and cellular proliferation. These findings were highlighted after treating the cells with its specific inhibitor LY294002.

NF-κB pathway is not involved in basal expression of the tested surface markers while it is involved in the upregulation of CD54 and MHC II. NF-κB pathway has no effect on the CpG-ODN induced cytokine synthesis, but it highly involved in the CpG-ODN induction of cellular proliferation, consistent with others findings (Lin A *et al.*, 2003; Shishodia Sh *et al.*, 2005; Shakibaei *et al.*, 2007). These findings were investigated by the use of NF-κB inhibitor, Curcumin.

In summary, the present study indicates a novel molecular effects of the signalling pathways in BJAB cell's immune response, suggesting that MAPK (ERK and $p38^{MAPK}$) and PI3K/AKT pathways play a major role in the CpG-ODN mediated responses. Taken together, these data indicate that signalling through ERK and p38 MAP kinases play an important role in cellular growth, differentiation, apoptosis and inflammatory response. Inhibiting such signals would affect those cellular events. Whereas, PI3K/AKT pathway, is believed to regulate both growth and survival mechanisms in cancer cells. As a result, this study provides a valuable tool to determine the cellular role of CpG-ODN/TLR9 mediated response which can lead to the development of the therapeutic agents needed for the treatment of proliferative tumours.

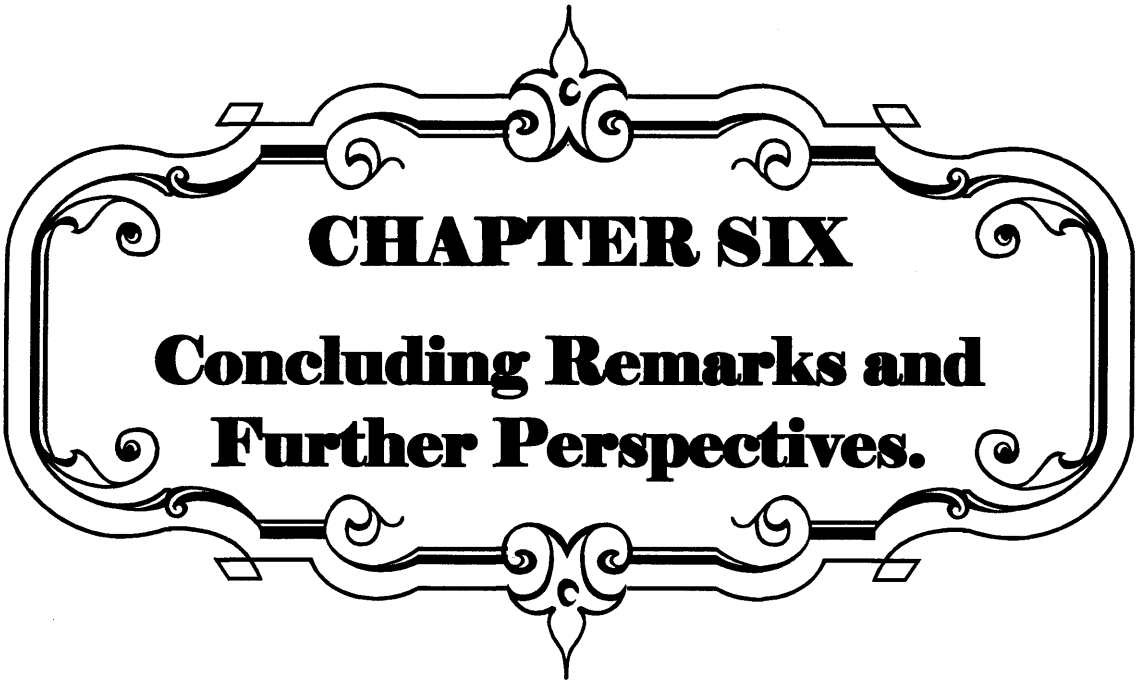

CHAPTER SIX

Concluding Remarks and Further Perspectives.

CHAPTER SIX
Concluding remarks

Despite that many studies have investigated the expression and role of hTLR9 in normal immune and non-immune cells, less is known about its expression and function in tumour cells. To understand the mechanism of action of hTLR9 in stimulating the immune system in tumour cells, its agonist CpG-ODN was used to shed new light on the immunotherapeutic potentials to the treatment of cancer, and in particular B-cell malignancies.

Studying the mRNA expression of TLR9, the RT-PCR method showed that most B cell tumour lines, representing different stages of B cell differentiation, expressed TLR9, with the exception of myeloma cell lines U266 and Karpas 707H, and the EBV transformed lymphoblastoid HMy-2 cell line, whereas all non-haematological cell lines tested were negative or very weakly positive for TLR9 mRNA expression (Figures 2.6-2.10 and Tables 2.2 & 2.3). A semi-quantitative RT-PCR assay was established, to estimate levels of TLR9 mRNA expression. There was a good correlation between RT-PCR and qRT-PCR data for the expression of TLR9 mRNA, and in addition there was a correlation between the level of expression of TLR9 mRNA as determined by qRT-PCR and the ability of the cells to respond to CpG-ODN, suggesting a direct relationship between TLR9 expression and responsiveness to CpG-ODN.

Determining the protein expression of TLR9 in normal and tumour cells showed no clear evidence of surface expression by flow cytometry (Tables 2.4-2.6 and Figures 2.12 & 2.14). All cell lines tested appeared to be weakly positive for the intracellular stain (Tables 2.4-2.6 and Figures 2.13 & 2.15), although cell lines positive for TLR9 expression by PCR tended to show a higher level of expression than those that were TLR9 negative by PCR. In addition, CpG-ODN treatment of PBMCs and BJAB cells resulted in an upregulation of intracellular TLR9 expression as detected by monoclonal antibody staining with flow cytometry (Figure 2.16). Confocal microscopy data were consistent with the detection of intracellular, but not extracellular, TLR9 protein expression in TLR9 transfected Hek293 cells (Figures 2.22 & 2.23), with correlation with flow cytometry results (Table 2.5 and Figures 2.14 and 2.15). Among the B-cells tested for TLR9 protein expression by confocal microscopy, multiple myeloma U266

and Karpas 707H cell lines showed no expression, whereas the rest showed an intracellular expression of TLR9 protein (Figure 2.24), in keeping with the expression of TLR9 as determined by flow cytometry (Table 2.4) and RT-PCR methods. No consistent bands of the correct size were detected by IP/WB for TLR9 protein expression in any of the cell lines tested (Figures 2.17 & 2.21). TLR9 transfected Hek293 and HeLa cells showed a positive TLR9 mRNA expression by PCR (and confocal microscopy for Hek293 cells Figures 2.22 & 2.23) while untransfected and mock transfected Hek293 and HeLa cells were negative. TLR9 transfected Hek293 cells showed a stronger positive TLR9 mRNA expression by PCR than TLR9 transfected HeLa cells (Figures 2.7 & 2.10 and Table 2.3).

As a conclusion, RT-PCR and qRT-PCR methods appeared to provide reliable methods for the detection of TLR9 mRNA expression. Immunoflourescent confocal microscopy and flow cytometry also showed promise as methods for the detection of TLR9 protein expression, although more data are required to confirm their usefulness. In contrast, IP/WB method did not provide a reliable method for the detection of TLR9 protein expression. Finally, Hek293 cells and to a lesser extent HeLa cells were successfully transfected with TLR9 construct gene, as detected by PCR methods.

CpG-ODN mediated responses of normal B-cells and tumour cells were studied for both intracellular signalling and extracellular responses. Intracellular signalling mediated responses were studied for MEK/ERK and p38 (MAPK) pathways, PI3K/AKT pathway and IκB-α/NF-κB pathway. Burkitt's lymphoma BJAB cells, the model of the study, showed a basal activation level at time zero for ERK, $p38^{MAPK}$ and PI3K/AKT pathways. In response to CpG-ODN, phosphorylated ERK 1/2 was reduced after 10 and 30 minutes, returning to basal activation at 60 and 120 minutes, whereas total ERK was fairly stable (Figure 3.3). BJAB cells showed an activation and phosphorylation in p38-dependent ATF-2 at 60 minutes (Figures 3.4 & 3.5), while it showed a PI3K-dependent phosphorylation of AKT-1 after 90 minutes of activation (Figure 3.6). IκB-α/NF-κB pathway was studied in BJAB cells as well as other tumour and normal B-cells. BJAB cells showed an activation peak for pIκB-α after 60 minutes of activation, while total IκB-α was fairly constant (Figures 3.9 & 3.10). Ramos, another Burkitt's lymphoma cell line, showed IκB-α/NF-κB pathway activation and pIκB-α production as early as 15minutes after CpG-ODN activation (Figure 3.8). The activation of IκB-α/NF-κB

pathway was seen in BJAB and RPMI tumour B-cell lines as well as normal PBMCs and B-CLL *ex vivo* B-cells (Table 3.4). Therefore MAP kinase (MEK/ERK and p38), PI3K/AKT and NF-κB pathways were all involved in the cellular response to CpG-ODN. NF-κB activation was also determined by luciferase assay in all TLR9 positive *ex vivo* cells and tumour cell lines.

Cytokine release was determined in several *ex vivo* B-cells and cell lines (TLR9 positive by PCR) to show an increase in the release of at least one of the cytokines (IL-6, IL-10 or TNF-α) in all TLR9 positive *ex vivo* B-cell and tumour B-cell lines, whereas no cytokine release was detected in U266 and Karpas 707H multiple myeloma cell lines (TLR9 negative by PCR, flow cytometry and confocal microscopy) following treatment with CpG-ODN (Table 3.5).

Determining the extracellular effects of CpG-ODN stimulation, responses varied between B-cells for the surface marker upregulation, but broadly correlated with TLR9 expression status (as detected by PCR) (Table 3.7), in that all TLR9 positive cells responded by upregulation of at least one of the four surface markers tested (CD54, CD80, CD86 and MHC II), whilst TLR9 negative cells showed no response. CpG-ODN mediated cellular proliferation also correlated with TLR9 expression. TLR9 positive cells were responding to CpG-ODN activation by changing the proliferative rate, while TLR9 negative cells showed no changes in the cellular proliferation rate. All TLR9 positive cells showed an increase in cellular proliferation except for Burkitt's lymphoma BJAB cells which showed inconsistent responses where in experiments carried out early in the project, it increased proliferation whereas in late experiments proliferate responses to CpG-ODN were decreased (Table 3.8 and Figure 5.11). The reasons for this difference were not clear, but other responses of this cell line to CpG-ODN activation remained consistent throughout the project.

Taking these results together, the tested haematological tumour derived cells (with the exception of myeloma cell lines U266 and Karpas, and EBV transformed lymphoblastoid HMy2 cells), not only highly expressed TLR9, but displayed functional characteristics (activating signalling pathways, cytokine release, surface marker upregulation and cellular proliferation) also observed in normal B-cells in response to CpG-ODN, whilst TLR9 negative cells showed no response to CpG-ODN.

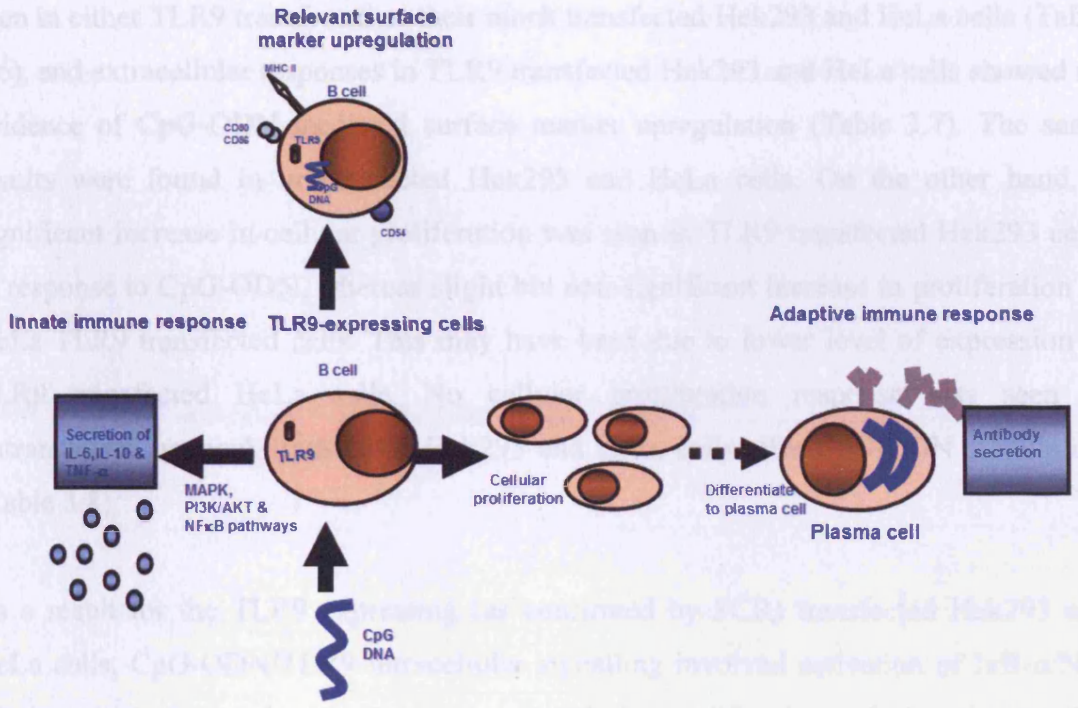

Figure 6.1. TLR9-dependent CpG DNA mediated responses. CpG DNA stimulates B cells expressing TLR9 in their ER by initiating the two main immune responses, the innate immune response leading to the upregulation of surface markers, cellular proliferation, cytokine release and the adaptive immune response by B cell differentiation to plasma cells leading to the secretion of antibodies.

Figure 6.1 summarises the TLR9-dependent CpG-ODN mediated responses in B-cells as suggested by the results. The binding of CpG-ODN to TLR9 in B-cells would initiate the two main immune responses; the innate immune response, leading to the activation of signalling pathways, secretion of cytokines/chemokines, upregulation of the relevant surface markers, and cellular proliferation, and the adaptive immune response by activating B cell differentiation to plasma cells and antibody secretions (not studied in this project).

Studying the activation responses of CpG-ODN on the positive control of TLR9 transfected Hek293 and HeLa cell lines showed an intracellular signalling response involving the IκB-α/NF-κB pathway, where TLR9 transfected Hek293 and HeLa cells showed an activation response by the production of pIκB-α, while their mock transfectants showed no effect (Figures 3.11-3.16). TLR9 transfected Hek293 and HeLa cells also showed NF-κB activation in luciferase assays, whereas their mock transfected and untransfected cells failed to activate NF-κB (Table 3.4). Together with the PCR data on these cells, the results suggest expression of a functional TLR9 gene in the transfected cells. However, no increase in IL-6, IL-10 and TNF-α cytokine release was

seen in either TLR9 transfected or their mock transfected Hek293 and HeLa cells (Table 3.6), and extracellular responses in TLR9 transfected Hek293 and HeLa cells showed no evidence of CpG-ODN mediated surface marker upregulation (Table 3.7). The same results were found in untransfected Hek293 and HeLa cells. On the other hand, a significant increase in cellular proliferation was seen in TLR9 transfected Hek293 cells in response to CpG-ODN, whereas slight but non-significant increase in proliferation of HeLa TLR9 transfected cells. This may have been due to lower level of expression in TLR9 transfected HeLa cells. No cellular proliferation response was seen in untransfected or mock transfected Hek293 and HeLa cells after CpG-ODN stimulation (Table 3.8).

As a result for the TLR9 expressing (as confirmed by PCR) transfected Hek293 and HeLa cells, CpG-ODN/TLR9 intracellular signalling involved activation of IκB-α/NF-κB that was associated with an increase in cellular proliferation, which indicates that TLR9 is functional, but they did not upregulate surface markers (CD54, CD80, CD86 and MHC II) or release IL-6, IL-10 and TNF-α cytokines. This would raise a question of "do these data reflect lack of response in these cells, or were we just looking for the wrong markers/cytokines?".

Cells	Cell type	TLR9 expression	Surface marker upregulation	Cytokine release	IκB-α phosphor.	NF-κB activation	Cellular proliferation
PBMCs	Normal *ex vivo* B-cells	PCR + Confocal: ND	CD54, CD80, CD86, MHC II	IL-6, IL10, TNF-α	YES	YES	YES
B-CLL	Tumour *ex vivo* B-cells	PCR + Confocal: ND	CD54, CD80, CD86, MHC II	IL-6, IL10, TNF-α	YES	YES	YES
TH044	*Ex vivo* mantle cell lymphoma	PCR+, Confocal +	ND	IL-6, IL10, TNF-α	ND	ND	YES
FC029		PCR + Confocal: ND	ND	IL-6, IL10, TNF-α	ND	ND	ND
BJAB	Burkitt's lymphoma cell lines	PCR+, Confocal +	CD54, CD86, MHC II	IL-6, IL10, TNF-α	YES	YES	YES
Ramos		PCR+ Confocal: ND	CD54, CD80, CD86, MHC II	IL-6	YES	YES	YES
Raji		PCR+ Confocal: ND	CD86	ND	ND	ND	YES
Lila	Precursor B-ALL cell line	PCR + Confocal +	CD54	IL-6, IL10, TNF-α	ND	YES	ND
RPMI	Multiple myeloma cell lines	PCR + Confocal: ND	CD54, CD80, CD86, MHC II	TNF-α	ND	YES	YES
U266		PCR – Confocal -	NO	NO	ND	ND	NO
Karpas		PCR-, Confocal -	NO	NO	ND	ND	NO

Table 6.1 Summary of some haematological tumour cells/cell lines (and normal PBMCs) used in this study and their CpG-ODN mediated responses, showing the methods used to detect their TLR9 expression. ND: Not done.

Tables 6.1 and 6.2 summarise some of the cells used in this study, showing the method(s) that confirmed their TLR9 expression, and indicating the different responses mediated by CpG-ODN activation.

Cells	Cell type	TLR9 expression	Surface marker upregulation	Cytokine release	IκB-α phosphor.	NF-κB activation	Cellular proliferation
Hek293	Human embryonal kidney	PCR – Confocal: ND	NO	NO	ND	ND	NO
HeLa	Human cervical carcinoma	PCR – Confocal: ND	NO	NO*	ND	ND	NO
MCF-7	Breast cancer adenocarcinoma	PCR – Confocal: ND	NO	NO*	ND	ND	NO
DU-145	Prostate carcinoma	PCR – Confocal: ND	NO	NO*	ND	ND	NO
HRT-18	Rectum-anus, adenocarcinoma	PCR – Confocal: ND	NO	NO*	ND	ND	NO
WM1361A	Melanoma	PCR – Confocal: ND	NO	NO*	ND	ND	NO
Hek293 TLR9	TLR9 transfected Human embryonal kidney	PCR + Confocal +	NO	NO	YES	YES	YES
Hek293 HA/TLR9		PCR + Confocal +	NO	NO	ND	YES	YES
HeLa TLR9	TLR9 transfected Human cervical carcinoma	PCR + Confocal: ND	NO	NO	ND	YES	NO
HeLa HA/TLR9		PCR + Confocal: ND	NO	NO	YES	YES	NO
Hek293 pCl-neo	Mock transfected Human embryonal kidney	PCR – Confocal –	NO	NO	ND	NO	NO
Hek293 pDisplay		PCR – Confocal –	NO	NO	NO	NO	NO
HeLa pCl-neo	Mock transfected Human cervical carcinoma	PCR – Confocal: ND	NO	NO	ND	NO	NO
HeLa pDisplay		PCR – Confocal: ND	NO	NO	NO	NO	NO

Table 6.2. Summary of non-haematological tumour cell lines used in this study and their CpG-ODN mediated responses, showing the methods used to detect their TLR9 expression. ND: Not done. *Data taken from Helia Esteves, BSc project, University of Leicester.

Studying the CpG-ODN mediated tolerance on TLR9 positive B-cells/cell lines (Table 6.3) showed evidence of a tolerising effect on NF-κB activation and reduced surface markers upregulation when cells were pretreated with 0.1μg/ml 10103 CpG-ODN before their subsequent CpG-ODN activation. A variable effect on cytokine release was induced in the pretreated cells after their activation, with inhibition of some cytokines (e.g. IL-6) in some cells (B-CLL and BJAB), but the results were not consistent between

different cell lines. No clear effect on cellular proliferation was induced in the pretreated *ex vivo* cells and RPMI cell line after the subsequent activation whilst BJAB B-cell lines induced a refractory state. These data suggested that NF-κB activation (which was consistently inhibited in these experiments) was not involved in all of the cellular responses to CpG-ODN that were investigated.

B-cells	Time Of pretreatment	0.1μg/ml 10103 CpG Non-activating:	NF-κB activation	Cytokines release	Surface markers	Cellular proliferation
BJAB	Up to three weeks	NF-κB, all cytokines & surface markers (except MHCII), proliferation	Complete inhibition in day one to three weeks	IL-6, One & Three days TNF-α, Day Three	All (less in CD80). Partial tolerance from first day to two weeks	Inhibition from first day to Three weeks
RPMI	Up to four weeks	NF-κB, all cytokines & surface markers, proliferation	Short term inhibition in day one and three only.	IL-10 & TNF-α release enhanced in day three*	All mostly in long term (one week and two weeks)	Short term inhibition of One and Three days
PBMCs	One and three days	NF-κB, IL-10 & TNF-α in one day. CD54, CD86 & MHC II	Inhibition in day one and three.	TNF-α, partial inhibition in IL-10 after three days	CD54, CD86 & MHC II in days One & Three	Decrease with time. No clear inhibition.
B-CLL	One and three days	NF-κB, All cytokines, partial inhibition in all surface markers	Inhibition in day one and three.	IL-6 partial inhibition, IL-10 strong inhibition & enhance TNF-α* in day three.	Partial inhibition of all, mostly in day three	Decrease with time. No clear inhibition.

Table 6.3. Summary of the inhibitory effect of low dose CpG-ODN on B-cell/cell lines on the immune responses to subsequent challenge with optimal doses of CpG-ODN. Table illustrates the inhibited responses that are affected with the low dose of CpG-ODN and the time of their effect. * Cells showed an activation response to CpG by enhancing the cytokine release.

Data on the effect of low dose CpG-ODN indicates that tolerance to CpG-ODN can be induced, but that it is a refractory state that follows the initial phase of B-cell activation and is characterised by the reduction in the ability of B-cells to induce the expected CpG-ODN mediated responses in response to subsequent CpG-ODN challenges. The mediated responses that were not activated with the low CpG-ODN, showed a tolerance status towards the subsequent CpG-ODN activation, while those which were activated did not. Low dose of CpG-ODN appeared to tolerise effectively NF-κB signalling, and partially for surface marker upregulation and cellular proliferation, with variable effects on cytokine production, showing inhibition of some in some cells but not consistent. A relatively stable refractory state was established in BJAB cells after three days of pretreatment with 0.1μg/ml CpG-ODN that lasted at least one week before the cell line regained its responsiveness to NF-κB activation. In conclusion, data suggest that low

doses of CpG-ODN can tolerise NF-κB activity, also different signalling pathways mediate different functional effects of CpG-ODN/TLR9 activation, and so looking at tolerising effects on signalling pathways other than NF-κB is crucial. These data have potentially important implications for dosing schedules, where CpG-ODN is being used in immunotherapy regimes.

The final set of experiments was designed to determine the signalling pathways involved in BJAB cell activation by CpG-ODN, and their role in the different functional responses, using several selective inhibitors of different cellular signalling pathways (Table 6.4). As expected, the data indicate that Curcumin inhibits NF-κB pathway, U0126 inhibits MEK/ERK pathway, SB203580 inhibits $p38^{MAPK}$ /ATF-2 pathway and LY294002 inhibits PI3K/AKT pathway. Determining the effect of the inhibitors on intracellular NF-κB signalling pathway showed a complete inhibition of NF-κB activation with CpG-ODN when MAPK inhibitors (U0126 and SB203580) and Curcumin were used, while PI3K/AKT inhibitor (LY294002) reduced CpG-ODN induced NF-κB activation compared with the non-inhibited BJAB cells (Figure 5.10). CpG-ODN induced release of IL-6, IL-10 and TNF-α in BJAB cells, which was not affected by Curcumin. BJAB cells treated with U0126 showed a complete inhibition of IL-6 and TNF-α release, with a reduction in IL-10 release in response to CpG activation. SB203580 inhibitor showed a complete inhibition in IL-6 cytokine, but only partially inhibited IL-10 release and had no effect on TNF-α cytokine. In contrast, LY94002 strongly inhibited all three cytokines before and after CpG-ODN activation (Table 5.2).

BJAB	Activated pathway			NF-κB Activation	Cytokines Release			Surface markers Upregulation				Cellular proliferation
	MAPK		PI3K									
	ERK	p38	AKT		IL-6	IL-10	TNF-α	CD54	CD80	CD86	MHCII	
Medium	YES	YES	YES	YES	YES	YES	YES	YES	YES[x]	YES	YES	YES*
Curcumin	ND	ND	ND	NO	YES	YES	YES	YES	NO	NO	YES	NO
U0126	NO	ND	ND	NO	NO	YES	NO	NO	NO	NO	NO	NO
SB203580	ND	NO	ND	NO	NO	YES	YES	NO	NO	YES	YES	NO
LY294002	ND	ND	NO	YES	NO	NO	NO	YES^	NO	NO	YES	YES¥

Table 6.4. Summary for the effect of selective inhibitors of different cellular signalling pathways on CpG-ODN mediated activation of Burkitt's lymphoma BJAB B-cell line. [x]CD80 expression did not show a clear effect as the other surface markers tested. * 60% reduction in cellular proliferation. ^CD54 basal level was decreased in the presence of PI3K/AKT inhibitor, but it was enhanced after CpG-ODN activation. ¥ Basal cellular proliferation was inhibited by LY294002, but enhanced after CpG-ODN activation. YES: Enhancement Response, NO: Inhibition Response. ND: Not done.

The upregulation of the surface markers (CD54, CD80, CD86 and MHC II) was strongly inhibited with U0126 inhibitor before and after CpG-ODN activation. Curcumin showed no clear effect on the expression of the four surface markers in resting, but partially inhibited CD54 and MHC II upregulation in CpG-ODN activated cells. SB203580 enhanced CD86 and MHC II expression in resting cells and CpG-ODN activated cells, but inhibited CD54 upregulation in CpG-ODN activated cells. LY294002 strongly inhibited costimulatory CD80 and CD86 expression in resting and CpG-ODN activated cells, whereas CD54 expression was inhibited in resting cells, but CD54 and MHC II expressions were increased by CpG-ODN activation compared with non-inhibited cells (Figure 5.11). CpG-ODN mediated cellular responses showed a reduced cellular proliferation in non-inhibited BJAB cells. Curcumin showed no effect on cellular proliferation in resting and CpG-ODN activated cells. U0126 markedly inhibited proliferation of resting cells with a slight further reduction on activation. SB203580 showed no effect on resting cells and no reduction or change in proliferation rate on activated cells. Whereas LY294002 markedly inhibited basal cellular proliferation in resting BJAB cells, but slightly enhanced cellular proliferation after CpG-ODN activation, less than in control (non-inhibited) cells (Figure 5.12).

Taken together, the data indicate that different inhibitors have different effects on basal and CpG-ODN activated surface marker expression, cellular proliferation and cytokine release. Also, NF-κB activation was affected by all except LY294002 inhibitor which suggests that NF-κB could be a downstream mediators of CpG-ODN mediated MAP kinase signalling, but not of PI3K/AKT signalling. In addition, cellular proliferation is positively regulated by NF-κB activation, and that was also detected in the work of others such as Lin A *et al.*, (2003) and Shishodia S *et al.*, (2005).

There is growing interest in determining which signalling pathways are mediated by CpG-ODN/TLR9 activation and their effects on the CpG-ODN mediated immune responses. Table 6.5 and Figure 6.2 summarise the effects of the signalling pathways resulting from CpG-ODN/TLR9 mediated responses in Burkitt's lymphoma BJAB cell lines, as found in this work.

The results indicate that ERK/MEK pathway is the main pathway that is involved in most of the activating processes, as it regulates NF-κB pathway, IL-6 and TNF-α

release, CD54, CD80, CD86 and MHC II surface marker upregulation and cellular proliferation. On the other hand IL-10 was found to be mostly regulated by PI3K/AKT pathway, showing a negatively regulating response towards IL-6 and TNF-α release as also been indicated in others work (Yi AK *et al.*, 2002; Saegusa K *et al.*, 2007). IL-6 cytokine release was found to be mostly dependent on MAPK and PI3K/AKT pathways, but not NF-κB pathway, whereas IL-10 release is mainly dependent on PI3K/AKT pathway and negatively controlled by MAPK pathways. TNF-α release correlated broadly with IL-6 release, but it was less dependent on $p38^{MAPK}$ pathway.

Pathways	Activation	Biological activity	Response of CpG-ODN activated Burkitt's lymphoma BJAB B-cells
MAPK pathways	ERK 1/2	• Mediates cellular proliferation and survival	• Activates NF-κB . • Induces IL-6 and TNF-α. • Suppresses IL-10 release. • Upregulates surface markers CD54, CD80, CD86 and MHC II • Enhances cellular proliferation.
	$p38^{MAPK}$	• Activated in response to cellular stress. • Have a protective and pro-apoptotic functions.	• Activates NF-κB. • Induces IL-6 cytokine release. • Suppresses TNF-α cytokines release. • Enhances cellular proliferation. • Upregulates CD54 expression. • Suppresses costimulatory molecules CD80 and CD86.
PI3K/AKT pathway	AKT	• Negatively regulates NF-κB transcriptional factor. • Prevents apoptosis induced by cytokines and cellular stress.	• Inhibits NF-κB. • Enhances Cytokine release, especially IL-10. • Inhibits cellular proliferation. • Upregulates costimulatory molecules CD80 and CD86. • Suppresses CD54 and MHC II upregulation.
NF-κB pathway	NF-κB	Regulates • Cell survival and antiapoptotic factor. • Cell division. • Innate and cellular responses to stress.	• Negatively regulates IL-10 release • Regulates IL-6 and TNF-α release • Enhances cellular proliferation. • Upregulates CD54 and MHC II expression.

Table 6.5. Summary of the suggested effects of the signalling pathways on CpG-ODN/TLR9 mediated responses in Burkitt's lymphoma BJAB cell lines as concluded from this work.

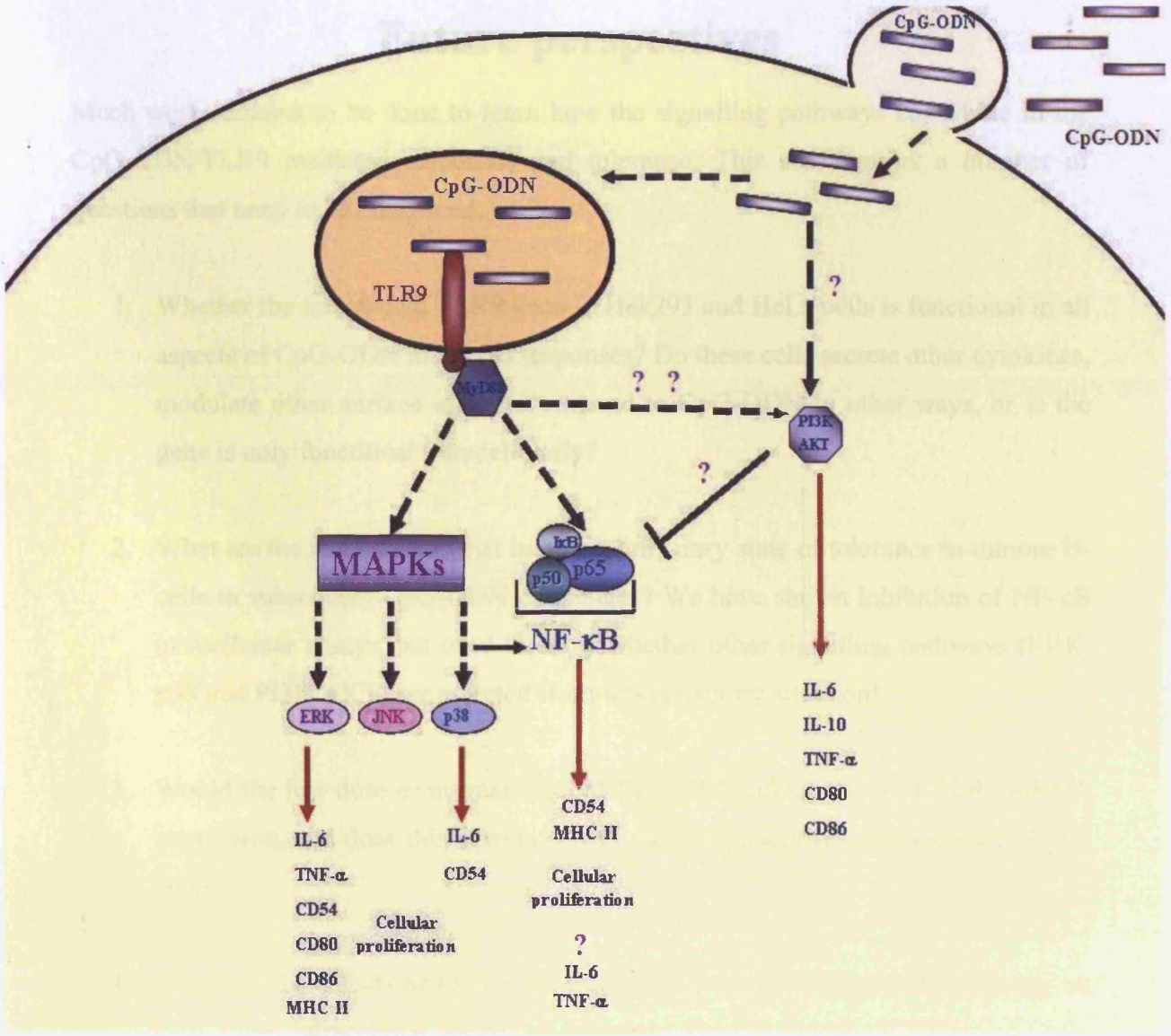

Figure 6.2. Suggested summary of the signalling pathways and their effect on the other functional immune responses involved in TLR9 activation by CpG-ODN in Burkitt's lymphoma BJAB cell lines as has been concluded from this work. Red arrows indicate the suggested CpG-ODN stimulated responses.

Taken together, these data strongly implicate TLR9 as the receptor for CpG-ODN, as its expression correlated with CpG-ODN responsiveness, and varied between the different human tumour cell lines. Furthermore, TLR9 positive tumour cells differ in their responsiveness to CpG-ODN, and different signalling pathways mediate different functional effects of CpG-ODN/TLR9 activation. Understanding the complex relationships between the different signalling pathways and CpG-ODN/TLR9 function, should enable development of therapies aimed at modulating the immune response.

Future perspectives

Much work remains to be done to learn how the signalling pathways contribute in the CpG-ODN/TLR9 mediated responses and tolerance. This study raises a number of questions that need to be confirmed, such as:

1. Whether the transfected TLR9 gene in Hek293 and HeLa cells is functional in all aspects of CpG-ODN mediated responses? Do these cells secrete other cytokines, modulate other surface markers, respond to CpG-ODN in other ways, or is the gene is only functional intracellularly?

2. What are the mechanisms that induce a refractory state of tolerance in tumour B-cells to subsequent CpG-ODN challenges? We have shown inhibition of NF-κB in luciferase assays, but need to show whether other signalling pathways (ERK, p38 and PI3K/AKT) are affected from this refractory situation!

3. Would the low dose or normal dose of CpG-ODN affect levels of TLR9 mRNA expression, and does this correlate with the subsequent responsiveness to CpG-ODN?

4. What are the effects of each CpG-ODN/TLR9 mediated signalling pathway on both, other intracellular signalling pathways and the functional effects of CpG-ODN/TLR9?

5. Is the PI3K/AKT pathway independent of the other signalling pathways? Is its activation following TLR9 signalling dependent on the same upstream events (e.g. MyD88)?

The above questions are currently under investigation to understand the exact molecular mechanisms involved in the activation of TLR9 by CpG-ODN.

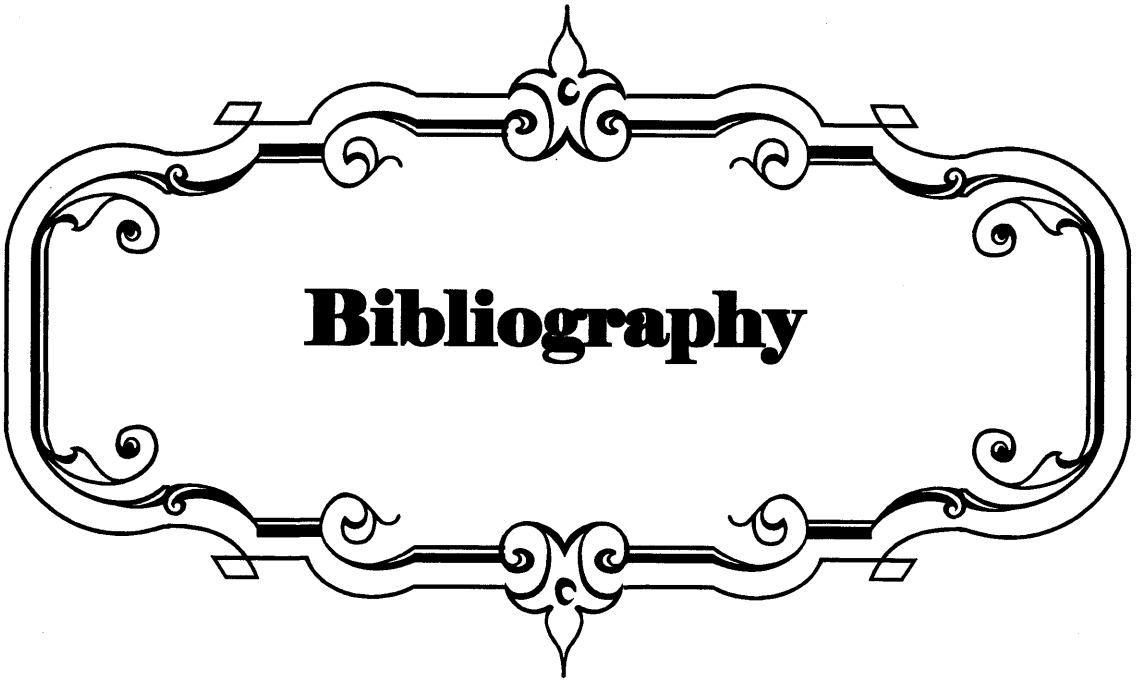

Bibliography

Bibliography:

Ahmad-Nejad P, Hacker H, Rutz M, Bauer S, Vabulas RM, Wagner H. Bacterial CpG-DNA and lipopolysaccharides activate Toll-like receptors at distinct cellular compartments. Eur J Immunol. 2002; 32:1958-68.

Aderem A, Hume D.A. How do you see CG? Cell. 2000; 103:993-996.

Akira S, Hemmi H. Recognition of pathogen-associated molecular patterns by TLR family. Immunol Lett. 2003; 85:85-95.

Akira S and Takeda K. Toll-like receptor signalling. Nat Rev Immunol. 2004; 4:499-511.

Akira S. Toll-like receptors and innate immunity. Adv Immunol. 2001; 78:1-56.

Akira S, Takeda K, Kaisho T. Toll-like receptors: critical proteins linking innate and acquired immunity. Nat Immunol. 2001; 2:675-80.

Akira S., Uematsu S. and Takeuchi O. Pathogen recognition and innate immunity. Cell. 2006; 124: 783–801.

An H, Xu H, Yu Y, Zhang M, Qi R, Yan X, Liu S, Wang W, Guo Z, Qin Z, Cao X. Up-regulation of TLR9 gene expression by LPS in mouse macrophages via activation of NF-kappaB, ERK and p38 MAPK signal pathways. Immunol Lett. 2002; 81(3):165-9.

Baines J, Celis E. Immune-mediated tumor regression induced by CpG-containing oligodeoxynucleotides. Clin Cancer Res. 2003; 9:2693-700.

Baiyee EE, Flohe S, Lendemans S, Bauer S, Mueller N, Kreuzfelder E, Grosse-Wilde H. Expression and function of Toll-like receptor 9 in severely injured patients prone to sepsis. Clin Exp Immunol. 2006; 145:456-62.

Barton GM, Kagan JC, Medzhitov R. Intracellular localization of Toll-like receptor 9 prevents recognition of self DNA, but facilitates access to viral DNA. Nat Immunol. 2006; 7:49-56.

Bauer, S., C. J. Kirschning, H. Hacker, V. Redecke, S. Hausmann, S. Akira, H. Wagner, G. B. Lipford. Human TLR9 confers responsiveness to bacterial DNA via species-specific CpG motif recognition. Proc. Natl. Acad. Sci. USA 2001; 98:9237.

Broad A, Kirby JA, Jones DE; Applied Immunology and Transplantation Research Group. Toll-like receptor interactions: tolerance of MyD88-dependent cytokines but enhancement of MyD88-independent interferon-beta production. Immunology. 2007 ;120:103-11.

Bourke E, Bosisio D, Golay J, Polentarutti N, Mantovani A. The toll-like receptor repertoire of human B lymphocytes: inducible and selective expression of TLR9 and TLR10 in normal and transformed cells. Blood. 2003; 102:956-63.

Boyd AW, Dunn SM, Fecondo JV. Regulation of expression of a human intercellular adhesion molecule (ICAM-1) during lymphohematopoietic differentiation. Blood. 1989; 73: 1896–1903.

Brinkmann MM, Spooner E, Hoebe K, Beutler B, Ploegh HL, Kim YM. The interaction between the ER membrane protein UNC93B and TLR3, 7, and 9 is crucial for TLR signaling. J Cell Biol. 2007; 177:265-75.

Cario E, Podolsky DK. Differential alteration in intestinal epithelial cell expression of toll-like receptor 3 (TLR3) and TLR4 in inflammatory bowel disease. Infect Immun. 2000; 68:7010-7.

Chang JH, Park JY, Kim SK. Dependence on p38 MAPK signalling in the up-regulation of TLR2, TLR4 and TLR9 gene expression in Trichomonas vaginalis-treated HeLa cells. Immunology. 2006; 118:164-70.

Chaperot L, Plumas J, Jacob MC, Bost F, Molens JP, Sotto JJ, Bensa JC. Functional expression of CD80 and CD86 allows immunogenicity of malignant B cells from non-Hodgkin's lymphomas. Exp Hematol. 1999; 27:479-88.

Chen W, Wang J, An H, Zhou J, Zhang L, Cao X. Heat shock up-regulates TLR9 expression in human B cells through activation of ERK and NF-kappaB signal pathways. Immunol Lett. 2005; 98:153-9.

Chiu D, Ma K, Scott A, Duronio V. Acute activation of Erk1/Erk2 and protein kinase B/akt proceeds by independent pathways in multiple cell types. FEBS J. 2005; 272:4372-84.

Chu W, Gong X, Li Z, Takabayashi K, Ouyang H, Chen Y, Lois A, Chen DJ, Li GC, Karin M, Raz E. DNA PKcs is required for activation of innate immunity by immunostimulatory DNA. Cell. 2000; 103:909-18.

Chuang, TH., J. Lee, L. Kline, J. C. Mathison, R. J. Ulevitch. Toll-like receptor 9 mediates CpG-DNA signaling. J. Leukocyte Biol. 2002; 71:538.

Chuang TH, Ulevitch RJ. Cloning and characterization of a sub-family of human toll-like receptors: hTLR7, hTLR8 and hTLR9. Eur Cytokine Netw. 2000; 11:372-8.

Cornélie S, Hoebeke J, Schacht AM, Bertin B, Vicogne J, Capron M, Riveau G. Direct evidence that toll-like receptor 9 (TLR9) functionally binds plasmid DNA by specific cytosine-phosphate-guanine motif recognition. J Biol Chem. 2004; 279:15124-9.

Crabtree TD, Jin L, Raymond DP, Pelletier SJ, Houlgrave CW, Gleason TG, Pruett TL, Sawyer RG. Preexposure of murine macrophages to CpG oligonucleotide results in a biphasic tumor necrosis factor alpha response to subsequent lipopolysaccharide challenge. Infect Immun. 2001; 69:2123-9.

Cuenda A, Rouse J, Doza YN, Meier R, Cohen P, Gallagher TF, Young PR, Lee JC. SB 203580 is a specific inhibitor of a MAP kinase homologue which is stimulated by cellular stresses and interleukin-1. FEBS. Lett. 1995 May 8; 364:229-33.

Cunningham-Rundles C, Radigan L, Knight AK, Zhang L, Bauer L, Nakazawa A. TLR9 activation is defective in common variable immune deficiency. J Immunol. 2006; 176:1978-87.

Dalpke AH, Heeg K. CpG-DNA as immune response modifier. Int J Med Microbiol. 2004; 294:345-54.

Dalpke AH, Lehner MD, Hartung T, Heeg K. Differential effects of CpG-DNA in Toll-like receptor-2/-4/-9 tolerance and cross-tolerance. Immunology. 2005; 116:203-12.

Dasari P, Nicholson IC, Hodge G, Dandie GW, Zola H. Expression of toll-like receptors on B lymphocytes. Cell Immunol. 2005; 236:140-5.

Decker T, Schneller F, Kronschnabl M, Dechow T, Lipford GB, Wagner H, Peschel C. Immunostimulatory CpG-oligonucleotides induce functional high affinity IL-2 receptors on B-CLL cells: costimulation with IL-2 results in a highly immunogenic phenotype. Exp Hematol. 2000a; 28:558-568.

Decker T, Schneller F, Sparwasser T, Tretter T, Lipford GB, Wagner H, Peschel C. Immunostimulatory CpG-oligonucleotides cause proliferation, cytokine production, and an immunogenic phenotype in chronic lymphocytic leukaemia B cells. Blood. 2000b; 95:999-1006.

Dobrovolskaia MA, Medvedev AE, Thomas KE, Cuesta N, Toshchakov V, Ren T, Cody MJ, Michalek SM, Rice NR, Vogel SN. Induction of in vitro reprogramming by Toll-like receptor (TLR)2 and TLR4 agonists in murine macrophages: effects of TLR "homotolerance" versus "heterotolerance" on NF-kappa B signaling pathway components. J Immunol. 2003; 170:508-19.

Dragoi AM, Fu X, Ivanov S, Zhang P, Sheng L, Wu D, Li GC, Chu WM. DNA-PKcs, but not TLR9, is required for activation of Akt by CpG-DNA. EMBO J. 2005; 24:779-89.

Droemann D, Albrecht D, Gerdes J, Ulmer AJ, Branscheid D, Vollmer E, Dalhoff K, Zabel P, Goldmann T. Human lung cancer cells express functionally active Toll-like receptor 9. Respir Res. 2005; 6:1.

Du, X., A. Poltorak, Y. Wei, and B. Beutler. Three novel mammalian toll-like receptors: gene structure, expression, and evolution. Eur Cytokine Netw. 2000; 11:362-71.

Eaton-Bassiri A, Dillon SB, Cunningham M, Rycyzyn MA, Mills J, Sarisky RT, Mbow ML. Toll-like receptor 9 can be expressed at the cell surface of distinct populations of tonsils and human peripheral blood mononuclear cells. Infect Immun. 2004; 72:7202-11.

Eisenstein EM, Chua K, Strober W. B cell differentiation defects in common variable immunodeficiency are ameliorated after stimulation with anti-CD40 antibody and IL-10. J Immunol. 1994; 152:5957-68.

Favata MF, Horiuchi KY, Manos EJ, Daulerio AJ, Stradley DA, Feeser WS, Van Dyk DE, Pitts WJ, Earl RA, Hobbs F, Copeland RA, Magolda RL, Scherle PA, Trzaskos Identification of a novel inhibitor of mitogen-activated protein kinase. J Biol Chem. 1998; 273:18623-32.

Fransson M, Benson M, Erjefält JS, Jansson L, Uddman R, Björnsson S, Cardell LO, Adner M. Expression of Toll-like receptor 9 in nose, peripheral blood and bone marrow during symptomatic allergic rhinitis. Respir Res. 2007; 28:8-17.

Funami K, Matsumoto M, Oshiumi H, Akazawa T, Yamamoto A, Seya T. The cytoplasmic 'linker region' in Toll-like receptor 3 controls receptor localization and signaling. Int Immunol. 2004; 16:1143-54.

Grandjenette C, Kennel A, Faure GC, Béné MC, Feugier P. Expression of functional toll-like receptors by B-chronic lymphocytic leukemia cells. Haematologica. 2007; 92:1279-81.

Gursel M, Verthelyi D, Klinman DM. CpG oligodeoxynucleotides induce human monocytes to mature into functional dendritic cells. Eur J Immunol. 2002; 32:2617-22.

Häcker H, Vabulas RM, Takeuchi O, Hoshino K, Akira S, Wagner H. Immune cell activation by bacterial CpG-DNA through myeloid differentiation marker 88 and tumor necrosis factor receptor-associated factor (TRAF) 6. J Exp Med. 2000; 192:595-600.

Häcker G, Redecke V, Häcker H. Activation of the immune system by bacterial CpG-DNA. Immunology. 2002; 105:245-51.

Han Y, Weinman S, Boldogh I, Walker RK, Brasier AR. Tumor necrosis factor-alpha-inducible IkappaBalpha proteolysis mediated by cytosolic m-calpain. A mechanism parallel to the ubiquitin-proteasome pathway for nuclear factor-kappab activation. J Biol Chem. 1999; 274:787-94.

Hartmann G, Krieg AM. Mechanism and function of a newly identified CpG DNA motif in human primary B cells. J Immunol. 2000;164:944-53.

Hatao F, Muroi M, Hiki N, Ogawa T, Mimura Y, Kaminishi M, Tanamoto K. Prolonged Toll-like receptor stimulation leads to down-regulation of IRAK-4 protein. J Leukoc Biol. 2004; 76:904-8.

Hayashi F., Means T.K. and Luster A.D. Toll-like receptors stimulate human neutrophil function. Blood. 2003; 102:2660–2669.

Hazeki K, Nigorikawa K, Hazeki O. Role of phosphoinositide 3-kinase in innate immunity. Biol Pharm Bull. 2007; 30:1617-23.

Hemmi H, Takeuchi O, Kawai T, Kaisho T, Sato S, Sanjo H, Matsumoto M, Hoshino K, Wagner H, Takeda K, Akira S.A. Toll-like receptor recognizes bacterial DNA. Nature. 2000; 408:740-5.

Henault M, Lee LN, Evans GF, Zuckerman SH. The human Burkitt lymphoma cell line Namalwa represents a homogenous cell system characterized by high levels of Toll-like receptor 9 and activation by CpG oligonucleotides. J Immunol Methods. 2005; 300:93-9.

Herbst-Kralovetz MM, Quayle AJ, Ficarra M, Greene S, Rose WA 2nd, Chesson R, Spagnuolo RA, Pyles RB. Quantification and Comparison of Toll-Like Receptor Expression and Responsiveness in Primary and Immortalized Human Female Lower Genital Tract Epithelia. Am J Reprod Immunol. 2008; 59:212-24.

Hirano T, Yasukawa K, Harada H, Taga T, Watanabe Y, Matsuda T, Kashiwamura S, Nakajima K, Koyama K, Iwamatsu A. Complementary DNA for a novel human interleukin (BSF-2) that induces B lymphocytes to produce immunoglobulin. Nature. 1986; 324:73-6.

Hoene V, Peiser M, Wanner R. Human monocyte-derived dendritic cells express TLR9 and react directly to the CpG-A oligonucleotide D19. J Leukoc Biol. 2006; 80:1328-36.

Hornung V, Rothenfusser S, Britsch S, Krug A, Jahrsdorfer B, Giese T, Endres S, Hartmann G. Quantitative expression of toll-like receptor 1-10 mRNA in cellular subsets of human peripheral blood mononuclear cells and sensitivity to CpG oligodeoxynucleotides. J Immunol. 2002; 168:4531-7.

van Horssen R, Ten Hagen TL, Eggermont AM. TNF-alpha in cancer treatment: molecular insights, antitumor effects, and clinical utility. Oncologist. 2006; 11:397-408.

Howard, M., and A. O'Garra. Biological properties of interleukin 10. Immunol. Today. 1992; 13:198–200.

Ishii KJ, Akira S. Innate immune recognition of nucleic acids: beyond toll-like receptors. Int J Cancer. 2005; 117:517-23.

Ishii KJ, Akira S. Innate immune recognition of, and regulation by, DNA. Trends Immunol. 2006; 27:525-32.

Ishii KJ, Takeshita F, Gursel I, Gursel M, Conover J, Nussenzweig A, Klinman DM. Potential role of phosphatidylinositol 3 kinase, rather than DNA-dependent protein kinase, in CpG DNA-induced immune activation. J Exp Med. 2002; 196:269-74.

Iwasaki A, Medzhitov R. Toll-like receptor control of the adaptive immune responses. Nat Immunol. 2004; 5:987-95.

Jahrsdörfer B, Hartmann G, Racila E, Jackson W, Muhlenhoff L, Meinhardt G, Endres S, Link BK, Krieg AM, Weiner GJ. CpG DNA increases primary malignant B cell expression of costimulatory molecules and target antigens. J Leukoc Biol. 2001;69:81-8.

Jahrsdorfer B, Muhlenhoff L, Blackwell SE, Wagner M, Poeck H, Hartmann E, Jox R, Giese T, Emmerich B, Endres S, Weiner GJ, Hartmann G. B-cell lymphomas differ in their responsiveness to CpG oligodeoxynucleotides. Clin Cancer Res. 2005; 11:1490-9.

Kadowaki N, Ho S, Antonenko S, Malefyt RW, Kastelein RA, Bazan F, Liu YJ. Subsets of human dendritic cell precursors express different toll-like receptors and respond to different microbial antigens. J Exp Med. 2001; 194:863-9.

Kamstrup S, Verthelyi D, Klinman DM. Response of porcine peripheral blood mononuclear cells to CpG-containing oligodeoxynucleotides. Vet Microbiol. 2001; 78:353-62.

Kajita E, Nishiya T, Miwa S. The transmembrane domain directs TLR9 to intracellular compartments that contain TLR3.Biochem Biophys Res Commun. 2006; 343:578-84.

Kawai T, Akira S. TLR signaling. Semin Immunol. 2007; 19:24-32.

Kawai T, Sato S, Ishii KJ, Coban C, Hemmi H, Yamamoto M, Terai K, Matsuda M, Inoue J, Uematsu S, Takeuchi O, Akira S. Interferon-alpha induction through Toll-like receptors involves a direct interaction of IRF7 with MyD88 and TRAF6. Nat Immunol. 2004; 5:1061-8.

Kim CS, Kawada T, Kim BS, Han IS, Choe SY, Kurata T, Yu R. Capsaicin exhibits anti-inflammatory property by inhibiting IkB-a degradation in LPS-stimulated peritoneal macrophages. Cell Signal. 2003; 15:299-306.

Kim YM, Brinkmann MM, Paquet ME, Ploegh HL. UNC93B1 delivers nucleotide-sensing toll-like receptors to endolysosomes. Nature. 2008; 452:234-8.

Kim YI, Park JE, Martinez-Hernandez A, Yi AK. CpG DNA prevents liver injury and shock-mediated death by modulating expression of IL-1R-associated kinases. J Biol Chem. 2008; [Epub ahead of print].

Kishimoto T. The biology of interleukin-6. Blood. 1989; 74:1-10.

Klinman DM, Yi AK, Beaucage SL, Conover J, Krieg AM. CpG motifs present in bacteria DNA rapidly induce lymphocytes to secrete interleukin 6, interleukin 12, and interferon gamma. Proc Natl Acad Sci U S A. 1996; 93:2879-83.

Klinman D.M. Immunotherapeutic uses of CpG oligodeoxynucleotides. Nat Rev Immunol. 2004; 4:249-58.

Kraatz J, Clair L, Rodriguez JL, West MA. Macrophage TNF secretion in endotoxin tolerance: role of SAPK, p38, and MAPK. J Surg Res. 1999; 83:158-64.

Krieg AM, Yi AK, Matson S, Waldschmidt TJ, Bishop GA, Teasdale R, Koretzky GA, Klinman DM. CpG motifs in bacterial DNA trigger direct B-cell activation. Nature. 1995; 374:546-9.

Krieg AM. Mechanisms and applications of immune stimulatory CpG oligodeoxynucleotides. Biochimica et Biophysica Acta - Gene Structure and Expression. 1999; 1489:107-116.

Krieg, AM., Yi, A. K., Hartmann, G. Mechanisms and therapeutic applications of immune stimulatory CpG DNA Pharmacol. Ther. 1999; 84;113-120.

Krieg, AM., Hartmann, G., Yi, A. K. Mechanism of action of CpG DNA. Curr. Top. Microbiol. Immunol. 2000; 247:1-21.

Krieg AM. Now I know my CpGs. Trends Microbiol. 2001; 9:249-52.

Krieg AM. From A to Z on CpG. Trends Immunol. 2002a; 23:64-5.

Krieg AM. CpG motifs in bacterial DNA and their immune effects. Annu Rev Immunol. 2002b; 20:709-60.

Krieg AM. Development of TLR9 agonists for cancer therapy. J Clin Invest. 2007; 117:1184-94.

Krug A, Towarowski A, Britsch S, Rothenfusser S, Hornung V, Bals R, Giese T, Engelmann H, Endres S, Krieg AM, Hartmann G. Toll-like receptor expression reveals CpG DNA as a unique microbial stimulus for plasmacytoid dendritic cells, which synergizes with CD40 ligand to induce high amounts of IL-12. Eur. J. Immunol. 2001; 31:3026–3037.

Lagneaux L, Delforge, A., Bron, D., De Bruyn, C., Stryckmans, P. Chronic lymphocytic leukemic B cells, but not normal B cells, are rescued from apoptosis by contact with normal bone marrow stromal cells. Blood. 1998; 91:2387-2396

Latz E, Visintin A, Espevik T, Golenbock DT. Mechanisms of TLR9 activation. J Endotoxin Res. 2004a;10:406-12.

Latz E, Visintin A, Lien E, Fitzgerald KA, Monks BG, Kurt-Jones EA, Golenbock DT, Espevik T. Lipopolysaccharide rapidly traffics to and from the Golgi apparatus with the toll-like receptor 4-MD-2-CD14 complex in a process that is distinct from the initiation of signal transduction. J Biol Chem. 2002; 277:47834-43.

Latz E, Schoenemeyer A, Visintin A, Fitzgerald KA, Monks BG, Knetter CF,Lien E, Nilsen NJ, Espevik T, Golenbock DT. TLR9 signals after translocating from the ER to CpG DNA in the lysosome. Nat Immunol. 2004b; 5:190-8.

Lebre MC, van der Aar AM, van Baarsen L, van Capel TM, Schuitemaker JH, Kapsenberg ML, de Jong EC. Human keratinocytes express functional Toll-like receptor 3, 4, 5, and 9. J Invest Dermatol. 2007; 127:331-41.

Leifer CA, Kennedy MN, Mazzoni A, Lee C, Kruhlak MJ, Segal DM. TLR9 is localized in the endoplasmic reticulum prior to stimulation. J Immunol. 2004; 173:1179-83.

Li J, Kartha S, Iasvovskaia S, Tan A, Bhat RK, Manaligod JM, Page K, Brasier AR, Hershenson MB. Regulation of human airway epithelial cell IL-8 expression by MAP kinases. Am J Physiol Lung Cell Mol Physiol. 2002; 283:690-9.

Li J, Ma Z., Tang Z.L., Stevens T., Pitt B. and Li S., CpG DNA-mediated immune response in pulmonary endothelial cells. Am J Physiol Lung Cell Mol Physiol 2004; 287 :552–558.

Lim EJ, Lee SH, Lee JG, Kim JR, Yun SS, Baek SH, Lee C. Toll-like receptor 9 dependent activation of MAPK and NF-kB is required for the CpG ODN-induced matrix metalloproteinase-9 expression. Exp Mol Med. 2007; 39:239-45.

Lin A, Karin M. NF-kappaB in cancer: a marked target. Semin Cancer Biol. 2003; 13:107-14.

Link BK, Ballas ZK, Weisdorf D, Wooldridge JE, Bossler AD, Shannon M, Rasmussen WL, Krieg AM, Weiner GJ. Oligodeoxynucleotide CpG 7909 delivered as intravenous infusion demonstrates immunologic modulation in patients with previously treated non-Hodgkin lymphoma. J Immunother. 2006; 29:558-68.

Locksley RM, Killeen N, Lenardo MJ. The TNF and TNF receptor superfamilies: integrating mammalian biology. Cell. 2001; 104:487-501.

Longo PG, Laurenti L, Gobessi S, Petlickovski A, Pelosi M, Chiusolo P, Sica S, Leone G, Efremov DG. The Akt signaling pathway determines the different proliferative capacity of chronic lymphocytic leukemia B-cells from patients with progressive and stable disease. Leukemia. 2007; 21:110-20.

Marchand P, Resch K, Radeke HH. Selective inhibition of monocyte chemoattractant protein-1 gene expression in human embryonal kidney cells by specific triple helix-forming oligonucleotides. J Immunol. 2000;164:2070-6.

McFarlane SM, Pashmi G, Connell MC, Littlejohn AF, Tucker SJ, Vandenabeele P, MacEwan DJ. Differential activation of nuclear factor-kappaB by tumour necrosis factor receptor subtypes. TNFR1 predominates whereas TNFR2 activates transcription poorly. FEBS Lett. 2002; 515:119-26.

Medvedev AE, Kopydlowski KM, Vogel SN. Inhibition of lipopolysaccharide-induced signal transduction in endotoxin-tolerized mouse macrophages: dysregulation of cytokine, chemokine, and toll-like receptor 2 and 4 gene expression. J Immunol. 2000; 164: 5564-74.

Medzhitov R.Toll-like receptors and innate immunity. Nat Rev Immunol. 2001; 1:135-45.

Medzhitov R, Preston-Hurlburt P, Janeway CA. "A human homologue of the Drosophila Toll protein signals activation of adaptive immunity". Nature. 1997; 388: 394–7.

Muzio M, Bosisio D, Polentarutti N, D'amico G, Stoppacciaro A, Mancinelli R, van't Veer C, Penton-Rol G, Ruco LP, Allavena P, Mantovani A. Differential expression and regulation of toll-like receptors (TLR) in human leukocytes: selective expression of TLR3 in dendritic cells.J Immunol. 2000; 164:5998-6004.

Nagase H, Okugawa S, Ota Y, Yamaguchi M, Tomizawa H, Matsushima K, Ohta K, Yamamoto K, Hirai K. Expression and function of Toll-like receptors in eosinophils: activation by Toll-like receptor 7 ligand. J Immunol. 2003; 171:3977-82.

Naka T, Nishimoto N, Kishimoto T. The paradigm of IL-6: from basic science to medicine. Arthritis Res. 2002; 4:233-42.

Nakano S, Morimoto S, Suzuki J, Nozawa K, Amano H, Tokano Y, Takasaki Y.Role of pathogenic auto-antibody production by Toll-like receptor 9 of B cells in active systemic lupus erythematosus. Rheumatology (Oxford). 2008; 47:145-9.

Nishimura M, Naito S. Tissue-specific mRNA expression profiles of human toll-like receptors and related genes. Biol Pharm Bull. 2005; 28:886-92.

O'Neill LA. Immunology. After the toll rush. Science. 2004; 303:1481-2.

Park Y, Lee SW, Sung YC. Cutting edge: CpG DNA inhibits dendritic cell apoptosis by up-regulating cellular inhibitor of apoptosis proteins through the phosphatidylinositide-3'-OH kinase pathway. J Immunol. 2002; 168: 5–8

Pedersen G, Andresen L, Matthiessen MW, Rask-Madsen J, Brynskov J. Expression of Toll-like receptor 9 and response to bacterial CpG oligodeoxynucleotides in human intestinal epithelium. Clin Exp Immunol. 2005; 141:298-306.

Peng SL. Signaling in B cells via Toll-like receptors. Curr. Opin. in immunology. 2005; 17:230-236.

Platz J., Beisswenger C. and Dalpke A. Microbial DNA induces a host defense reaction of human respiratory epithelial cells. J Immunol. 2004; 173:1219–1223.

Prakash S, Swerdlow SH.Nodal aggressive B-cell lymphomas: a diagnostic approach. J Clin Pathol. 2007; 60:1076-85.

Richardson B. DNA methylation and autoimmune disease. Clin Immunol. 2003; 109:72-9.

Redford TW, Yi AK, Ward CT, Krieg AM. Cyclosporin A enhances IL-12 production by CpG motifs in bacterial DNA and synthetic oligodeoxynucleotides. J Immunol. 1998; 161:3930-5.

Rock FL, Hardiman G, Timans JC, Kastelein RA, Bazan JF. A family of human receptors structurally related to Drosophila Toll. Proc Natl Acad Sci U S A. 1998; 95:588-93.

Roda JM, Parihar R, Carson WE 3rd. CpG-containing oligodeoxynucleotides act through TLR9 to enhance the NK cell cytokine response to antibody-coated tumor cells. J Immunol. 2005; 175: 1619-27.

Sato S, Takeuchi O, Fujita T, Tomizawa H, Takeda K, Akira S. A variety of microbial components induce tolerance to lipopolysaccharide by differentially affecting MyD88-dependent and -independent pathways. Int Immunol. 2002; 14:783-91.

Saegusa K, Yotsumoto S, Kato S, Aramaki Y. Phosphatidylinositol 3-kinase-mediated regulation of IL-10 and IL-12 production in macrophages stimulated with CpG oligodeoxynucleotide. Mol Immunol. 2007; 44:1323-30.

Scheid MP, Duronio V. Phosphatidylinositol 3-OH kinase activity is not required for activation of mitogen-activated protein kinase by cytokines. J Biol Chem. 1996; 271:18134-9.

Schnare M, Barton GM, Holt AC, Takeda K, Akira S, Medzhitov R. Toll-like receptors control activation of adaptive immune responses. Nat Immunol. 2001; 2:947-50.

Schwab G, Siegall CB, Aarden LA, Neckers LM, Nordan RP. Characterization of an interleukin-6-mediated autocrine growth loop in the human multiple myeloma cell line, U266. Blood. 1991; 77:587-93.

Sehgal PB, Walther Z, Tamm I. Rapid enhancement of beta 2-interferon/B-cell differentiation factor BSF-2 gene expression in human fibroblasts by diacylglycerols and the calcium ionophore A23187. Proc Natl Acad Sci U S A. 1987; 84:3663-7.

Sester DP, Brion K, Trieu A, Goodridge HS, Roberts TL, Dunn J, Hume DA, Stacey KJ, Sweet MJ. CpG DNA activates survival in murine macrophages through TLR9 and the phosphatidylinositol 3-kinase-Akt pathway. J Immunol. 2006; 177:4473-80.

Shakibaei M, John T, Schulze-Tanzil G, Lehmann I, Mobasheri A. Suppression of NF-kappaB activation by curcumin leads to inhibition of expression of cyclo-oxygenase-2 and matrix metalloproteinase-9 in human articular chondrocytes: Implications for the treatment of osteoarthritis. Biochem Pharmacol. 2007; 73:1434-45.

Shishodia S, Amin HM, Lai R, Aggarwal BB. Curcumin (diferuloylmethane) inhibits constitutive NF-kappaB activation, induces G1/S arrest, suppresses proliferation, and induces apoptosis in mantle cell lymphoma. Biochem Pharmacol. 2005;70:700-13.

Singh S, and B.B Aggarwal. Activation of transcription factor NF-κB is suppressed by curcumin. J. Biol. Chem. 1995; 270:24995-25000.

Smith JB, Wickstrom E. Antisense c-myc and immunostimulatory oligonucleotide inhibition of tumorigenesis in a murine B-cell lymphoma transplant model. J Natl Cancer Inst. 1998; 90:1146-54.

Stacey K, Young GR, Clark F, Sester DP, Roberts TL, Naik S, Sweet MJ, Hume DA. The molecular basis for the lack of immunostimulatory activity of vertebrate DNA. J Immunol. 2003; 170:3614-3620.

Song PI, Abraham TA, Park Y, Zivony AS, Harten B, Edelhauser HF, Ward SL, Armstrong CA, Ansel JC. The expression of functional LPS receptor proteins CD14 and toll-like receptor 4 in human corneal cells. Invest Ophthalmol Vis Sci. 2001; 42:2867-77.

Sukkar MB, Xie S, Khorasani NM, Kon OM, Stanbridge R, Issa R, Chung KF. Toll-like receptor 2, 3, and 4 expression and function in human airway smooth muscle. J Allergy Clin Immunol. 2006; 118:641-8.

Takeda K, Kaisho T, Akira S.Toll-like receptors. Annu Rev Immunol. 2003; 21:335-76.

Tasker L, Marshall-Clarke S. Functional responses of human neonatal B lymphocytes to antigen receptor cross-linking and CpG DNA. Clin Exp Immunol. 2003; 134:409-19.

Takeshita F, Gursel I, Ishii KJ, Suzuki K, Gursel M, Klinman DM. Signal transduction pathways mediated by the interaction of CpG DNA with Toll-like receptor 9. Semin Immunol. 2004; 16:17-22.

Takeshita F, Ishii KJ, Ueda A, Ishigatsubo Y, Klinman DM. Positive and negative regulatory elements contribute to CpG oligonucleotide-mediated regulation of human IL-6 gene expression. Eur J Immunol. 2000; 30:108-16.

Takeshita F, Leifer CA, Gursel I, Ishii KJ, Takeshita S, Gursel M, Klinman DM. Cutting edge: Role of Toll-like receptor 9 in CpG DNA-induced activation of human cells. J Immunol. 2001; 167:3555-8.

Takeshita F, Suzuki K, Sasaki S, Ishii N, Klinman DM, Ishii KJ. Transcriptional regulation of the human TLR9 gene. J Immunol. 2004; 173:2552-61.

Terol MJ, Tormo M, Martinez-Climent JA, Marugan I, Benet I, Ferrandez A, Teruel A, Ferrer R, García-Conde J. Soluble intercellular adhesion molecule-1 (s-ICAM-1/s-CD54) in diffuse large B-cell lymphoma: association with clinical characteristics and outcome. Ann Oncol. 2003; 14:467-74.

Tominaga K, Saito S, Matsuura M, Nakano M. Lipopolysaccharide tolerance in murine peritoneal macrophages induces downregulation of the lipopolysaccharide signal transduction pathway through mitogen-activated protein kinase and nuclear factor-kappaB cascades, but not lipopolysaccharide-incorporation steps. Biochim Biophys Acta. 1999; 1450:130-44.

Underhill DM, Ozinsky A. Toll-like receptors: key mediators of microbe detection. Curr Opin Immunol. 2002; 14:103-10.

Vasselon T, Detmers PA. Toll receptors: a central element in innate immune responses. Infect Immun. 2002; 70:1033-41.

Verthelyi D, Ishii KJ, Gursel M, Takeshita F, Klinman DM. Human peripheral blood cells differentially recognize and respond to two distinct CPG motifs. J Immunol. 2001; 166:2372-7.

Viglianti GA, Lau CM, Hanley TM, Miko BA, Shlomchik MJ, Marshak-Rothstein A. Activation of autoreactive B cells by CpG dsDNA. Immunity. 2003; 19:837-47.

Visintin A, Mazzoni A, Spitzer JH, Wyllie DH, Dower SK, Segal DM. Regulation of Toll-like receptors in human monocytes and dendritic cells.J Immunol. 2001; 166:249-55.

Vollmer J. Progress in drug development of immunostimulatory CpG oligodeoxynucleotide ligands for TLR9. Expert Opin Biol Ther. 2005; 5:673-82 .

Vollmer J, Weeratna R, Payette P, Jurk M, Schetter C, Laucht M, Wader T, Tluk S, Liu M, Davis HL, Krieg AM. Characterization of three CpG oligodeoxynucleotide classes with distinct immunostimulatory activities. Eur J Immunol. 2004a; 34:251-62.

Vollmer J, Weeratna RD, Jurk M, Samulowitz U, McCluskie MJ, Payette P, Davis HL, Schetter C, Krieg AM.. Oligodeoxynucleotides lacking CpG dinucleotides mediate Toll-like receptor 9 dependent T helper type 2 biased immune stimulation. Immunology. 2004b; 113:212-23.

Wang H, Rayburn ER, Wang W, Kandimalla ER, Agrawal S, Zhang R. Chemotherapy and chemosensitization of non-small cell lung cancer with a novel immunomodulatory oligonucleotide targeting Toll-like receptor 9. Mol Cancer Ther. 2006; 5:1585-92.

Wei L, Hong Z, Jiang Z, Guofu D, Hongwei C, Liangxi W, Yongling L, Bin L, Ping L. Decreased intracellular TLR9 confers hyporesponsiveness of RAW264.7 cells to subsequent CpG ODN challenge. Int Immunopharmacol. 2006; 6:935-46.

Wesche H, Henzel WJ, Shillinglaw W, Li S, Cao Z. MyD88: an adapter that recruits IRAK to the IL-1 receptor complex. Immunity. 1997; 7:837-47.

Wooldridge JE, Ballas Z, Krieg AM, Weiner GJ. Immunostimulatory oligodeoxynucleotides containing CpG motifs enhance the efficacy of monoclonal antibody therapy of lymphoma. Blood. 1997; 89:2994-8.

Wysocka M, Robertson S, Riemann H, Caamano J, Hunter C, Mackiewicz A, Montaner LJ, Trinchieri G, Karp CL. IL-12 suppression during experimental endotoxin tolerance: dendritic cell loss and macrophage hyporesponsiveness. J Immunol. 2001; 166:7504-13.

Yeo SJ, Yoon JG, Hong SC, Yi AK. CpG DNA induces self and cross-hyporesponsiveness of RAW264.7 cells in response to CpG DNA and lipopolysaccharide: alterations in IL-1 receptor-associated kinase expression.J Immunol. 2003; 170:1052-61.

Yi AK, Krieg AM. Rapid induction of mitogen-activated protein kinases by immune stimulatory CpG DNA. J Immunol. 1998, 161:4493-7.

Yi AK, Yoon JG, Yeo SJ, Hong SC, English BK, Krieg AM. Role of mitogen-activated protein kinases in CpG DNA-mediated IL-10 and IL-12 production: central role of extracellular signal-regulated kinase in the negative feedback loop of the CpG DNA-mediated Th1 response. J Immunol. 2002; 168:4711-20.

Yi AK, Yoon JG, Krieg AM. Convergence of CpG DNA- and BCR-mediated signals at the c-Jun N-terminal kinase and NF-kappaB activation pathways: regulation by mitogen-activated protein kinases. Int Immunol. 2003; 15:577-91.

Yi AK, Chace JH, Cowdery JS, Krieg AM. IFN-gamma promotes IL-6 and IgM secretion in response to CpG motifs in bacterial DNA and oligodeoxynucleotides. J Immunol. 1996; 156:558-64

Yi AK, Yoon JG, Hong SC, Redford TW, Krieg AM. Lipopolysaccharide and CpG DNA synergize for tumor necrosis factor-alpha production through activation of NF-kappaB. Int Immunol. 2001; 13:1391-404.

Yung RL, Quddus J, Chrisp CE, Johnson KJ, Richardson BC. Mechanism of drug-induced lupus. I. Cloned Th2 cells modified with DNA methylation inhibitors in vitro cause autoimmunity in vivo. J Immunol. 1995; 154:3025-35.

Zarember KA, Godowski PJ. Tissue expression of human Toll-like receptors and differential regulation of Toll-like receptor mRNAs in leukocytes in response to microbes, their products, and cytokines. J Immunol. 2002; 168:554-61